

**ASSESSMENT OF THE ADHESION OF POWDERS
TO A METAL SURFACE**

by

KWOK KAI LAM

Thesis submitted for the degree of

DOCTOR OF PHILOSOPHY

in the

Faculty of Medicine

of the

UNIVERSITY OF LONDON

Department of Pharmaceutics,
The School of Pharmacy,
University of London,
29-39 Brunswick Square,
London WC1N 1AX.

November, 1991.

ProQuest Number: U055663

All rights reserved

INFORMATION TO ALL USERS

The quality of this reproduction is dependent upon the quality of the copy submitted.

In the unlikely event that the author did not send a complete manuscript and there are missing pages, these will be noted. Also, if material had to be removed, a note will indicate the deletion.



ProQuest U055663

Published by ProQuest LLC (2017). Copyright of the Dissertation is held by the Author.

All rights reserved.

This work is protected against unauthorized copying under Title 17, United States Code
Microform Edition © ProQuest LLC.

ProQuest LLC.
789 East Eisenhower Parkway
P.O. Box 1346
Ann Arbor, MI 48106 – 1346

ABSTRACT

A centrifuge method has been employed to study, statistically, the adhesion of individual particles of some pharmaceutical powder excipients to stainless steel. The surface of the steel substrate was characterized by profilometry, which was defined by the various surface roughness parameters. By altering the relative position of the steel disk in a specially designed rotor tube, the centrifugal force can act both as a compression force as well as a detachment force.

Preliminary pressing of powder particles on to the steel surface was found to increase the strength of particle adhesion. The relative adhesiveness of different solid excipient materials was compared quantitatively by means of the adhesion ratio derived in this study, which allows a more objective means of assessment. In general, adhesion to stainless steel was stronger for soft materials than hard ones, on the basis that plastic deformation has occurred. Moreover, the strengths of adhesion bonds were appreciably affected by the duration that the adhering particles were initially under a compression force before separation. Particulate materials having an inherent weak solid structure was particularly sensitive to such effect.

Variation of particle adhesion forces to stainless steel was shown to be due partly to the non-uniformity of particle size in a powder sieve fraction. Though bigger particles exhibited greater forces of adhesion, due to their larger masses, they were more easily dislodged than the smaller particles by centrifugation.

Investigations into two powder-steel adhesive systems indicated a considerable role played by the molecular van der Waals forces in the particle adhesion. Adhesive interactions were examined in terms of surface energetics, from which an apparent energy of adhesion was calculated for either system, which may provide an alternative means of evaluating particles-substrate adhesion.

A form of Arrhenius relationship was found between temperature and the median adhesion force or the amount of median adhesion force established per unit of the preliminary press-on force, from which the apparent activation energy for an adhesion process was obtained. With less energy of activation was required for a soft material, as found, an implication of this is that, adhesion bond formation would be energetically more favourable for a soft solid.

For my parents

For my brothers and sister

CONTENTS

	Page
Title Page	1
Abstract	2
List of Figures	10
List of Tables	14
List of Plates	16
List of Symbols	17
Acknowledgements	21
CHAPTER 1: GENERAL INTRODUCTION	22
1.1 Concepts of Adhesion	23
1.2 Adhesion and Fracture Mechanics	24
1.3 Adhesion and Tribology	25
1.4 Deformation of Materials	27
1.4.1 Elastic Deformation	27
1.4.2 Plastic Deformation	28
1.5 True Contact Area	32
1.5.1 Measurement of Real Area of Contact	35
1.6 Mechanisms of Adhesion	37
1.6.1 Contact Interaction Forces	37
1.6.1.1 Molecular van der Waals Forces	38
1.6.1.2 Electrical Forces of Adhesion	48
1.6.1.3 Capillary Forces	50
1.6.2 Relative Contributions of the Different Components of Adhesive Forces	52
1.6.3 Other Reactions at the Particle-Substrate Interface	54
1.7 Influence of Solid Surface Condition on Adhesion	55

	Page
1.8	Kinetics of Particle-Substrate Adhesion 56
1.8.1	Hertz's Theory of Elastic Contact 57
1.8.2	Particle Roughness on an Elastic Contact 59
1.9	Kinetics of Particle Detachment from a Plane Surface 62
1.9.1	The Thermodynamic Force and Energy Approaches 62
1.9.2	The Contact Mechanics Approach 66
1.9.3	Field of Applicability of the JKR and DMT Models 68
1.10	Measurement of Particle-Substrate Adhesion 72
1.10.1	Experimental Methods for Measuring Adhesion Forces 72
1.10.1.1	The Aerodynamic and Hydrodynamic Techniques . . . 74
1.10.1.2	The Weighing Technique 75
1.10.1.3	The Pendulum Technique 77
1.10.1.4	The Inclined Plane Technique 77
1.10.1.5	The Centrifuge Technique 78
1.10.1.6	Some other Specific Techniques 79
1.10.2	Merits of the Centrifuge Technique 80
1.11	Objectives of this Work 83
CHAPTER 2: PREPARATION AND CHARACTERIZATION	
OF EXPERIMENTAL MATERIALS 84	
2.1	Characterization of Powder Materials 85
2.1.1	Choice of Powder Materials 85
2.1.2	Description and Pharmaceutical Usages of the Powders 85
2.1.3	Sources of Materials 86
2.1.4	Size Separation of the Powders 86
2.1.5	Apparent Particle Densities 88
2.1.6	Single Particle Mass Determination 88
2.1.7	Particle Microscopical Morphology 91
2.1.8	Storage of Materials 91
2.2	Surface Characterization of the Substrate Material 95
2.2.1	Substrate Material 95

	Page
2.2.2 Surface Topography Analysis of the Stainless Steel Disks	95
2.2.2.1 Introduction	95
2.2.2.2 Experimental	99
2.2.2.3 Results and Discussion	99
2.2.3 Surface Texture Parameters	102
2.2.3.1 Introduction	102
2.2.3.2 Results and Discussion	105
2.2.4 Conclusions	105
CHAPTER 3: TECHNIQUE FOR MEASUREMENT OF ADHESIVE FORCES BETWEEN PARTICLES AND A SUBSTRATE SURFACE	107
3.1 Determination of Particle-Substrate Adhesion Forces	108
3.1.1 Introduction	108
3.1.2 Experimental Technique for Measuring Adhesive Forces	109
3.2 Apparatus	110
3.2.1 Centrifuge	110
3.2.2 Purpose-Built Centrifuge Cells	110
3.2.3 Counting of Adhering Particles on a Substrate Surface	116
CHAPTER 4: EFFECT OF APPLIED COMPRESSION ON THE ADHESION OF POWDERS TO STAINLESS STEEL . . .	120
4.1 Introduction	121
4.2 Experimental Method	123
4.2.1 Preparation of Particle-Steel Adhesive System	123
4.2.2 Adhesion Measurements of Powder Materials Without Preliminary Compression	124
4.2.2.1 Method	124
4.2.2.2 Results and Discussion	124
4.2.3 Adhesion Measurements of Powder Materials With Preliminary Compression	128
4.2.3.1 Method	128

	Page
4.2.3.2 Results	129
4.2.3.3 Discussion	143
4.3 Conclusions	152
CHAPTER 5: INVESTIGATION OF PRELIMINARY COMPRESSION DURATION ON PARTICLE ADHESION TO STAINLESS STEEL	153
5.1 Introduction	154
5.2 Experimental Method	156
5.3 Results	157
5.4 Discussion	175
5.5 Conclusions	179
CHAPTER 6: INFLUENCE OF PARTICLE SIZE ON POWDER ADHESION TO STAINLESS STEEL	180
6.1 Introduction	181
6.2 Experimental Method	185
6.3 Results	186
6.4 Discussion	197
6.5 Conclusions	204
CHAPTER 7: EFFECT OF LOW TEMPERATURES ON POWDER ADHESION TO STAINLESS STEEL	205
7.1 Introduction	206
7.2 Experimental Method	208
7.3 Results	210
7.4 Discussion	220
7.5 Conclusions	229

	Page
CHAPTER 8: GENERAL CONCLUSIONS	230
Suggestions for Further Work	235
Bibliography	237

LIST OF FIGURES

		Page
FIG. 1.1	Edge-dislocation - consecutive movement of the dislocation through a crystal lattice	30
FIG. 1.2	Screw dislocation	31
FIG. 1.3	Diagrammatic illustration of a typical 'clean' polished metal surface	34
FIG. 2.1	Diagrammatic illustration of the principle of surface profilometry	98
FIG. 2.2	Roughness, waviness and errors in form	100
FIG. 2.3	Diagrammatic representations of some surface roughness parameters	103
FIG. 3.1	A schematic diagram of the specially designed rotor tube . . .	115
FIG. 4.1	Adhesion profiles of particulate materials to stainless steel, without preliminary forcing the powder solids to the substrate	126
FIG. 4.2	Adhesion profiles of PEG 4000 to stainless steel at different preliminary press-on forces (indicated by RPM)	130
FIG. 4.3	Adhesion profiles of Starch 1500 to stainless steel at different preliminary press-on forces (indicated by RPM)	131
FIG. 4.4	Adhesion profiles of spray-dried lactose to stainless steel at different preliminary press-on forces (indicated by RPM)	132
FIG. 4.5	Adhesion profiles of heavy precipitated calcium carbonate to stainless steel at different preliminary press-on forces (indicated by RPM)	133
FIG. 4.6	Log-probability plots of the adhesion of PEG 4000 to stainless steel at different preliminary compression forces (indicated by RPM)	134
FIG. 4.7	Log-probability plots of the adhesion of Starch 1500 to stainless steel at different preliminary compression forces (indicated by RPM)	135

	Page
FIG. 4.8	Log-probability plots of the adhesion of spray-dried lactose to stainless steel at different preliminary compression forces (indicated by RPM) 136
FIG. 4.9	Log-probability plots of the adhesion of heavy precipitated calcium carbonate to stainless steel at different preliminary compression forces (indicated by RPM) 137
FIG. 4.10	Effect of preliminary compression force on the scattering of particle-steel adhesion force expressed by the geometric standard deviation 140
FIG. 4.11	Relationship between median adhesion force and preliminary press-on force 141
FIG. 4.12	Inverse relationship between the literature values of the yield pressure of the powder solids and their adhesion ratios 151
FIG. 5.1	Adhesion profiles of PEG 4000 to stainless steel, as a function of the duration (in seconds) of preliminary compression 158
FIG. 5.2	Adhesion profiles of Starch 1500 to stainless steel, as a function of the duration (in seconds) of preliminary compression 159
FIG. 5.3	Adhesion profiles of spray-dried lactose to stainless steel, as a function of the duration (in seconds) of preliminary compression 160
FIG. 5.4	Adhesion profiles of heavy precipitated calcium carbonate to stainless steel, as a function of the duration (in seconds) of preliminary compression 161
FIG. 5.5	Log-probability plots of the adhesion of PEG 4000 to stainless steel, as a function of the duration (in seconds) of preliminary compression 162
FIG. 5.6	Log-probability plots of the adhesion of Starch 1500 to stainless steel, as a function of the duration (in seconds) of preliminary compression 163
FIG. 5.7	Log-probability plots of the adhesion of spray-dried lactose to stainless steel, as a function of the duration (in seconds) of preliminary compression 164

	Page
FIG. 5.8	Log-probability plots of the adhesion of heavy precipitated calcium carbonate to stainless steel, as a function of the duration (in seconds) of preliminary compression 165
FIG. 5.9	Relationship between median adhesion force and duration of preliminary compression 168
FIG. 5.10	Effect of the duration of preliminary compression on the amount of median adhesion force established per unit of the press-on force applied to PEG 4000 171
FIG. 5.11	Effect of the duration of preliminary compression on the amount of median adhesion force established per unit of the press-on force applied to Starch 1500 172
FIG. 5.12	Effect of the duration of preliminary compression on the amount of median adhesion force established per unit of the press-on force applied to spray-dried lactose 173
FIG. 5.13	Effect of the duration of preliminary compression on the amount of median adhesion force established per unit of the press-on force applied to heavy precipitated calcium carbonate 174
FIG. 6.1	Adhesion profiles of different particle size fractions of Starch 1500 to stainless steel, after preliminary compression 187
FIG. 6.2	Adhesion profiles of different particle size fractions of spray-dried lactose to stainless steel, after preliminary compression 188
FIG. 6.3	Log-probability plots of the adhesion of different particle size fractions of Starch 1500 to stainless steel, after preliminary compression 189
FIG. 6.4	Log-probability plots of the adhesion of different particle size fractions of spray-dried lactose to stainless steel, after preliminary compression 190
FIG. 6.5	Relationship between the median adhesion force and the calculated average particle size, when the powder solids have initially been forced on to the stainless steel surface 194
FIG. 6.6	Relative extent of adhesion of the different calculated average particle sizes of the powder sieve fractions to stainless steel, after preliminary compression 196

	Page
FIG. 7.1	Adhesion profiles of PEG 4000 to stainless steel at different preliminary press-on temperatures 212
FIG. 7.2	Adhesion profiles of heavy precipitated calcium carbonate to stainless steel at different preliminary press-on temperatures . . 213
FIG. 7.3	Log-probability plots of the adhesion of PEG 4000 to stainless steel at different preliminary press-on temperatures 214
FIG. 7.4	Log-probability plots of the adhesion of heavy precipitated calcium carbonate to stainless steel at different preliminary press-on temperatures 215
FIG. 7.5	Effect of lowering the preliminary press-on temperature on the relative extent of particle adhesion to stainless steel 219
FIG. 7.6	Arrhenius plots of the median adhesion force of particles to stainless steel, as a function of the press-on temperature 225
FIG. 7.7	Arrhenius plots of the relative extent of particle-steel adhesion (τ), as a function of the press-on temperature 226

LIST OF TABLES

		Page
TABLE 1.1	London-van der Waals interactions at small separation, h , for some geometrical contact models, from the microscopic Hamaker theory	42
TABLE 1.2	London-van der Waals interactions at small separation, h , for some geometrical contact models, from the macroscopic Lifshitz theory	46
TABLE 2.1	Sources of powder materials	87
TABLE 2.2	The mean apparent particle densities of some powder fractions	89
TABLE 2.3	Mean particle masses of different sieve fractions of the powders	92
TABLE 2.4	Statistical surface texture parameters of the polished and unpolished stainless steel disks	106
TABLE 3.1	The relative centrifugal forces (RCF) at the particles at some of the rotation speeds	117
TABLE 4.1	Geometric median adhesion forces of the powders and their respective geometric standard deviation, σ_g , at the various compression forces	139
TABLE 4.2	Values of the ratio of the geometric median adhesion force to the preliminary compression force	142
TABLE 4.3	Yield pressures of the powder materials	150
TABLE 5.1	Geometric median adhesion forces of powders and their corresponding geometric standard deviations, σ_g , over a press-on time period from 60 to 960 seconds, at 17,000rpm	166
TABLE 5.2	Ratios of the geometric median adhesion force to the preliminary compression force, over a compression duration of 60 to 960 seconds, at 17,000rpm	170
TABLE 6.1	Values of the median adhesion force and geometric standard deviation, σ_g , of the various particle size fractions of Starch 1500 and spray-dried lactose	191

	Page
TABLE 6.2 Ratios of the median adhesion force to the preliminary compression force for the various calculated particle sizes of the test powders	195
TABLE 7.1 Results of the statistical analysis of the control experiment . . .	211
TABLE 7.2 Values of the two log-probability statistical parameters at the various experimental temperatures, for the two powder excipients	216
TABLE 7.3 Relative adhesions of the powder materials to the steel substrate, at the various press-on centrifugation temperatures	218
TABLE 7.4 Values of the apparent activation energy of bonding, E_a (kJmol^{-1}) and A_0 , from Arrhenius plots for PEG 4000 and heavy precipitated calcium carbonate	227

LIST OF PLATES

	Page
PLATE 2.1	The Perkin Elmer AD-2 Autobalance 90
PLATE 2.2	Scanning electron micrographs of some sieve size fractions of the powder materials 93
PLATE 2.3	The polished and unpolished stainless steel substrate disks 96
PLATE 2.4	Talysurf profilometer records of the polished and unpolished stainless steel disks 101
PLATE 3.1	The MSE High-Speed 18 Ultracentrifuge 111
PLATE 3.2	Control panel of the MSE High-Speed 18 Ultracentrifuge . . . 112
PLATE 3.3	Positioning of the two adhesion rotor tubes in a fixed angle rotor 113
PLATE 3.4	Two specially designed adhesion rotor tubes 114
PLATE 3.5	Particle counting microscope system 118
PLATE 3.6	A close-up view showing the positions of the light guides relative to the metal disk 119

LIST OF SYMBOLS

A	'Non-retarded' Hamaker constant
A_o	Arrhenius equation constant
A_t	Total contact area
a	Contact zone radius
a_l	Liquid film thickness
a_m	Slope value
a_o	Radius of finite contact area
B	'Retarded' Hamaker constant
b	Particle rough shell thickness
b_i	Ordinate intercept value
C	Radius of curvature of liquid surface
C_r	Correction factor
c	Parameter characterizing rigidity of a spring
c_l	Shape factor of liquid bridge
D	Edge-length of a cube
D_o	Particle diameter
d	Sphere diameter
E	Young's modulus of elasticity
E_a	Activation energy
E^*	Effective elastic modulus
F	Centrifugal force
F_{ad}	Adhesion force
F_B	Force due to capillary liquid bridge
F_c	Capillary force
F'_c	Empirical capillary force relating to air relative humidity
F_{def}	Additional van der Waals forces due to deformation
F_{el}	Elastic repulsion force
F_H	Compressive (Hertz) force
F_{hyd}	Hydrodynamic force

F_{im}	Electrostatic image force
F_m	Total molecular attraction force
F'_m	Molecular force inside contact zone
F''_m	Molecular force in the annular zone
F_p	Force due to difference of pressure outside and inside a liquid bridge
F_R	Surface tension force
F_r	'Retarded' van der Waals forces
F_{vdw}	Van der Waals forces of adhesion
F'_{vdw}	Total van der Waals forces
F_w	Electrostatic double layer force of attraction
g	Gravitational acceleration
H	Micro-hardness of material
H_d	Particle-plane separation distance
h_o	Minimum equilibrium distance of separation
K	Proportional constant relating to model
K_e	Elastic properties relating to Young's modulus and Poisson's ratio
L	Surface profilometry assessment length
M	Surface hardness
m	Average measured particle mass
m_p	Mass of a powder layer
N	Load index
n	Number of oxyethylene groups in a molecule
P_k	Capillary pressure
$P_{(\xi)}$	Local normal pressure
p	Adhesive surface area radius
Q	Electrical charge
R	Particle radius
R_a	Surface roughness
R_c	Bulk particle radius
R_h	Harmonic mean radius
R_{ku}	Kurtosis parameter of surface profile

R_o	Molar gas constant
R_p	Maximum peak height
R_{pm}	Mean of R_p
R_q	Root-mean-square parameter of R_a
R_{sk}	Skewness parameter of surface profile
R_t	Maximum peak-to-valley height
R_{tm}	Mean of maximum peak-to-valley
R_v	Maximum valley depth
R_y	Largest maximum peak-to-valley height
r	Radius of centrifugation
S	Mean spacing of adjacent local peaks
S_c	Contact area
T	Absolute temperature
t	Time under a compressive stress
U	Contact potential difference
V_i	Median adhesion force or Ratio of the median adhesion force to the preliminary press-on force
V_{vdw}	Van der Waals energy of interaction
v	Terminal velocity
v_c	Modified shear stress factor
W	Load
z	Atomic separation distance
α	Amount of deformation
α_d	Coefficient relating to dielectric constant and uniformity of surface charge density
α_l	Liquid bridge angle
β	Radius of curvature of asperity tip
γ	Surface free energy of solid
γ_l	Surface tension of liquid
δ_c	Elastic displacement
δ_l	Spring elongation
$\delta\gamma$	Change in surface energy per unit area
ϵ	Dielectric constant of medium

ϵ_0	Permittivity of vacuum
ϵ_x	Strain in x-direction
η	Liquid viscosity
θ	Modified adhesion parameter
θ_c	Contact angle
θ_t	Tilted angle to the horizontal
λ	Plasticity index
μ	Integral equation solution parameter
μ_c	Proportional constant
ν	Poisson's ratio
ξ	Distance from axis of symmetry
ρ	Particle density
ρ_c	Effective mean radius of curvature of asperity peaks
σ	Standard deviation
σ_g	Geometric standard deviation
σ_l	Surface tension of liquid
σ_r	Effective joint roughness
σ_x	Deforming stress in x-direction
σ_y	Deforming stress in y-direction
σ_z	Deforming stress in z-direction
τ	Ratio of the median adhesion force to the preliminary compression force
ϕ	Potential of interaction
ϕ_a	Apparent adhesive interaction energy
φ	Angle of inclination
φ_c	Critical angle of inclination
ω	Angular velocity
$\hbar\bar{\omega}$	Lifshitz-van der Waals constant
$1/\Delta_c$	Adhesion parameter

ACKNOWLEDGEMENTS

I would like firstly to express my sincere thanks to my Supervisor, Professor J.M. Newton (Head of Department of Pharmaceutics) for his invaluable advice, guidance and constant encouragement throughout the project and in preparing this thesis.

I would also like to thank Mrs. M. Fielder (Secretary of the Department of Pharmaceutics) for her kindness and using her facilities when preparing some of my thesis materials.

I am very grateful to Mr. J.H. McAndrew (Laboratory Superintendent of the Department of Pharmaceutics) and Mr. K. Barnes for their considerable technical assistance, and to other technical staff, in particular, Mr. D. Hunt and Mr. C. Ingram for manufacturing the adhesion rotor cells. My appreciation also extends to my colleagues who have so freely given their advice.

I wish to express my gratitude to Mr. W.C. Baldeo and Ms. L. Randall of the Department of Pharmaceutical Chemistry for their help with the operation of the Perkin Elmer Autobalance.

I am also greatly indebted to my family for their continuous moral support and patience throughout the three years of my research, and I wish here to express my heartfelt thanks. Last but not the least, I wish to thank the ORS Committee for the provision of a research studentship for this project.

CHAPTER 1

General Introduction

1. GENERAL INTRODUCTION

1.1 CONCEPTS OF ADHESION

A review of the literature regarding adhesion between solid bodies reflects a widespread interest and activity in various fields related to solid-solid adhesion. An understanding of the term adhesion would constitute one of the main elements of a theory of adhesion.

Generally, the term adhesion and the practice of sticking two pieces of material together are in common use, though the term bonding (or sticking) is sometimes used to denote the processes through which a molecular bond between two bodies is established, and the term adhesion is reserved to mean the strength that this bond achieves. In fact, the term adhesion conjures up different concepts in the minds of the workers (e.g. chemist, physicist, engineer, mathematician) engaged in different fields of scientific work.

On the one hand, adhesion is understood to be a process through which two bodies are brought together and bonded to each other in such a manner that an applied force or thermal motion is required to break the bond, i.e., the kinetics of joining the bodies. It is usually applied in this sense in colloid research and coagulation phenomena, where sticking generally implies that a certain barrier be overcome by means of an external force or thermal energy.

On the other hand, adhesion can be defined as a molecular coupling between two unlike contiguous bodies. Patrick (1967) defined adhesion to be the state in which two surfaces are held together by valence forces, or mechanical interlock, or both. Alternatively, the mechanism of adhesion was defined by Good (1973) as the means by which mechanical force or work is transferred from one solid body to another, in tension or shear without slip. Adamson (1982) described adhesion as the physical state where two solid surfaces are maintained in intimate interfacial contact by mechanical

interlocking or chemical interactions across the interface. The term practical adhesion was used by Mattox & Rigney (1986) to describe the physical strength of an interface between two regions of a material system.

Furthermore, adhesion can be interpreted to mean the normal force or energy required to separate two bodies in contact. In this case, the intensity of adhesion is considered in terms of the process of breaking a bond between solids that are already in contact. This area of study is of particular interest in such applications as small particle adhesion to a substrate surface, after the former has initially adhered to the latter. In this situation, there are no factors to hinder contact and the formation of an adhesive bond. This kind of phenomenon is commonly encountered in many pharmaceutical and technological processes.

At adhesional equilibrium, the attractive forces between two adherents are balanced by repulsive forces resisting further deformation at their interface. These forces are generally not measurable. The commonly used terminology such as force of adhesion, adhesive strength or their equivalents, are usually interpreted to denote that force which is numerically equal to but opposite in direction to an applied removal force which is the minimum force necessary to cause detachment of an adherent particle from a fixed substrate, in a specified period of time.

1.2 ADHESION AND FRACTURE MECHANICS

An adhesive contact represents, in the general case, the plane of contact of solid bodies of substantially different structure, a naturally weak spot. The loss of adhesion under a pull-off force can occur by fracture of the material at or near the interface. This mechanical failure of an adhesive interface is essentially a fracture phenomenon.

A substantial body of fracture mechanics theory for the failure at an interfacial contact, with particular reference to adhesion, was developed by several workers (e.g.

Kendall, 1971, 1975; Maugis & Barquins, 1978; Maugis, 1984). It is widely employed to describe adhesion fracture of polymers.

1.3 ADHESION AND TRIBOLOGY

Tribology is the science of interacting surfaces in relative motion. The approach of considering the adhesion between two solids when they are pressed together has a close connection with the behaviour of solids which are placed together and slid over one another. Investigations on the friction between unlubricated solids indicate that, adhesion plays an important role in such tribological processes as friction and wear (*Bowden & Tabor, 1950, 1964; Archard, 1953a; James & Newton, 1985*). For real surfaces which are rough on an atomic scale, intimate contact occurs only where the asperities on one surface touch the others, and it is at these regions that adhesional and tribological actions take place.

The familiar theory of friction (*Bowden & Tabor, 1950, 1964; Archard, 1953a*) is based on the adhesion and shear fracture of asperity junctions. Archard (1953a) developed wear models which emphasize adhesive contacts and fracture in material away from the contact junctions. Basically, friction between two solid surfaces involves two main elements, plastic flow at the contact regions and strong adhesion or welding at the points of intimate contact, which lead to the formation of solid junctions. If one surface is now caused to slide over the other, the frictional force resisting motion is primarily the force required to shear the solid adhesive junctions so formed. This adhesion mechanism of friction explains the basic laws of friction, which are that, frictional force is proportional to the load and is independent of the size of the bodies. Moreover, it also provides an explanation for the general phenomenon of frictional wear, as being due to strong adhesion occurring at the points of real contact that shearing does not take place at the interface but within the bulk of the weaker of the two solids, i.e., an adhesive wear.

The adhesion theory of friction considers situations where asperity deformation is plastic on surfaces of complex topography, and the contact junctions must possess

a constant specific shear strength. However, contacts between bodies are not always plastic, and the above conditions can be violated by very hard surfaces, or those having a large elastic range, or by the presence of brittle or weak surface layers. Criticisms of the adhesion theory regarding friction phenomenon and the modifications required to combat them are reviewed by Rabinowicz (1965) and Teer & Arnell (1975). Two main criticisms of the theory are the lack of emphasis placed on the importance of surface structure, and the controversy over the concept of adhesion at the asperity junctions. A review by Bikerman (1976) proposes that adhesion does not cause friction and has no influence on the friction phenomena. However, little support for this view is published except that, measured adhesional forces are often extremely low, and the effect is particularly more noticeable if the asperity junctions work harden and become brittle. This was explained (*McFarlane & Tabor, 1950; Bowden & Tabor, 1964; Deryaguin et al., 1975c*) as due to the rupturing of the asperity junctions by the elastic stresses released on removal of the normal load, which is inevitable if an adhesion force is to be measured. On the other hand, in friction measurements, the normal load is maintained on the surfaces.

Friction is influenced by not only the forces of adhesion acting on the sections of true contact, but can also by forces of non-contact adhesion acting on the sections of the surface that are not directly touching but are close enough to each other to be within the radius of action for molecular attraction. Non-contact adhesion is a factor in the interaction between any two contacting surfaces if the true contact area is less than the normal contact area. The lower the mean height of the projections on the contacting surfaces, the greater will be the non-contact adhesion. This non-contact adhesion will, however, be minimized when the surfaces are so rough that all protuberances, other than those in actual contact, are far enough away from the closest points of the opposite surface that they are outside the range of actions of surface forces, and also if the contact is completely plastic.

Whereas friction is known to prevent the relative tangential displacement, i.e., sliding, of two contacting bodies, adhesion is commonly used to represent the resistance to relative displacement in a direction normal to the contacting surfaces. In

broad terms, friction is essentially a measure of the shear strength and adhesion a measure of the tensile strength of the junctions formed at the regions of real contact.

Studies of friction and adhesion of solids both focus the attention directly on the solid-solid interface. Adhesion is a complex phenomenon and, similar to friction, is also highly dependent on the specific nature of the contacting surfaces. This is because both mechanical and physico-chemical bondings are possible. Therefore, the surface structural and mechanical characteristics of materials are vitally important, as is the geometry of the true contact.

1.4 DEFORMATION OF MATERIALS

The way that two solids behave on contact and the production of adequate areas of contact depend critically on the mechanical properties of the adherents, which govern the deformation behaviour of the materials at the contact interface. Under an applied load, surface deformations at an adhesive contact include elastic, plastic, elastoplastic or viscoelastic.

1.4.1 Elastic Deformation

If a stress within the elastic limit is imposed, a solid will be deformed but not break. Moreover, it will return to its original shape when the stress is released. Such deformations are said to be elastic. The relation between the deforming stress, σ_x , and the resulting strain, ϵ_x , is known as the Hooke's law:

$$\sigma_x = E\epsilon_x \quad (1.1)$$

where E is the modulus of elasticity in tension. Since extension of an element in the x-direction is accompanied by lateral contractions, a more generalized form of the Hooke's law, extended to three dimensions, x, y and z, for an isotropic solid (i.e., the elastic properties are the same in all directions) is:

$$\epsilon_x = \frac{1}{E} [\sigma_x - \nu(\sigma_y + \sigma_z)] \quad (1.2)$$

where ν is the Poisson's ratio. For many materials, Poisson's ratio can often be taken equal to $\frac{1}{4}$; the value for structural steel is about 0.3. In practice, Poisson's ratio varies only between 0 and $\frac{1}{2}$.

Elastic deformations in a crystal may arise not only by the action of external forces on it, but can also be due to internal structural defects present in the crystal (*Landau & Lifshitz, 1975*).

1.4.2 Plastic Deformation

Plastic deformation occurs in a material when it has been subjected to a stress greater than the yield stress; the deformation follows with increasing load and continues until the area of the material normal to the maximum resultant stress induced by the applied load, is capable of supporting that stress. On removal of the stress, a permanent strain is left. Most systems, however, store a residual strain energy which gives some elastic recovery on release of the load. In single crystals, plastic deformation occurs by a process called slip, in which two planes of atoms or molecules move relative to each other, but leaving the configuration unchanged, or less commonly, by a process known as twinning, where the configuration of the atoms or molecules is modified when the sheared portion of the crystals is transformed into a mirror image of the unshaded portion.

Slip is structure-sensitive and generally occurring on planes of greatest atomic density in the direction of greatest linear density (*Caddell, 1980*). The shear stress necessary to produce this slip is the critical shear stress and in real crystals, this may be several orders of magnitude lower than that calculated for an ideal crystal. This discrepancy was suggested by some workers (e.g. *Taylor, 1934*) to be due to the presence of dislocations (or defects) within the real crystal, which allow slip to occur

at much lower stresses than those required to cause simultaneous movement of full atomic planes. Moreover, slip can be considered as the passage of dislocations across the crystal, with attention being concentrated on the movement of dislocations rather than planes of atoms.

Dislocations may be pure edge, pure screw or a mixture of these two extreme types. Consider that an 'extra' half-plane of atoms is introduced into a crystal lattice, the edge of this half-plane is then called an edge dislocation. In the immediate neighbourhood of this dislocation, the crystal lattice is greatly distorted; displacement of the atoms occurs normal to the direction of motion of the dislocation (Fig. 1.1). The screw type of dislocation may be visualized as the result of 'cutting' the lattice along a half-plane and then shifting the parts of the lattice on either side of the cut in opposite directions parallel to the edge of the cut. Such dislocation converts the lattice planes into a helicoidal surface (Fig. 1.2).

Inbuilt dislocations are only a minor source for the yielding process because they may not lie in a slip plane for the structure or they may be pinned in place by impurities in the crystal and are therefore immobile. Dislocation defects causing plastic deformation are generated as required, by dislocation interaction such as the Frank-Read source where an edge dislocation is anchored by an obstacle and an applied shear stress causes dislocation loops to form repeatedly. This increase in dislocation density will continue until the expanding dislocation loops meet a resistance which impedes their movement. The continuing pile-up of dislocations results in tangled networks due to the intersection of different slip planes, and causes a back pressure which shuts off further generation from the Frank-Read source. A consequence of this is that, there is an irreversible consolidation of mass, and greater stresses are required to deform the crystal plastically, a phenomenon known as strain or deformation hardening (*Hayden et al., 1965*). The crystal will exhibit an increase in strength and a more brittle behaviour.

Polymeric materials often show plastic behaviour but the mechanisms responsible for absorbing the energy of the applied stress are somewhat different. Such

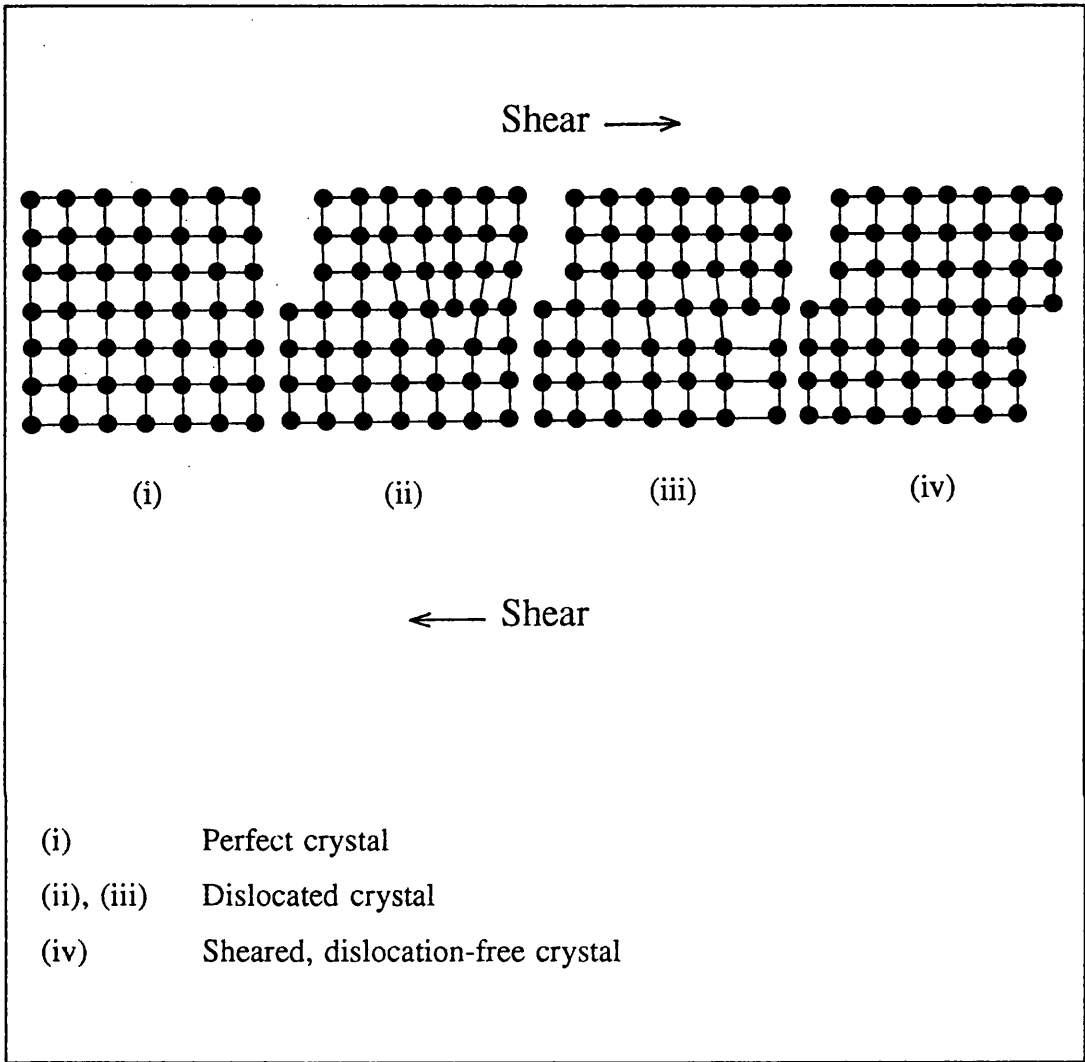


FIG. 1.1 Edge dislocation - consecutive movement of the dislocation through the crystal lattice (from Cook, 1987).

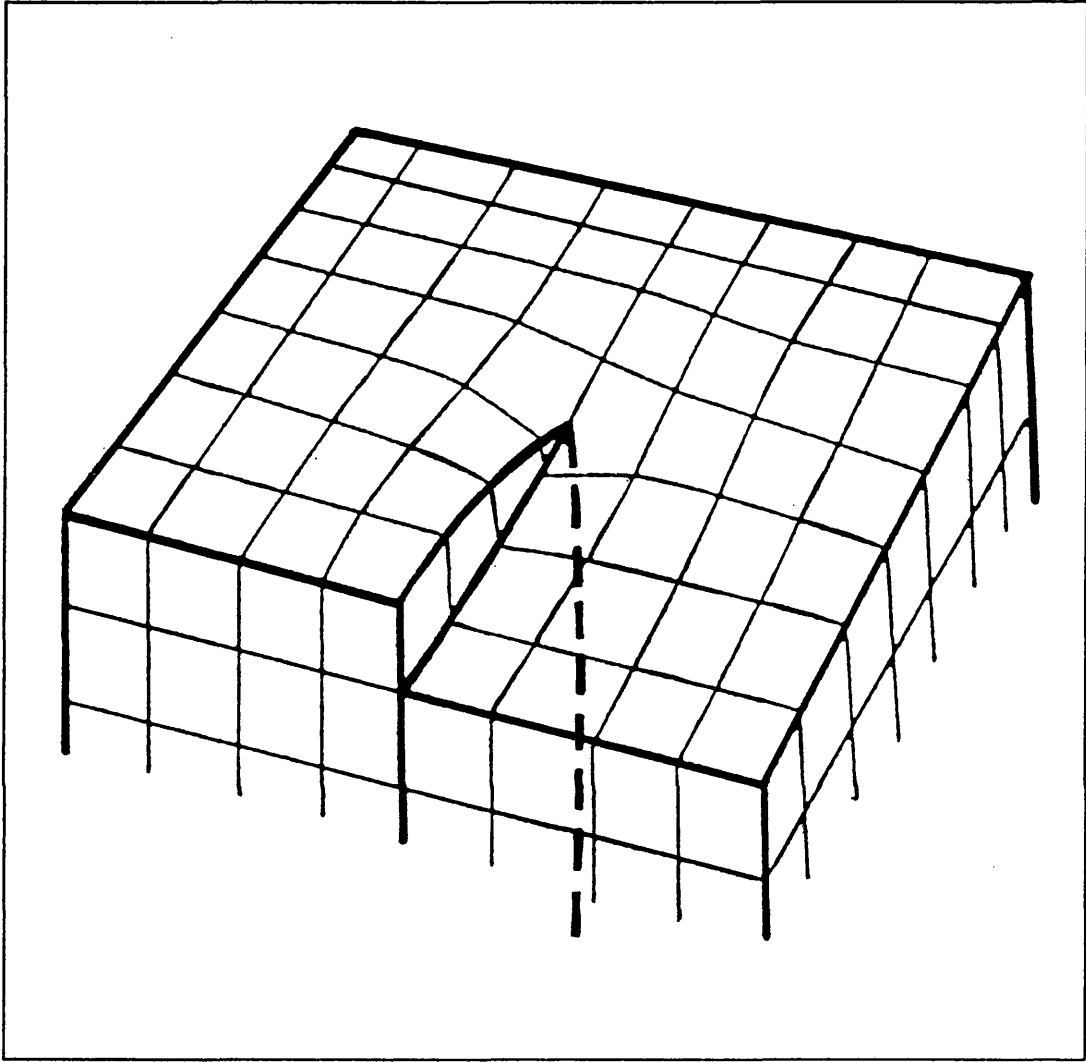


FIG. 1.2 Screw dislocation (from Landau & Lifshitz, 1975).

materials consist of long chain molecules which are arranged in a way that is at least partially crystalline. The chains are folded or coiled so that bonding by secondary forces occurs between the chains. When the material is stressed, energy is absorbed in unfolding these chains and breaking the secondary bonds so that the solid deforms plastically before it breaks.

For engineering surfaces, the dominant mode of contact deformation may be predicted by a plasticity index, λ (*Greenwood & Rowe, 1965; Greenwood & Williamson, 1966*). It is expressed as:

$$\lambda = \frac{E^*}{M} \left(\frac{\sigma_r}{\rho_c} \right)^{1/2} \quad (1.3)$$

where E^* is the effective elastic modulus of the joint (given by $1/E^* = (1-\nu_1^2)/E_1 + (1-\nu_2^2)/E_2$, where E_1 and E_2 are the elastic moduli and ν_1 and ν_2 are the Poisson's ratios of the two surfaces 1 and 2 forming the joint), M is the surface hardness of the softer of the two materials comprising the joint, σ_r is the effective joint roughness, and ρ_c is the effective mean radius of curvature of the asperity peaks. It was found that when $\lambda < 0.7$, the possibility of plastic deformation occurring is very small.

1.5 TRUE CONTACT AREA

Under normal conditions, solid surfaces of macroscopic objects do not adhere together when brought into contact, except perhaps after severe plastic deformation or at high temperatures, etc. It is usually argued that this is primarily due to the protective action of adsorbed gases and other surface films, which themselves provide poor adhesive strength and, in addition, prevent the formation of adhesive bonding between the adherents. This was found experimentally to be the situation for most metals whose surfaces are 'cleaned' in air, since their surfaces would still be covered by a thin film of oxide, some physically adsorbed gases and certain impurities

(Bowden & Tabor, 1950; Bowden & Rowe, 1956). A diagrammatic illustration is shown in Fig. 1.3. In many cases, this surface film consists predominantly of the metal oxide, which is usually considered as a material of higher elastic modulus than the parent metal itself. Whilst this is a major factor in preventing adhesion, the topographical nature or degree of flatness of the surfaces is also of importance, because it controls the proportion of the surface area that can be brought within the range of the short-range surface forces of the two adhering bodies, i.e., it governs the real area of contact.

When real particles come into contact with a rough substrate surface, two extreme cases of contact are possible. Either the particle diameter is greater than the interval between the substrate surface asperities, or the particle diameter is smaller than the interval between those protuberances. In the case of relatively large particles, the bulk of the particles will be directly in contact with the tops of the substrate surface rugosities. The parameters of the atomic-molecular roughness of the latter asperities, under those circumstances, can be treated as more or less constant values (Zimon, 1982). Very fine particles, on the other hand, will be located randomly on the side surface of a substrate asperity. Several typical cases characterizing the adhesion of ideally smooth spherical particles to rough substrate surfaces of different classes of surface finish, are distinguished in a study by Zimon & Volkova (1965). Under practical conditions, the adhesion of particles to a plane surface can encounter a variety of forms of surface irregularities, in which case, the bulk of a particle may occupy any position relative to the summit or base of a substrate asperity.

Since two rough surfaces in contact touch only in isolated regions, the real contact area, being the sum of the flattened tips of the asperities, will be much less than the apparent area of contact, which is the region covering the macroscopic deformation. Within the range of elastic deformation, the process of deformation is completely reversible, and the surfaces return to their original configuration on removal of the load. For bodies which deform one another plastically, there is additional relaxation of the elastic stresses in the bodies when the load is reduced. If the adhesive junctions formed are strong, they may not be ruptured by the released

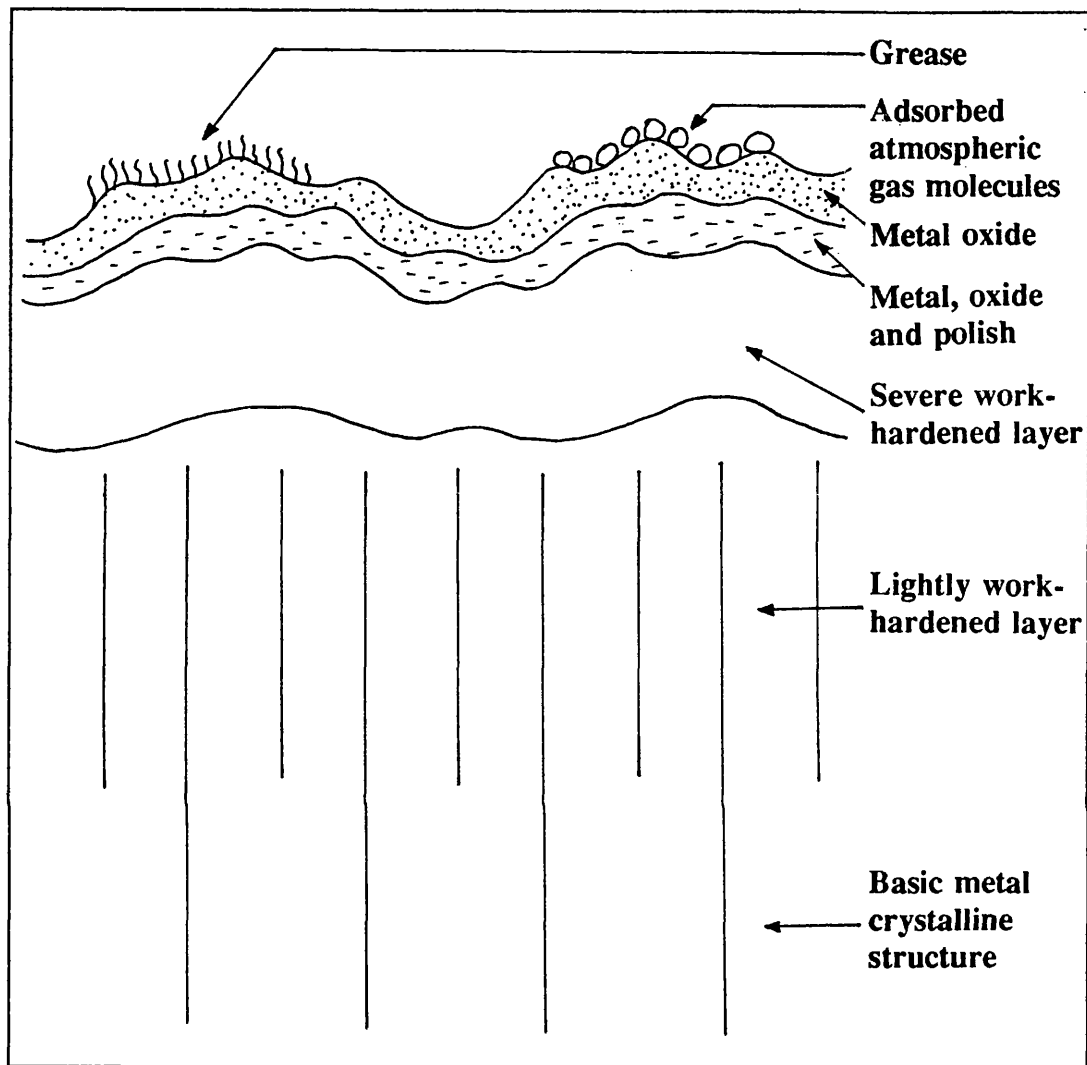


FIG. 1.3 Diagrammatic illustration of a typical 'clean' polished metal surface (adapted from Bowden & Tabor, 1950).

elastic stresses and, as a result, the true area of contact may not decrease appreciably with decreasing load. For adhesion studies, an accurate estimation of the total areas of true contact is therefore crucial, as it determines the magnitude of the adhesion force.

1.5.1 Measurement of Real Area of Contact

Owing to the experimental difficulties involved in directly determining the true area of contact, analytical models are developed in order to predict the approximate magnitude of the real contact area or to illustrate how it may vary with the normal load and contact topography. Archard (1953a) considered two extreme types of deformation, namely, purely plastic and purely elastic, of a surface covered with asperities of spherical shape. For completely plastic deformation, the area of contact is directly proportional to the load, W , whereas for completely elastic deformation, the area of contact of each asperity will be proportional $W^{2/3}$, in accordance with the Hertz's equation (*Hertz, 1881; Timoshenko & Goodier, 1951*).

With regard to elastic deformation, Archard considered two possible ways in which such deformation can take place. Firstly, if contact occurs over a fixed number of asperities, the effect of increasing the load is then simply to increase the elastic deformation of each asperity. In this case, the area of real contact is proportional to $W^{2/3}$. Secondly, if contact occurs over a large number of asperities, with the average area of each deformed asperity being constant, increasing the load in this case will then proportionately increase the number of regions of contact. Under this situation, the area of real contact is directly proportional to W .

The total contact area, A_r , was shown to relate to the load, W , by the following general equation form (*Archard, 1953b*):

$$A_r = K(W/E)^N \quad (1.4)$$

where E is the Young's modulus of the two similar surfaces in contact, K is a constant depending on the model used, and N , though its value also depends on the test model, generally lies between $\frac{2}{3}$ and unity. With real surfaces, there may be expected an intermediate behaviour. If the small asperities have even smaller asperities on them, the area of true contact will vary by a power of W still closer to unity. A general conclusion given is that, with multi-point contact, even elastic deformation can give an area of contact almost linearly proportional to the load.

By means of a statistical approach to the asperity heights and distributions, Fuller & Tabor (1975) extended the models of single asperity contacts to multiple asperity contacts.

Though difficult to perform in practice, experimental measurements of the true area of contact between solids are, nevertheless, attempted. Much of the information comes mainly from the studies of friction and wear, and reviews of some of the techniques used to examine real contact configurations are given by several workers (e.g. *Grunberg et al., 1961; D'Yachenko et al., 1964; Greenwood & Rowe, 1965; Woo & Thomas, 1979*). Electrical resistance measurements can be used if the region of contact is essentially metallic (*Bowden & Tabor, 1950; Gane et al., 1974*). This method provides a reasonable estimate of the true contact area established between two clean metal surfaces when the resistivities are known. Similarly, variations of the real area of contact could also be indicated qualitatively by changes in thermal conductance at the contacts (*Snaith et al., 1986*).

For elastic contacts, the contact configuration may be observed directly by loading a surface against a transparent glass optical flat (*Chestinov, 1954; Dyson & Hirst, 1954; Fuller & Tabor, 1975*) or against a prism (*Kragelskii & Demkin, 1960*). This optical method works on the principle of light reflection or transmission at the points of contact, and light scattering at the regions of no contact, and is suitable for use when one or both solids are transparent.

Permanent impressions result from plastic deformations of rough hard surfaces loaded against optically flat opaque surfaces (*O'Callaghan & Probert, 1970*) or when the asperities of soft rough surfaces are flattened permanently by pressing them against hard opaque optical flats (*Uppal & Probert, 1972; Uppal et al., 1972*); their dimensions can be measured directly after removal of the load.

Moreover, the arrays of micro-contacts may be quantified photometrically by, for examples, phase contrast microscopy (*Dyson & Hirst, 1954*) and Nomarski interferometry (*O'Callaghan & Probert, 1970; Uppal et al., 1972*), or by examining the deposits of paints, surface films or radioactive coatings disrupted or transferred from one surface to the other forming the contact (*Grunberg et al., 1961; D'Yachenko et al., 1964; Fujiwara, 1978*). Grunberg *et al.*, (1961) reported that freshly deformed surfaces are capable of emitting electrons which can be observed with highly sensitive Geiger counters. Cottrell (1978), on the other hand, measured the electrical charge densities developed across rubber-filled contacts. The chemical reactivity of certain deformed surfaces may also change with deformation.

Furthermore, estimation of the total plastically deformed asperities may be accomplished using a technique called three-dimensional relocation profilometry (*Williamson & Hunt, 1968; Edmonds et al., 1977; O'Callaghan & Probert, 1987*). Measurement would usually be carried out between various stages of loading of a hard flat surface against a softer rougher surface.

1.6 MECHANISMS OF ADHESION

1.6.1 Contact Interaction Forces

Once the real areas of contact between two solids have been established by deformation processes, the bonds that form at the interface, together with the area and mechanical properties, govern the adhesive strength. Attractions between two solid surfaces arise from the interatomic forces between atoms on the two surfaces, the

intensity of which will determine the resistance of the contact to breaking, i.e., a quantitative measure of adhesion.

The main components of the physical forces primarily important in the adhesive interaction of small particles to surfaces, in air, include molecular van der Waals forces, electrical forces comprising electrical double layers at the contact points and Coulombic interactions of the electrical charges distributed over the particle surface due to previous electrification, and capillary effects in the annular zone surrounding each side of contact between particle and substrate, from condensation of vapour present in the gas medium (*Krupp, 1967; Bhattacharya & Mittal, 1978; Deryaguin et al., 1978a; Khilani, 1988; Ranade et al., 1988*).

According to Zimon (1982), the above forces determining adhesive interaction can broadly be divided into two groups. The first group of forces determines the interaction of particles with a surface prior to direct contact of the two bodies; the magnitude of these forces drops off with increasing distance between the contiguous surfaces. Molecular forces and to some degree, Coulomb forces are examples of such forces. The second group of forces arises when the particles come into contact with a solid surface; without the actual contact, these forces could not exist. The forces concerned are the forces of interactions due to the electrical double layer in the contact zone, capillary forces as well as the disjoining action of the liquid layer between the contiguous solids.

1.6.1.1 Molecular van der Waals Forces

Van der Waals forces can be understood as follows. Even at absolute zero temperature, solids can contain local electric fields which originate from polarizations of the constituent atoms and molecules. According to quantum mechanics, the electrons of an electrically neutral solid cannot occupy fixed states of a sharply defined minimum energy. The changes in the electron positions result in spontaneous electric and magnetic polarizations, varying quickly with time (*Krupp, 1967*). The atoms of two bodies in close proximity can interact through their electric fields. Phase

correlation of the fluctuating electric fields reduces the energy of the system, which is thus the origin of van der Waals forces. Van der Waals forces include forces between molecules possessing dipoles and quadrupoles caused by the polarizations of the atoms and molecules in the material. This can include both natural as well as induced instantaneous dipoles and quadrupoles.

Of the several components to van der Waals forces, the one of greatest concern is the non-polar van der Waals forces, except in the case where the polarizability is small and the dipole moment is large. The non-polar van der Waals effect is completely general and operates whenever two molecules, ions or atoms are in close contact. It is the result of an interaction between the random motions of the electrons in the two species. Although non-polar molecules have zero permanent dipole moment over a period of time, because of the extremely rapid motion of the electrons resulting in a symmetrical distribution of electric charge, there will exist instantaneous dipole moments. In the case of facing bodies, this will occur within the dielectric medium in between. These instantaneous dipole moments will be influenced by the corresponding moments in neighbouring molecules and distributions, which correspond to an attractive potential. This potential will be favoured over that corresponding to repulsion, leading consequently to a net attractive potential between the molecules. The range of attractive interactions between two condensed bodies is approximately of the order of the size of a molecule, i.e., 0.2 to 1nm (*Visser, 1989*), and the maximum surface interval to be by order of magnitude of about 1000\AA (*Rumpf, 1977*).

The non-polar van der Waals forces are also referred to as London-van der Waals dispersion forces, because London associated these forces with the cause of optical dispersion, i.e., spontaneous polarizations (*London, 1937; Corn, 1966*). Van der Waals dispersion interactions are the basis for the theories of molecular interactions.

Since the dispersion interaction energy between two neutral atoms varies with the inverse sixth power of their mutual distance, London-van der Waals forces vanish very rapidly with increasing distance, and so will be very sensitive to surface roughness which tend to keep the particles apart. Historically, there are two theoretical

methods of deriving van der Waals attractive forces between solids; they are the microscopic and macroscopic approaches.

MICROSCOPIC THEORY OF VAN DER WAALS FORCES

The microscopic theory of Hamaker starts with considering the interaction of one molecule of one adherent with an arbitrary molecule of the other adherent. London dispersion effects are postulated to be additive, which means that if three molecules act simultaneously upon each other, the three interaction potentials between the three pairs can simply be added together, and any influence of a third molecule upon the interaction between the first two is only a small perturbation effect of a smaller order of magnitude than the interaction itself (*London, 1937*). Taking this assumption, Hamaker (1937) evaluated the van der Waals interactions between two adjacent macroscopic bodies by a summation of the pairwise molecular interaction energies over all molecule pairs of the adherents concerned. The result showed that van der Waals forces depend on the geometry of the adherents and a constant, A , called the Hamaker constant, which is characteristic of the materials involved, and is definable by order of magnitude only, being generally within the range 10^{-20} to 10^{-19} J.

Under certain circumstances, van der Waals forces are considered repulsive, in which case, the material constant, A , will become negative. A discussion of negative Hamaker constants is given by some researchers (e.g. *Visser, 1981; Neumann et al., 1984*).

For an idealized case of a spherical particle adhering to a semi-infinite surface (i.e., a smooth plane), the van der Waals forces of adhesion, F_{vdw} , at point contact, based on the microscopic approach, are given by the following formula (*Deryaguin et al., 1984; Leenaars, 1988*):

$$F_{vdw} = AR/6h_0^2 \quad (1.5)$$

where A is the Hamaker constant, R is the particle radius, and h_0 is the distance of closest approach between the facing layers of molecules, which is not zero because some adsorbed gas layers must be present on solid surfaces in air, and is typically assumed to be about 3-6Å. The summation procedure is also carried out for other geometries of the interacting bodies (*van den Tempel, 1972; Lodge, 1983; Hays, 1988; Visser, 1989*), and the results of the derivations for the limiting case where the interaction distance (h) between the undeformed adherents is very small compared to the other dimensions of the system, are summarized in Table 1.1. These geometrical configurations considered all have a simple shape and orientation.

An investigation by Vold (1954) on cubes of edge-length, D , whose edges are parallel showed that the van der Waals energy, V_{vdw} , between two oriented cubes, if the line connecting the centres is perpendicular to the opposing faces, is as follows:

$$V_{vdw} = AD^2/12\pi h^2 \quad (1.6)$$

For anisometric particles, further studies of several typical cases by Vold (1954) indicated the magnitude of the interaction can generally be considered intermediate between that for spheres and cubes. The order of attractive energies is found to be: plates > rectangular rods > cylinders > spheres. Van den Tempel (1961) then arbitrarily suggested that, an average value of the interactions may be obtained by considering the attraction as intermediate between that for spheres and for well-oriented cubes. Based on this postulation, van den Tempel proposed an equation for the average interaction energy, as:

$$V_{vdw} = AD_0^{1.5}/12h^{1.5} \quad (1.7)$$

where D_0 is the equivalent particle diameter. The derived van der Waals attractive force between consecutive particles in a chain, in absolute value, is then equal to:

TABLE 1.1 London-van der Waals interactions at small separation, h , for some geometrical contact models, from the microscopic Hamaker theory.

Geometrical system	Force, F_{vdw}	Energy, V_{vdw}
2 semi-infinite parallel planes, per unit area	$\frac{A}{6\pi h^3}$	$\frac{A}{12\pi h^2}$
Sphere/semi-infinite plane	$\frac{AR}{6h^2}$	$\frac{AR}{6h}$
2 spheres	$\frac{AR}{12h^2}$	$\frac{AR}{12h}$

$$F_{vdw} = AD_0^{1.5}/8h^{2.5} \quad (1.8)$$

Surface deformation can result in an increased contact area. In the absence of the 'long-range' forces such as electrical double layer interactions, the enhanced London-van der Waals forces, F'_{vdw} , may be described by the following formula (*van den Tempel, 1972*):

$$F'_{vdw} = \frac{AR}{6h^2} \left(1 + \frac{A}{6\pi h^3 H} \right) \quad (1.9)$$

where H is the micro-hardness of the softer of the two bodies.

As can be seen from the above equations, London-van der Waals forces between two adherents are dependent on the distance between the solids. Owing to the electromagnetic nature of the dispersion interactions, as the separation distance is increased, the propagation of the interaction will take a finite time, resulting in a different separation-dependence of the force of attraction. The London forces are then said to be 'retarded', and will be smaller at a given separation because of a phase difference between the electronic oscillations of the interacting molecules than if they had remained 'non-retarded' (*Gregory, 1969, 1981; Visser, 1972; Lodge, 1983*). The mutual distance at which such change in the dependence of the attractive interactions on separation distance occurs, was shown experimentally by Tabor & Winterton (1968) to be between about 100 and 200Å. For a particle adhering to a smooth hard plane, the 'non-retarded' attractive forces are given by Equation (1.5) above, whereas for the 'retarded' van der Waals forces, F_r , they are given by (*Tabor, 1977*):

$$F_r = 2\pi BR/3h^3 \quad (1.10)$$

where B is the 'retarded' Hamaker constant.

Since the Hamaker constant depends on the number of molecules per unit of volume of matter, in the case of anisotropic solids, this material property will therefore vary with the crystal plane under observation. Consequently, Hamaker constants will be different for different crystal planes in anisotropic crystals, which would lead to variations in the London dispersion forces at different contact regions on the crystal face. The influence of anisotropy on the Hamaker constant was demonstrated experimentally (*Good et al., 1971*) by the anisotropy of contact angles on oriented polymers. Direct determination of Hamaker coefficients can, however, be carried out by direct measurement of the adhesion force (*Gregory, 1969*). Alternatively, the material constant can be derived from, for instance, colloid chemistry experiments (*Visser, 1972*), surface and interfacial tension measurements (*van Oss et al., 1986*) and rheological data (*Visser, 1972*).

MACROSCOPIC THEORY OF VAN DER WAALS FORCES

To avoid the assumption of additivity made in the determination of the material (Hamaker) constant, a physically more satisfactory approach was later developed by Lifshitz (1956), which can give a more accurate evaluation of the Hamaker coefficient. It is called the macroscopic approach, and is based on quantum electrodynamics and statistical physics. This continuum theory of Lifshitz treats the interacting condensed bodies and the phase which separates them as continuous media, and involves only bulk material properties, namely, the optical properties of the materials, over the complete electromagnetic spectrum. The resulting attractive interactions are expressed as an electromagnetic radiation in wavelengths characteristic of the material pairing, allowing for electromagnetic lag.

The principle of the macroscopic Lifshitz approach to van der Waals forces is that, a particle ‘sees’ another particle only through the fluctuating electromagnetic field originating from the rapidly rotating atomic dipoles. This dispersion interaction is, in turn, completely determined by the interaction of this fluctuating electromagnetic field with the atomic dipoles in each particle. The fluctuating electromagnetic field, and its interaction with any other condensed material, can be measured directly by recording the amount of light reflected from the surface of the material body, over the entire

range of frequencies from zero to infinity. However, the quantity that determines the interaction is the amount of electromagnetic energy absorbed at each frequency. For most systems, contributions from the far ultraviolet region of the spectrum are the most important. This is because retardation of lower frequency carries not much energy, whereas the very high frequencies are not readily absorbed by most materials. Some further details of the macroscopic approach is given in a discussion by Hough & White (1980).

The resulting expression for the London-van der Waals forces is a function of a decisive material value known as the Lifshitz-van der Waals constant, $\hbar\bar{\omega}$, which can be defined as an integral of functions of the imaginary dielectric constants above the frequency. It is independent of geometry and can be computed from known or measurable continuum material values. The Lifshitz constant of the van der Waals interaction is of the order between 0.1 and 10eV (*Rumpf, 1977*), and for two real materials, generally ranges from about 0.6 to 9eV (*Krupp, 1967*). Qualitatively, since the Lifshitz-van der Waals constant is related to the optical absorptivity of a body, materials with strong optical absorption will have strong spontaneous fields, and thus will be bound by greater forces of adhesion due to van der Waals interactions.

Under certain conditions and depending on materials combination, the Lifshitz constant, $\hbar\bar{\omega}$, can be related to the Hamaker constant, A , by the following equation (*Krupp, 1967; Visser, 1972; Rumpf, 1977; Zimon, 1982*):

$$\hbar\bar{\omega} = 4\pi A/3 \quad (1.11)$$

The approximate equivalent London-van der Waals equations, based on the macroscopic approach, for several geometrical contact systems, are listed in Table 1.2. All these equations, however, apply only to non-deformable solids. Should deformations occur at the contact point under the effect of attraction force, the van der Waals forces would be increased by the increased contact area. The additional van der

TABLE 1.2 London-van der Waals interactions at small separation, h , for some geometrical contact models, from the macroscopic Lifshitz theory.

Geometrical system	Force, F_{vdw}	Energy, V_{vdw}
2 semi-infinite parallel planes, per unit area	$\frac{\hbar \bar{\omega}}{8\pi^2 h^3}$	$\frac{\hbar \bar{\omega}}{16\pi^2 h^2}$
Sphere/semi-infinite plane	$\frac{\hbar \bar{\omega} R}{8\pi h^2}$	$\frac{\hbar \bar{\omega} R}{8\pi h}$
2 spheres	$\frac{\hbar \bar{\omega} R}{16\pi h^2}$	$\frac{\hbar \bar{\omega} R}{16\pi h}$

Waals forces, F_{def} , due to this deformation may be given as follows (*Osborne-Lee, 1988*):

$$F_{def} = \hbar\bar{\omega}p/8\pi h^3 \quad (1.12)$$

where p is the radius of the adhesive surface area. For a solid semi-infinite half-space and a sphere contact system, assuming only the sphere undergoes deformation and on the basis of the Lifshitz theory, the overall van der Waals forces of adhesion, F'_{vdw} , may be obtained by transforming Equation (1.9) to give the following expression:

$$F'_{vdw} = \frac{\hbar\bar{\omega}R}{8\pi h^2} \left(1 + \frac{\hbar\bar{\omega}}{8\pi^2 h^3 H} \right) \quad (1.13)$$

For materials with hardness, H , above 10^7Nm^{-2} , the second term in brackets could be neglected (*Massimilla & Donsi, 1976*).

The Hamaker approach is limited to non-absorbing materials, which therefore precludes its application to metals. In contrast, the Lifshitz theory is applicable to all materials. Since in the derivation of the van der Waals material constant, the assumptions made in the macroscopic approach are only minor, the Lifshitz-van der Waals constant can be regarded as more correct (*Visser, 1972*), provided that all the optical data over the whole electromagnetic spectrum of the material in question, which are required for its evaluation, are available. Owing to lack of sufficient necessary optical information, the Lifshitz constant is known only for a restricted number of materials (*van den Tempel, 1972; Visser, 1972; Parsegian & Weiss, 1981*). Nevertheless, it receives sound experimental substantiation from direct measurement of van der Waals forces (*Deryaguin et al., 1988*).

Despite a number of shortcomings, e.g., the problem of attenuation by media, and linear non-additivity of the dispersion effect because the Hamaker theory does not

consider cross-correlation of charge (*Krupp, 1967*), the microscopic approach is still quite widely used, mainly because explicit functions in the theory may be derived containing parameters to which values can be fairly readily ascribed (*Vincent, 1973*). Moreover, in the limiting cases where the two approaches may be compared, their agreement is reasonably acceptable and for many practical systems, the results are comparable (*Gregory, 1969*).

1.6.1.2 Electrical Forces of Adhesion

In addition to the van der Waals forces, forces of electrical origin can also contribute substantially to the adhesion of particles to a plane surface. They are composed of two types of forces, the electrical double layer forces at the contact sites and Coulomb forces. The range of these forces is larger than that of the van der Waals forces by a few decimal orders of magnitude (*Krupp, 1967*). On the other hand, the strength of these attractive forces decreases as a function of time rather than distance, provided that there is no appreciable neutralization of the charges during the separation process. In this respect, the electrical forces differ radically from the molecular forces. As electrostatic forces are dependent on the physical nature of a solid, they would be adversely affected by, for instance, surface roughness as edges and corners tend to assist discharge from the particles.

An important electrical force for small particles is electrostatic contact potential induced electrical double layer forces. Two essentially unlike materials, when in contact, will develop a contact potential due to differences in the local energy states and electron work functions. Electrons will be transferred from one solid to another until an equilibrium is reached, where the current flow in both directions is equal. The resulting potential difference is called a contact potential difference, U . It sets up a double layer charge region which has a high surface charge density, and thereby creating the electrostatic attraction force. For a spherical particle adhering to a plane surface, this electrostatic double layer force of attraction, F_w , can be calculated by the following equation (*Visser, 1972; Bowling, 1988*):

$$F_w = \pi \epsilon_0 R U^2 / z \quad (1.14)$$

where ϵ_0 is the permittivity of vacuum, R is the particle radius, and z is the atomic separation distance.

Coulomb forces (or electrostatic image forces) are electrical forces due to charges of particles. They are governed by interaction of charged particles with a surface when there is a definite gap between the contiguous bodies. These forces are manifested at the initial moment of particles contact with the surface, on the condition that the particles are pre-charged. Alternatively, bulk excess charges on the particles may be acquired by triboelectrification. The charged particle then induces equal and opposite charges on the counterpart surface, and as a result, image forces are established. Under this condition, Coulomb forces are greater than the molecular van der Waals forces as well as the electrostatic forces arising from contact potential difference, and in such instance, the Coulomb forces will determine the particle adhesion.

If, however, the particle material or that of the contact zone is conductive, or if moisture is present, charges will tend to leak off, thereupon, reducing the electrostatic forces and hence, reducing adhesion. The electrostatic image force, F_{im} , for a spherical dielectric particle in contact with a conducting surface is (*Overbeek, 1984; Bowling, 1988; Hays, 1988*):

$$F_{im} = \alpha_d Q^2 / 4\pi \epsilon \epsilon_0 h^2 \quad (1.15)$$

where Q is the charge, α_d is a coefficient that depends on the dielectric constant and uniformity of the surface charge density (and for a uniformly charged sphere in contact with a substrate, α_d is equal to 1 for dielectric constant of 1), ϵ_0 is the permittivity of free space, ϵ is the dielectric constant of the medium between the particle and surface, and h is the distance between the charge centres.

1.6.1.3 Capillary Forces

The adhesion of solid particles on a plane surface can be substantially controlled by atmospheric moisture (*Hiestand, 1972; Massimilla & Donsi, 1976*). Small amount of moisture in air may adsorb on the solid surface and affect the surface energy of the materials concerned. Furthermore, moisture may provide sufficient surface conductivity to reduce the electrostatic charge accumulation to a low level, thereby decreasing the electrostatic component of the forces of attraction. If the air relative humidity is high, for example, close to 100%, condensation of water vapour will take place in the gap at each site of contact between the adhering particles and substrate surface due to closeness of the body surfaces near those regions, thus forming a liquid bridge or meniscus.

If a liquid of low viscosity forms a bridge between two particles, the force, F_B , acting between them consists of two components, the surface tension force, F_R , and a force, F_P , due to the difference of the pressure outside and inside the bridge:

$$F_B = F_R + F_P \quad (1.16)$$

While the surface tension force always brings about an attraction, the capillary pressure, P_K , expressed by (*Schubert, 1984*):

$$P_K = \sigma_l (1/C_1 + 1/C_2) \quad (1.17)$$

where σ_l is the surface tension of the liquid, and C_1, C_2 are the radii of curvature of the liquid surface, can only contribute a positive component to the adhesion force if it produces a pressure deficiency within the bridge. For spheres of equal size, the adhesion, F_B , is given in the following functional expression (*Schubert, 1984*):

$$F_B = d\sigma_l f(\alpha_1, \theta_c, a_l/d) \quad (1.18)$$

where d is the sphere diameter, α_1 is the bridge angle, θ_c is the contact angle, and a_l is the liquid film thickness. The adhesion forces between equal spheres, unequal spheres, and for other two-particle geometries are also reported, both on the basis of a circular approximation and for an exact liquid-profile description of the bridge (Gillespie & Settineri, 1967; Princen, 1969; Hotta *et al.*, 1974; Mehrotra & Sastry, 1980).

For particulate media, different states are described for the presence of water on solids (Massimilla & Donsi, 1976). Coelho & Harnby (1978) showed that the form of water retention in a powder is a function of the nature of the solid (i.e., hydrophilic or hydrophobic), the relative water vapour pressure in the ambient medium, temperature and pressure. A more in-depth treatment of capillary forces and their influence on the behaviour of solid particles is given in a review paper by Schubert (1984).

In the case of a particle-substrate system, similar factors above will also govern the phenomenon of liquid bridge formation. In addition, the extent of the meniscus will also be dependent upon the geometry of the gap between the contacting bodies, as well as the properties of the solid-liquid system under consideration, i.e., contact angle and surface tension of the liquid. The critical humidity level at which moisture condensation can affect adhesion was found to be in excess of 60% by Hiestand (1966), at 65-80% by Turner & Balasubramanian (1974) and exceeding 60-70% by Zimon (1982).

When a liquid film is formed between a particle and the substrate surface, the force of particle adhesion is attributed entirely to the capillary forces (Larsen, 1958; Kordecki & Orr, 1960; Zimon, 1982). For a spherical particle adhering on a plane surface, the capillary force, F_c , can be expressed as follows (Massimilla & Donsi, 1976; Bardina, 1988):

$$F_c = 4\pi c_l R \gamma_l \quad (1.19)$$

where R is the particle radius, γ_l is the surface tension of the liquid, and c_l is a shape factor of the liquid bridge. On the other hand, for hard materials and clean surfaces in air, Hinds (1982) postulated an empirical equation to relate the level of humidity with the adhesion force, F'_c (in dynes):

$$F'_c = d \left[75 + 0.65(\%RH) \right] \quad (1.20)$$

where $\%RH$ is the percentage relative humidity and d is the particle diameter (in cm).

1.6.2 Relative Contributions of the Different Components of Adhesive Forces

For a dry particle-substrate adhesive system in air, with ambient humidity below the critical humidity level, van der Waals forces and electrical double layer forces are generally considered to be the prevailing force components affecting small particle adhesion.

A greater importance of the electrical component is claimed for weakly adhering particles. This is explained by Zimon (1982) who suggested that, since these particles are located on the peaks of a rough substrate surface, and therefore the contact area established will be at a minimum for such particles, though both the electrical and molecular forces of adhesion decrease with increasing distance between the contacting bodies, the molecular force decreases more rapidly than the electrical forces, due to the former having a shorter range of action. In this particular case, adhesion is determined mainly by the electrical component.

Deryaguin *et al.* (1976, 1977b) suggested that, the contact of elastic kind between small particles and a solid substrate determines the prevalent role of the

electrostatic double layer forces in the detachment process. The London forces are overcome on various areas of the contact zone during the elastic recovery process, not all at once, but consecutively, diminishing the role of the molecular component. Then, the adhesion component conditioned by the double electric layer is determined, due to the long-range action of the electrostatic forces, by the maximum value of the initial contact area, and is retained as the latter decreases during elastic recovery in the tearing-off process, provided that no appreciable neutralization of the double layer charges occurs (*Deryaguin et al., 1984*). In view of this, a greater contribution of the electrostatic component to the adhesion would be expected for the case of breaking the contact of two parallel planes, as compared with that of breaking a sphere-plane contact. The reason is that, in the former case, the electrostatic component remains virtually constant until a gas discharge starts, whereas in the latter instance, the interaction forces of the electric double layer charges, concentrated on small areas, rapidly decrease in accordance with Coulomb's law (*Deryaguin et al., 1977b*).

Comparisons between the molecular and electric double layer force components making up adhesion, were made by some investigators (*Aleinikova et al., 1968; Deryaguin et al., 1968/69, 1984*) for certain systems. A review of some methods used for such differentiation is given by Zimon (1982). Basically, these comparisons revealed that the electrical forces can contribute appreciably to adhesion on certain occasions; in other instances, these forces are commensurate with the molecular forces.

Charged particles and/or charged substrate surface would add an additional electrostatic image force to the molecular forces. A view expressed by Krupp (1967) is that, a surface charge which does not owe its origin to the existence of a contact potential between the adherents, but has been additionally imposed (and thus, is not in equilibrium and leaks off in finite time), will normally not contribute significantly to the adhesive force. This is because its effect will usually be much smaller than that due to equilibrium charges which owe their existence to a relatively not small contact potential difference between the partners of the interaction. Consider also that real particles or surfaces inevitably carry adsorbed films of different substances, the latter would impart some degree of surface conductance to the materials. Zimon (1982)

similarly suggested that, although the adsorbed 'contaminated' layers do not have any great effect on the electrical forces created at the expense of the double-layer charge, if the surface is made conductive enough, a decrease in Coulomb interactions as time elapses could be expected.

Wet systems can have an additional capillary force acting to hold the particles from detachment. Apparently, even at the critical humidity level, the effect of capillary forces does not act immediately, but appear to proceed with time. Zimon (1963) observed that, for the contact of 80-100 μ m glass particles with a quartz glass substrate in air at relative humidity near 100%, the increase in adhesive force took about 30 minutes to complete. Thus, it seems that the effect of capillary condensation will not be manifested fully immediately after an adhesional contact has taken place, if the experimentation time period is comparatively short and the material concerned is not hydrophilic.

It can therefore be seen that, the adhesive interaction between a particle and a substrate surface can be a complicated mixture of several types of the fundamental physical forces, which can act concurrently or successively to varying degrees. Under real conditions, the particular combination of these force components governing the adhesion and their relative contributions may be quite different from one case to another. This may be considered as a factor for the disagreement or poor reproducibility of some adhesion results obtained by different investigators under different experimental conditions, even though the adhesive system used may apparently be identical. On the other hand, there is as yet no evidence of the direct additivity of these different force components making up the overall adhesion.

1.6.3 Other Reactions at the Particle-Substrate Interface

There are certain processes according to which significant interface growth and strong bonding between different adherents may occur, mechanisms other than the van der Waals and electrostatic forces. These include sintering, diffusive mixing, mutual dissolution, and dissolution and alloying. Conceptually, these various effects cannot

strictly be separated, though these different concepts are often applied separately in different fields. Sintering between two solids is generally defined as a growth of their common adhesive area, usually by one and/or the other of the following mechanisms, re-crystallization, evaporation and recondensation, surface or bulk diffusion, and creep (*Goetzel, 1950*). It is not unusual that special conditions such as high temperatures are required for the above effects to occur (*Jones, 1960; Lontz, 1964; Jayasinghe & Pilpel, 1970; Shapiro, 1983*). Investigations on the mutual diffusion of solid polymer materials into each other were carried out by *Voyutskii (1963)*.

Particle-substrate adhesion may also arise from contributions of very short-range interactions, which consist of chemical bonds of all types as well as intermediate bonds such as hydrogen bondings (*Krupp, 1967*). This group of forces, however, can add to adhesion only after the establishment of an adhesion contact area. Owing to the surfaces of real adherents are ordinarily chemically saturated, chemical bond formation across an adhesive interface will be rather improbable under ambient conditions (*Krupp, 1967*).

1.7 INFLUENCE OF SOLID SURFACE CONDITION ON ADHESION

The surface condition of a solid referred to is the cleanliness of the adherent surface, i.e., the presence or absence of foreign substances on the surface, such as surface active materials, grease, moisture, etc. These surface-adsorbed layers of different substances can grossly affect adhesive interactions. Some authors make no mention of the methods adopted for cleaning surfaces and particles before tests. It is suggested by *Zimon (1982)* that this is one reason why greatly different results were sometimes reported for measured forces of adhesion, even for contacts between identical materials, if measurements are treated on an individual basis.

The state of surface cleanliness is determined, on the whole, by the quality of surface cleaning. Various methods of surface cleaning are reported in the literature. For example, mica, aluminium, Plexiglas and brass could be cleaned by washing with alcohol, then distilled water and finally dried at 100°C (*Kordecki & Orr, 1960*). Corn

(1961) suggested using chromic acid, demineralized water and acetone in that sequence, for cleaning quartz, Pyrex and platinum. Steel can be treated with purified benzene, distilled water, activated charcoal and ethyl alcohol to remove grease and surface active matter (*Deryaguin & Zimon, 1961*). Glass surface may be cleaned with chromic acid mixture and then water; other recommendations include the use of distilled water and acetone (*Zimon & Volkova, 1965*). If a particular thorough treatment of a surface is required, depending on the material, the last stage of cleaning can involve a flame, in which case, any residual organic impurities will be burned off.

1.8 KINETICS OF PARTICLE-SUBSTRATE ADHESION

Real surfaces, with the exception of field ion tips in field ion microscope experiments (*Buckley et al., 1986*) and some freshly cleaved materials such mica sheets (*Richmond & Ninham, 1972; Luckham, 1989*), are not smooth and flat. This is particularly so for pharmaceutical materials, where crystals of many drugs and excipients are of various shapes, neither smooth nor regular, and usually possess sharp corners and edges. These inevitably complicate any analysis of stress or strain of an adhesion contact.

The various complexities can, however, be minimized and the kinetics of particle-substrate adhesion be more easily modelled and understood, if a geometrically particularly simple adhesive system is considered, namely that between a small solid particle and the surface of a solid plane. Its simplicity stems from the fact that, the particle may be approximated by a perfect sphere and that, ideally, the plane substrate may be represented by half-space (*Krupp, 1967*). In other words, at least at and in the immediate vicinity of the sphere-plane interface, the area can be assumed to be very smooth. Hence, the adhesive system under consideration presents rotational symmetry around an axis which is parallel to the surface normal to the substrate, and passes through the centre of the sphere. This geometry can further simplify the analysis of the stress-strain field established during an adhesion.

When a sphere approaches a half-space from a large distance, assuming that the latter is comparatively hard and rigid, at a finite distance of separation, the long-range forces of attraction, such as van der Waals and electrostatic forces lead to deformation of the sphere, the extent of which increases with decreasing distance. In this phase, the effect of gravity may generally be neglected for particles of small size. Upon contact, the sphere and the smooth plane will initially touch at one point, the area of which is of atomic dimension. Owing to the long-range attraction forces, the sphere will generally subject to a moment of forces so that several contacts are established, which is particularly so for a non-perfectly smooth particle. In the latter case, the contacting surface asperities will be flattened by the interaction forces. Then, the contact area increases until the attractive forces between the two adherents are balanced by the repulsive forces resisting the further deformation at their interface. A frictionless, adhesive area of finite size is thus formed, where the deformed surfaces of the contiguous bodies are parallel to each other.

If a perfectly smooth sphere is brought into an elastic contact with a smooth hard plane, the stresses between the contiguous solids can be analysed by means of the Hertz's theory for elastic deformation (*Timoshenko & Goodier, 1951*).

1.8.1 Hertz's Theory of Elastic Contact

The Hertz's theory is used by different theorists (e.g. physicists, engineers and material scientists) as a tool for predicting the area of contact and stresses between elastic bodies pressed together.

Basically, for a sphere that is in a state of adhesional equilibrium on a hard plane surface, the contact zone can be represented by a circle (with radius, a). Within this zone, the dependence of the local normal pressure, $P(\xi)$, on the distance, ξ , to the axis of symmetry, under the effect of a compressive (Hertz) force, F_H , can be described by the Hertz's equation for elastic deformation:

$$P(\xi) = \frac{3F_H}{2\pi a^2} \left(1 - \frac{\xi^2}{a^2} \right)^{1/2} \quad (1.21)$$

When no surface forces act, the force F_H is related to the size of the contact zone, a , by:

$$a^3 = RF_H/K_e \quad (1.22)$$

where R is the sphere radius and $K_e = 4E/3(1-\nu^2)$, of which E is the Young's modulus of the sphere and ν is the Poisson's coefficient. Alternatively, Equation (1.22) is also commonly expressed in the following way:

$$F_H = \frac{4Ea^3}{3(1-\nu^2)R} \quad (1.23)$$

Resulting from local compression near to the contact region, the shift, α , of the centre of the sphere toward the rigid plane (i.e., the distance of approach or the amount of deformation) is related to the radius of the sphere, R , by the following relationship:

$$\alpha^3 = F_H^2/K_e^2R \quad (1.24)$$

By combining Equations (1.22) and (1.24), a simplified formula is obtained:

$$a^2 = \alpha R \quad (1.25)$$

Hence, the contact area, S_c , can be determined from the following expression:

$$S_c = \pi a^2 = \pi \alpha R \quad (1.26)$$

According to the Hertz's theory, in which surface attractive forces are not taken into account, for two bodies in elastic contact under zero normal load, both S_c and a will therefore be equal to zero, since there is no deformation of the contacting materials at the contact zone.

Many real surfaces, though, are never smooth as Hertz assumes. When two rough surfaces are pressed into contact, they touch at the tips of their surface irregularities so that the real area of contact is only a fraction of the nominal contact. In the case of elastic spheres, true contact is thus not made continuously over the circular area envisaged by Hertz, but through an archipelago of small discrete 'islands' roughly clustered within a circular region. As a consequence, the true contact pressure is also discontinuous, which will be very high within the 'islands' of real contact, but falling to zero in between. However, if the scale of the surface asperities is small compared with the bulk scale of the bodies themselves, so that it may be perceived that there are a very large number of 'islands' of real contact, the discontinuous pressure distribution may be conceived as being 'smoothed out' into a continuous one (*Johnson, 1958*).

1.8.2 Particle Roughness on an Elastic Contact

A detailed theoretical analysis of the influence of surface roughness on the adhesion of elastic solids was carried out by Fuller & Tabor (1975). The rough surface is modelled by asperities all of the same radius of curvature and with heights following a Gaussian distribution of standard deviation, σ . Based on the contact model suggested by Johnson *et al.* (1971), which will be discussed in the following Section 1.9.2, the result of the analysis predicts that, the adhesion, expressed as a fraction of the maximum value, is dependent upon a single dimensionless parameter, $1/\Delta_c$. It is defined as the ratio of σ to the elastic displacement, δ_c , that the tip of an asperity can sustain before it breaks off from the other surface, and is expressed as follows:

$$\frac{1}{\Delta_c} = \frac{\sigma}{\delta_c} = 3\sigma \left(\frac{2K_e}{9\pi\beta^{1/2}\delta\gamma} \right)^{2/3} \quad (1.27)$$

where β is the radius of curvature of the asperity tips, K_e is the elastic properties of the solid concerned, and $\delta\gamma$ is the net change in surface energy per unit area on the formation of an adhesive contact. For a soft rubber of Young's modulus, E , and Poisson's ratio 0.5, in contact with a rigid plane surface, the above equation assumes the following form:

$$\frac{1}{\Delta_c} = \frac{4\sigma}{3} \left(\frac{4E}{3\pi\beta^{1/2}\delta\gamma} \right)^{2/3} \quad (1.28)$$

Since $1/\Delta_c$ is dimensionless, by raising Equation (1.28) to the power of 3/2 and omitting any numerical terms, Fuller & Tabor (1975) came up with a modified adhesion parameter, θ , given by:

$$\theta = \frac{E\sigma^{3/2}\beta^{1/2}}{\beta\delta\gamma} \quad (1.29)$$

The denominator gives a measure of the adhesive force experienced by the rubber sphere, whereas the numerator is a measure of the elastic force needed to push the sphere to a depth, σ , into an elastic solid of modulus E . The physical meaning for this is that, the adhesion parameter $1/\Delta_c$ may be regarded as representing the statistical average of a competition between the compressive forces exerted by the higher asperities which are trying to separate the surfaces and the adhesive forces between the lower asperities which are trying to hold the surfaces together. When the adhesion parameter is small, the adhesive factor dominates and the adhesion is high. As the surface roughness and hence the adhesion parameter increases, the higher asperities will prise the contacting surfaces apart and, as a result, the true contact area will

reduce and adhesion falls to a very low value. Satisfactory experimental agreement with this analytical model was given later by Briggs & Briscoe (1976).

Czarnecki & Dabros (1980) employed the method of integration of the pairwise interactions of molecules to estimate the influence of surface roughness (of isotropic distribution) of a globular particle on the energy of its attraction to a plane. A statistical analysis of surface asperities is first carried out, which yields a radial mass distribution function, from which the attraction energy in a rough sphere/half-space system is calculated. The results obtained by this means, for various particle sizes, thicknesses of the rough layer and separation values are then compared with the adhesion energies evaluated for smooth spheres of the same size and at the same separation. A correction factor, C_r , was then derived to account for the attenuation of the van der Waals attraction energy due to the roughness of the particle surface. It is given as:

$$C_r = 1 + 0.5b/H_d \quad (1.30)$$

where b is the thickness of the rough shell of the particle, and H_d is the separation distance between the particle and the plane surface. This model, however, does not take into account any contact deformations.

Later, Sparnaay (1983) showed that surface roughnesses begin to exert its influence when its height exceeds 10 to 20% of the distance between the surfaces.

After contact is made between a particle and a plane, local surface deformations can lead to an increase in the adhesion force and energy (*Krupp, 1967*). Experimental data on particle adhesion to a rough surface (*van den Tempel, 1972; van Blokland & Overbeek, 1979*) suggests that the attenuation of adhesion energy due to surface roughness is considerably greater than its increase caused by local surface deformations. Nevertheless, the lack of any information on the micro-mechanical

properties of many materials means that an exact theory of local material creeping and its influence on the van der Waals energy is still not formulated.

1.9 KINETICS OF PARTICLE DETACHMENT FROM A PLANE SURFACE

It is known that clean, smooth surfaces when lightly pressed into intimate contact may adhere strongly together because of surface molecular attraction forces (*Bowden & Tabor, 1964*). In this particular circumstance, a finite area of elastic contact will be established though at zero applied load, and a certain force is required to separate the surfaces, as opposed to the Hertz's theory (in Section 1.8.1). Various steps in the development of a theory of breaking an elastic contact of particles adhering to a plane surface while taking into consideration surface forces, are reflected mainly in the work carried out by Deryaguin and his associates, as well as in those of Johnson and his colleagues.

1.9.1 The Thermodynamic Force and Energy Approaches

The primary aim of the force approach is to determine the influence of the geometric shape of the surfaces near the contact zone on the force of adhesion, taking into account both contact and non-contact forces. Molecular forces are considered to be the sole forces causing adhesion. The basic premises of the force method is that, adhesion at convex contact takes place under the influence of surface forces, which can be regarded as a reversible process in thermodynamic equilibrium, provided that the radii of curvature of both surfaces are considerably greater than the radius of action of the surface forces. In this approach, an elastic sphere is assumed to deform according to the Hertzian equations for the elastic deformation of spherical surfaces, and that such deformation will not be modified by the molecular attraction forces (*Deryaguin et al., 1975c*). Non-elastic deformation is not considered.

In the absence of external applied forces, the equilibrium contact deformation is due to the joint effect of molecular attraction forces and elastic repulsion forces. There are two components of the force of molecular attraction, F_m , acting, namely, the

component, F'_m , which acts inside the contact area and the other component, F''_m , which acts in the annular zone outside. Attraction between the contacting surfaces is provided by the molecular force component acting outside the contact zone, since the molecular attraction force within the contact zone enters into an elastic reaction. If an external load is now applied, the area of contact will increase. Owing to the presence of surface forces, the circle of contact is larger than that predicted by the Hertz's theory. Since all the deformations due to this applied force are reversible, the contact area returns to its finite equilibrium value on removal of the load.

The elastic repulsion force, F_{el} , arising as a result of deformation can be derived from the Hertz's theory (*Landau & Lifshitz, 1975*), and is given as follows:

$$F_{el} = \frac{4R^{1/2}E\alpha^{3/2}}{3(1-\nu^2)} \quad (1.31)$$

where R is the sphere radius, E is the Young's modulus of the sphere material; the plane (or half-space) is assumed absolutely hard, ν is the Poisson's coefficient and α is a measure of deformation. With regard only to the molecular attraction forces, analytical calculations (*Deryaguin et al., 1975a, b; Muller & Yushchenko, 1980*) show that the component, F'_m , practically does not depend on deformation. Also, due to the width of the annular zone surrounding the contact area will decrease in the radial direction as the degree of flattening is increased (*Deryaguin et al., 1975b*), when the deformation, α , becomes greater than the equilibrium distance of contact, h_0 (about $3-6\text{ \AA}$ (*Muller et al., 1980*)), F''_m could be neglected. The results yield that, the molecular attraction forces, F_m , may then be regarded as constant and at this stage, is equal to:

$$F_m = AR/12h_0^2 \quad (1.32)$$

where A is the 'non-retarded' Hamaker constant. When no external force is applied, adhesional equilibrium can be determined from the condition of equality of Equation

(1.31) to Equation (1.32). From this, α can be evaluated, which when substituted into Equation (1.26), the finite equilibrium contact area can be obtained.

The existence of a finite area of contact between a sphere and plane under purely the effect of surface molecular forces implies that, a finite force is required to achieve separation of the contacting surfaces. Upon application of this pull-off force, the circle of contact diminishes whilst the annular region surrounding the contact zone becomes correspondingly larger. With increasing pull-off force, it is shown (*Deryaguin et al., 1975a, b; Muller et al., 1980*) that, at point contact (i.e., zero deformation),

$$F'_m = F''_m = AR/12h_0^2 \quad (1.33)$$

The total molecular attraction force, F_m , is now equal to (*Deryaguin et al., 1975c, 1977; Muller et al., 1983a*):

$$F_m = F'_m + F''_m = AR/6h_0^2 \quad (1.34)$$

Thus, the pull-off force reaches its maximum absolute value at this stage when simultaneously, the elastic repulsion force, F_e , is zero. This may be regarded as a measure of the strength of adhesion of an elastic sphere to a plane surface.

The contact phenomenon above illustrates that, a reversible decrease in the contact of deformation occurs in the process of breaking an elastic contact, the deformation having been set up by the molecular forces in the annular region outside the contact area. Moreover, elastic contact deformations, with or without preliminary pressing of a sphere to a hard surface, cannot increase the effective molecular component of the force of adhesion. Owing to the elastic reaction with deformation, the force of adhesion due to the action of surface forces is at maximal, with point contact of the sphere.

This thermodynamic force approach to the breakup of an elastic contact is based on the proposition that the force of adhesion is a function of the clearance separating the contacting surfaces of two bodies. It can then be envisaged that, the opposite influence of the rigidity of spheres on the molecular force of adhesion can be attributed to the fact that, as the elastic modulus of the sphere decreases, there will be a corresponding increase in the distance to which a sphere needs to be drawn apart in order to separate at the contact site (*Muller et al., 1983b*). On breaking an elastic contact, a change in the spacing of the interacting bodies occurs simultaneously with a variation in the form on the deformed surface of the sphere as well as in the size of the interaction zone, so that the molecular forces are not overcome at once, but consecutively on different areas of the contact zone. Thus, this decreases their role as compared with the case of breaking a plastic contact of a particle with a hard plane surface, where a variation in the force of interaction may be connected only with a variation in the distance between them (*Deryaguin et al., 1977b*).

An attempt was made by Dahneke (1972) to take into account the effect of elastic contact deformation on the force of adhesion. However, this work was criticized by Deryaguin *et al.* (1975b, c) as fallacious. The main drawback of Dahneke's approach is that, contact deformations are accounted for incorrectly, thus leading to an erroneous conclusion that, on accounting for elastic contact deformation on the basis of the Hertz's theory, an increase in particle adhesion force should have resulted. This is contradictory to the generally accepted notion (*Deryaguin et al., 1975a; Rumpf, 1977; Tabor, 1977*) as described above that, elastic properties play no important part in these circumstances. Despite van der Waals forces being capable of increasing the area of an elastic contact, the maximum pull-off force only occurs just when the contiguous surfaces become tangential, i.e., at point contact.

On the other hand, analysis of the influence of a deformed sphere surface profile on the magnitude of adhesion was also being carried out using a thermodynamic energy approach. The method for calculating the force of adhesive interaction for the elastic contact model is based on derivations of the total energy of adhesive interactions. This energy is consisted of two parts, the volume energy of

elastic deformation and the surface energy of molecular forces. At point contact of a sphere with a rigid plane, the following expression was derived (*Deryaguin et al., 1975c*):

$$F = 2\pi R\delta\gamma \quad (1.35)$$

where F is the maximum pull-off force, and $\delta\gamma$ is the specific energy of adhesion. The same equation was also obtained by Bradley (1932), but using a pairwise summation method. For adherents of the same material, Equation (1.35) can be re-written as follows:

$$F = 4\pi R\gamma \quad (1.36)$$

where γ is the surface free energy per unit area, of the material concerned.

The thermodynamic force and energy methods for a sphere-plane model, called the DMT approach, allow the elastic stresses and the shape of the surface of a deformed sphere around the contact zone to be defined. The approach also provides a means of calculating the pull-off force while taking into consideration the contact deformation of the elastic sphere.

1.9.2 The Contact Mechanics Approach

A different approach to evaluate the force required to detach a sphere from a hard plane surface, after an elastic contact is established, was adopted by Johnson *et al.*, (1971). Their method is based on the hypothesis that the forces of interaction between two adherents (both attraction and repulsion) may be considered as purely contact forces. In the central region of the contact zone, there will be compression (which corresponds to a region of interfacial repulsion) and in the periphery of the contact, there will be tension (which corresponds to interfacial attraction). Thus, all

the important interaction forces are confined within the immediate contact area, outside of which, they become, by comparison, negligible. According to this model, there will be a sharp discontinuity of the stress distribution at the edge of the contact zone. In practice, however, the edge region will somewhat be rounded off, so that stresses at this place will not exceed the limiting attractive forces that the interface can withstand (*Tabor, 1977*).

This method by Johnson *et al.* (1971), which also takes into account the elastic deformation of the adhering surfaces, involves determination of the surface energy for the adhering surfaces through measurement of the change of contact radius with a press-on force. The rationale for this is that, to separate two bodies in intimate contact, mechanical work must be expended to overcome the adhesive forces. This work will go to create 'new' surfaces, and the energy required to create unit area of a new surface is related to the surface free energy of the solid.

Analysis of this sphere-plane elastic contact model similarly indicates that, under the action of surface forces alone, the contacting surfaces will be drawn together and a finite area of contact (radius, a_0) will be established for zero applied load. However, the shape of the deformed sphere is quite different from that associated with the Hertzian deformation, and shows a small neck around the contact zone (*Tabor, 1977*). If an external load is applied, the area will increase, which is attributed to a net release of surface energy resulting from the replacement of two 'free' surfaces by a contact interface of lower surface energy, the size of which, however, is always greater than that given by the Hertz's equations.

On reducing the load, the area decreases reversibly to its original finite size. If the external load is now made negative, the smallest pull-off force will reduce the radius of the circle of contact. This will proceed until a stage is reached when the rate of release of the mechanical energy in the contact zone is greater than the surface energy requirements, then the contiguous surfaces separate immediately. This stage of instability was found to occur at a finite size of the contact circle of about $0.63a_0$, and the pull-off force, F , when separation just occur, is given by:

$$F = 3\pi R\delta\gamma/2 \quad (1.37)$$

where $\delta\gamma$ is the thermodynamic energy of adhesion per unit area of contact. If the contacting materials concerned are identical, the coefficient 3/2 in Equation (1.37) is replaced by 3. This analytical approach is referred to as the JKR method. The elastic properties of the solids are not involved in the final force expression, and the force F is independent of the initial joining load.

Experiments with rubber and gelatin (of respective Young's modulus of the order of magnitude of 10^5Nm^{-2} and 10^4Nm^{-2}) showed good agreement with the JKR equation (*Johnson et al., 1971*). Whilst it is promising for such low modulus materials, *Johnson et al. (1971)* also commented that this approach may not well suited to hard surfaces in contact, because of the inevitable difficulty in forming a good and measurable contact between materials of high elastic modulus. Later, *Gane et al. (1974)* and *Kohno & Hyodo (1974)* both reported a reasonable agreement of their experimental data for some hard solids with the JKR equation.

1.9.3 Field of Applicability of the JKR and DMT Models

The mechanics of the adhesion of curved elastic bodies, with reference to the JKR and DMT models, were discussed by *Tabor (1977)*. There are two particular aspects regarding these two approaches in dispute (*Deryaguin et al., 1978b, 1980; Tabor, 1978, 1980*). One aspect concerns the elastic deformation during an adhesive contact and especially just before two contacting surfaces separate, on whether or not the surface profile should follow the Hertzian mode as in the absence of surface molecular attraction forces. The other aspect of dispute concerns the pull-off force at the instance of separation. To quote a comment from *Tabor (1978)*, “*Any attempt to analyse the adhesion between elastic solids without combining surface forces with the principles of contact mechanics is bound to be erroneous.*” In reply, *Deryaguin et al. (1980)* gave, “*.... it is incomparable more correct and objective to regard the contact*

mechanics as a combination of the theory of elasticity and the theory of surface forces”.

In accordance with the DMT theory, under an external compressive force, curved elastic bodies (relatively rigid, of $E \geq 10^9 \text{Nm}^{-2}$) in contact undergo a Hertzian-type deformation. On reversing the external force, the bodies should come apart when the area of contact has just fallen to zero, i.e., at the stage where the surfaces assume their original undistorted shape, and the pull-off (or adhesive) force is given by Equation (1.35). On the contrary, the JKR theory states that the shapes of elastic bodies (of rather low elastic modulus) in contact are always non-Hertzian, and acquire the form of a neck; detachment occurs spontaneously at a finite contact radius when the force will then be defined by Equation (1.37).

Some workers (*Muller & Yushchenko, 1980; Muller et al., 1980*) suggested a self-consistent approach to the analysis of the interaction of elastic bodies, taking into account the dependence of surface molecular forces of attraction and repulsion on the distance between the bodies. An integral equation was formulated to define the profile of the deformed surface for the case of a deformable sphere on a hard rigid substrate, on the assumption that the interaction between the atoms of the sphere and those of the substrate can be described by the Lennard-Jones potential. The solution of this equation is determined by just a single dimensionless parameter, μ , which is a function of the radius of the sphere, R , the characteristics of elasticity of the sphere (i.e., Young's modulus, E and Poisson's coefficient, ν), the equilibrium separation distance, h_0 , and the potential of interaction of the sphere with the substrate, ϕ , and is given as follows:

$$\mu = \frac{32}{3\pi} \left(\frac{2\phi^2 R (1 - \nu^2)^2}{\pi E^2 h_0^3} \right) \quad (1.38)$$

By further considering only the molecular component of the work of adhesion ϕ , Equation (1.38) is expressed in the following form:

$$\mu = \frac{8}{3\pi^2} \left(\frac{A^2 R (1 - \nu^2)^2}{2E^2 h_0^7} \right)^{1/3} \quad (1.39)$$

where A is the ‘non-retarded’ Hamaker coefficient. From this expression, amongst the parameters determining the type of solution of the problem of adhesion of elastic particles, the particle radius and Young’s modulus are those that can be varied over the widest limits.

Investigations then of the dependence of the tearing-off force on the value of μ , led to the limits of applicability of each of the two existing approaches (the JKR and DMT) to be ascertained (*Muller & Yushchenko, 1980, 1982; Muller et al., 1980, 1983a, b*). The results indicate that, at small values of the parameter (i.e., $\mu < 1$), which correspond to sufficiently ‘hard’ particles and/or to materials with relatively low specific energy, the DMT model holds, whereas at high values of the parameter (i.e., $\mu \gg 1$), which correspond to ‘soft’ particles, the JKR approach is observed. Moreover, there are no relevant grounds for defining either of these two approaches as contact mechanics, in as much as both are particular limiting cases of the more general approach that has been set forth.

On the other hand, analytical calculations carried out by Tabor (1977) yielded a possibility that, under some limiting situations, the contact mechanics analysis must be modified. At which stage, a suggested consequence is that, the tearing-off force might reach a limiting value, following closely the formula derived from the DMT approach.

Besides the theoretical approach to determine between the JKR and DMT theories, direct experimentations, which may largely resolve the controversy, were performed using special rubber and molecularly smooth curved surfaces. Studies that were carried out involve determination of the surface profile of adhering rubber or mica surfaces (*Tabor, 1977*), and measurement of the pull-off force between two mica surfaces each coated with a monolayer of a surfactant (namely, calcium stearate or

hexacetyltrimethylammonium bromide) whose surface free energy is accurately known (*Israelachvili et al., 1980*). The results show that, the equilibrium surface profile is non-Hertzian, and that, the JKR theory provides a better description of the macroscopic deformation of surfaces in elastic contact, and also just before detachment. In particular, when pulled apart, the surfaces separated spontaneously once their contact area radius fell to a value of approximately 0.57 of the radius under zero external force. This experimental value is close to the theoretical value of 0.63 obtained by the JKR method. However, even though the contact profile was better described by the JKR theory, the force needed for their separation, for a known specific work of adhesion, was more accurately predicted by the DMT method.

While the adhesion force is, by and large, independent of the elastic properties of the adhering particle and hence, its deformation on contact, the adhesion energy between the adherents will increase as the contact area increases, due to this energy being very sensitive to the elastic modulus of the particle. Thus, provided all things being equal, softer particles would exhibit a greater adhesion energy at equilibrium (*Israelachvili, 1982*).

The extension of these models to materials that deform plastically on contact is, however, much less developed. Eventual separation of two solid surfaces may not always occur at the interface (i.e., 'brittle' or adhesive rupture), but may occur in the bulk of one of the two materials (i.e., 'ductile' or cohesive rupture). The latter was shown to be the case for relatively 'clean' metals in contact where, on separation, transfer of materials from one solid to the other occurred (*McFarlane & Tabor, 1950*). An implication from this phenomenon is that, the adhesive junction established is at least as strong as the intrinsic strength of the cohesively weaker metal. The conditions for the existence of different fracture modes, for adherence at metal micro-contacts, were defined by Maugis & Pollock (1984), which are expressed as a function of five parameters, Young's modulus, elastic limit, surface energy, radius of curvature and load.

1.10 MEASUREMENT OF PARTICLE-SUBSTRATE ADHESION

1.10.1 Experimental Methods for Measuring Adhesion Forces

Measurement of the adhesion of small size particles represents a methodological difficulty, mainly because the forces involved are generally small and the surfaces are not smooth. However, theoretical advancement in the treatment of particle interactions together with technological developments, have produced quantitative methods for assessing particle adhesion.

There are, essentially, two different approaches for studying particle-substrate interactions. For the first approach, one technique involves the determination of van der Waals attraction forces between two macroscopic bodies, as a function of the finite distance of separation between their surfaces. A type of experiment concerned was to measure the interaction between a large number of particles, as a function of a mean value of surface separation (*Cairns et al., 1976; Homola & Robertson, 1986*), e.g. measurement of osmotic pressure with respect to volume fraction of particles.

An alternative method is to measure the molecular attraction forces between just two bodies as they are brought together in a controlled manner, and with their distance of separation accurately defined. With this technique, difficulties inevitably arise concerning the necessity of combining a high rigidity of instruments (for stabilizing the gap as the objects will tend to jump into contact under the effect of growing molecular attraction forces) with a high sensitivity to the measured forces (*Deryaguin et al., 1988*), since interpretations of the measured forces in terms of known mechanisms of interactions (the microscopic and macroscopic theories) require detailed information about the mutual distance between the adhering bodies, which is of atomic dimensions over a large part of the contact area (*Deryaguin et al., 1977a, 1978c; Luckham, 1989*). A separate problem involves precise measurement and pre-setting of the gap width. Besides, due to a severe limitation in the selection of a well-defined surface composition (such as freshly cleaved mica sheet), a further problem therefore resides in the choice, nature and preparation of the surfaces of solids, between which the forces are to be measured (*Lodge, 1983*).

A conceptual model for the above force measurements is two flat plates. However, the experimental use of this system presents problems in the form of edge effects and their precise parallel alignment (*Lodge, 1983*). A more favoured geometrical model which is devoid of these shortcomings is a crossed-cylinder arrangement, in which two elastic cylinders (or filaments) in contact are at right angles to each other (*Deryaguin et al., 1964, 1977a, 1978c; Tabor & Winterton, 1968, 1969; Tabor, 1969, 1977; Gane et al., 1974*). The contact region obtained from this geometrical configuration is exactly analogous to those of a sphere-sphere contact and a sphere-plane contact (*Muller et al., 1983a; Buckley et al., 1986; Bickel & Wentzel, 1988*).

Different techniques based on the above force-distance measurement principle are developed, for examples, the 'simple' and 'complex' deflection methods (*Kitchener & Prosser, 1957; Deryaguin et al., 1977a; Rabinovich et al., 1982*), the dynamic and dynamic-jump methods (*Overbeek & Sparnaay, 1952; Lodge & Mason, 1982a, b*) and the resonance method (*Israelachvili & Tabor, 1972*). A review of some of these methods is given by Lodge (1983). Since the results only provide a value of a function of force at a certain distance of separation, this technique will not determine the adhesive (or pull-off) forces when the adherents are already in contact with each other.

The second approach for investigating particle-substrate interactions involves determination of the applied force that is just sufficient to separate the adherents, i.e., the pull-off force or the force of adhesion. In this approach, two general types of methods are used, one for bulk powder as a whole, and the other for individual particles. For bulk powders, the experimental methods employed measure, basically, the cohesive behaviour of particles in a powder bed, e.g. measurement of shear strength by a shear cell (*Hiestand, 1972*) and tensile strength by a split-plate tensile tester (*Hartley et al., 1985*). By these methods, any attempt to understand single particle-particle or substrate-single particle interaction is complicated by multi-interparticle interactions. In this respect, the approach to investigate individual

particles could be considered to allow more insight into such fundamental type of particle adhesion.

There are, principally, five techniques for measuring the adhesion of small particles to a solid substrate (*Böehme et al., 1962; Krupp, 1967; Zimon, 1982*), the aerodynamic and hydrodynamic method, the weighing method, the pendulum method, the inclined plane method and the centrifuge method. According to Zimon (1982), these five methods of adhesive force measurement can broadly be classified into two groups, on the basis of the specific features of action of the detaching force. One group of methods, in which the detachment force acts on only one single particle, includes the aerodynamic and hydrodynamic, weighing and pendulum methods. The other group consists of methods based on the detachment of a relatively large number of particles, viz., the inclined plane and centrifuge methods. Here, the detaching force acts simultaneously on all of the adherent particles present on the surface. Also, of these five techniques, only the aerodynamic and hydrodynamic and the centrifuge methods are useful for micron-sized particles.

1.10.1.1 The Aerodynamic and Hydrodynamic Techniques

Particle separation is measured as a function of the rate and direction of an air (or liquid) jet. For the aerodynamic technique, a compressed air (or nitrogen gas) jet is usually the source of high velocity air current (*Jordan, 1954; Larsen, 1958*). It is generally effective in dislodging large particles ($>10\mu\text{m}$) from a substrate surface, but ineffective for small particle sizes.

A means to evaluate the adhesive ability of a powder can be by observing the adhesion of particles after their impingement, by an air stream, on to a solid surface. This method is employed by Jordan (1954) who assessed the adhesion of quartz and ground glass particle to a surface, as a function of the air jet speed. Gillespie (1955) also adopted an aerodynamic technique by which, a horizontal air stream of particles was directed towards a vertical cylinder. The number of adhering particles is then determined in relation to their distribution on the cylinder surface.

Apart from air current, liquids (such as water) have also been used as a flow medium (*Kuo & Matijević, 1980; Kallay & Matijević, 1981*). In this situation, the force is exerted on the particle by the drag of a flowing liquid. For a single sphere in an infinite sea of liquid and a flow of sufficiently low Reynolds number, the hydrodynamic force, F_{hyd} , can be expressed according to the Stoke's law, as follows:

$$F_{hyd} = 6\pi\eta vR \quad (1.40)$$

where η is the viscosity of the liquid medium, v is the terminal velocity and R is the sphere radius. This viscous drag method bears an advantage of not being dependent on particle density. The effect of a solid flat boundary in contact with the sphere is an increased drag force by a factor of about 1.70 (*Goldman et al., 1967*), and the corresponding equation is:

$$F_{hyd} = 1.7 \times 6\pi\eta v_c R \quad (1.41)$$

where $v_c = (\text{wall shear stress}/\text{viscosity})R$. In this case, the shear stress at the substrate surface needs to be determined, which can be obtained by means of a concentric cylinder apparatus (*Visser, 1970*). A discussion of the role of drag on particle removal by air as well as by liquid flow is given by Zimon (1982).

1.10.1.2 The Weighing Technique

Various types of devices (e.g. spring balance, beam balance, microbalance) are used for the determination of the interaction force between contacting spherical surfaces or between a sphere and plane contact, but all operate on a similar principle. Basically, there is a spring or balance arm to which one of the contacting bodies is attached, an attachment for mounting the other contacting body and a readout system. Bradley (1932) used a spring balance for investigating the adhesion of quartz and of borate spheres. It consisted of a sensitive helical spring whose extension could be

measured by a travelling microscope, and the adhesion force then evaluated by reference to the elongation of the spring at the instant of particle detachment. Provided that the extension of the spring is within its elastic limit, the adhesion force, F_{ad} , can be calculated, in accordance with the Hooke's law, by the following formula:

$$F_{ad} = c \delta l \quad (1.42)$$

where c is a parameter characterizing the rigidity of the spring and δl is the amount of spring elongation at the moment that adhesion fails. A beam balance was described by McFarlane & Tabor (1950) in their study of the adhesion properties of hard and soft metals.

Adhesive force could be expressed in terms of the deflection of an elastic beam. Corn (1961) reported a study in which the adhesional force between micron-sized particles and solid surfaces were measured using a microbalance. With this particular apparatus, the quantity, δl , in Equation (1.42) corresponds to the deflection of the balance arm which carries, at the end, the materials under investigation. Kohno & Hyodo (1974) employed a torsion microbalance to evaluate the microadhesion between tungsten or fused quartz styli and a steel flat, as a function of the loading force.

A special instrumentation was designed by Mitrejev & Augsburger (1980) for measuring the adhesion of tablets to the lower punch face in a rotary tablet press. Here, adhesion force was measured by means of a strain-gauged cantilever beam affixed to the feed frame in front of the sweep-off blade. The tablet was detached from the lower punch by striking the blade, and the net adhesion force expressed as the total force measured by the beam less that due to the momentum of the tablet. Using also a system of cantilever and strain gauges, Fuller & Tabor (1975) examined the effect of surface roughness on the adhesion of elastic solids.

1.10.1.3 The Pendulum Technique

In this method, only the component of full gravitational force of the measuring object, which is normal to the area of contact, becomes effective as the separating force. Generally, a vertical plate is brought up to a freely suspending sphere or the fused end of a fibre until contact is just achieved. The gravity component, which tends to separate the sphere, can be continuously increased by shifting the plate in a direction perpendicular to the contact area in order to increase the angle of inclination, φ , to the vertical. At the instant of separation, the adhesive force can be derived from the mass, m , of the particle and the critical angle of inclination, φ_c , by the equation below:

$$F = mg \sin \varphi_c \quad (1.43)$$

By means of the gravity method, McFarlane & Tabor (1950) measured the adhesion between different pairs of materials under various experimental conditions.

1.10.1.4 The Inclined Plane Technique

The inclined plane method is a technique used mainly for measuring the adhesion of an ensemble of particles to a substrate. A defined amount of powder is uniformly distributed on the substrate, which is then tilted at an ever-increasing angle to the horizontal until the bulk of the powder starts to slide under gravity. This angle of inclination can be taken as a measure of the adhesion of the particle layer. Hiestand (1966) further described this process with an equation, similar to the Laws of Friction, as follows:

$$m_p g \sin \theta_i = \mu_c (m_p g \cos \theta_i + A) \quad (1.44)$$

where m_p is the investigated mass of the powder, g is 9.82ms^{-2} , θ_i is the tilted angle, A is the adhesion force of the powder to the plate when the shear plane is between

the powder and the plate, and μ_c is a proportional constant. This equation indicates that, apart from the normal reaction force component due to the weight of the particle ensemble, the frictional force is also governed by an adhesive component. Thus, when the sliding force, on the left hand side of the above equation, is equal to or just greater than the combined frictional and adhesional forces, on the right hand side of the equation, the powder mass will begin to slide down the slope.

Bowden & Tabor (1950) claimed that with large objects, this friction manifestation of adhesion is readily observed, whereas with fine powders, this relationship is more intricate and will be dependent on the system under examination. The technique of determining adhesion force by tilting the substrate surface is reviewed by Zimon (1982).

1.10.1.5 The Centrifuge Technique

The adhesion between a particle and a solid surface can be defined by the amount of centrifugal force necessary to cause their separation. A particles-laden surface can be made to rotate around a horizontal or vertical axis, which is accelerated to a speed at which the adherents are detached from each other. In the former instance when the 'dusted' substrate surface is rotated around a horizontal axis, the force of gravity will tend to assist the detachment of hanging particles and oppose the breakaway of particles lying on the surface. The gravitational effect can, however, be neglected if the solid surface is rotated around a vertical axis and the separating force acts in the direction normal to the contact plane.

A frequently employed geometrical adhesive system for the centrifuge method is a plane surface with particulate materials adhering on its surface. This configuration is also of considerable interest in problems of deposition and filtration, because the particles are usually so much smaller than the collector that the sphere-infinite plane model is a justifiable assumption.

Beams *et al.* (1955) applied the principle of centrifugation to determine the adhesive strength of silver films electrodeposited on steel rotors. In a study by Kordecki & Orr (1960), the adhesion of particles to a solid flat was evaluated by comparing the number and size distribution of the particles initially sprinkled on a glass microscope slide with those obtained after subjecting the adhesive system, in discrete steps, to successively higher fields of centrifugal force. Böehme *et al.* (1962) also used a centrifuge method to investigate the variation of adhesion force for a narrow size range of test particles. The influence of capillary condensation (Zimon, 1963) and the effect of surface roughness (Zimon & Volkova, 1965), on the adhesion of individual particles was also studied by means of the centrifuge technique. With the centrifugal method, Krupp (1967) determined the forces of adhesion of fine spherical powders on plane metal substrates, and Asakawa & Jimbo (1967) quantified the adhesiveness of some mineral powders to flat plates. The adhesional forces of some glass and mineral powders to a glass plate were calculated by Sano *et al.* (1984), following the theory of the centrifuge technique.

1.10.1.6 Some other Specific Techniques

In addition to the above general force measurement methods, there are reported some specific techniques for determining particle-substrate adhesion force. One technique is vibration at high frequencies. Particles are deposited usually on a metal support which is connected to an acoustic transducer or an ultrasonic vibrator (Deryaguin & Zimon, 1961; Dybwad, 1988). Adhesion of particles to the metal substrate is expressed as a function of the frequency and amplitude of the vibration. By varying the oscillation frequency, the detaching force can be varied over a wide range. Using this technique, Larsen (1958) determined the force of adhesion of spherical particles to fibres, at a frequency range of 10 to 90Hz. Further references regarding the use of this technique for separating submicron particles, which requires much higher vibration frequency, are given by Ranade *et al.* (1988).

Another technique is the impact-separation method, an example of which is illustrated in a work of Otsuka *et al.* (1983), which described the determination of

adhesion forces between powdered organic drugs and a glass substrate by using a pendulum type shock testing machine. Basically, the adhering particles are caused to detach from a test surface by an impact on the opposite side of the substrate plane. The same method was employed by Otsuka *et al.* (1988) to investigate the effect of some material properties on particle adhesion. Based on the impact-separation principle, Deryaguin *et al.* (1968/69) proposed a pulse method for studying the effect of electrostatic forces on the adhesion of polymer powders to solid surfaces. In this study, the adhesion of the particles deposited on the plane surface of a target was overcome by the impact of a pellet, shot from the barrel of a pneumatic adhesiometer, at the reverse side of the target plate. By means of this method, Muller *et al.* (1976) examined the influence of elastic contact deformation on particle adhesion. This technique is used particularly for removing small particles (diameter < 30 μm), which usually requires separating forces corresponding to accelerations of the order of 10^5 - 10^6 g that most ultracentrifuges cannot achieve.

For metallic particles adhering to a conductive surface, the use of electric fields to remove these particles can be employed as a method of determining the strength of adhesion (Cooper *et al.*, 1988). This principle is commonly applied in xerographic processes where charged electrophotographic toner particles are detached from a photoconductor surface to paper by an electric field (Lee & Jaffe, 1988). The theoretical concepts for electric field detachment of single charged particles and particle layers are reviewed by Hays (1988).

1.10.2 Merits of the Centrifuge Technique

When compared with the other four adhesion force measuring techniques, the centrifuge method is more extensively and frequently used. Böehme *et al.* (1962) demonstrated experimentally that, a major merit of the centrifuge technique lies in its simultaneous determination of the adhesive forces of many particles, resulting in large statistical accuracy.

Both the weighing and pendulum methods are difficult to set up, and only allow measurement of comparatively large particles (diameter of the order of 1mm). Moreover, they become very delicate with decreasing particle size, whereas the centrifuge technique bears certain advantages in its simplicity of operation, accessibility and large measuring sensitivity (particle diameter 1-100 μ m, depending on material properties of the solids).

Unlike a centrifuge method for which, basically, the force of adhesion can be equated to the centrifugal force that is just sufficient to detach a particle from the surface of a substrate, in an aerodynamic method, a particle is moved by an air current in a direction parallel to the substrate surface, and so it is subjected to an additional torque. The force required to start the rolling motion of the particle along the surface may therefore be quite different from the adhesive force. Furthermore, the aerodynamic method is considered not to provide direct data on the adhesion between a substrate and particles; it yields, at best, reference values (*Zimon, 1982*).

For the inclined plane method, the powder mass must be practically rigid. This condition is, however, not satisfied by many particulate ensembles as usually, varying degrees of partial sliding within the powder layer or rolling of the powder mass on a first layer of particles, acting as ball bearings, would take place. This is further complicated by the varying degrees of particle agglomeration, which could significantly affect the results obtained. Also, because of the insufficiently explored relationship between adhesion and friction, as well as the complicated nature of the sliding process, the inclined plane technique is indeed not an objective method for measuring adhesion forces.

During operation of the vibration or the impact-separation method, the impact force will tend to cause the particles to press against the test surface before their detachment, which would result in deformation and, perhaps, also a change in the initial geometry of the contact zone. This could thereby complicate the subsequent interpretations of results. Since also many pharmaceutical particulate materials would be liable to plastic deformation under such experimental conditions, for which the

present theory only accounts for elastic deformation, these methods are therefore not particularly suitable for determining adhesion forces for these powder materials.

1.11 OBJECTIVES OF THIS WORK

During processing of pharmaceutical powders, particulate solids will come into contact with a variety of substrate surfaces, in particular, metal surfaces. Therefore, the primary aim of this work is to examine the adhesion properties of some of these solid materials to a stainless steel surface. Since the arrangement of a particle on a rough surface is random, to ensure contacts are made on the tops of the touching asperities, the topographic nature of the steel surface should be characterized, and the test particle size carefully selected. Adhesion forces between the substrate and particles can then be measured by means of a centrifuge, whereby separation forces of defined magnitudes will be acting in a direction normal to the interface.

In a contact process, some kind of impact force is usually experienced at the interface between two unlike solids, which would result in strengthening of the adhesion junctions. Thus, it will be necessary to study the effect on adhesion of variable contact stress imposed normal to the sites of adhesion. Additionally, the influence of the duration of applied load will be investigated. As these variables will be influenced by the mechanical properties of the particles, thereby, this will be studied by the use of different types of powder.

The particle size of a powder is a common major concern in many pharmaceutical processing operations, its effect on the adhesional behaviour of solid materials will be investigated, with reference also to the theory related to the nature of the adhesion force. Generally, particle-substrate adhesion is strengthened by deformation of the materials at the contact interface, a process arising from energy dissipation within the bulk of the solids concerned, which will be sensitive to temperature. Hence, the role of ambient temperature on the adhesional response of powder solids will also be evaluated in this study.

CHAPTER 2

Preparation and Characterization of Experimental Materials

2. PREPARATION AND CHARACTERIZATION OF EXPERIMENTAL MATERIALS

2.1 CHARACTERIZATION OF POWDER MATERIALS

2.1.1 Choice of Powder Materials

Pharmaceutical particulate excipients are widely used in solid dosage formulations, their selection for this work is therefore of practical relevance to further research and development.

The materials which could be considered suitable for this study must be, non-corrosive, of suitable particle size, possess appropriate material properties and be relatively insensitive to ambient condition changes within a laboratory. Of the various kinds of pharmaceutical excipients available, Starch 1500, spray-dried lactose, polyethylene glycol 4000 and heavy precipitated calcium carbonate were considered to have satisfied the above requirements and were thus chosen. Moreover, with reference to the literature, the material properties of these solids, in the form of powders, were considered capable of exhibiting differentiable adhesive properties.

2.1.2 Description and Pharmaceutical Usages of the Powders

Starch 1500

Starch 1500 is partially pre-gelatinised starch. It differs from compendial maize starch principally in its water solubility and particle size analysis, and offers the advantages of being free flowing, self-lubricating and directly compressible. Starch 1500 is used mainly as a bulking agent in solid dosage forms.

Spray-dried lactose

Spray-dried lactose is made up mainly of α -lactose but also contains a proportion of the amorphous form. It is widely used as a diluent or bulking agent in pharmaceutical formulations.

Polyethylene glycol 4000

Polyethylene glycols (PEG) are commonly used as suppository and ointment bases. They are manufactured by condensation of water and polymers of ethylene oxide, and are represented by the following chemical formula:



where n stands for the average number of oxyethylene groups. The number which follows the name, PEG, indicates the average molecular mass of that compound. PEG 4000 (with n=69-84), for example, has an average molecular mass of 3000-4800. It has a density of 1.212 g/cm³ (*The Merck Index, 1983*). PEG of higher molecular weights (>1000) are solids which vary from pastes to waxy flakes.

Precipitated calcium carbonate

Precipitated calcium carbonate is made by double decomposition of calcium chloride and sodium carbonate in aqueous solutions. The heavy forms of the precipitated calcium carbonate are produced by using high concentrations of the reacting solutions. It is used as a tablet diluent and an ingredient in certain effervescent preparations.

2.1.3 Sources of Materials

The sources of the experimental powder excipients are listed in Table 2.1.

2.1.4 Size Separation of the Powders

The powders were used in their 'as received' conditions. Unmilled samples of these materials were fractionated into the required size fractions with the use of an Air Jet Sieve (Alpine, Augsburg, Germany). The test sieves used were British Standard (BS 410: 1969) 200mm Haver & Boecker stainless steel sieves of aperture sizes 32µm, 40µm, 45µm, 56µm, 63µm and 75µm.

TABLE 2.1 Sources of powder materials.

Material	Manufacturer	Batch number
Starch 1500	Colorcon Inc., USA	012003
Lactose, spray-dried	Dairy Crest, UK	033505
PEG 4000	Hoechst AG, Germany	618535
Calcium carbonate, heavy precipitated	BDH, UK	---

2.1.5 Apparent Particle Densities

The apparent particle density of a powder material is defined as the mass of the particles divided by the volume, excluding open pores but including closed pores (BS 2955: 1958 amended 1965). In this work, the apparent particle densities of the particulate samples were determined using a Beckman (Model 930) air comparison pycnometer (Beckman Instruments Inc., California, USA).

The pycnometer was used in its standard atmosphere operation mode. The zero offset of the instrument was measured by performing a volume determination with the sample cup empty, and subsequent volume measurements were appropriately adjusted. The accuracy of the unit was then checked by making volume measurements with the two steel test balls, supplied by the manufacturer, in the sample cup. The results obtained agreed well with those stated by the manufacturer.

Ten determinations were carried out for the required size fractions of the materials and the mean values obtained are shown in Table 2.2.

2.1.6 Single Particle Mass Determination

The masses of the powder particles were measured by means of a Perkin-Elmer AD-2 Autobalance (Perkin Elmer Corp., Connecticut, USA) (see Plate 2.1).

PRINCIPLE OF OPERATION OF THE AUTOBALANCE

The AD-2 Autobalance is an electromagnetic ultramicrobalance which has a sensitivity of $\pm 0.1\mu\text{g}$. It consists of a Weighing Unit and a Control Unit. The balance operates as a high gain electromechanical servo system. When a sample is placed on the Sample Pan, the beam that supports the Sample Pan deflects. A beam position detector measures the deflection with an optical sensor and uses electrical current to return the beam essentially to its original position. The amount of current needed is a measure of the weight on the beam. This current is amplified and filtered and then displayed on the digital panel meter in milligram.

TABLE 2.2 The mean apparent particle densities of some powder fractions.
(s.d.=standard deviation)

Material	Size fraction (μm)	Apparent particle density (g/cm^3)	s.d. ($\times 10^{-3} \text{g}/\text{cm}^3$)
PEG 4000	-56+45	1.222	2.75
Starch 1500	Unsieved sample	1.508	7.26
	-56+45	1.500	3.78
Lactose, spray-dried	Unsieved sample	1.514	3.98
	-56+45	1.509	4.09
Calcium carbonate, heavy precipitated	-45+32	2.681	3.82

WEIGHING UNIT

Optics cover box

Side window

Sample weight tray

Metal tin pot

Carriage bolts

CONTROL UNIT

Digital meter

Coarse zero control

Fine zero control

Range switch

Hi/Lo filter switch

Power switch

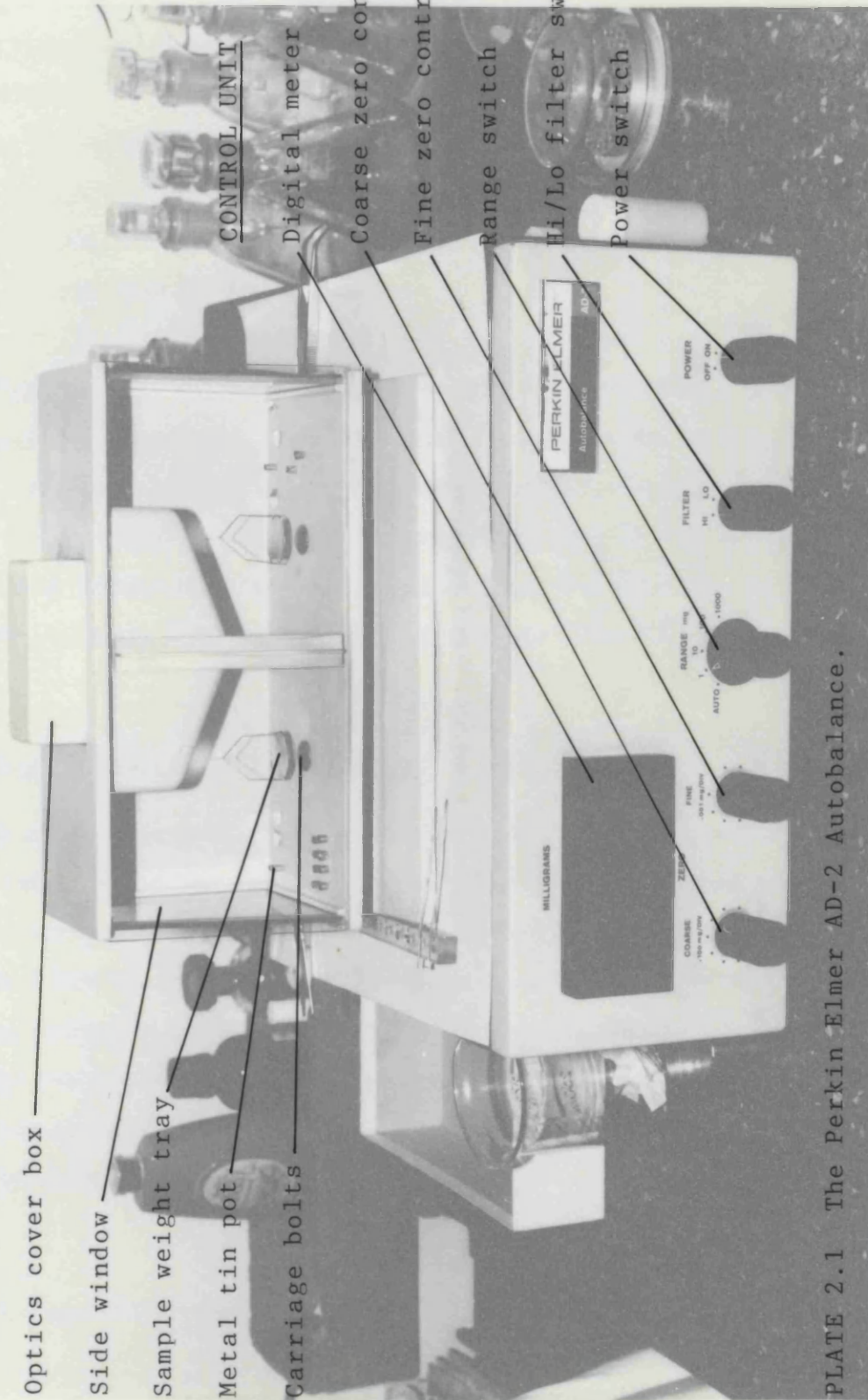
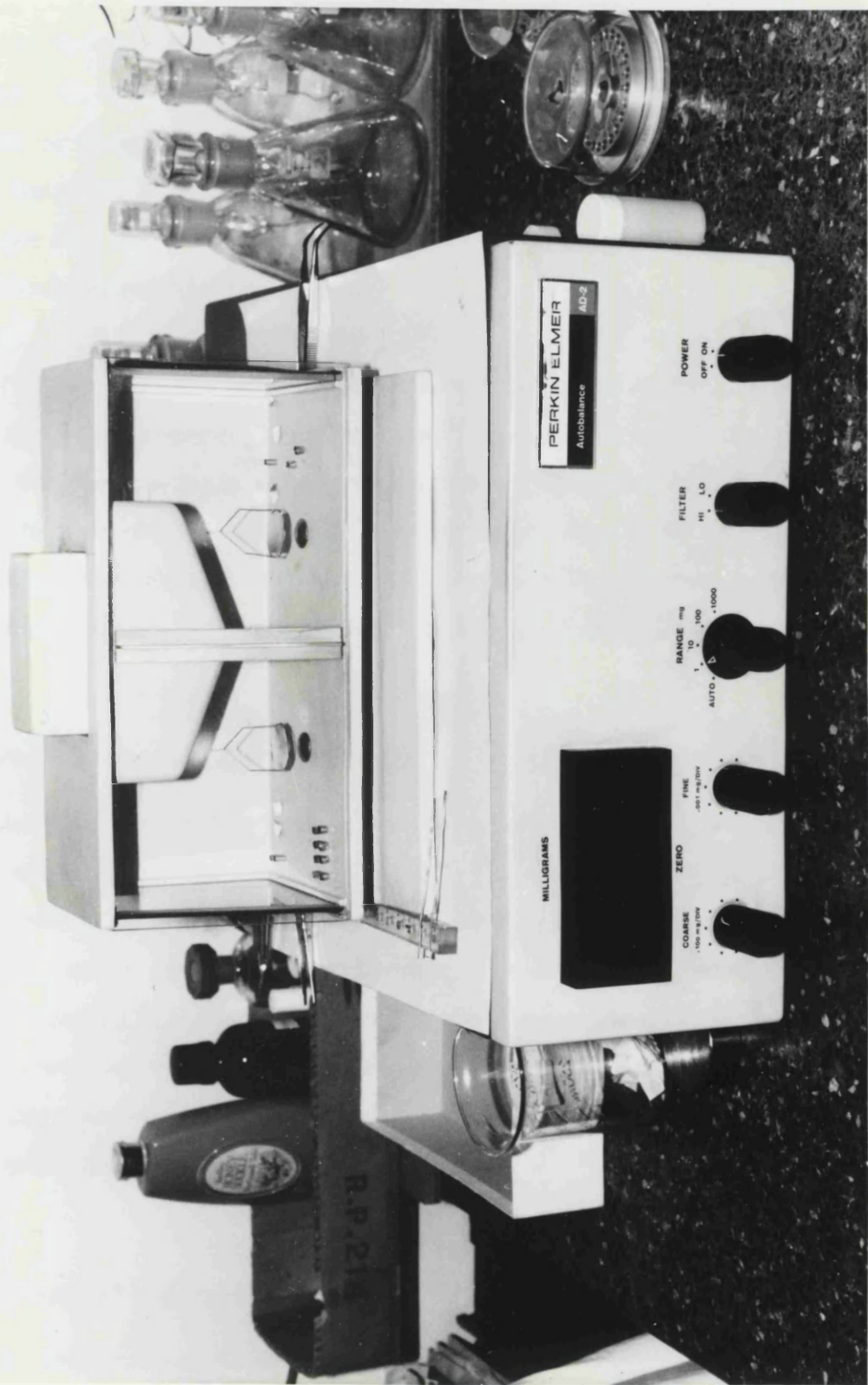


PLATE 2.1 The Perkin Elmer AD-2 Autobalance.



The AD-2 was zeroed before measurements. All the powder samples used for weighing were not more than 1mg in mass, so the Range Switch on the AD-2 was adjusted to the 1mg setting for all the measurements. A small fraction of each sample was transferred, by means of a micro-spatula, to a small metal tin pot, which was then placed on the Sample Pan of the Autobalance. After stabilization, the initial digital readout was noted. The particles in the pot were subsequently poured on to a glass microscope slide and the tin pot was re-weighed. The total mass of the particles was the difference between the two readouts.

The glass slide was gently tapped on its sides to spread the particles out into a single layer. The number of particles contained in the weighed out fraction, between 500 and 3000, was counted under an optical microscope. The average mass of a single particle was calculated by dividing the measured sample mass by the corresponding particle count. Measurements were carried out in triplicate for each sieve fraction and the mean value taken. The results obtained are shown in Table 2.3.

2.1.7 Particle Microscopical Morphology

Scanning electron micrographs were taken of some sieve fractions of the powder materials, and are shown in Plate 2.2. The crystals of calcium carbonate appear cubical in shape, though some crystalline micro-aggregates were also observed. Spray-dried lactose particles show, in general, a rounded outline appearance. PEG 4000 was obtained in a milled form from the manufacturer, the photomicrograph of a size fraction sample of which shows that the particles are generally plate-like in shape. Also appearing crystalline are particles of Starch 1500, probably as a result of the pre-gelatinization process.

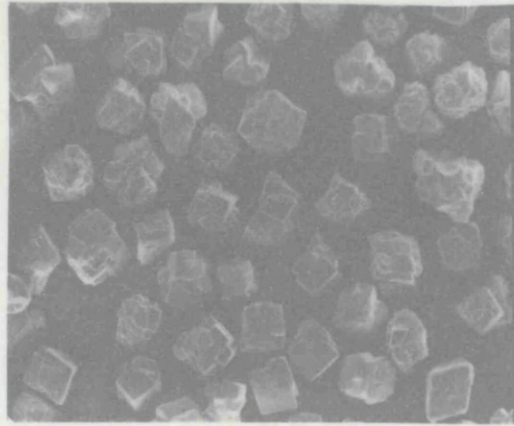
2.1.8 Storage of Materials

In most pharmaceutical manufacturing processes, powders are usually used in their 'as received' conditions. Drying a powder before use, for example, by heating, could affect its material properties such as its binding, flowing and handling

TABLE 2.3 Mean particle masses of different sieve fractions of the powders.
(s.d.=standard deviation)

Material	Size fraction (μm)	Particle mass (μg)	s.d. ($\times 10^{-3} \mu\text{g}$)
Starch 1500	-40+32	0.045	2.96
	-45+40	0.072	6.70
	-56+45	0.116	2.08
	-63+56	0.239	6.08
	-75+63	0.255	7.00
Lactose, spray-dried	-40+32	0.038	1.48
	-45+40	0.057	0.60
	-56+45	0.116	3.06
	-63+56	0.207	5.03
	-75+63	0.251	4.73
PEG 4000	-56+45	0.120	0.90
Calcium carbonate, heavy precipitated	-45+32	0.084	3.03

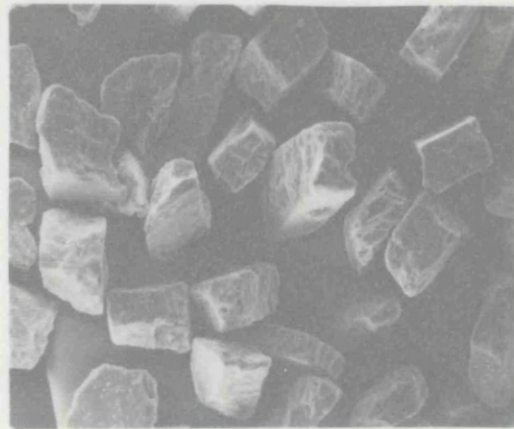
Heavy ppt'd. calcium carbonate
(-45+32 μ m)
Mag. x220



Spray-dried lactose
(-56+45 μ m)
Mag. x220



PEG 4000
(-56+45 μ m)
Mag. x220



Starch 1500
(-56+45 μ m)
Mag. x220

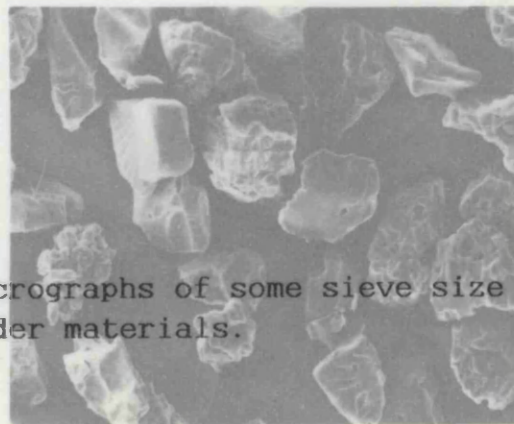
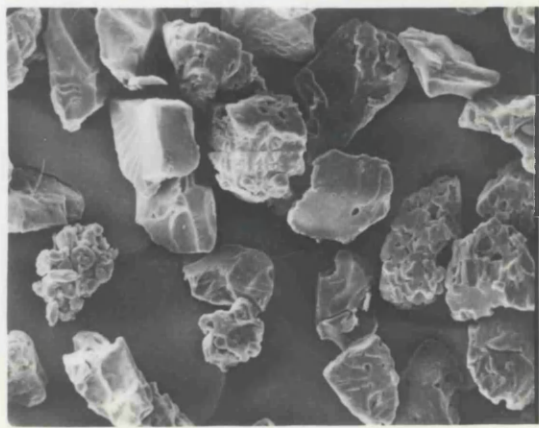
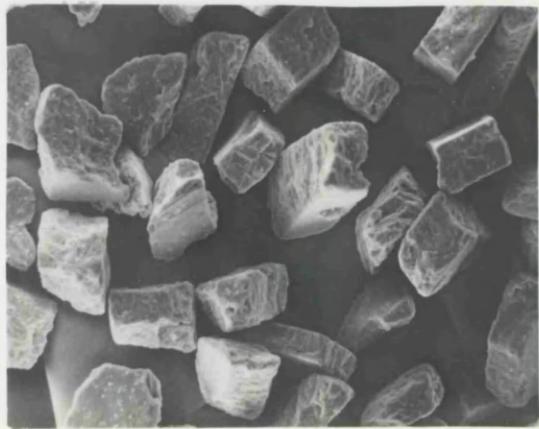
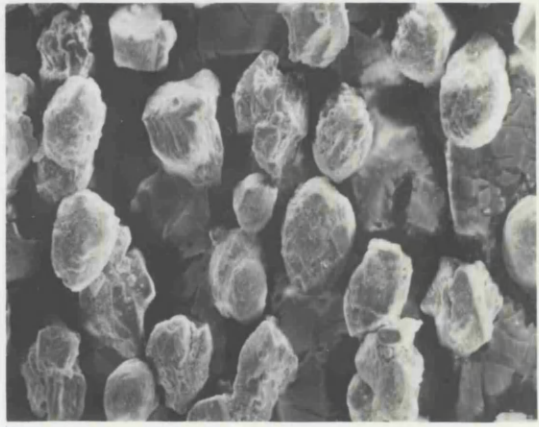
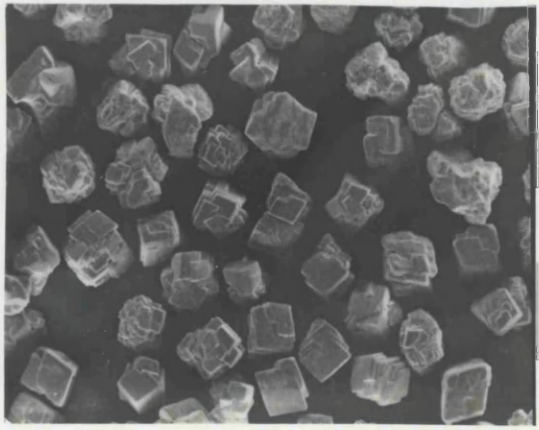


PLATE 2.2 Scanning electron micrographs of some sieve size fractions of the powder materials.



behaviour. In this work, the sieved powder fractions were untreated but stored at room temperatures in glass containers over silica gel crystals in a desiccator, until required for use.

2.2 SURFACE CHARACTERIZATION OF THE SUBSTRATE MATERIAL

2.2.1 Substrate Material

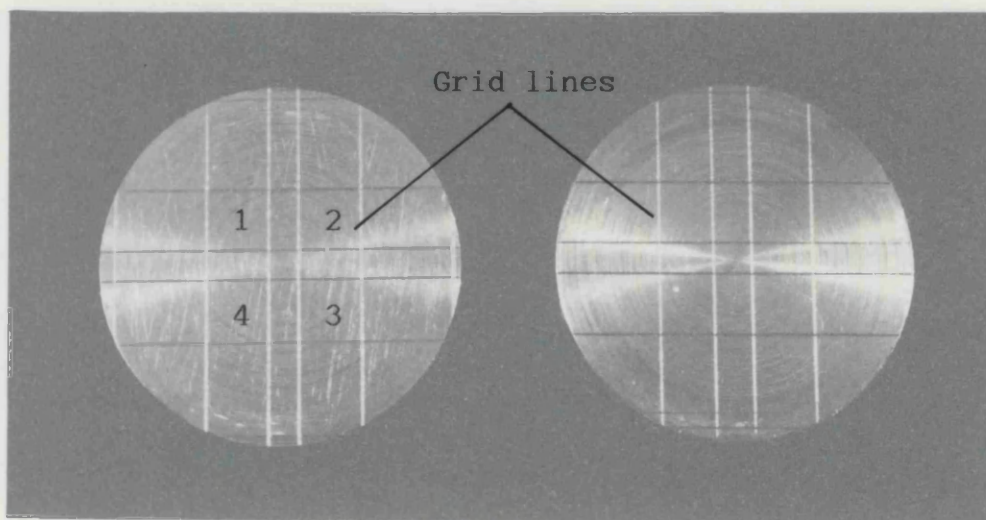
During processing of pharmaceutical powders, particles often come into contact with surfaces of a variety of substrate materials such as steel, plastics (e.g. Perspex, polypropylene, polytetrafluoroethylene (PTFE)), aluminium and glass. Amongst the various substrates, stainless steel is very frequently encountered and commonly used in industry. For this reason, stainless steel (BS 1449: 2, steel 304 S 16) was chosen as the substrate material for this study.

Two small stainless steel disks were cut, by a lathe, from a larger specimen and machined to 12mm in diameter and 3mm in thickness. One disk was polished using standard polishing techniques, while the other disk was left untreated. Although machine turning marks are still visible on the polished disk, it has a more shiny appearance than its unpolished counterpart (see Plate 2.3). Stainless steel surfaces used for pharmaceutical industrial operations are usually polished, though to different extent of surface finish. From the two metal disks, the polished one was chosen to be the substrate for adhesion experiments in this work. The polished disk was finally prepared with grid lines marked over its polished face. This is to facilitate counting of the adhering particles by microscopy (see Section 3.2.3 later). Only the particles that were deposited within the grid squares (1-2-3-4) were counted.

The substrate disk was cleaned with acetone in an ultra-sonic bath. No effort, though, was made to remove any adsorbed gases or to reduce any metallic oxide that may be present on the disk surface in order to simulate its general surface condition in ordinary practical use situations.

2.2.2 Surface Topography Analysis of the Stainless Steel Disks

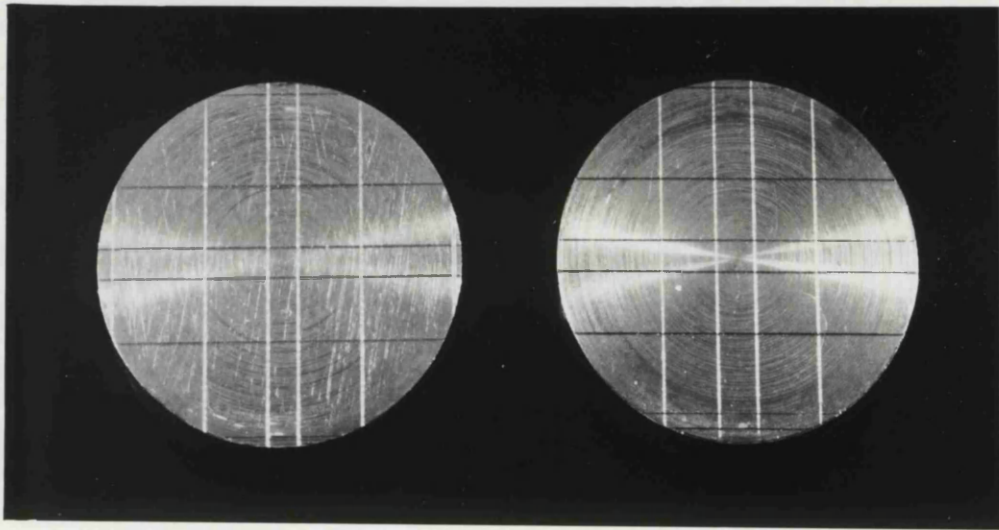
2.2.2.1 Introduction



Polished disk

Unpolished disk

PLATE 2.3 The polished and unpolished stainless steel substrate disks.



The first diagram illustrates the wave pattern produced by a point source in a medium. The concentric circles represent the wavefronts expanding outwards from the source. The grid lines provide a reference for the wave's position and direction of travel.

The second diagram illustrates the wave pattern produced by a source that is moving through the medium. The wavefronts are compressed in the direction of motion and stretched out behind it, resulting in the interference fringes seen along the horizontal axis.

The diagrams demonstrate how the motion of the source affects the resulting wave pattern. In the first case, the source is stationary, and the wavefronts are symmetric. In the second case, the source is moving, and the wavefronts are asymmetric, leading to the formation of interference fringes.

These patterns are characteristic of wave phenomena and are used to study the properties of waves and the effects of motion on wave propagation.

The various theories of adhesion all place an emphasis on the significance of the properties of the interacting surfaces and to various extent, the importance of surface topography.

A number of techniques are developed for studying or examining the surface structure of solid surfaces, for examples, electron microscopy, multiple optical beam interferometry, stylus method, oblique sectioning, pneumatic gauging and reflectometry. These methods are reviewed by Halling (1972) and Thomas (1975). Another possible method, which has been used for estimating plastically deformed micro-contact areas, is the three-dimensional relocation profilometry (*Edmonds et al., 1977; O'Callaghan & Probert, 1987*).

The stylus method is widely used in examining solid surface profiles. A fine, sharply pointed stylus, usually a conical diamond or sapphire, attached to a transducer, is mounted in a pick-up arm, which is drawn across the specimen surface at a steady rate by a gearbox. The vertical undulating movement of the stylus, as it follows the surface contours, produces an electrical signal proportional to the total height of the surface. This signal modulates a carrier waveform and is amplified, demodulated and available for recording, computer analysis or use to drive a chart recorder (see Fig. 2.1). The surface profile traces thus obtained are representative of a cross-section of the solid surface and can be analysed in a variety of ways.

The ultimate sensitivity of this profilometric method is, however, limited by the finite size of the stylus with regard to the resolution attainable and the integrity of the profile trace in representing the trace surface. Information will be lost by the filtering action of the stylus, which is unable to penetrate the finest irregularities whose widths are less than that of the stylus tip. Moreover, the stylus is liable to traverse the shoulder of a peak, as opposed to directly across its highest point, because of the lateral movement possible within the pick-up arm. As a result, the profile trace does not fully represent the true surface structure but provides a realistic model for further analysis.

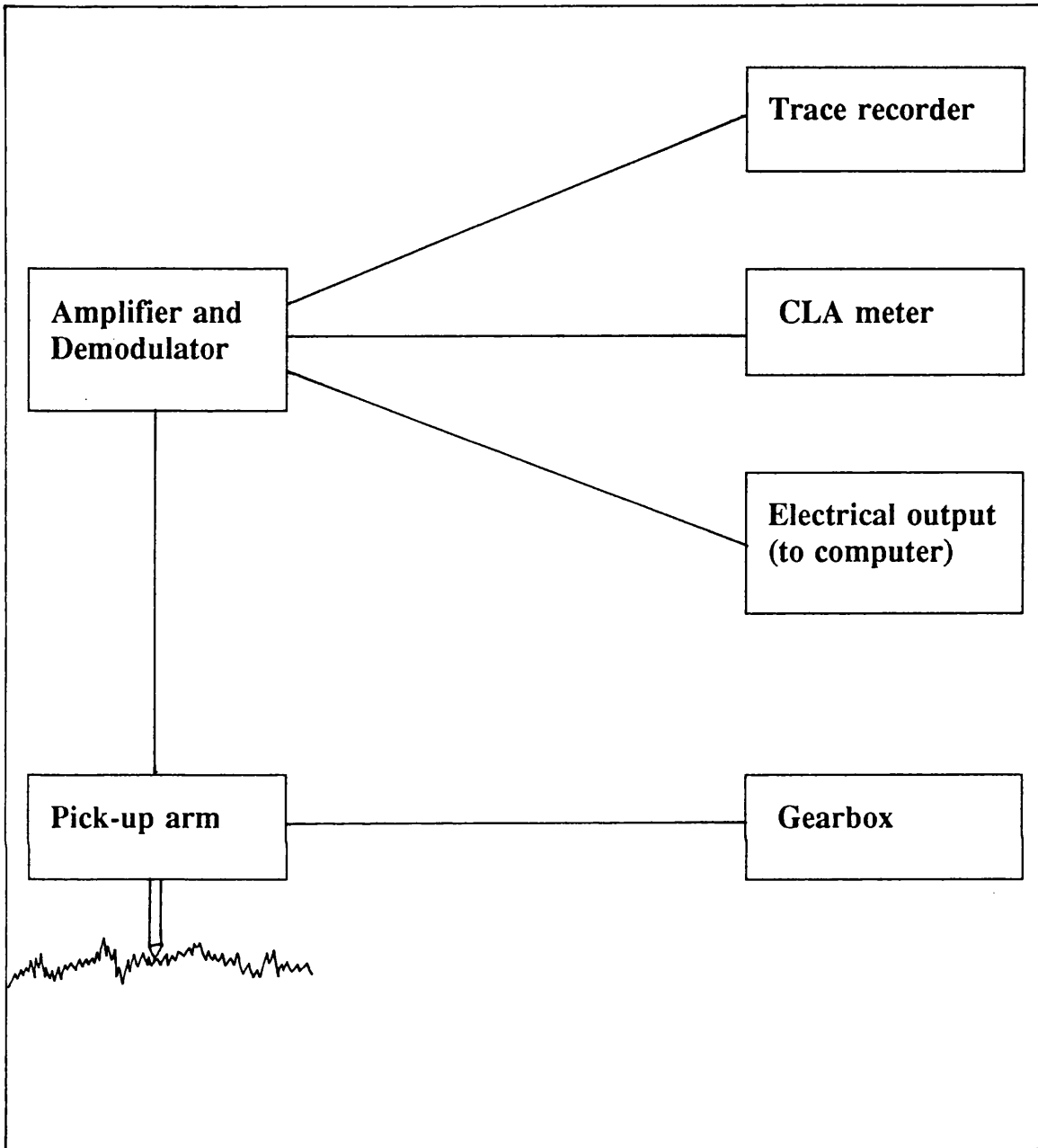


FIG. 2.1 Diagrammatic illustration of the principle of surface profilometry (adapted from James, 1986).

Nevertheless, Nakamura (1966) claimed that the errors due to the stylus dimensions were insignificant, and Guerrero & Black (1972) showed that lateral movement and stylus hopping were not serious problems. In addition, a great advantage of the stylus technique is that it can give a record of the surface profile more quickly and conveniently than many other methods, and does not cause destruction of the testing surfaces.

2.2.2.2 Experimental

Surface texture measurement was carried out on the polished stainless steel disk surface. It was also performed on the unpolished disk to observe the differences, due to polishing, that resulted in the surface topography of the polished disk. The analyses were accomplished using a Rank Taylor Hobson stylus profilometer, Talysurf 6 (Rank Precision Industries Metrology Division, Leicester, UK) at 20°C under laboratory conditions. A 2µm stylus tip was used in conjunction with a 0.25mm filter cut-off length. Four determinations were performed at random on each disk perpendicular to the lay of the surface (i.e., radially).

2.2.2.3 Results and Discussion

The three-dimensional variation of a solid surface can be considered to comprise a number of arbitrary classes of surface texture, defined by their horizontal scale. Large wavelength features are classified as errors in form, intermediate wavelengths as waviness, and short wavelength variations as roughness (see Fig. 2.2).

The surface profilometer records of the two stainless steel disks are illustrated in Plate 2.4. Visual inspection of the two profiles, taking into consideration of their different vertical magnifications, showed obvious differences in their errors in form. Less waviness of the surface profile was also observed in Plate 2.4b. In addition, the peaks shown in Plate 2.4b are more flat and the variation in surface height, i.e., roughness, is much less than that in Plate 2.4a. These various observed differences were possibly the results of plastic flow of the surface asperities of the polished disk

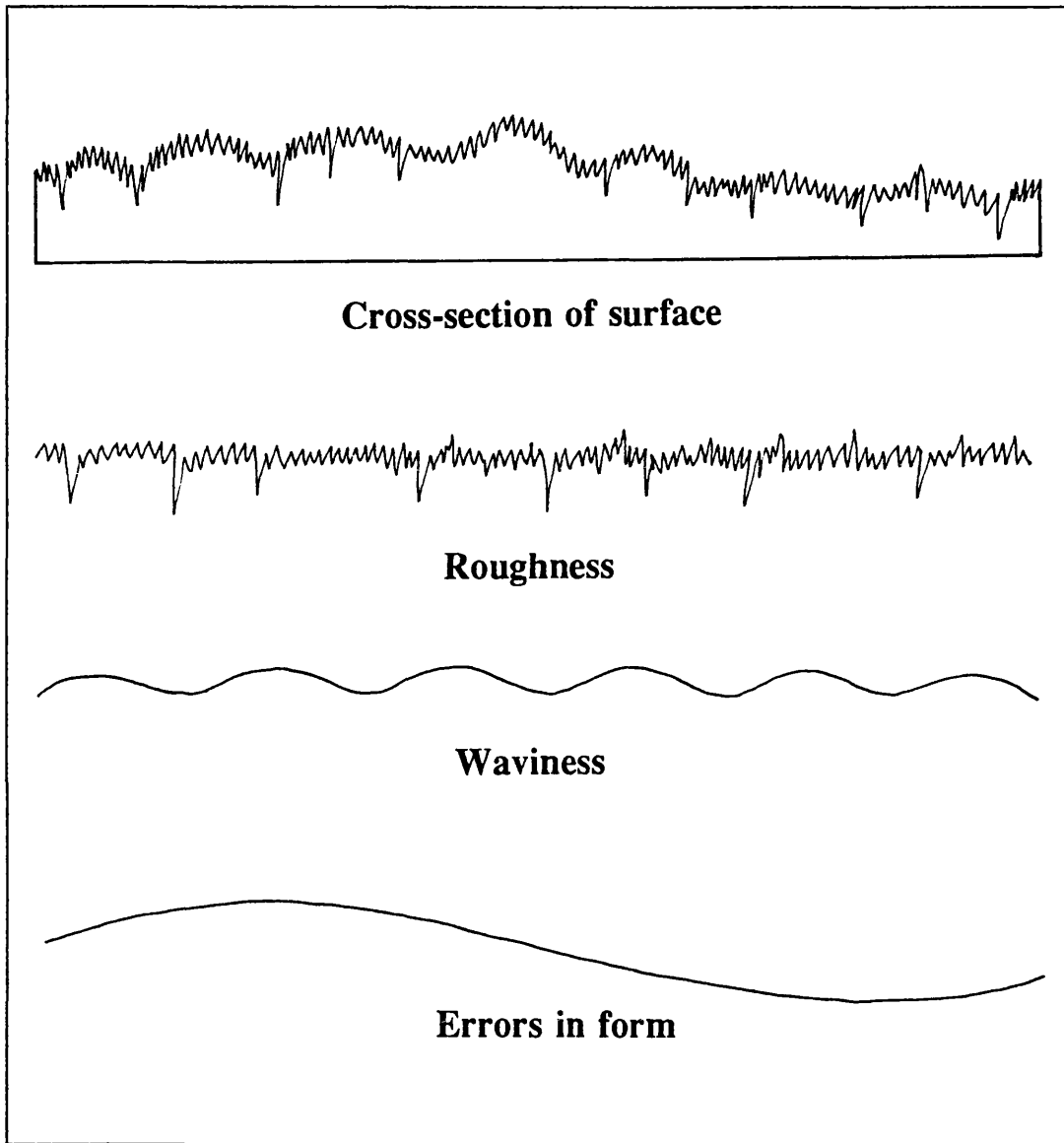
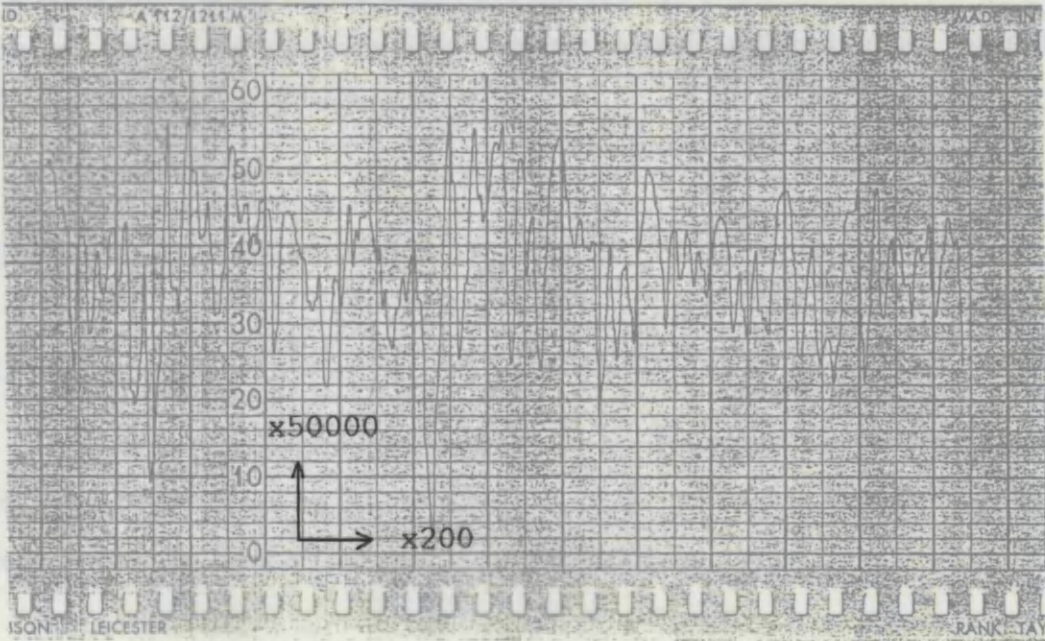
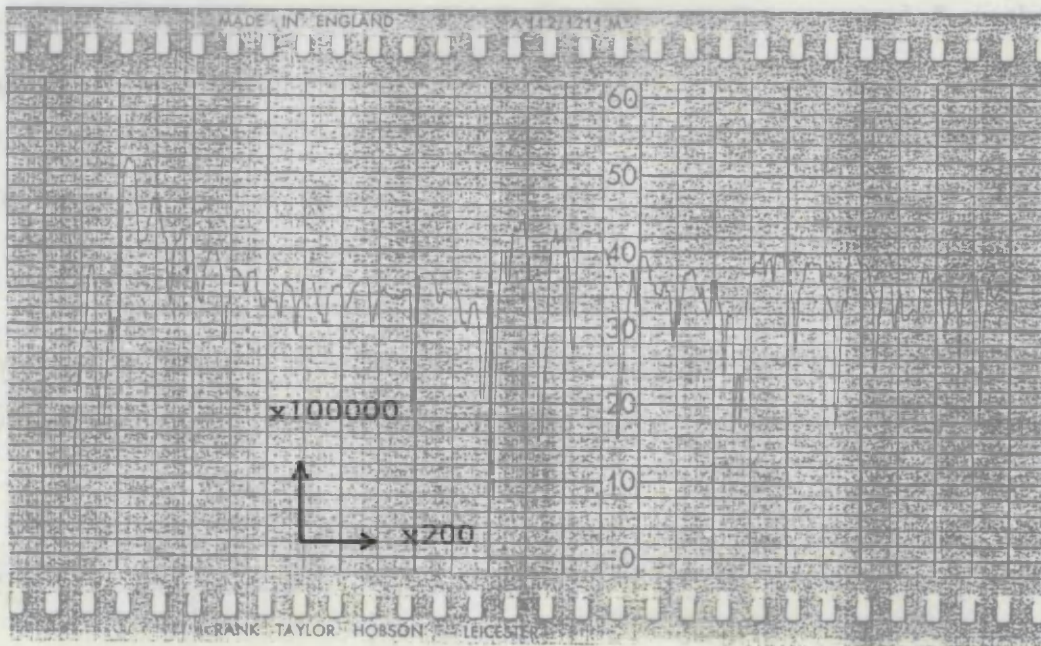


FIG. 2.2 Roughness, waviness and errors in form (from James, 1986).

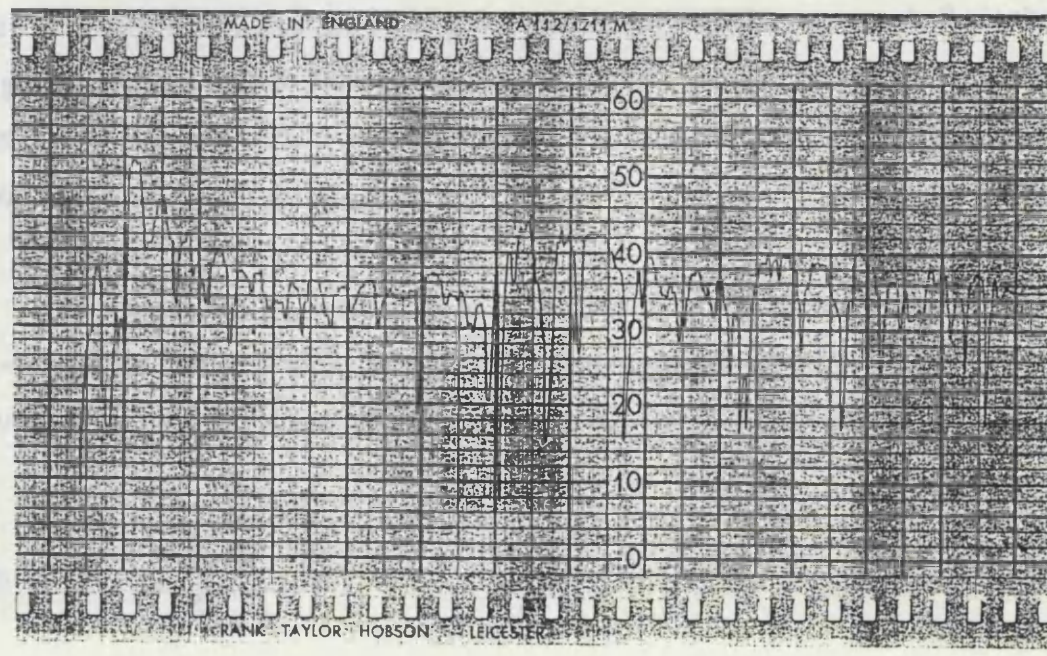
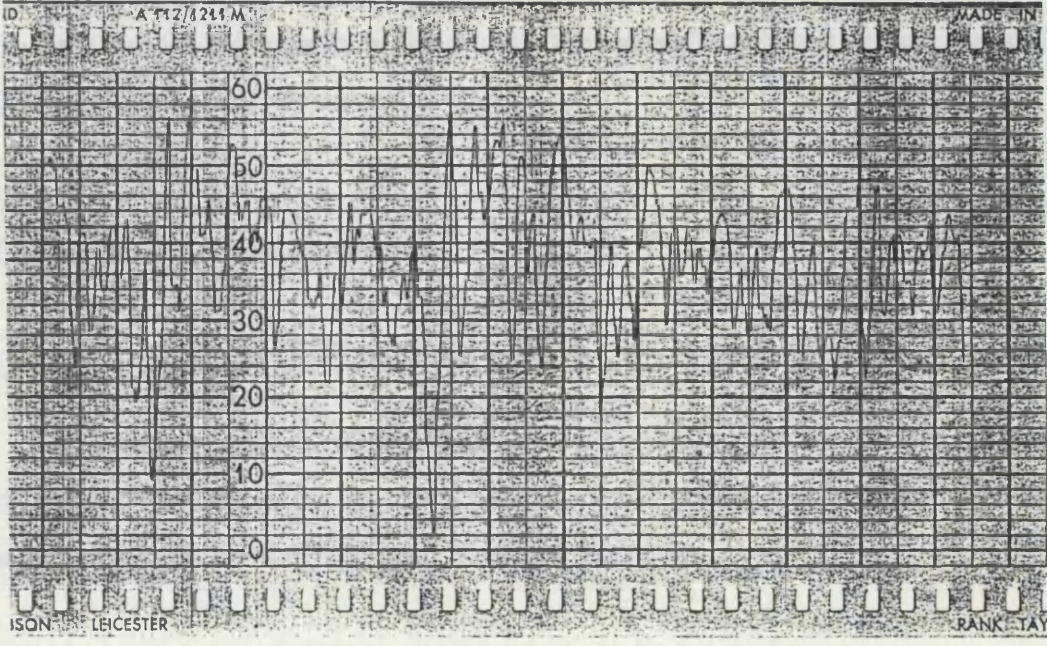


a) Surface profile of the unpolished stainless steel disk.



b) Surface profile of the polished stainless steel disk.

PLATE 2.4 Talysurf profilometer records of the unpolished and polished stainless steel disks.



during the process of polishing, due to the immense heat generated at the points of rubbing contact, which caused the surface material to soften or melt. Moreover the deep valley features are mostly absent in Plate 2.4b, probably as a consequence of these deep valleys being partially filled up by the thermally softened surface material which later cooled and re-hardened.

2.2.3 Surface Texture Parameters

2.2.3.1 Introduction

A number of surface roughness parameters are used to describe surface profiles and surfaces themselves by the characteristics of the height distribution within the assessment length, L , of a horizontal trace (see Fig. 2.3).

Parameters such as R_p , the maximum peak height and R_v , the maximum valley depth, are the corresponding maximum deviations of the profile above and below the mean line, within the assessment length. The mean (or reference) line is the line drawn in such a way that the areas above and below this line are equal. R_y is the largest maximum peak-to-valley height of the profile. These 3 parameters are very sensitive to atypical surface features such as localized scratches and represent the extremes of the height distribution.

The parameter, R_{tm} is the mean of R_p , the maximum peak-to-valley heights (ie., R_p+R_v) of the profile, within the assessment length. It was used by Nadkarni *et al.* (1975) to describe roughness of tablet surfaces. R_{tm} can be expressed as follows:

$$R_{tm} = \frac{R_{t1} + R_{t2} + R_{t3} + R_{t4} + R_{t5}}{5} \quad (2.2)$$

The rugosity of a surface is, however, very commonly expressed by R_a , the international parameter of roughness, which is defined as the arithmetic mean of the

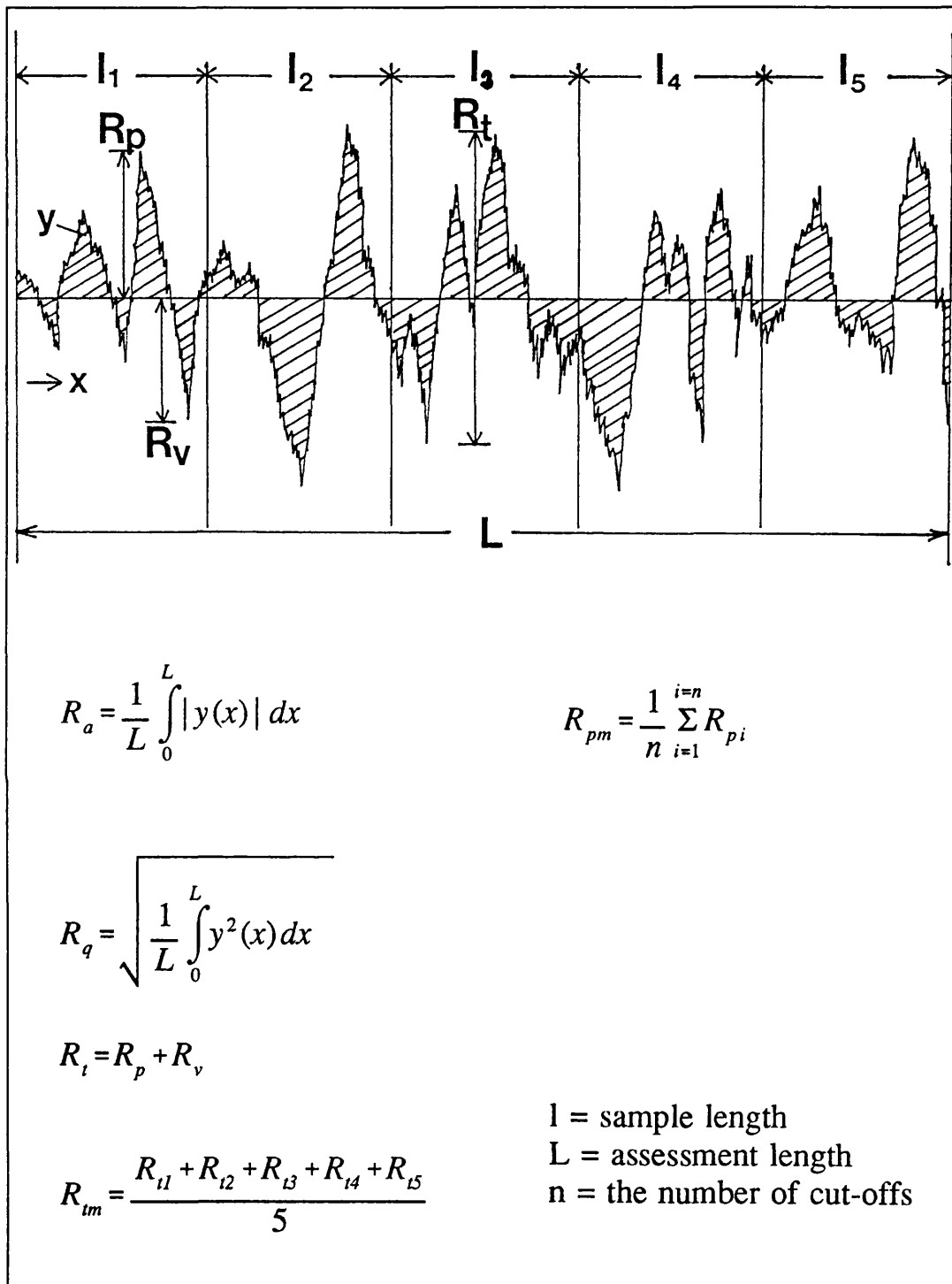


FIG. 2.3 Diagrammatic representations of some surface roughness parameters.

departures of the roughness profiles from the mean line. In general, the lower the R_a value, the smoother is the surface. Mathematically, R_a is given as:

$$R_a = \frac{1}{L} \int_0^L |y(x)| dx \quad (2.3)$$

This roughness parameter was used by Rowe (1977, 1978a) to quantify the surface appearance of film-coated tablets, as a function of some process conditions. On other occasions, R_a was employed to characterize tablet surface quality (Rowe, 1979) and as a quantitative measure of the adhesion of some effervescent powder formulations to compression tools (Sendall & Staniforth, 1986). Moreover, the R_a parameter was shown to be an indicator of the adhesion of polymer films to tablet surfaces (Rowe, 1978b), but no such relationship was found for the R_{tm} (Nadkarni *et al.*, 1975). R_q , the root-mean-square (rms) parameter of R_a , was used by Toyoshima *et al.* (1988) to evaluate quantitatively the phenomenon of tablet sticking to punch face. It is defined by the following mathematical formula:

$$R_q = \sqrt{\frac{1}{L} \int_0^L y^2(x) dx} \quad (2.4)$$

Other surface texture parameters such as R_{sk} and R_{ku} describe respectively, the skewness and kurtosis of a surface profile. The ISO ten point height parameter, R_z , is numerically the average height difference between the five highest peaks and the five lowest valleys within the assessment length. It is measured from an arbitrary line drawn parallel to the reference line but not crossing the profile, and would therefore require further data processing of the profile signal.

Whilst the amplitude (roughness) parameters give evaluations of the vertical characteristics of a surface deviation, information regarding the horizontal

characteristics can be obtained from the spacing parameters. One measurement of which, having particular relevance to the present adhesion study, is S, the mean spacing of adjacent local peaks.

2.2.3.2 Results and Discussion

The surface texture parameters obtained for the two stainless steel disks are shown in Table 2.4. A lower R_a value is indicated for the polished disk. Since all the other roughness values are also lower for the polished disk than for the unpolished one, this statistically substantiates the former having a smoother surface than the latter. The S value ($=12.4\mu\text{m}$) of the polished disk was used as a reference index in later adhesion experiments (see Section 4.2.2.2).

2.2.4 Conclusions

The surface topography of the polished stainless steel substrate has been characterized by a stylus profilometry technique, with the surface texture being defined by the various statistical roughness parameters obtained. The roughness parameter, R_a , was used in this work to represent the surface rugosity of the polished disk, the value obtained being $0.17\mu\text{m}$. This R_a value together with the S value for the polished disk, were utilized to elucidate the relative positioning of the adhering particles on the steel substrate surface.

TABLE 2.4 Statistical surface texture parameters of the polished and unpolished stainless steel disks.
(s.d.=standard deviation)

Surface roughness parameter	Polished disk			Unpolished disk		
	x (µm)	$X_{\min}-X_{\max}$ (µm)	s.d. (µm)	x (µm)	$X_{\min}-X_{\max}$ (µm)	s.d. (µm)
R_a	0.17	0.13-0.20	0.03	0.60	0.25-0.93	0.28
R_q	0.27	0.23-0.31	0.04	0.77	0.32-1.13	0.34
R_y	2.0	1.4-2.7	0.5	4.5	2.0-5.4	1.6
R_{tm}	1.2	1.1-1.5	0.2	3.4	1.5-4.8	1.4
R_v	1.1	0.9-1.4	0.2	2.7	1.2-3.4	1.0
R_p	1.1	0.5-2.4	0.9	1.8	0.8-2.7	0.8
R_{pm}	0.5	0.3-0.6	0.2	1.4	0.6-2.3	0.7
S	12.4	10.9-14.5	1.7	13.5	9.1-16.3	3.1

CHAPTER 3

Technique for Measurement of Adhesive Forces Between Particles and a Substrate Surface

3. TECHNIQUE FOR MEASUREMENT OF ADHESIVE FORCES BETWEEN PARTICLES AND A SUBSTRATE SURFACE

3.1 DETERMINATION OF PARTICLE-SUBSTRATE ADHESION FORCES

3.1.1 Introduction

The centrifuge technique is widely used in determining adhesive forces of particles to flat surfaces, in air. The principle of this method is to evaluate, statistically, the average particle-substrate adhesion force by separating the particles from the surface of a substrate by the application of centrifugal forces.

Pharmaceutically, the centrifuge technique was used by Gillespie & Rideal (1955) for studying the adhesion of aerosol drops on solid surfaces. A centrifuge method was used by Otsuka *et al.* (1983) to investigate the effect of temperature on the adhesion between some organic powders and a glass plane, and by Kulvanich & Stewart (1987a) to measure the adhesion of several powdered drugs to substrates. Booth & Newton (1987) studied the adhesion behaviour of two pharmaceutical powders on various types of metal and polymer materials.

By replacing the conventional inorganic substrate surface by the surface of a tablet made from compaction of a powder of interest, Okada *et al.* (1969) determined the interaction forces between the same and different kinds of pharmaceutical powder materials. On the other hand, a modified centrifuge method, in which a two-compartment cell separated by a crossed-wire screen, was used by Donald (1969) to evaluate the adhesion of particles on bead surfaces. A similar technique was described by Staniforth *et al.* (1980) in a study of the adhesion characteristics of some ordered mixes, and later (*Staniforth et al., 1981, 1982*) employed in measuring the interparticle forces between drug and excipient powder particles bound in binary and ternary ordered units. Laycock & Staniforth (1983) developed a thin brass plate, with a small

diameter hole to contain an interactive unit, for examining the adhesion of drug particles.

3.1.2 Experimental Technique for Measuring Adhesive Forces

In this work, the centrifuge technique was employed for determinations of adhesion forces of the test pharmaceutical powder excipients on the characterized stainless steel substrate. With regard to the design of the centrifuge tube to contain the particles-substrate interactive system (see following Section 3.2.2), the force of adhesion can be interpreted as equal in magnitude, but opposite in sign, to the centrifugal force required to dislodge the particles from the substrate. The generated centrifugal force, F , either to force the particles on to or to remove them from the steel disk surface, can be calculated by the following equation:

$$F = m\omega^2r \quad (3.1)$$

where m is the particle mass, ω is the angular velocity and r is the distance between the particle-substrate contact plane and the centre of the rotational axis.

3.2 APPARATUS

3.2.1 Centrifuge

All adhesion measurements were performed by means of an MSE High-Speed 18 Refrigerator Ultracentrifuge (Fisons, UK) (see Plates 3.1 & 3.2) with an 8×50ml fixed angle rotor (Plate 3.3), which allowed rotation speeds up to 18,000rpm, corresponding to a centrifugal acceleration of 38,000g (where g is the gravitational acceleration).

3.2.2 Purpose-Built Centrifuge Cells

Two specially designed, 50ml size, identical rotor tubes (Plate 3.4), as described by Booth & Newton (1987), were constructed to contain the particle-steel substrate adhesive system. The material chosen for construction was considered on grounds of its weight, rigidity and durability. Since transparency was not important in this work, Nylon was chosen because it was light in weight as well as easy to machine and thread. Also, its intrinsic rigidity would enable the rotor tubes to withstand high centrifugal forces.

A schematic drawing of one centrifuge tube is shown in Fig. 3.1. The lower half of the tube was split into two parts along a line parallel to the rotational axis. Into each part was inserted an aluminium holder in half, whose function together was to hold the steel disk firmly in place. Moreover, screws were used rather than pins as during spinning, the latter might be centrifuging out under their own weight. This not only would disengage the lower two halves of the centrifuge cell, but could cause damage to the wall of the rotor pocket.

Although the rotor tube was inclined to the vertical rotational axis when positioned in place in the rotor, it has been designed such that the steel disk was orientated with its test surface parallel to the vertical axis of rotation of the centrifuge and the acceleration forces acted in a direction normal to the substrate surface. The



PLATE 3.1 The MSE High-Speed 18 Ultracentrifuge.



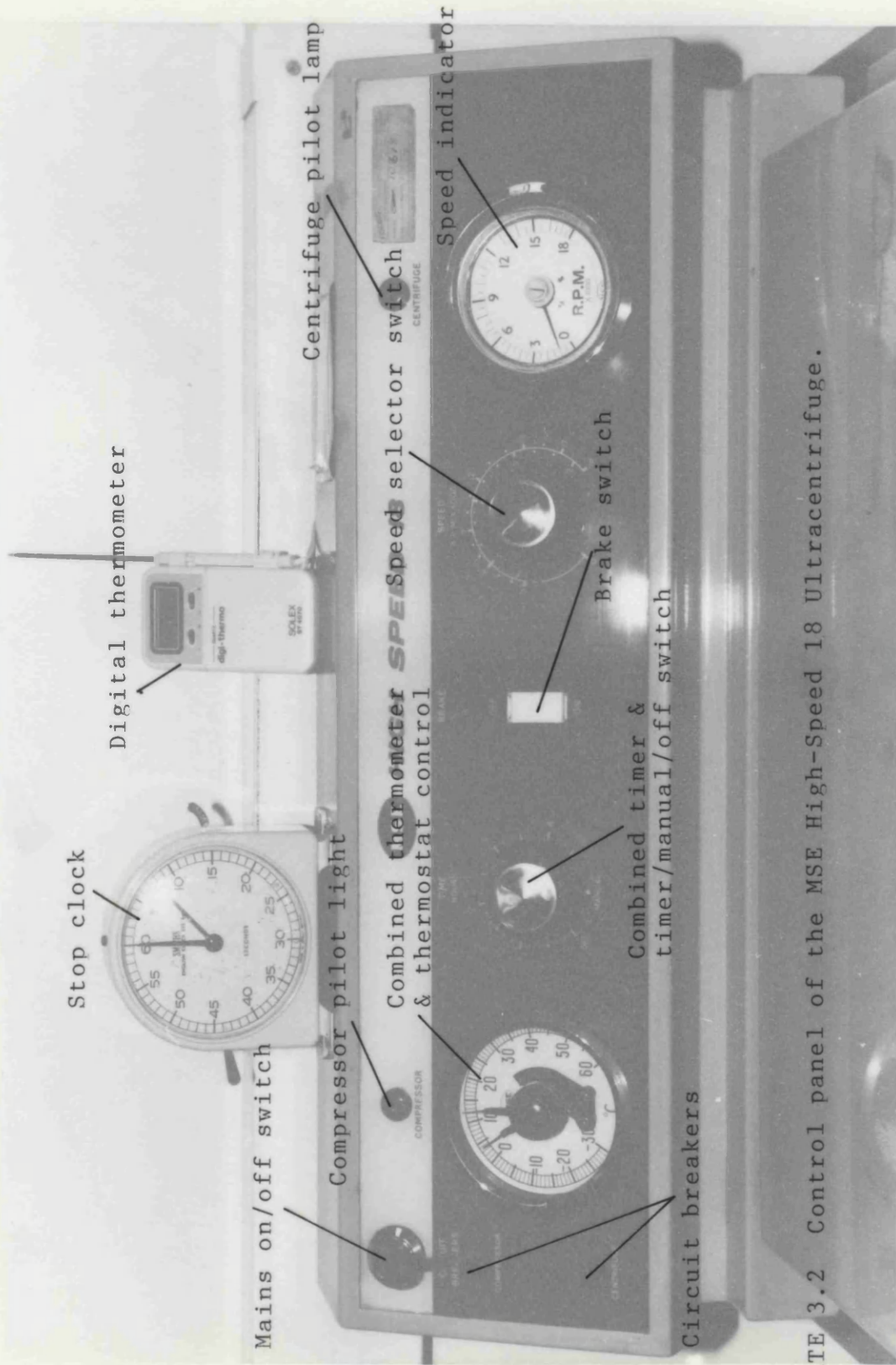
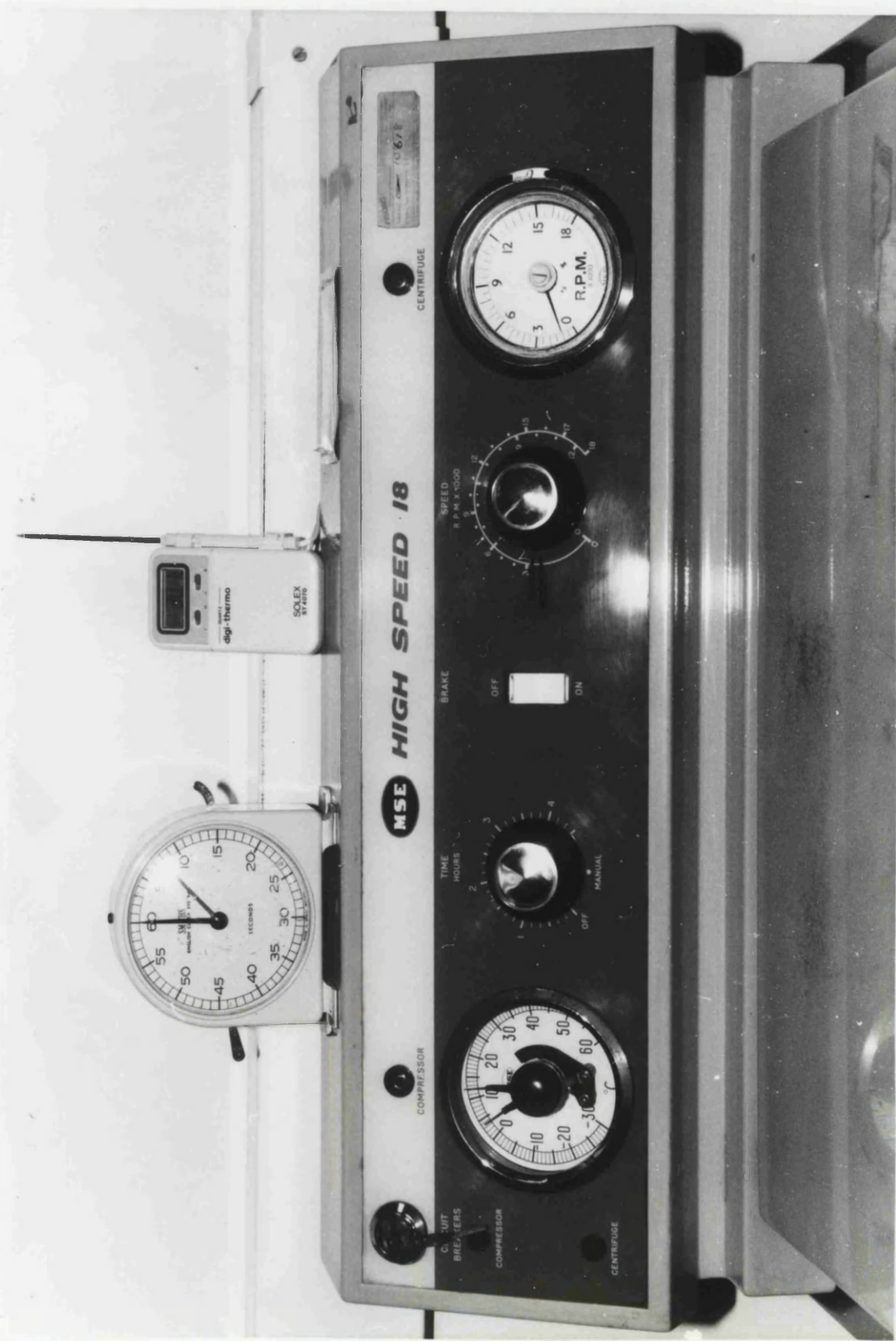
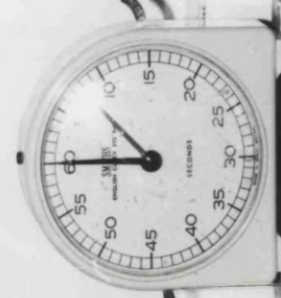


PLATE 3.2 Control panel of the MSE High-Speed 18 Ultracentrifuge.



10 678

MSE HIGH SPEED 18



SOLEX STAIN
digi-Thermo

COMPRESSOR

STOP BREAKERS COMPRESSOR

CENTRIFUGE

BRAKE

TIME HOURS

SPEED

COMPRESSOR

CENTRIFUGE

MANUAL

R.P.M. x 1000

CENTRIFUGE

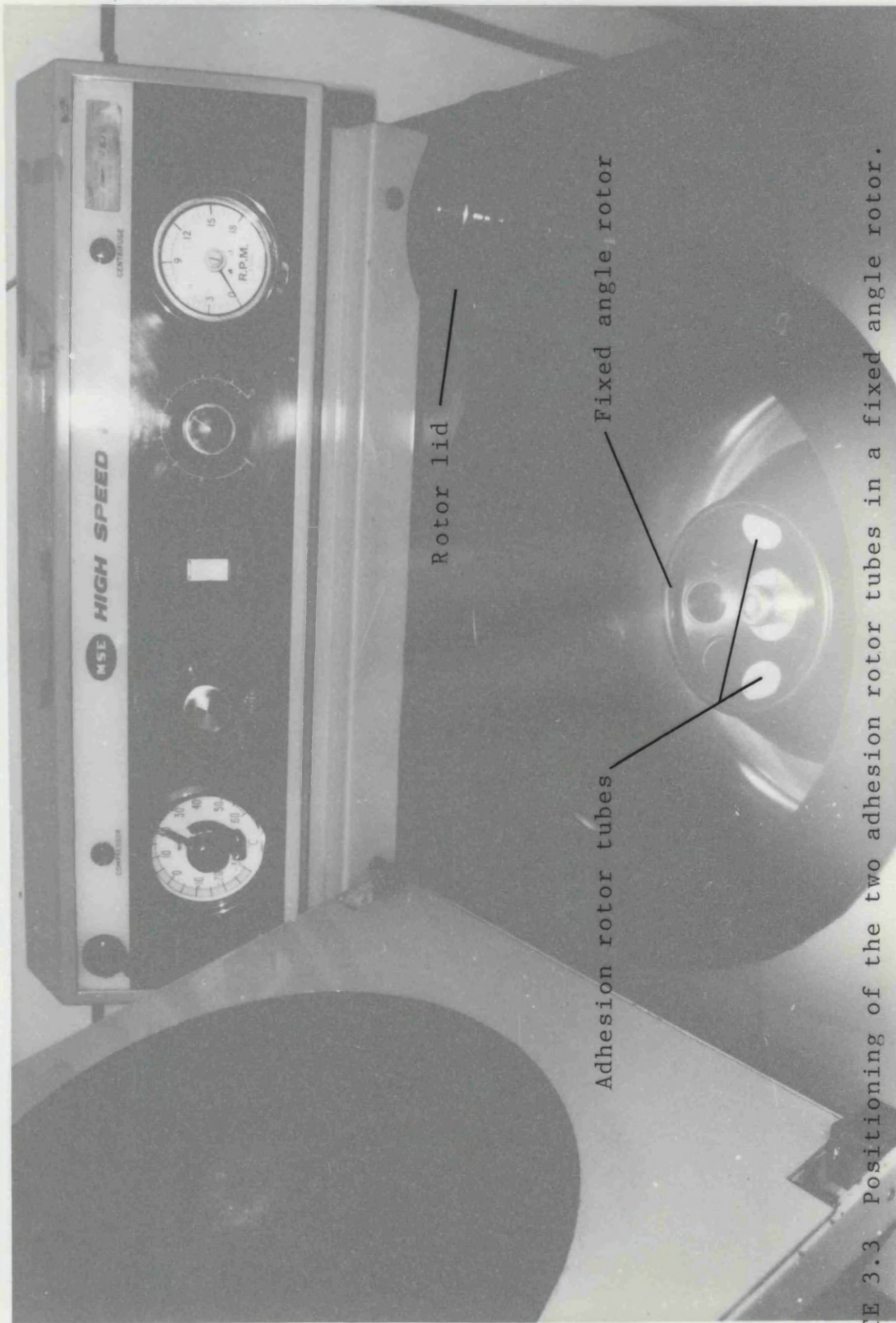


PLATE 3.3 Positioning of the two adhesion rotor tubes in a fixed angle rotor.



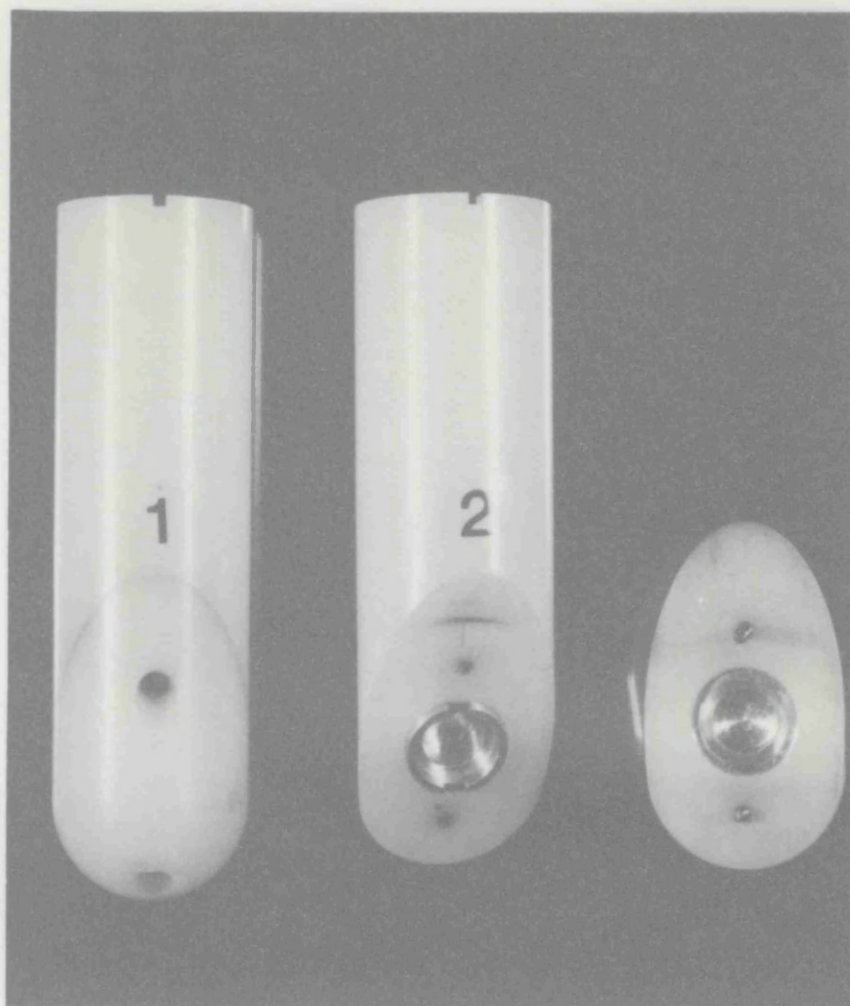


PLATE 3.4 Two specially designed adhesion rotor tubes.



Handwritten notes in the left margin, including the number '1' and some illegible text.

Faint, illegible handwritten text in the center of the page.

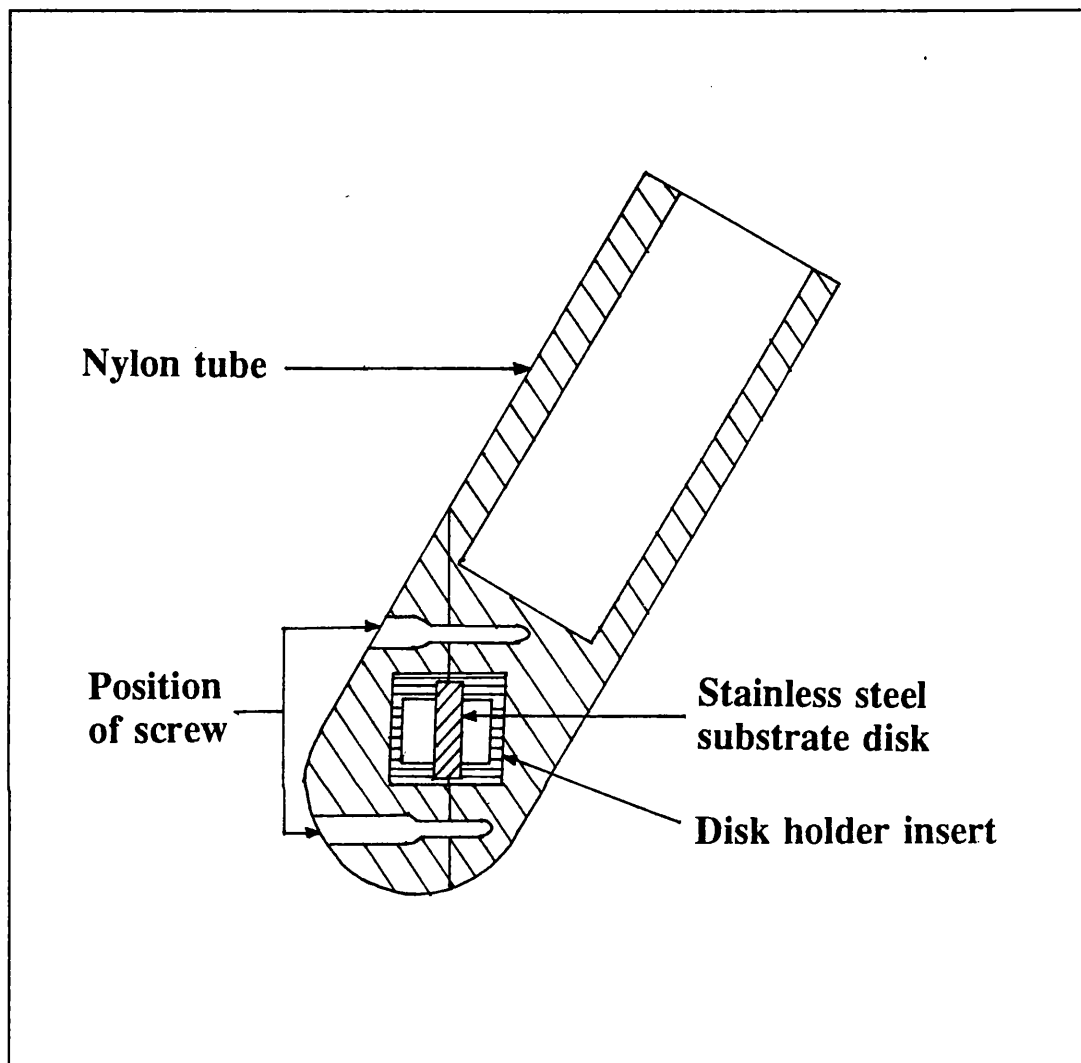


FIG. 3.1 A schematic diagram of the specially designed rotor tube (1:1).

relative centrifugal force (RCF) experienced by the particles can be calculated by the following formula:

$$RCF = \frac{\omega^2 r}{g} \quad (3.2)$$

where ω is the angular velocity, r is the centrifugal distance, and g is 9.82ms^{-2} , the gravitational acceleration. The RCF values at the particles at some of the centrifuge speeds used in experimentations are given in Table 3.1. The design of the rotor tube was also such that the distance of the test surface from the central rotational axis differed in the press-on and spin-off modes.

3.2.3 Counting of Adhering Particles on a Substrate Surface

Determination of the number of particles on the substrate before and after each centrifugation can be conveniently performed by counting the particles under a microscope. This method was used in a number of investigations (*Kordecki & Orr, 1960; Deryaguin & Zimon, 1961; Zimon & Volkova, 1965; Booth & Newton, 1987*).

The particle counting microscope system used throughout this work is shown in Plate 3.5. Only the particles that were deposited within the grid squares, 1-2-3-4, of the disk surface (see Plate 2.3) were counted and the total number was recorded. A ‘cold’ light source (Schott KL-1500T, Germany) was used to illuminate the ‘dusted’ surface of the steel disk because of the close positioning of the two light guides to the disk necessary to provide sufficient brightness for viewing (see Plate 3.6), and adhesive force can increase with rising temperature (*Otsuka et al., 1983*). This can therefore minimize any build up of heat in the vicinity of the particles adhering on the substrate, since the heat producing (infra-red) spectrum of the light was filtered out.

TABLE 3.1 The relative centrifugal forces (RCF) at the particles at some of the rotation speeds ($g=9.82\text{ms}^{-2}$).

Centrifuge speed (rpm)	Press-on RCF (g)	Spin-off RCF (g)
3000	871	901
5000	2419	2503
7000	4741	4906
10000	9676	10011
12000	13934	14417
15000	21772	22526
17000	27965	28933

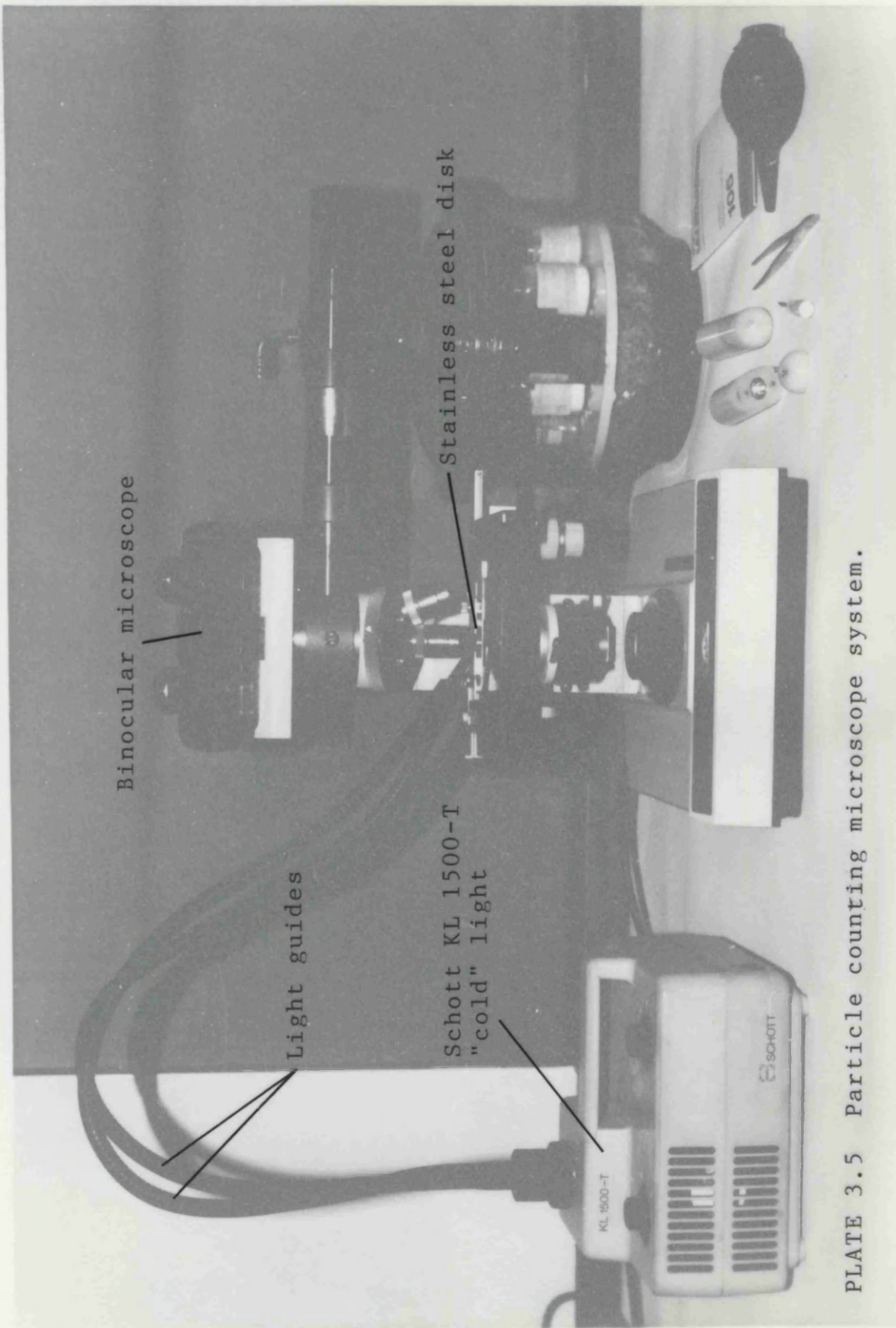
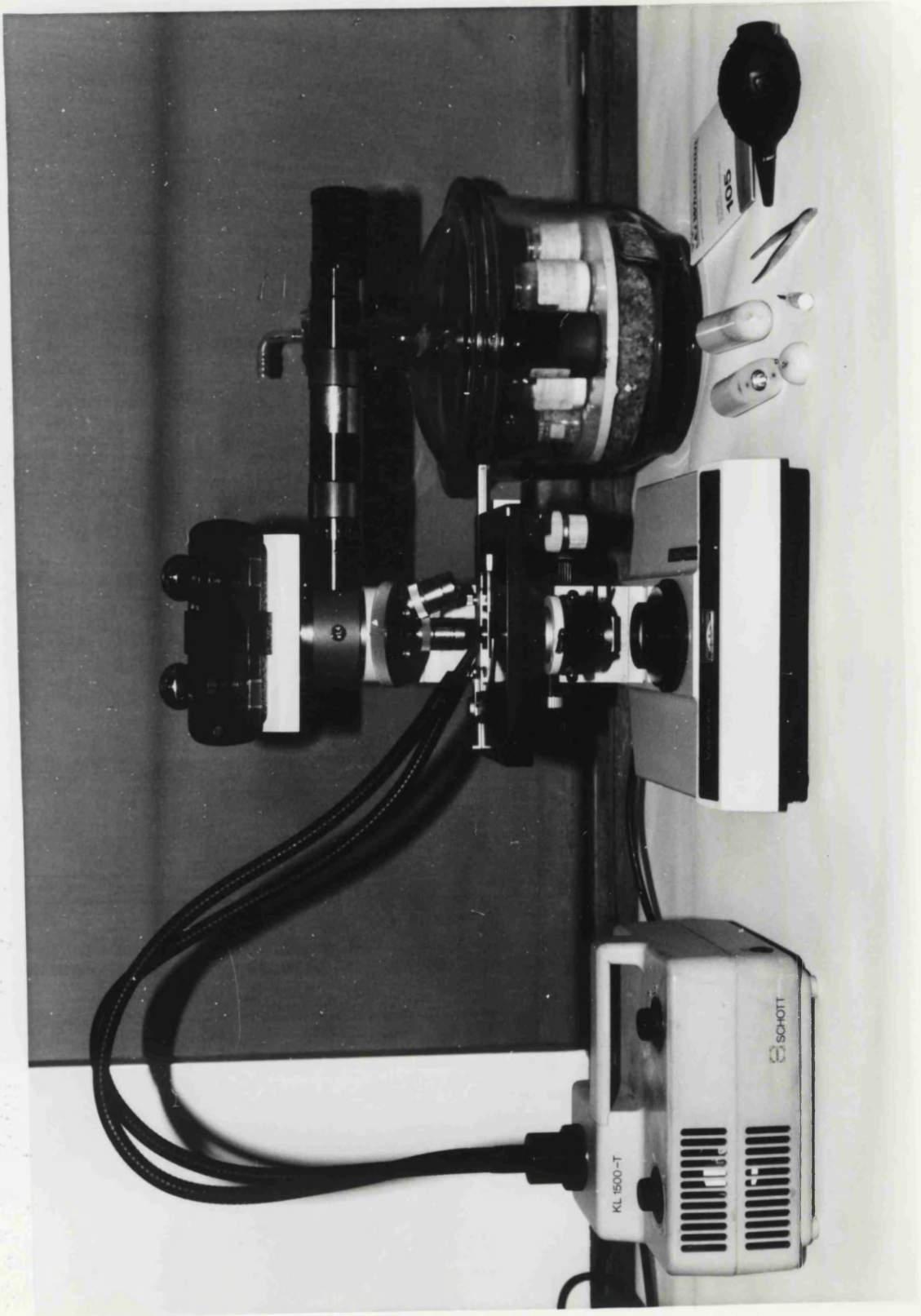


PLATE 3.5 Particle counting microscope system.



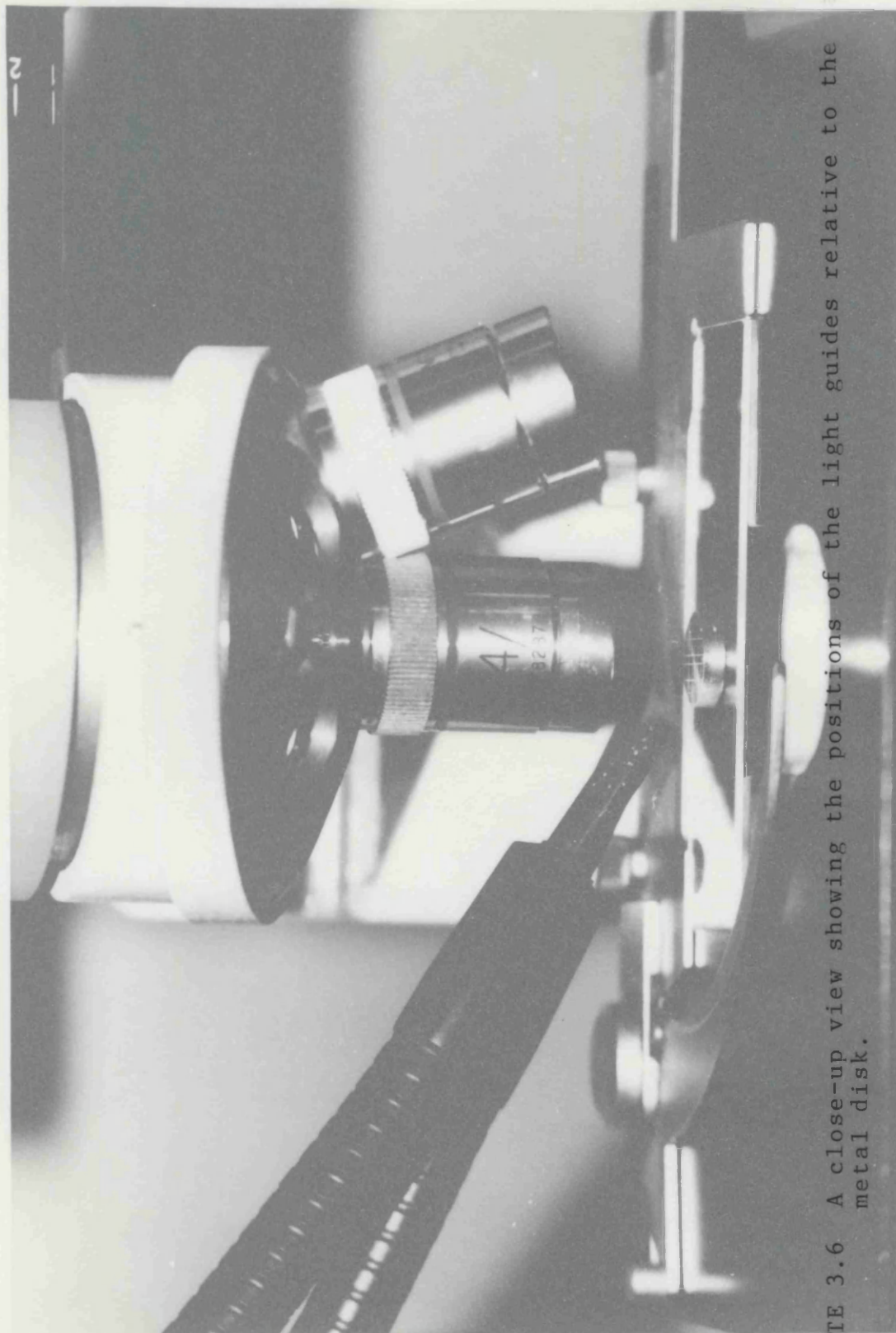
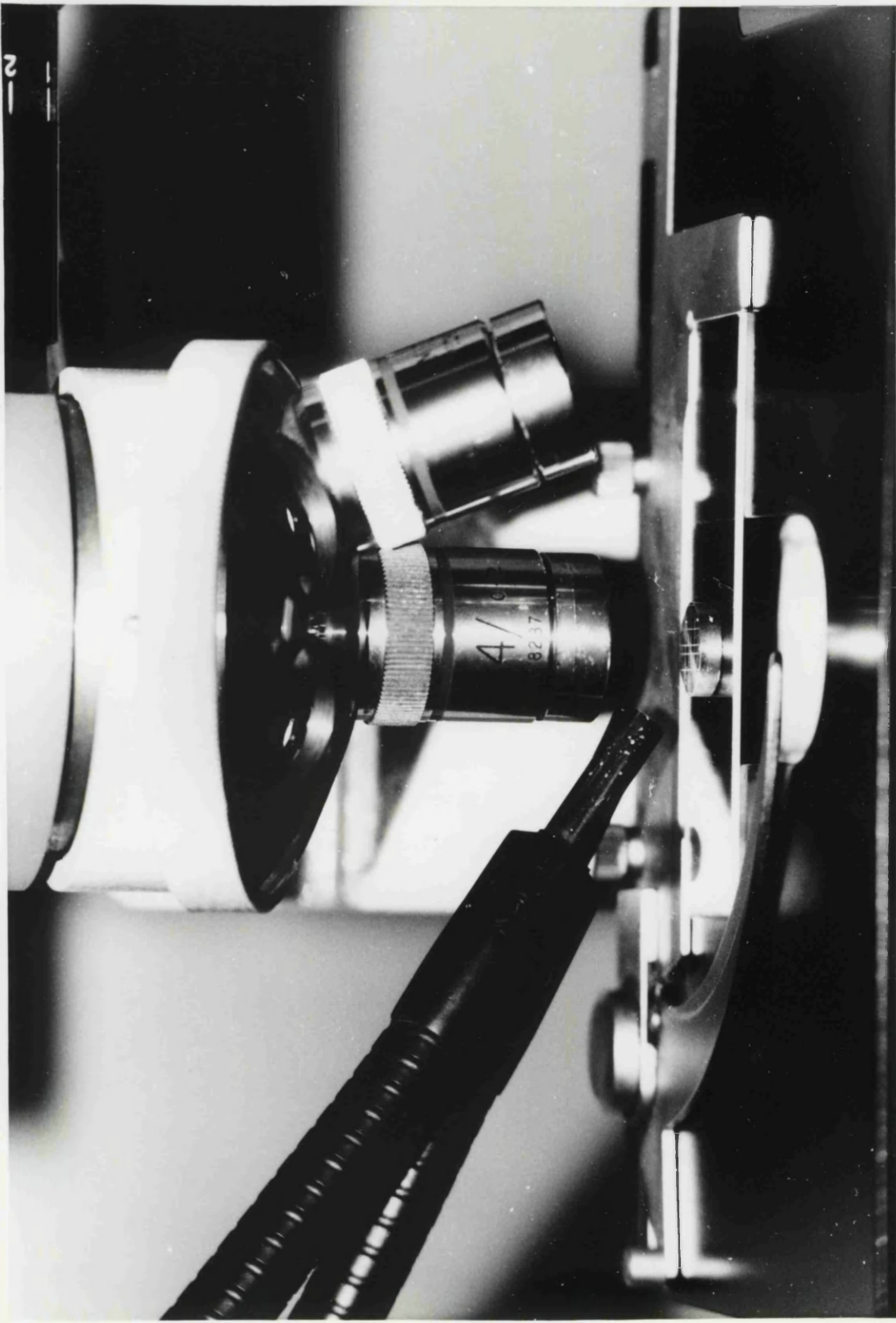


PLATE 3.6 A close-up view showing the positions of the light guides relative to the metal disk.



CHAPTER 4

Effect of Applied Compression on the Adhesion of Powders to Stainless Steel

4. ***EFFECT OF APPLIED COMPRESSION ON THE ADHESION OF POWDERS TO STAINLESS STEEL***

4.1 INTRODUCTION

Collisions between particles and a solid substrate, with subsequent adhesion under the effect of inertial forces, occur frequently in practice, for examples, in the precipitation of aerosol particles from a gas stream and in the deposition of dust particles, etc. Apart from the kind of compression forces that particulate solids are normally subjected to in tableting, forces of a much smaller nature, for instance, forces such as might be exerted by the weight of a powder bed in packing or the forces imposed by an auger in moving the material, will also be encountered.

The adhesion of an elastic sphere with a rigid surface, in the absence of an applied force, was considered by some researchers (e.g. *Deryaguin et al., 1975c; Muller et al., 1980*). Dahneke (1971) and Esmen *et al.* (1978) studied the adhesion of particles arising from impacts involving only elastic deformations of the impacting bodies. Plastic deformation caused by impact was discussed by Tabor (1948), and Richmond *et al.* (1974) investigated a rigid ball-plastic plate case. Brenner *et al.* (1981) examined the case of an impact of a purely plastic particle with a rigid surface with the recovery stage being due to elastic recovery processes. On the other hand, Rogers & Reed (1984) studied the adhesion of particles arising from elastic-plastic impacts with a surface, in which there was elastic deformation in both bodies as well as plastic deformation in one or other body. A feature of elastic-plastic impacts is that the geometry of the bodies is changed by the impact; the area of plastic deformation being surrounded by an annulus in which only elastic deformations occur. The effect of preliminary compression of particles, under an elastic compression wave, on their adhesion to a rigid surface was considered by Muller *et al.* (1976). A theoretical analysis of the influence of preliminary compression on the components of adhesion forces for the case of the contact of rigid elastic particles with a plane surface, was carried out by Deryaguin *et al.* (1984).

Much of the work pertinent to the subject of preliminary pressing-on on particle adhesion to a substrate was reported mainly outside of the pharmaceutical field, generally in metallurgical, material and colloid sciences. Pharmaceutical powders, in common with other types of materials, can exhibit characteristic adhesion properties. Bulk mechanical properties such as yield pressure and surface hardness are sometimes quoted as comparative parameters. A knowledge of the adhesion forces of pharmaceutical powder particles adhering to a solid surface would allow more insight into the adhesion behaviour of these types of particulate solids.

In practice, particles, especially pharmaceutical materials, are seldom spherical, but are highly irregular and rough. Thus, determinations of adhesive forces using formulae derived from ideal situations very often do not yield results which are reliable or have practical significance, as illustrated by Jordan (1954), Rumpf (1977) and Otsuka *et al.* (1988). An alternative approach is to examine the behaviour of many particles at one time to obtain a representative average value of the adhesion force; this can be achieved by practical experimentation. The aim of this chapter is to investigate the adhesion properties of the four powder excipients under the effect of various preliminary applied forces.

4.2 EXPERIMENTAL METHOD

4.2.1 Preparation of Particle-Steel Adhesive System

Prior to each experiment, the stainless steel substrate surface was wiped with a lens tissue soaked with acetone, and throughout the course of the work, the substrate was occasionally cleaned by immersion in the solvent in an ultra-sonic bath. Once cleaned, handling of it was kept to a minimum and then only with a pair of clean metal forceps. The size fraction of PEG 4000, Starch 1500 and spray-dried lactose used for this study was $-56+45\mu\text{m}$. Due to the small quantity of this size range of heavy precipitated calcium carbonate present in the sample, a lower size fraction ($-45+32\mu\text{m}$) was chosen. The powder material was gently 'dusted' onto the substrate surface at room temperature and relative humidities not exceeding 55%. Particle deposition was performed, first of all, by using a micro-spatula to sprinkle a small amount of a powder sample onto a Dural plate, which was inverted and positioned at a small height above the disk. The plate was then gently tapped a few times to dislodge the particles from its underside to fall, under gravity, on to the substrate surface.

The weight of the micron-sized test particles was considered generally small in comparison with the adhesion forces, and with the small distance of fall, the momentum acquired by the particles during free fall was assumed to be negligible (*Krupp, 1967*). After settling on the disk surface, the particles were probably rested on top of the substrate roughnesses rather than embedded within the troughs of the rugosities. At the same time, care was also taken to ensure the particles deposited on the substrate surface were separated from each other by an average distance larger than the size of the particle, to minimize the influence of interparticle interactions on adhesion. Finally, the 'dusted' disk was gently turned upside down to allow any loose particles to fall off.

4.2.2 Adhesion Measurements of Powder Materials Without Preliminary Compression

4.2.2.1 Method

The prepared particles-laden disk from above was subsequently mounted into a purpose-built centrifuge tube (Section 3.2.2), which was then placed inside a rotor boring. The rotor was counter-balanced by a similar adhesion cell set-up (but without particles) in the opposite rotor pocket. In a particle detachment process, there will probably be a time lapse between the application of the detaching force and the break-away of particles from the substrate surface, due to a certain duration is usually needed for the particles to acquire the necessary kinetic energy to overcome the work of adhesion (*Muller et al., 1976; Barouch et al., 1987*). A centrifugation time of several seconds at an attained speed was found by Kordecki & Orr (1960), from experiments on different kinds of powders, to be sufficient for particles detachment. Prolongation of this centrifuging period would not have any significant effect on the break-away of particles in air, as suggested by Zimon (1982). Zimon's (1982) proposition could probably be substantiated by the very similar centrifugation times (usually not more than 1 minute) used by different workers in various adhesion experiments (*Staniforth et al., 1981; Otsuka et al., 1983; Booth & Newton, 1987; Kulvanich & Stewart, 1988*). In this work, the process of centrifugation was, therefore, maintained for 1 minute at a desired, initially low, speed, before allowing the rotor to decelerate. After stopping, the number of particles which remained adhering was determined by microscopy (see Section 3.2.3). The particles were then subjected to consecutively higher centrifugal force field until the percentage of adhering particles was less than 10%. Six to ten replicates were carried out for each powder. The temperature of the centrifuge chamber was held between 15° and 20°C during all centrifugations.

4.2.2.2 Results and Discussion

Since the particle sizes (-45+32µm and -56+45µm) used were large in comparison to the average substrate surface roughness ($R_a=0.17\mu\text{m}$) and its mean peak

spacing ($S=12.4\mu\text{m}$), surface contact between the particles and the steel disk would thereby be effected through touching the tips of the asperities on the two adhering surfaces.

The adhesion profiles of the four powders, which are integral adhesive force distribution curves of the particles, are shown in Fig. 4.1. Adhesion forces were calculated according to Equation (3.1). A distribution of the adhesion forces is observed in all materials. This scatter in adhesion forces could partly be due to a variation in the Hamaker constant of molecular interaction, over different contact areas, since real solid surfaces are generally regarded as energetically inhomogeneous. The importance of the factor of surface heterogeneity on particle adhesion has already been recognised by Zimon (1982). Variations in particle sizes within a particular size fraction would also cause a distribution of the adhesion forces. In addition, the random statistical nature of the asperity contacts, i.e., the presence on the contacting surfaces of the different local irregularities and geometries, could add to the spread in the force measurements.

There was a rapid loss of particles from the steel surface after application of the minimum measurable separation force of each material (Fig. 4.1). At those detachment forces, about 80% of Starch 1500 particles and approximately 90% of both PEG 4000 and spray-dried lactose showed adhesion forces less than $1.2\times 10^{-7}\text{N}$, whilst for calcium carbonate, over 95% of its particles indicated adhesion forces less than $0.9\times 10^{-7}\text{N}$. The largest adhesive forces exhibited by the most tenaciously adhering particles, irrespective of the powder, did not exceed $20\times 10^{-7}\text{N}$. This apparent lack of adhesion could be accounted for mainly by the surface roughness effect. Surface asperities of the contacting surfaces increased the distance between the bulk of the adherents, thereby decreasing the mutual attraction. Moreover, because the radii of curvature of the effective contacting microasperities were minute, this led to a very small area of contact over which contact forces were able to act. In addition, due to the van der Waals forces of attraction of the particular protuberances were rather small in accordance with their small radii (see Section 1.6.1.1), the resultant adhesion would inevitably be low.

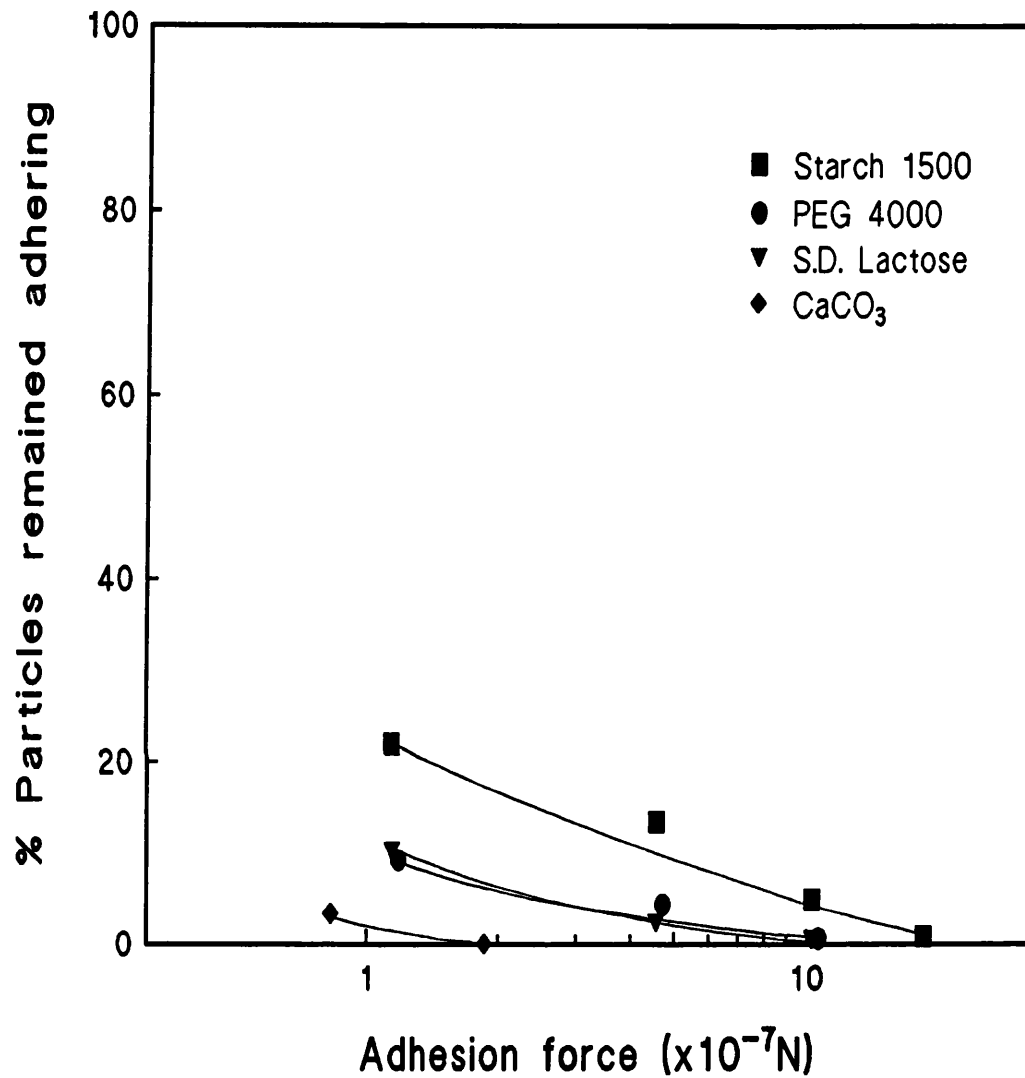


FIG. 4.1 Adhesion profiles of particulate materials to stainless steel, without preliminary forcing the powder solids to the substrate.

On the other hand, the scatter in adhesion forces could also be due to the powders being used in their 'as received' states. Under such conditions, the surfaces of the particles will undoubtedly be 'contaminated' by adsorbed gases and substances such as grease and lubricants, etc. These surface 'contaminants', although not changing the nominal contact between particles and the disk, could possibly decrease the fraction of the true contact area, thereby diminishing the adhesion, as exemplified by Brenner *et al.* (1981) on metal-metal contact.

It can be seen from Fig. 4.1 that, the adhesion profiles of PEG 4000 and spray-dried lactose are very close to each other. This suggested that, the adhesions of both solids to the steel surface were very similar. It would appear to be surprising since larger adhesive forces would be expected from the lamellar-shaped particles of PEG 4000 because of their, apparently, larger available 'flat' crystal faces to allow more contacts to be established. The observed results could, perhaps, be partly explained on the basis of the findings by Sano *et al.* (1984) and Otsuka *et al.* (1988). These workers found that, as a particle deviated from the spherical shape, its adhesive force to a plane substrate would decrease correspondingly, irrespective of the type of their experimental sample material. Moreover, the results of Otsuka *et al.* (1988) also indicated that, contacts between fibriform particles and a plane surface were dynamically less stable as compared with that of spherical particles. On the assumption that the PEG 4000 particles in this particular study were adhering to the steel surface mostly with their corners or edges, under such contacting states, the effective area of contact would be much^{more} decreased than expected, thereby resulting in similar adhesion as spray-dried lactose.

The overall results showed that, for the adhesion of the four powders to the stainless steel substrate without preliminary compression, Starch 1500 exhibited comparatively the highest adhesion whilst heavy precipitated calcium carbonate the lowest. Spray-dried lactose and PEG 4000 displayed a very similar adhesion profile, their adhesions being intermediate between that of the above two materials. The findings regarding Starch 1500 and PEG 4000 agreed very well with Booth & Newton

(1987) who also found the former powder depicted a greater adhesive strength than the latter to stainless steel, under similar condition.

4.2.3 Adhesion Measurements of Powder Materials With Preliminary Compression

4.2.3.1 Method

The effect of pressing-on on particle-steel adhesion was investigated by carrying out five preliminary compressions over the range of centrifuging speeds from 3,000 to 17,000rpm, on each powder sample. After each stage of forcing the particles on to the substrate, the corresponding adhesion profile was determined. The detailed procedure is described in the following.

In the first instance, the ‘dusted’ disk (Section 4.2.1) was mounted into a purpose-built rotor tube (see Section 3.2.2) with the particles-laden surface facing towards the axis of rotation so that during subsequent centrifugation, the particles were forced on to the steel surface by the centrifugal force. The rotor was dynamically balanced by positioning another centrifuge tube assemblies (but without powder) oppositely. The centrifuge was brought up to a pre-determined speed gradually, in order to avoid the effect of inertial forces on the particle-substrate adhesion. This press-on mode of centrifugation was held at a desired speed for an arbitrary time of 1 minute before bringing down the centrifuge speed. The influence of the duration of preliminary compression on particle adhesion will be investigated later (see Chapter 5). After the rotor has stopped, the ‘dusted’ substrate disk was taken out and the initial total number of adhering particles was counted under a microscope (see Section 3.2.3). The disk was next replaced in the centrifuge tube but with the ‘dusted’ surface now facing away from the rotational axis, by turning the disk through 180° from its previous orientation. Centrifugation to dislodge these ‘treated’ particles followed the procedure as described in Section 4.2.2.1. Throughout the whole process, the centrifugation temperature was maintained at about $20\pm 2^{\circ}\text{C}$.

4.2.3.2 Results

The adhesion profiles of the four powders at the various applied press-on forces are shown in Figs. 4.2 to 4.5. They were plotted on a semi-logarithmic scale with the percentage of residual particles remaining on the substrate after each step of spin-off centrifugation, as a function of the corresponding applied separation force expressed as the adhesion force. Each profile was obtained from results of 6 to 10 determinations. A greater width of distribution of the adhesion force as compared with that in Fig. 4.1, was observed. Also, the distribution of the particles with respect to the adhesion force, under different press-on forces, follows a similar pattern. Some of the plots show an initial flattened region where practically no or very few particles were removed, followed by a falling linear section, and finally the curves level off at higher forces.

The experimental data were treated statistically by plotting on logarithmic-probability coordinates (see representative Figs. 4.6 to 4.9). Linear relationships were obtained for all four powders around the 50% probability region. In practice, the experimental data yielding points on a log-probability plot will usually be scattered, the apparent degree of scattering being commonly greater at the extremities. For this reason, some investigators (e.g. *Drinker & Hatch, 1954*) ignore points beyond certain limits and fit the best straight line generally to those points within the 20% to 80% marks. In this study, a straight line could be drawn from the 80% to the 10% probability regions in most cases. Thus, over the range of the preliminary press-on speeds, the adhesion profiles of the four particulate solids were considered to be well represented by the logarithmic normal function, for the distribution of adherent particles with respect to the adhesion force, above about $5 \times 10^{-7} \text{N}$ for Starch 1500, $2 \times 10^{-7} \text{N}$ for spray-dried lactose and $1.5 \times 10^{-7} \text{N}$ for calcium carbonate, but this force value varied with the preliminary compression force for PEG 4000.

Each log-probability plot of a powder-steel adhesive system can be characterized by its geometric median adhesion force and geometric standard deviation, σ_g . The geometric median adhesion force can be defined as the force of adhesion at which 50% probability of the particles remains adhered to the substrate

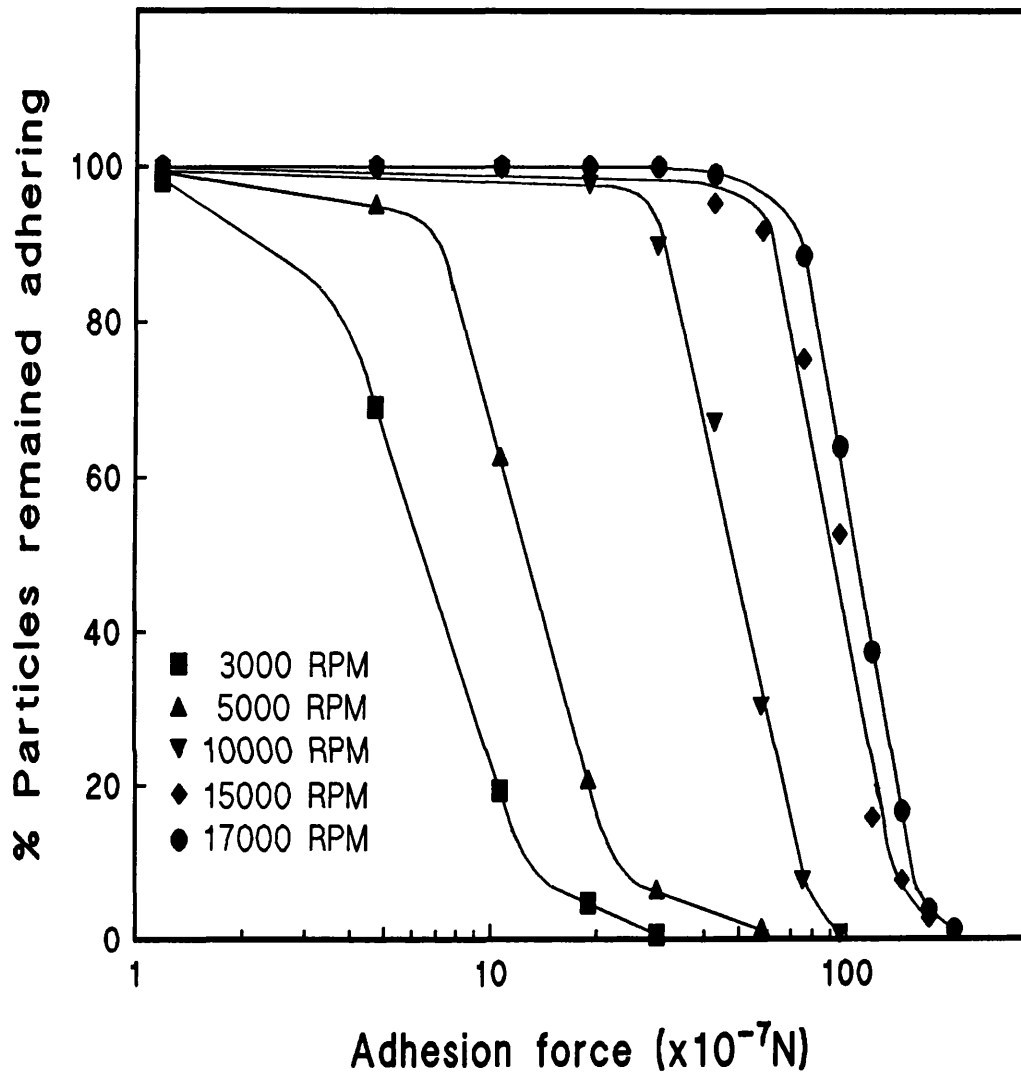


FIG. 4.2 Adhesion profiles of PEG 4000 to stainless steel at different preliminary press-on forces (indicated by RPM).

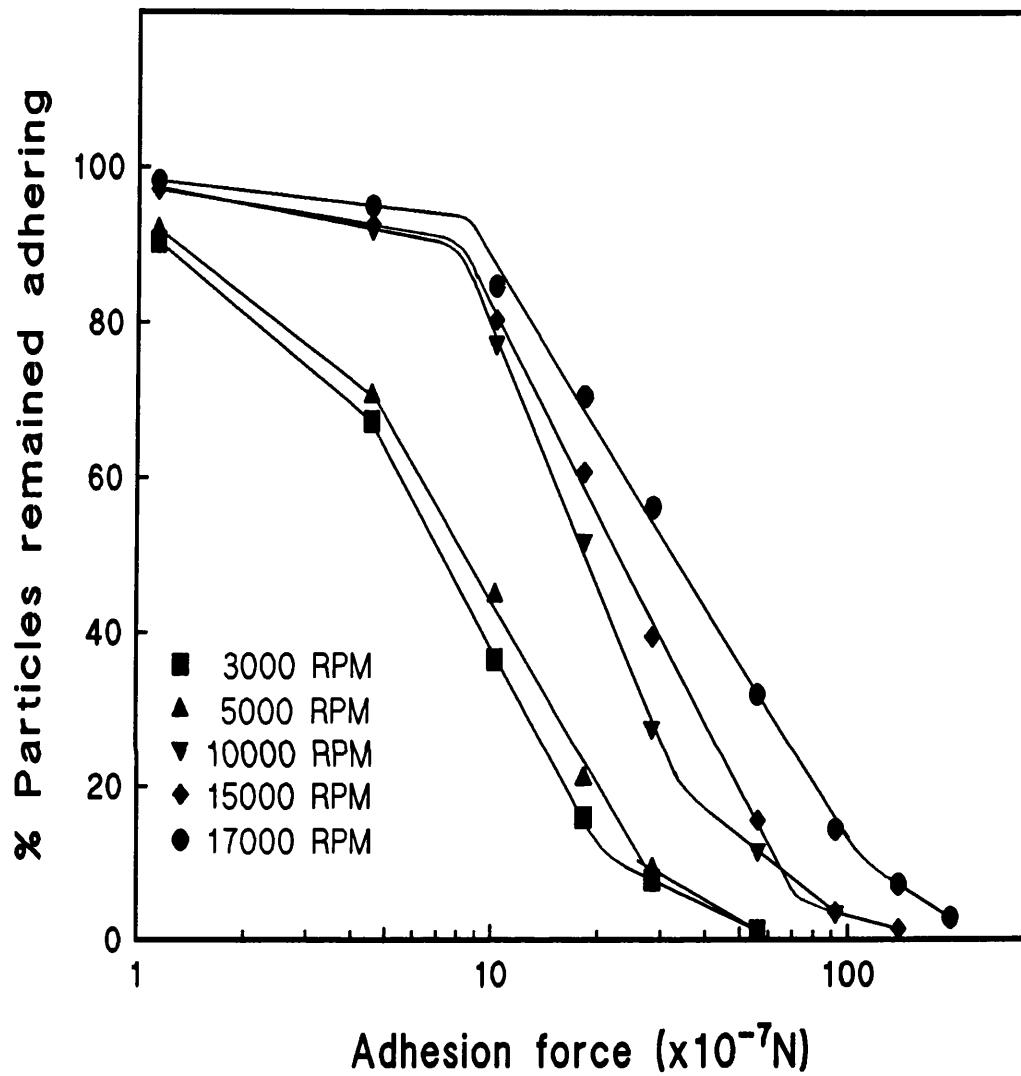


FIG. 4.3 Adhesion profiles of Starch 1500 to stainless steel at different preliminary press-on forces (indicated by RPM).

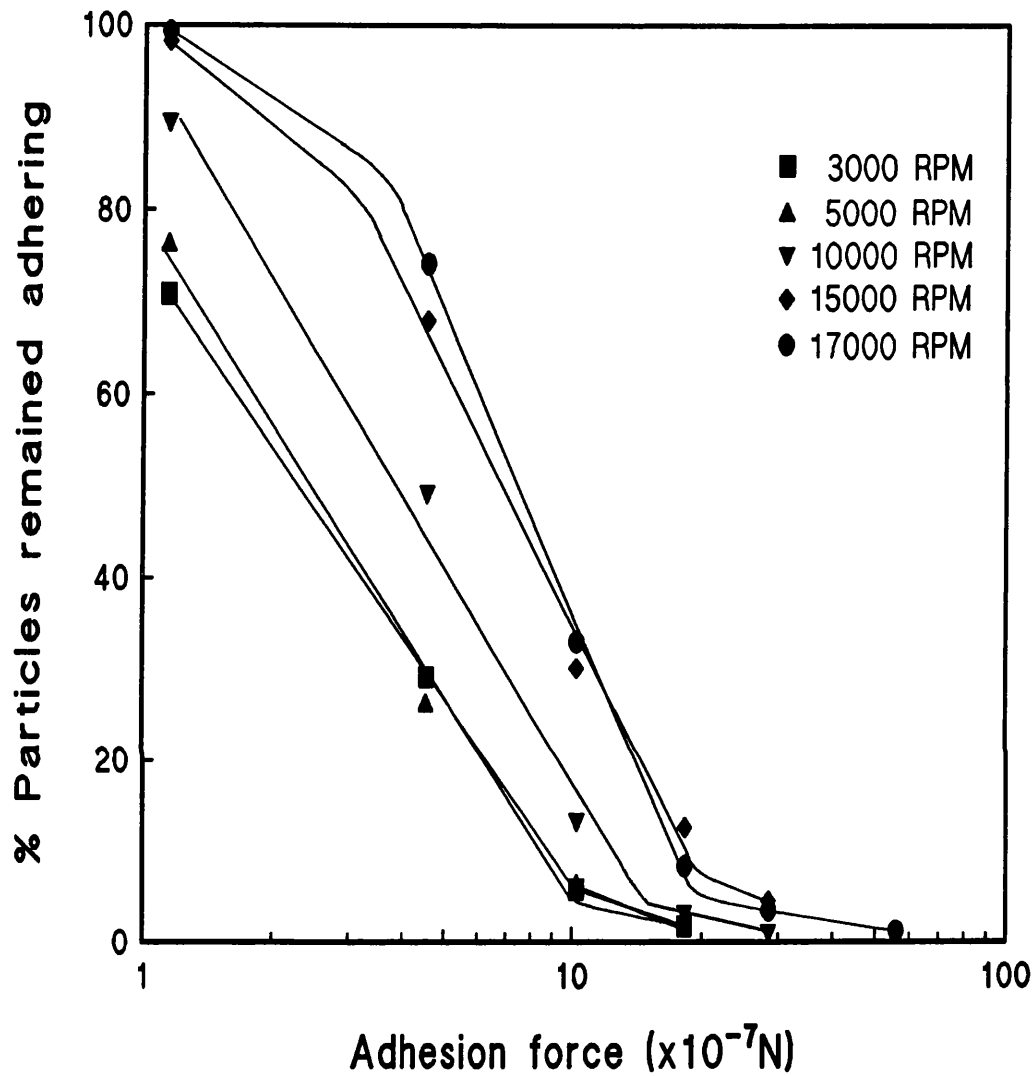


FIG. 4.4 Adhesion profiles of spray-dried lactose to stainless steel at different preliminary press-on forces (indicated by RPM).

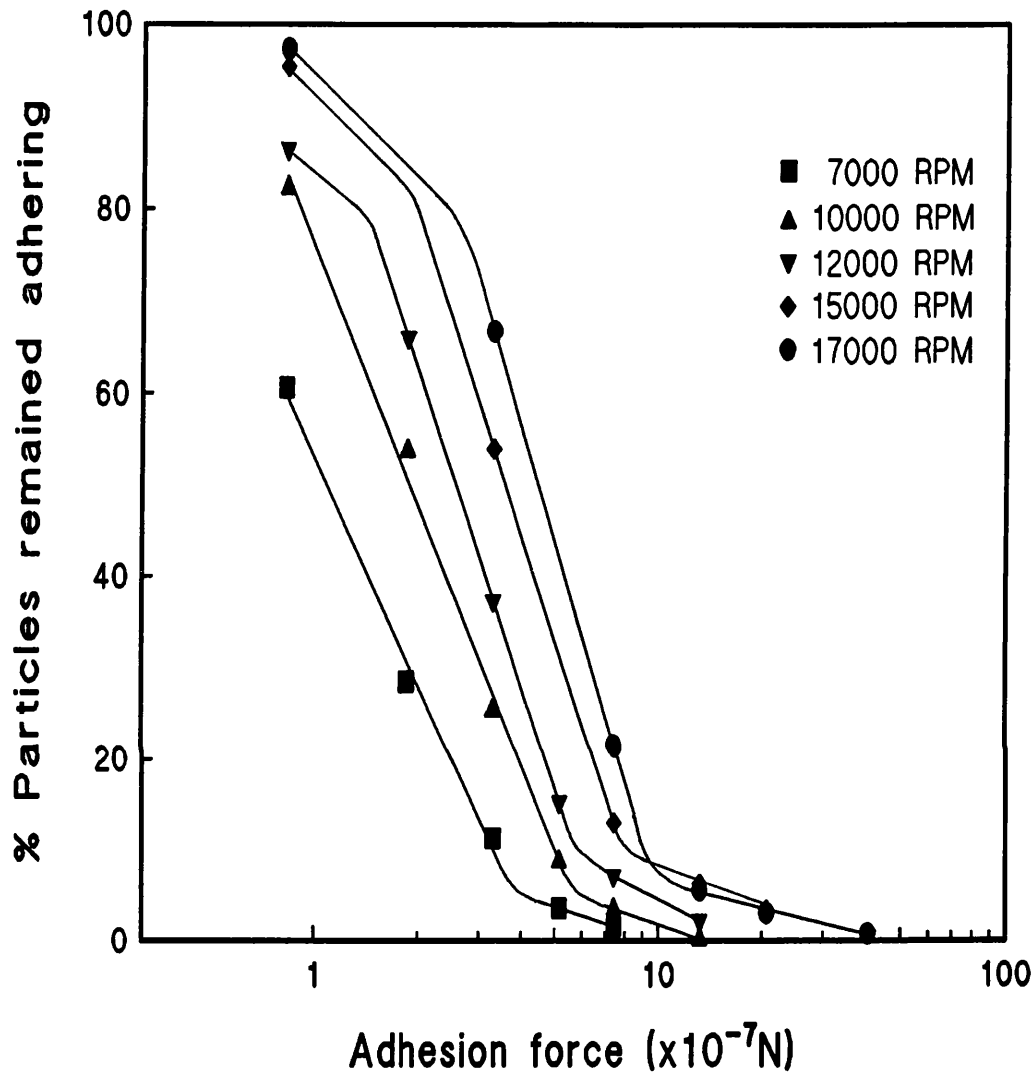


FIG. 4.5 Adhesion profiles of heavy precipitated calcium carbonate to stainless steel at different preliminary press-on forces (indicated by RPM).

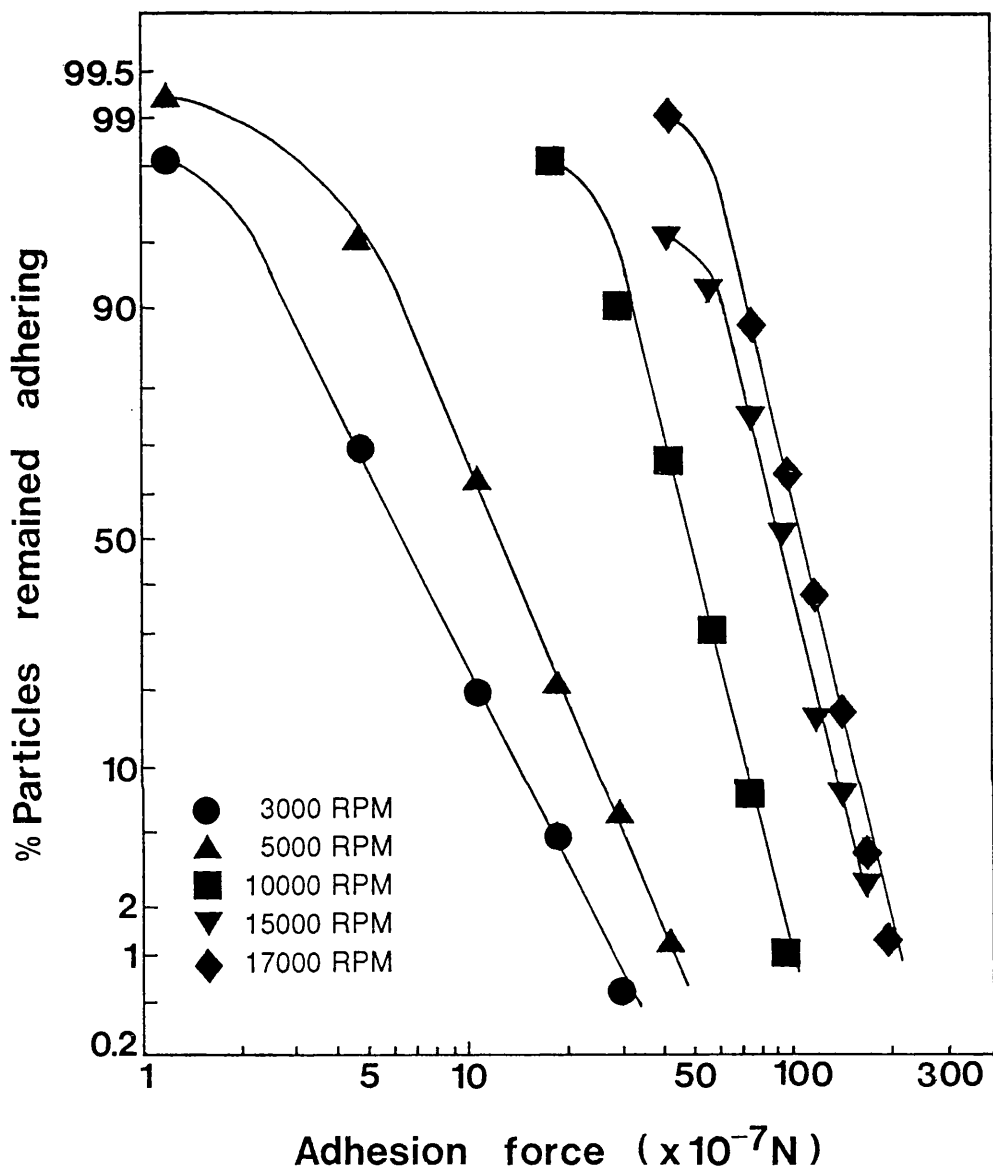


FIG. 4.6 Log-probability plots of the adhesion of PEG 4000 to stainless steel at different preliminary compression forces (indicated by RPM).

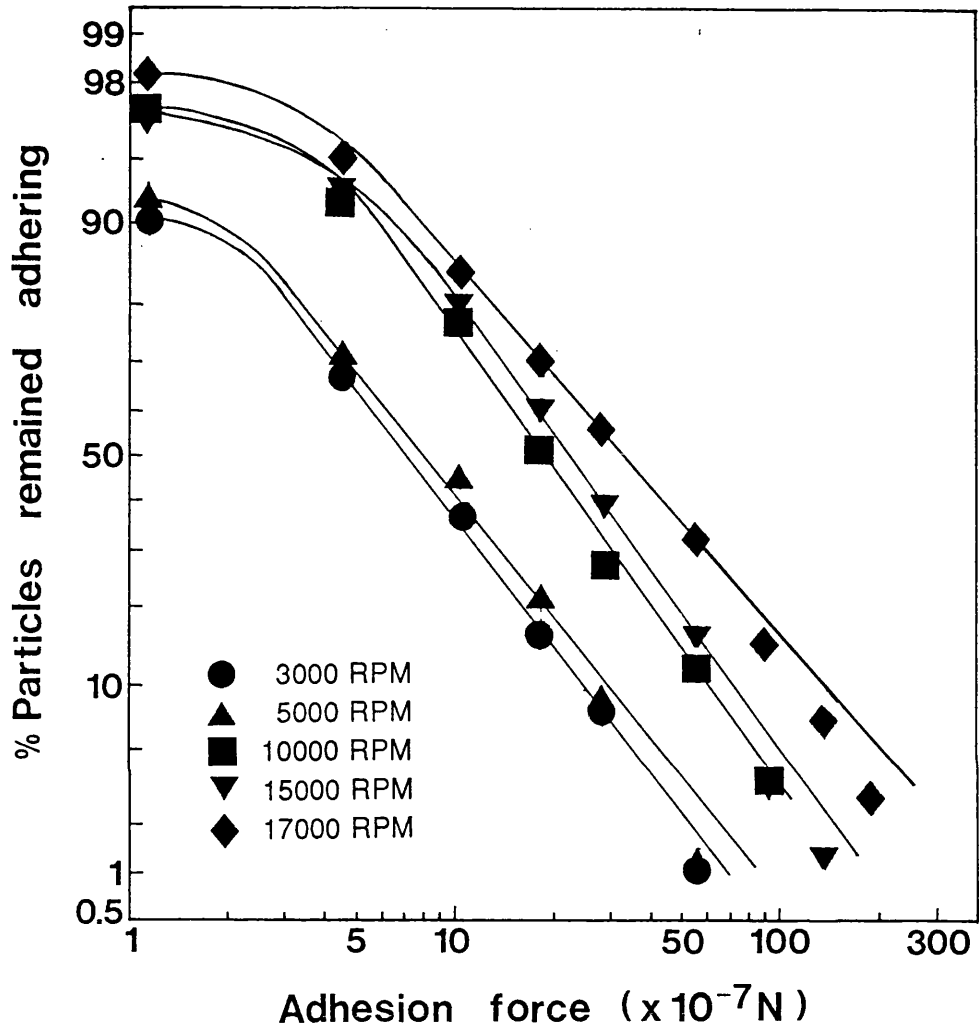


FIG. 4.7 Log-probability plots of the adhesion of Starch 1500 to stainless steel at different preliminary compression forces (indicated by RPM).

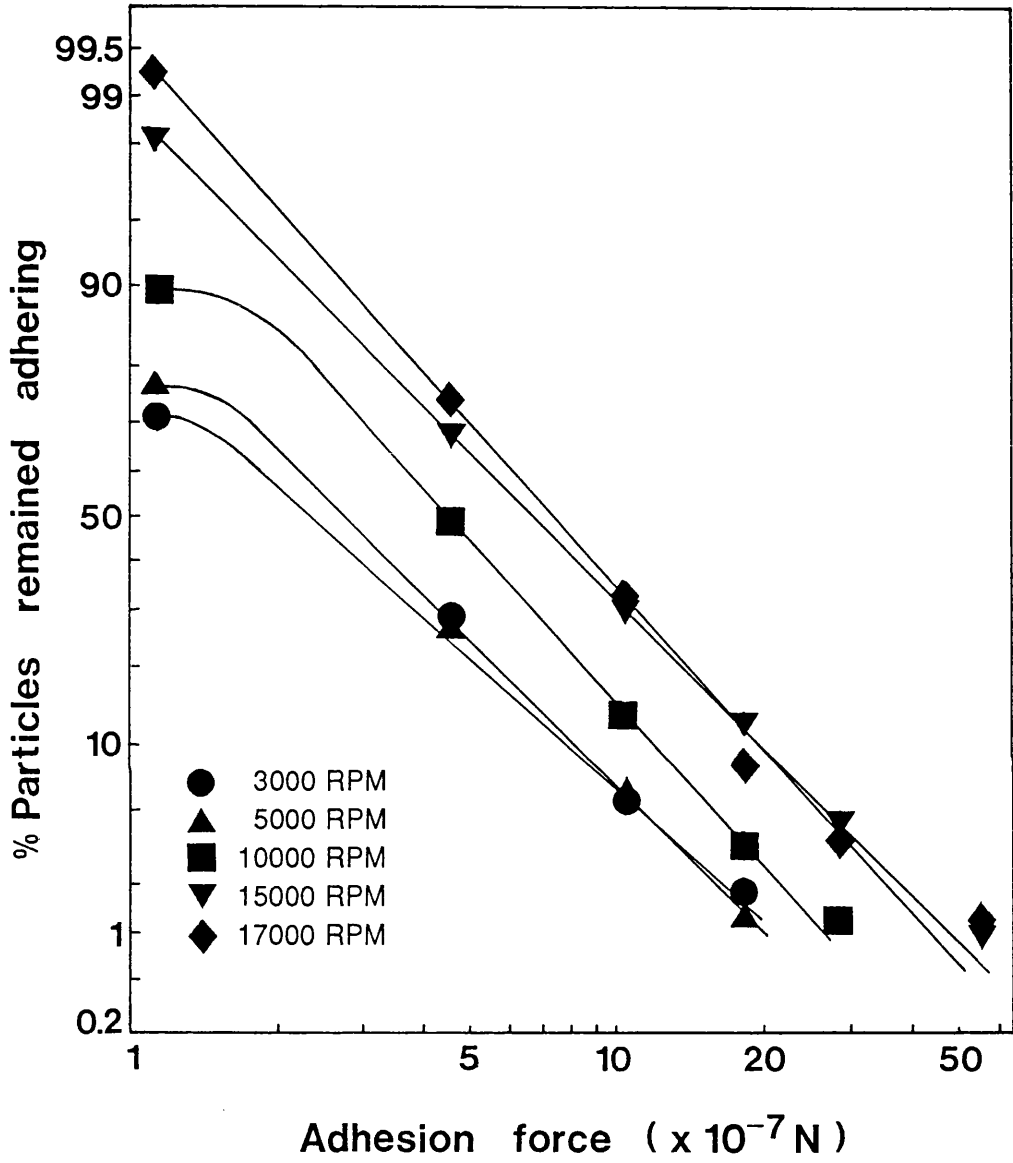


FIG. 4.8 Log-probability plots of the adhesion of spray-dried lactose to stainless steel at different preliminary compression forces (indicated by RPM).

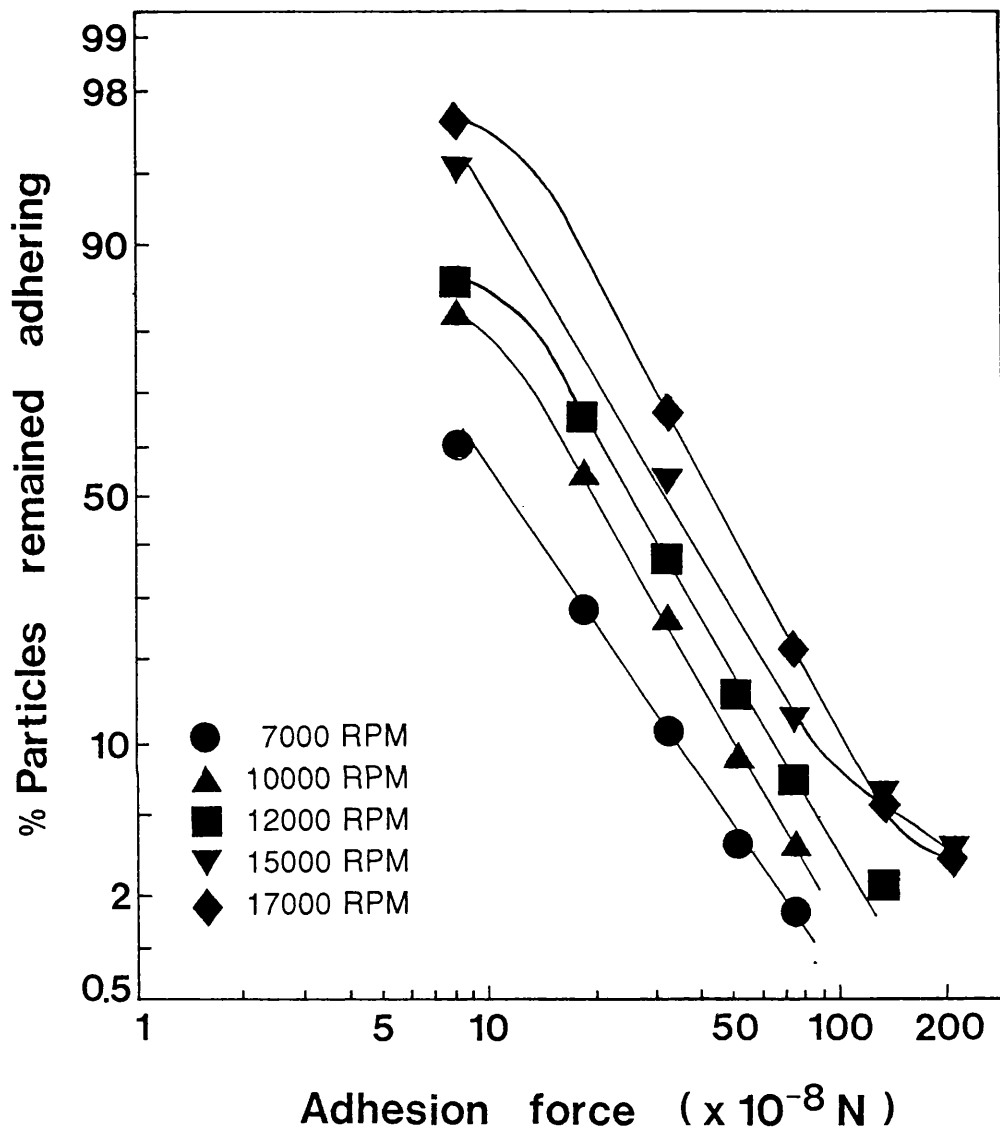


FIG. 4.9 Log-probability plots of the adhesion of heavy precipitated calcium carbonate to stainless steel at different preliminary compression forces (indicated by RPM).

after centrifugation. The numerical value of this statistical parameter can be obtained graphically, which may be used to evaluate the strength of adhesion of the particles on the steel disk. A higher median adhesion force value indicates a greater degree of adhesive interaction. On the other hand, the geometric standard deviation gives a quantitative measure of the scatter of the adhesion forces. It can be expressed as the ratio of the 50% probability force value to the 16% probability force value. Table 4.1 shows the values of these two statistical parameters for the four powder materials.

There was an increase in the median adhesion forces of the powders with the preliminary compression forces. At the common press-on speeds (namely, 10,000, 15,000 and 17,000rpm) for all powders, the largest measured median adhesion force, at the corresponding centrifuging speed, was always shown by PEG 4000, followed by Starch 1500, then spray-dried lactose and finally calcium carbonate. With regard to the values of σ_g obtained, no particular specific relationship with the preliminary compression forces was observed, although a trend of an increase of the former parameter with increment of the latter seemed to be shown by PEG 4000, spray-dried lactose and calcium carbonate (see Fig. 4.10).

The effect of preliminary compression on the adhesion of a powder to the steel substrate was illustrated by expressing the median adhesion force as a function of the corresponding press-on force. The resulting plots for the four powders are shown in Fig. 4.11. The line drawn through each set of experimental points was a best fit, using linear regression analysis. The correlation coefficients obtained for the data points of PEG 4000, Starch 1500, spray-dried lactose and heavy precipitated calcium carbonate were 0.9920, 0.9706, 0.9932 and 0.9943, respectively.

Table 4.2 shows the values of the ratio of the median adhesion force to the preliminary compression force, at each press-on speed. This ratio indicated the relative amount of adhesion force established per unit of the press-on force. In the main, the magnitude of this ratio decreased with increasing compression force, although the median adhesion force increased with the latter. This suggested that, the increase in the adhesion force was not in proportion with the increase of the compression force.

TABLE 4.1 Geometric median adhesion forces of the powders and their respective geometric standard deviations, σ_g , at the various compression forces. The standard error of mean for all force values was usually less than 6% of the mean.

Material	Press-on speed (rpm)	Compression force ($\times 10^{-6}$ N)	Median adhesion force ($\times 10^{-7}$ N)	σ_g (N)
PEG 4000	3000	1.03	6.46	0.546
	5000	2.85	12.56	0.586
	10000	11.40	48.75	0.713
	15000	25.66	98.21	0.676
	17000	32.95	108.25	0.734
Starch 1500	3000	0.99	7.19	0.388
	5000	2.76	7.88	0.360
	10000	11.02	18.97	0.444
	15000	24.80	22.70	0.409
	17000	31.86	32.42	0.344
Lactose, spray-dried	3000	0.99	2.37	0.400
	5000	2.76	2.43	0.388
	10000	11.02	4.33	0.467
	15000	24.80	6.79	0.436
	17000	31.86	7.36	0.483
Calcium carbonate, heavy ppt'd.	7000	3.91	1.16	0.437
	10000	7.98	1.97	0.483
	12000	11.49	2.52	0.484
	15000	17.96	3.29	0.475
	17000	23.07	4.44	0.511

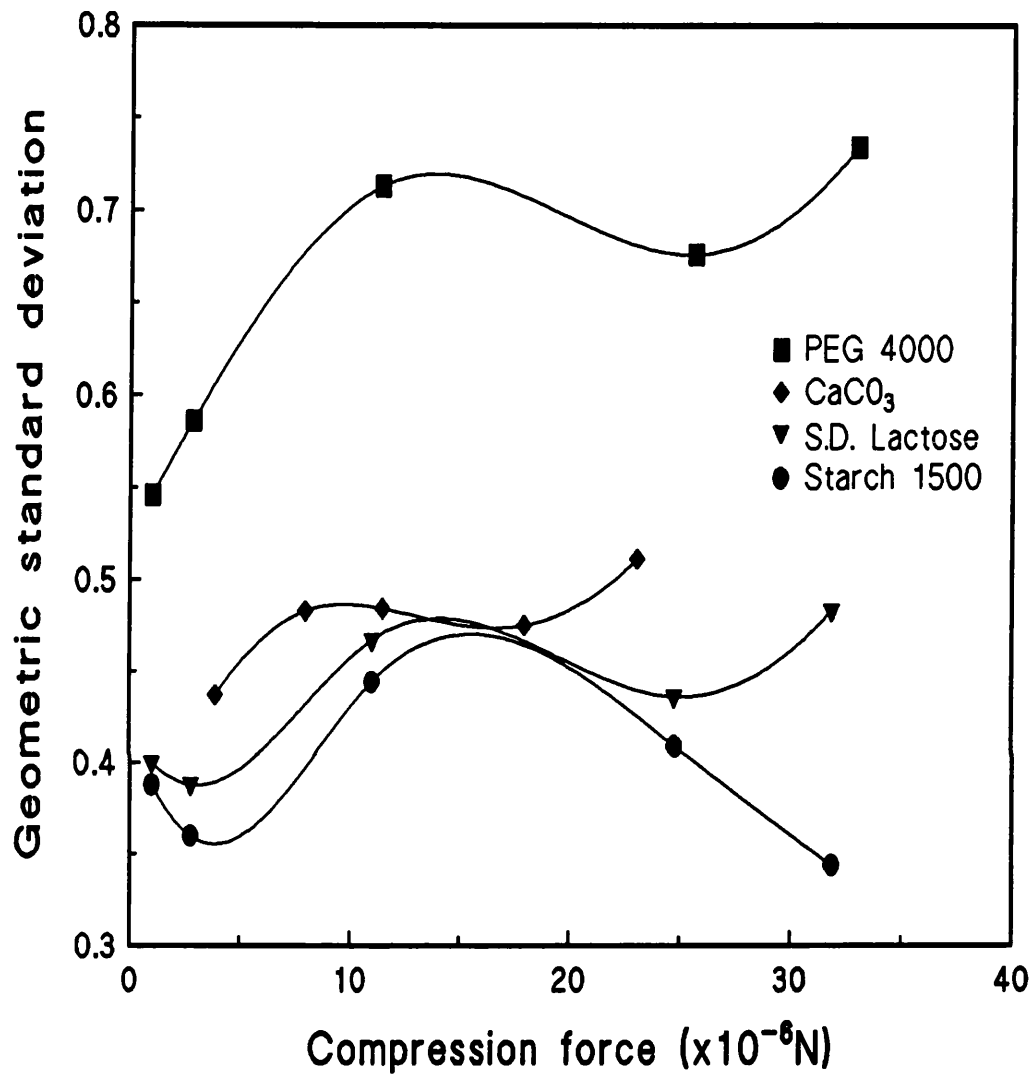


FIG. 4.10 Effect of preliminary compression force on the scattering of particle-steel adhesion force expressed by the geometric standard deviation.

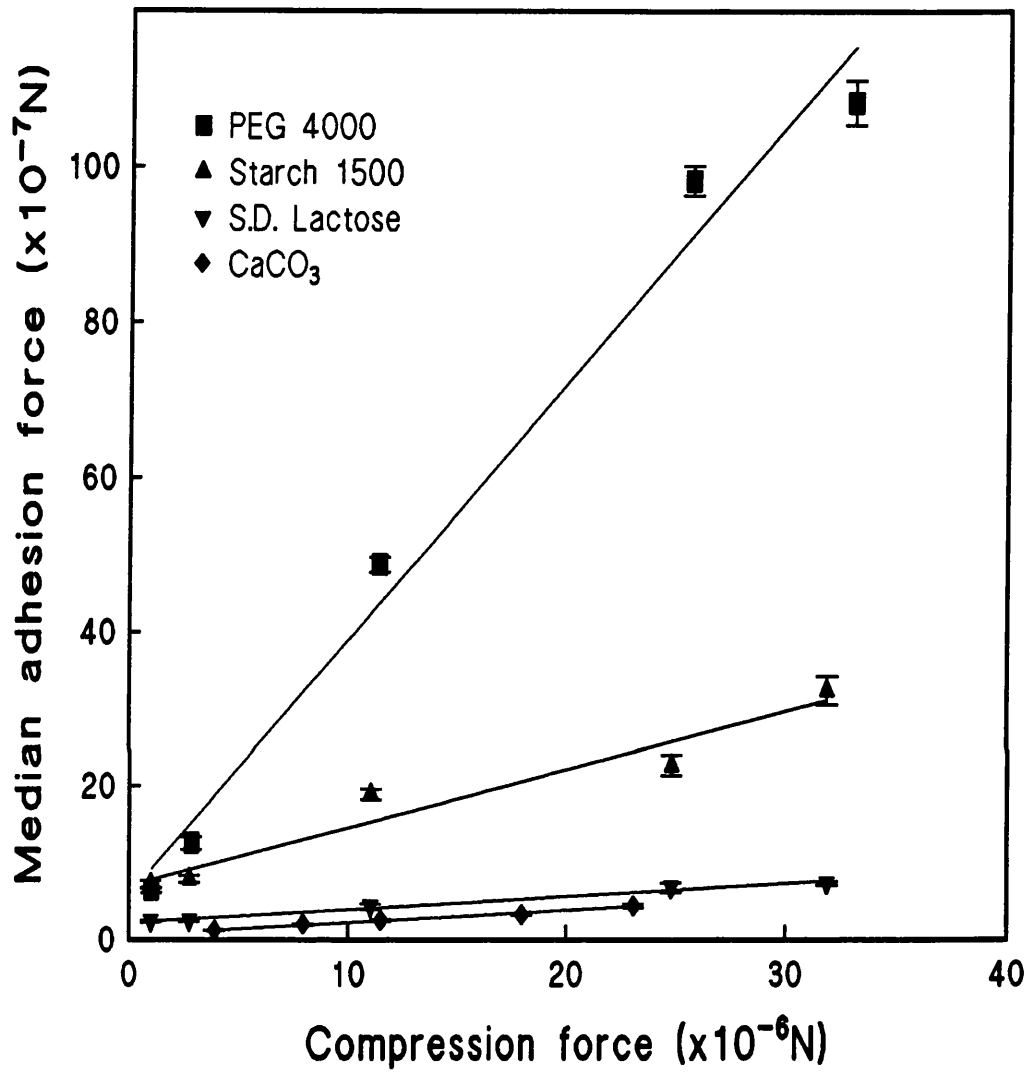


FIG. 4.11 Relationship between median adhesion force and preliminary press-on force. The error bar represents ± 1 s.e.m.

TABLE 4.2 Values of the ratio of the geometric median adhesion force to the preliminary compression force.

Material	Compression force	Median adhesion force	Median adhesion force
	($\times 10^{-6}$ N)	($\times 10^{-7}$ N)	$\frac{\text{Median adhesion force}}{\text{Compression force}}$ ($\times 10^{-2}$)
PEG 4000	1.03	6.46	62.7
	2.85	12.56	44.1
	11.40	48.75	42.8
	25.66	98.21	38.3
	32.95	108.25	32.9
Starch 1500	0.99	7.19	72.5
	2.76	7.88	28.6
	11.02	18.97	17.2
	24.80	22.70	9.15
	31.86	32.42	10.2
Lactose, spray-dried	0.99	2.37	23.9
	2.76	2.48	9.0
	11.02	4.33	3.93
	24.80	6.79	2.74
	31.86	7.36	2.31
Calcium carbonate, heavy ppt'd.	3.91	1.16	2.97
	7.98	1.97	2.47
	11.49	2.52	2.19
	17.96	3.29	1.83
	23.07	4.44	1.93

4.2.3.3 Discussion

The powder samples used for this study were not specifically cleaned, and as the experiments were carried out in the usual laboratory atmosphere, the particles were considered to be 'contaminated' by various adsorbed gases and vapours. Surface impurities can greatly affect the process of electrostatic charging between two dissimilar materials when they make and break contact, by providing a easier pathway for charge leakage. In addition, the sharp corners and edges of the contacting surfaces could aid electrical discharging. On the other hand, Boland & Geldart (1971/72) found that storage in glass containers would aid some degree of charge dissipation, which was previously suggested by Harper (1967) to be due to the glass surface which, when compared with a polymer surface, is capable of holding sufficient water molecules to promote certain extent of charge leakage. Kulvanich & Stewart (1987b) showed that longer storage time would allow greater discharging. Owing to these various common effects in affecting the electrostatic charging process, the influence of the latter on particle adhesion in this work was therefore neglected.

Triboelectrification is a manifestation of a contact electrification process in which rolling or frictional sliding is involved. It is still an incompletely understood effect, especially when non-metallic surfaces are involved. Similar to electrostatic charging, the triboelectric charging behaviour of materials is also sensitive to the atmospheric environment as well as to the presence of impurities on the contiguous surfaces. During the course of experimentations, up to the moment of contact, the particles being deposited have not been in any prior contact with the steel substrate, and in the absence of particle motion on the disk surface, the triboelectric effect was disregarded. Thus, particle-steel adhesion was then assumed to be due principally to the van der Waals interactions. Such an assumption could be supported by the work of Rumpf (1977) who from work on the role of contact potential in powders, suggested that, van der Waals interactions exceeded electrostatic and triboelectric effects by at least an order of magnitude. This view was also shared by Bailey (1984).

Plastic deformation is known to occur in many organic solids. There is an abundant of evidence to show that, lactose, when compacted, deforms by a mixed

mechanism of plastic flow at the contact points as well as particle fracture (*Hardman & Lilley, 1970; Fell & Newton, 1971a; Butcher et al., 1974; Salpekar & Augsburger, 1974; Cole et al., 1975; York & Bailey, 1977; Roberts & Rowe, 1986; Vromans et al., 1987*). Starch, on the other hand, deforms mostly by plastic deformation (*David & Augsburger, 1977; Rees & Rue, 1978; Paronen & Juslin, 1983; Paronen, 1987; Staniforth & Patel, 1989*). While adhesion contact points in practice almost always involve some plasticity when under a compression force, Krupp (1967) estimated that, non-elastic deformation may result from just the surface attraction forces alone between very small spherical particles, because of the minute regions of contact resulting in large contact pressure. The significance of surface forces was also indicated by the results of Pashley *et al.* (1984), which suggested surface forces alone were able to initiate plastic deformation of a metal microasperity.

In the case of the test powder particles contacting the steel surface, contacts would be made through touching the tips of the surface asperities of the contiguous surfaces. During the centrifuging stage when the particles were pressed against the disk surface, relative centrifugal forces (RCF) of the order of magnitude from 10^2 to 10^4g (see Table 3.1) would be exerted on the adherent particles, and as a result, a substantial localized pressure would be developed in the micro-contact areas. Under such stress concentrations, the elastic limits of the contacting particle asperities would likely be exceeded, plastic deformations then set in resulting in flattening of the contact regions. These contacts would be retained when the applied load was removed. The effect of strengthening the plastic adhesive contacts due to elastic deformation was disregarded, because the elastic strain energy that might be stored in the bulk of the particles during the pressing-on would be lost when the centrifuge decelerated. Moreover, several investigators (*Krupp, 1967; Johnson et al., 1971; Deryaguin et al., 1975b; Muller et al., 1976, 1983a; Rumpf, 1977*) concluded that, elastic contact deformations cannot possibly increase the molecular component of the adhesion force, simply because upon removal of the applied interfacial load, any elastically deformed areas will recover their original shapes.

The influence of externally applied forces on the adhesion of plastically deformable bodies to a solid surface was considered to be attributed to an increase in the interfacial bonding area as a result of smoothing out of the surface roughness, leading to a greater molecular van der Waals contribution to the adhesion force (*van den Tempel, 1972; Kohno & Hyodo, 1974; Fuller & Tabor, 1975*). Moreover, flattening of the surface irregularities would permit a closer proximity of the bulk of the particles to the steel surface, because of a reduction in the separation distance. This closer physical contact would further enhance the adhesion. Apart from the effect of microplasticity, under a compression force, the particle material beneath the microasperities might possibly be deformed, which would then bring new clusters of microasperities into contact with the steel surface to establish additional contact points. Consequently, the preliminary press-on force increased the degree of molecular interaction between the adherents. The higher the applied force, the greater would be the resultant total adhesion force.

The adhesion profiles of the four powders presented in Figs. 4.2 to 4.5 are an average of all the effects of all the forces, both attractive and repulsive. They show a shift to the right with higher press-on speed. An initial plateau region was observed in some of the plots, notably in PEG 4000 and Starch 1500. This implied that, these particles were adhering to the steel disk with such a force that the lower separation forces were not sufficient to effect any particles to be detached from the substrate. However, the same detachment forces have caused almost all the particles which had not been forced on to the steel surface, to be removed (see Section 4.2.2.2). These effects thus indicated that, forcing of the powders to the steel substrate can bring about marked increases in the adhesive forces. The minimum force of adhesion that needed to be overcome to initiate any particle detachment increased with the applied compression force, as depicted by the gradual lengthening of the flattened section or the appearance of a flattened region at higher press-on speeds. After this region has been exceeded, the percentage of adhering particles was found to decrease linearly with increasing logarithm of the separation force. The straight lines in this section were drawn using linear regression analysis. The magnitude of the detaching force corresponding to 50% of the remaining adhered particles was used by some

researchers (e.g. *Sano et al., 1984*) to represent the average particle-substrate adhesion force. With regard to the last part of each curve, i.e., that which tails off towards large detaching force, it was suggested by Krupp (1967) that, when a very smooth area on the particles happened to encounter a large flattened area on the substrate surface, much stronger adhesion after compression would result.

Treatment of adhesion results by statistical means was considered to be a more objective approach to evaluate adhesive interactions. In this study, linearization of an adhesion profile was achieved by logarithmic probability plot. The statistical results shown in Table 4.1 indicated that, PEG 4000 exhibited the largest median adhesion force at each corresponding press-on speed (with the exception at 3,000rpm where its force value is slightly less than that of Starch 1500). In the case of calcium carbonate, the lowest force values were displayed. At the press-on speed of 3,000rpm, the median adhesion force of PEG 4000 is about 5.6 times that of calcium carbonate at 7,000rpm, but this ratio increases to approximately 24 times at the common highest 17,000rpm press-on speed. This illustrated that, difference in the adhesive property between two powders to the steel substrate would be more clearly revealed at higher preliminary compression force.

The rough powder particles would adhere to the steel surface on multiple contacts with different strengths, which could be attributed to variation in local irregularities and non-homogeneity of solid surfaces, associated with different points of contact. A scattering of adhesion forces would therefore result, although the spread could be reduced by the preliminary compression process, as was found by Booth & Newton (1987). Nevertheless, with higher press-on forces allowing more contact sites to be established, the effect of the scattering could possibly be multiplied. This may perhaps explain the *trend of an increase in the geometric standard deviation value with the preliminary compression force*, as depicted in Fig. 4.10.

The plots in Fig. 4.11 indicate a proportional increase in the median adhesion force of the powders with the preliminary applied force. The slope of each regressed line expresses the change of the median adhesion force per unit increase of the press-

on force, and is termed the 'adhesion ratio', which is characteristic of each powder material. This dimensionless parameter may, therefore, be utilized as a means for comparing, in a quantitative way, the adhesiveness between different powders to the same substrate, over a particular range of compression force. In this study, the adhesion ratios obtained for the particulates are as follows, PEG 4000 33.3×10^{-2} , Starch 1500 7.57×10^{-2} , spray-dried lactose 1.72×10^{-2} and heavy precipitated calcium carbonate 1.63×10^{-2} . These values depict the rank order of the ability of the powders to adhere to the stainless steel substrate, after pressing-on, as: PEG 4000 > Starch 1500 > spray-dried lactose > calcium carbonate, which agrees well with other experimental results. If the same particle size fraction (-56+45 μ m) as the other materials was used, an even lower adhesion ratio value would be expected for calcium carbonate. This is because smaller particles, in general, adhere more strongly than larger particles of the same material.

Deformation hardening is a phenomenon whereby the elastic limit of a material increases with the extent of deformation. Upon further plastic flow, this limit will eventually become equal to the strength of the material; the solid will become relatively hard and brittle, and breakage of the surface within the deformed region might happen. The effect of work hardening generally does not occur where sections are so small that crystal dislocations are either not present or where they cannot move to generate new dislocation (see Section 1.4.2). The persistence of work hardened asperities on further plastic loading was discussed by Bowden & Tabor (1950). The phenomenon of work hardening is exhibited by many plastically deformable materials but to varying degrees. Though studies (e.g. *Ridgway et al., 1970*) involving typical pharmaceutical organic solids are scant, the mechanism could probably be the same, even though the relative occurrence or importance of various mechanisms may be different. Rice (1971) asserted that microplasticity may give rise to compression failure since the yield stress will be the upper limit of the compressive strength of many materials. Throughout this work, residues of any adherent particles after separation were not noticed, so separation of the particles from the steel substrate was assumed to have taken place at the interface, i.e., the detachment process represented an adhesional failure.

Owing to high localized pressures developing at the adhesive micro-contacts during the stage when the particles were forced on to the steel surface, the effect of deformation hardening was likely to occur in the contacting particle asperities; the steel surface was assumed comparably unaffected. For two metal surfaces in contact under an external load, O'Callaghan & Probert (1987) suggested that, material which was located within the intersections of surfaces would not be disrupted, but would be displaced to form the shoulders of the asperity contacts; such movement would also cause deformation hardening of the material in the asperities. At higher press-on forces, the increase in hardness with decreasing stressed volume would result in the total increase in the area of micro-contact to become less. Under such circumstances, this diminished the adhesive contribution due to plastic flattening of the particle asperities. This effect was probably reflected by the trend of the decrease in the magnitude of the ratio of the median adhesion force to the compression force, as the press-on force increased (see Table 4.2). The results suggested the significance of strain hardening in the adhesion of powders.

Nevertheless, the median adhesion force increased with the press-on force. This could be attributed to the increased physical closeness of the powder particles to the steel surface, which together with the formation of more micro-contacts at a higher preliminary compression force, possibly making their total van der Waals attractions significant.

Relationship Between Adhesion Ratios and Yield Pressures of the Powders

The surface mechanical property of a material is important in interfacial adhesion particularly when plastic deformation is involved, since the former is a principal factor in governing the true area of contact. A soft microasperity will be more inclined to form a bond whereas a harder one will have a lower bond-forming probability. By considering that the stressed volumes in the particle asperities were very small, their micro-mechanical properties may not be the same as those of the bulk material, as was demonstrated experimentally on metal contacts by Pashley *et al.* (1984). Unfortunately, relevant information regarding microplasticities of the surface

irregularities of the pharmaceutical solids concerned was not known, the values of which are usually only accessible through refined experiments.

One parameter which may be useful for describing surface plastic behaviour of a solid is the indentation hardness such as Brinell hardness or Vickers hardness. However, the hardness information for the experimental particulates was also not available. Another indicator for solids is the yield pressure of the particulate material. The yield pressure is that value which describes the tendency of a material to undergo total and plastic deformation, and is thus a means of characterizing plastic flow in contacts. Similar to the indentation hardness, the yield pressure of a solid could be affected by deformation hardening (*Ridgway et al., 1969*), nevertheless, it could remain a physically useful parameter. In view of the literature values for the yield pressures of the test powders (see Table 4.3), one would intuitively consider the microasperities of PEG 4000, a soft waxy solid, to be more compliant and would deform to greater extent, whereas those of calcium carbonate, a hard mineral salt, to be less liable to deform under the same press-on load, and those of starch and lactose to be behaving in between.

The relation of the adhesion ratios of the powders and their respective literature values of the yield pressure of the bulk materials is shown in Fig. 4.12. An inverse relationship was obtained between the two parameters; the coefficient of correlation being 0.9981. This suggested that, the relative adhesion behaviour between different particulate solids could be indicated or grossly assessed by the bulk mechanical properties of the materials.

TABLE 4.3 Yield pressures of the powder materials.

Material	Yield pressure (MPa)	Reference
PEG 4000	55	Al-Angari <i>et al.</i> (1985)
Starch 1500	216	Paronen (1987)
Lactose, spray-dried	354	Chowhan & Chow (1980)
Calcium carbonate	486	York (1978)

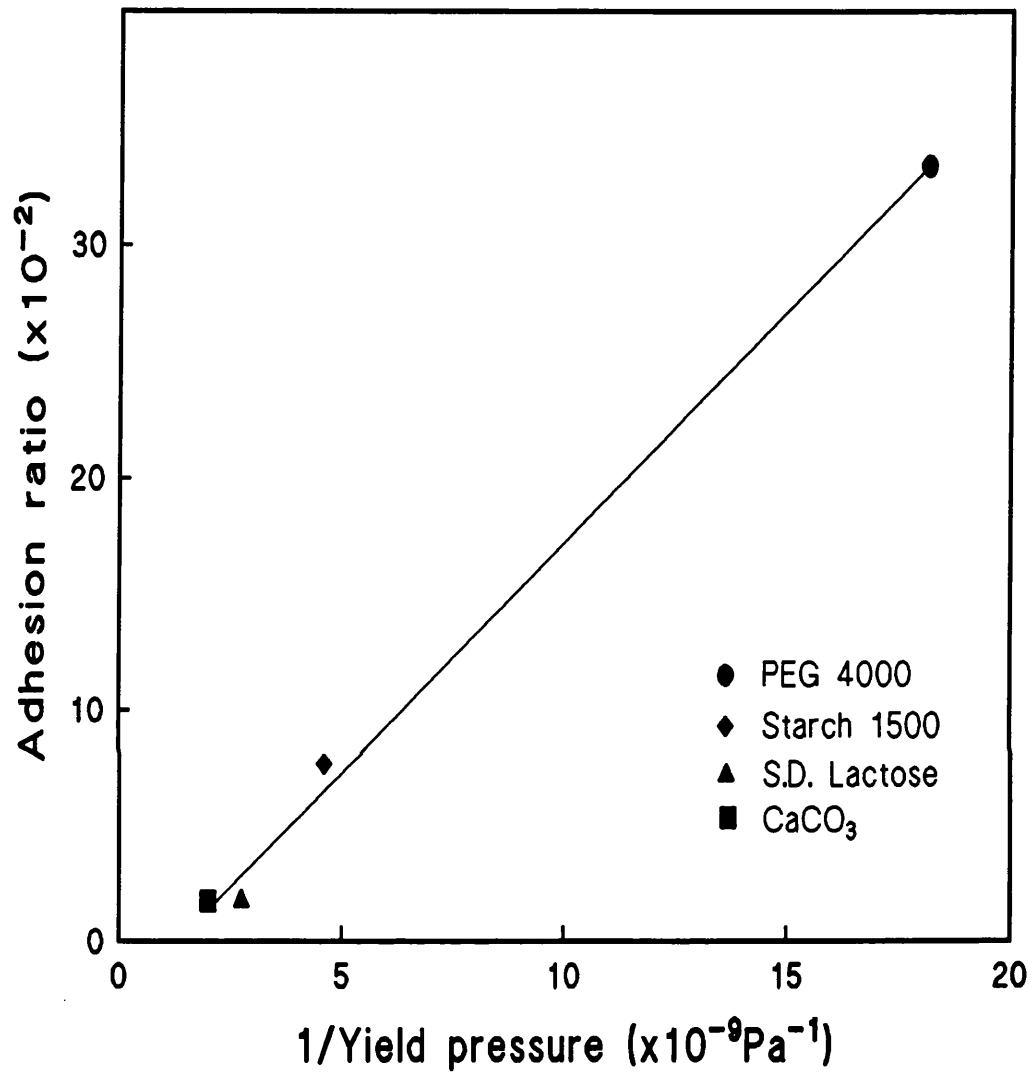


FIG. 4.12 Inverse relationship between the literature values of the yield pressure of the powder solids and their adhesion ratios.

4.3 CONCLUSIONS

In this chapter, the adhesion of powder materials to the stainless steel substrate, with and without the stage of preliminary compression, was studied by means of a centrifuge method. When the particles were deposited on to the steel disk without the subsequent pressing-on procedure, the adhesion profiles indicate that, Starch 1500 exhibited a relatively higher adhesion tendency, which was followed by both PEG 4000 and spray-dried lactose, and lastly, by heavy precipitated calcium carbonate.

Upon subjecting the particles to a preliminary compression, the adhesion behaviour of the four powders revealed marked changes from their previous circumstances, as well as between the materials. Distributions of the percentage of the adhering particles with respect to the adhesion force, were all found to follow a log-normal relationship, over the range of the preliminary press-on centrifuging speed. The increase in the median adhesion force was, for all materials, directly proportional to the force applied to the particles at the adhesive stage. The relative adhesiveness of the powders to the stainless steel was expressed by their respective adhesion ratio, which was obtained as the slope of the median adhesion force as a function of the compression force. The value of this ratio indicate the following rank order of adherence: PEG 4000 > Starch 1500 > spray-dried lactose > heavy precipitated calcium carbonate, which was equivalent to that for the reciprocal of the published values of the yield pressure of the powders. This may, perhaps, indicate that an assessment of the relative adhesiveness of powders could be grossly achieved from knowledge of their mechanical properties; in this study, from the yield pressures of the materials. Awareness of the effect of preliminary compression on particle adhesion is therefore essential when processing powders, particularly when plastic deformation will be involved.

CHAPTER 5

Investigation of Preliminary Compression Duration on Particle Adhesion to Stainless Steel

5. INVESTIGATION OF PRELIMINARY COMPRESSION DURATION ON PARTICLE ADHESION TO STAINLESS STEEL

5.1 INTRODUCTION

It is known that powders can exhibit some time dependent properties, e.g. time dependent shear strengths were reported in the 60's by Jenike (1961). In tableting, one parameter in powder compaction is the time for which a particulate material is held under load. The term 'contact time' was used by Jones (1977) to describe the total time for which a moving punch applies a detectable force to the die contents during the compression and decompression event, but excluding ejection. Compacts could also reveal the time dependent properties of the powders from which they are made, for instance, the tensile strengths of compressed powder masses were found by Rees *et al.* (1970) to be dependent upon the loading rate in a diametral compression test. The dimensional changes which took place in tablets after compression and possibly also on extended storage, were ascribed to creep strain recovery and stress relaxation (Shlanta & Milosovich, 1964; Aulton *et al.*, 1973; York & Bailey, 1977), both of which are time-dependent processes.

In an adhesion process, the attractive forces between the adherents can lead to elastic, plastic or elasto-plastic deformation at their interface. For many polymeric materials, such interfacial deformations will often vary with time, which would thus lead to a change in the adhesive area as time progresses. Under no applied force, the increase in the adhesive interaction between particles and a substrate surface with increasing time of contact is commonly termed 'ageing'. Krupp (1967) and van den Tempel (1972) found that 'ageing' was an important factor in altering the interaction energy between the adhering surfaces.

The effect of the length of time a powder is in contact with a solid surface on the adhesion forces, was investigated by some workers (Deryaguin & Zimon, 1961; Benjamin & Weaver, 1963; Zimon, 1963; Asakawa & Jimbo, 1967; Okada *et al.*,

1969). The reported adhesion data, obtained usually by measuring the adhesion forces over a certain time after deposition of a test powder on to a substrate surface, do not, however, reflect the circumstances in which the adhesive contacts are strengthened beforehand by an applied load. Though some reports were found in the fields of powder metallurgy and material sciences (*Bowden & Tabor, 1950; Corn, 1961; Roberts & Thomas, 1975; David & Augsburger, 1977*), such adhesion information for micron-sized pharmaceutical materials is meagre. Since those materials studied usually bear few physical properties in common with many pharmaceutical powders, the former information may not generally be applicable to the latter materials. The aim of this chapter is to examine the effect of the duration of contact under stress, on the adhesion of four pharmaceutical particulates to stainless steel.

5.2 EXPERIMENTAL METHOD

The adhesion of particles to the steel substrate as a function of time under load, was studied by determining the adhesion forces after the particles were forced on to the substrate for various time durations over 960 seconds. The powders investigated were those used previously, namely, PEG 4000, Starch 1500, spray-dried lactose and heavy precipitated calcium carbonate, and the particle size fractions experimented were $-56+45\mu\text{m}$ for the first three materials and $-45+32\mu\text{m}$ for the last. Each powder type was initially pressed on to the steel surface by centrifuging at 17,000rpm, the highest common rotation speed used in Chapter 4. This particular centrifuge speed was chosen because of its greater differentiating power than the lower speeds on the adhesion properties of the test solids (see Section 4.2.3.3). Thus, any subsequent adhesional changes that might occur as a result of longer durations of the preliminary compression would be more readily detected.

The pressing of the particles to the steel substrate followed the procedure as described in Section 4.2.3.1. After this stage, the corresponding adhesion profile was determined as in Section 4.2.2.1. The humidity levels throughout this part of the work did not exceed a R.H. of 50%, and the temperature in the centrifuge chamber was maintained at about $20\pm 2^\circ\text{C}$ at all stages of centrifugation.

5.3 RESULTS

The integral curves expressing the distribution of the adhesion forces of particles, at the various time duration of preliminary compression, are shown in a semi-log scale in Figs. 5.1 to 5.4. All the adhesion profiles show a somewhat initial plateau region, before the percentage of adhering particles decreased linearly with the adhesion force. Compared to spray-dried lactose, the adhesion profiles of PEG 4000, Starch 1500 and calcium carbonate are relatively less separated from each other, within the experimental time period from 60 to 960 seconds. It was also noticed that, no residue of the adherent particles of any powder was seen attaching to the stainless steel surface after separation was complete.

Adhesion data of the powders was plotted on logarithmic probability coordinates (see representative examples in Figs. 5.5 to 5.8). For PEG 4000, a linear section for its adhesion profiles was obtained between approximately the 90% and the 10% probability regions, for Starch 1500 95% to 20%, for spray-dried lactose 90% to 15% and for the calcium carbonate 80% to 10%. On the basis of the previous discussion (see Section 4.2.3.2), the adhesion profiles obtained for the four particulate materials were considered to follow the log-normal law, for the distribution of adherent particles with respect to the adhesion force. Owing to the pattern of the straight lines in the log-probability graphs, it was not possible to assign to each powder a specific value of the adhesion force, above which particle adhesion began to follow the log-normal law, but in general, this particular force value increased with the compression duration.

The above statistical treatment of the adhesion results allowed each adhesion profile to be characterized by the geometric median adhesion force and the geometric standard deviation, σ_g . Values of these two statistical parameters for the four adhesive systems are tabulated in Table 5.1. With regard to the values of σ_g , no specific relationship of it was observed with the duration of the preliminary compression. By assuming the adhesion data was normally distributed, the results of the one-way analysis of variance for PEG 4000 ($^4F_{25}=1.635$, $p=0.197$) and spray-dried lactose ($^4F_{26}=1.117$, $p=0.37$) indicated that, for either powder, there was no significant

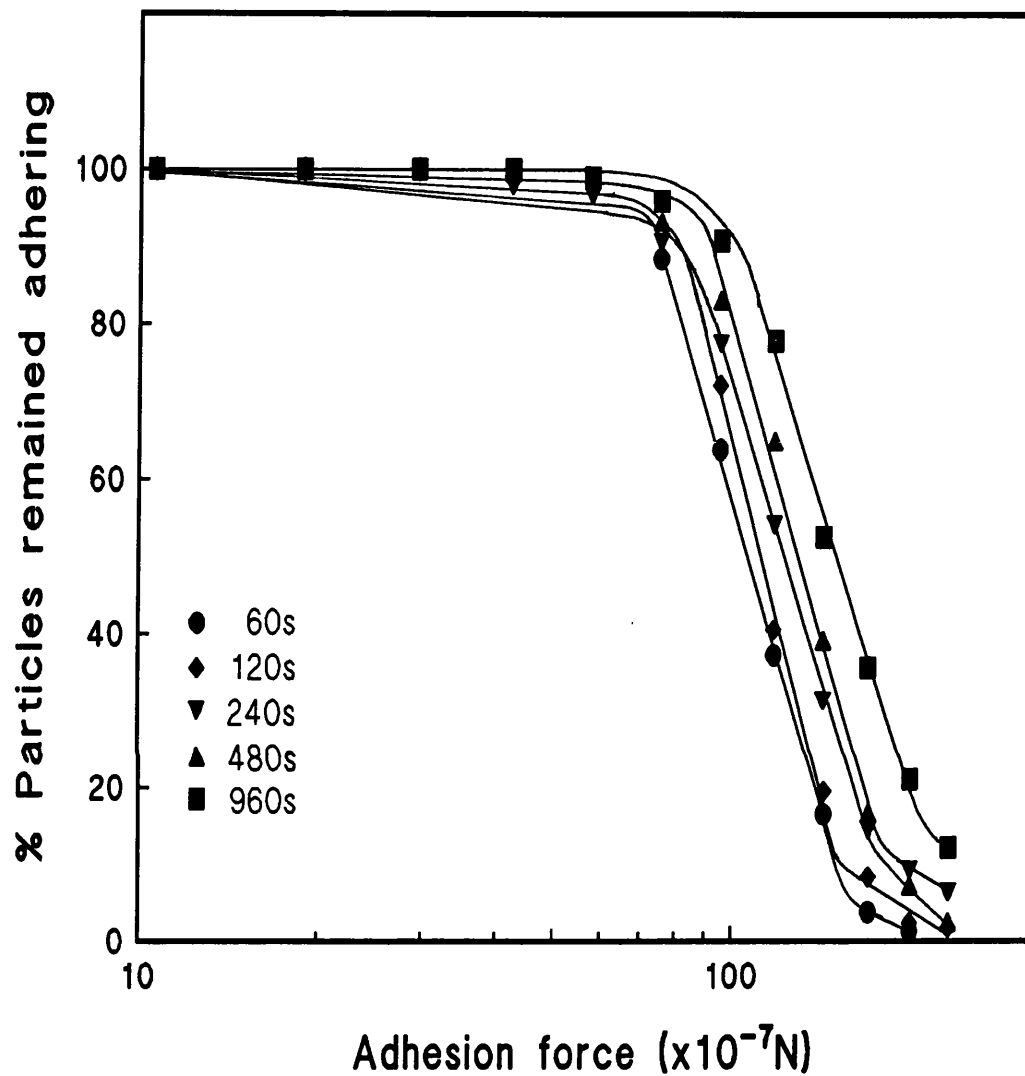


FIG. 5.1 Adhesion profiles of PEG 4000 to stainless steel, as a function of the duration (in seconds) of preliminary compression.

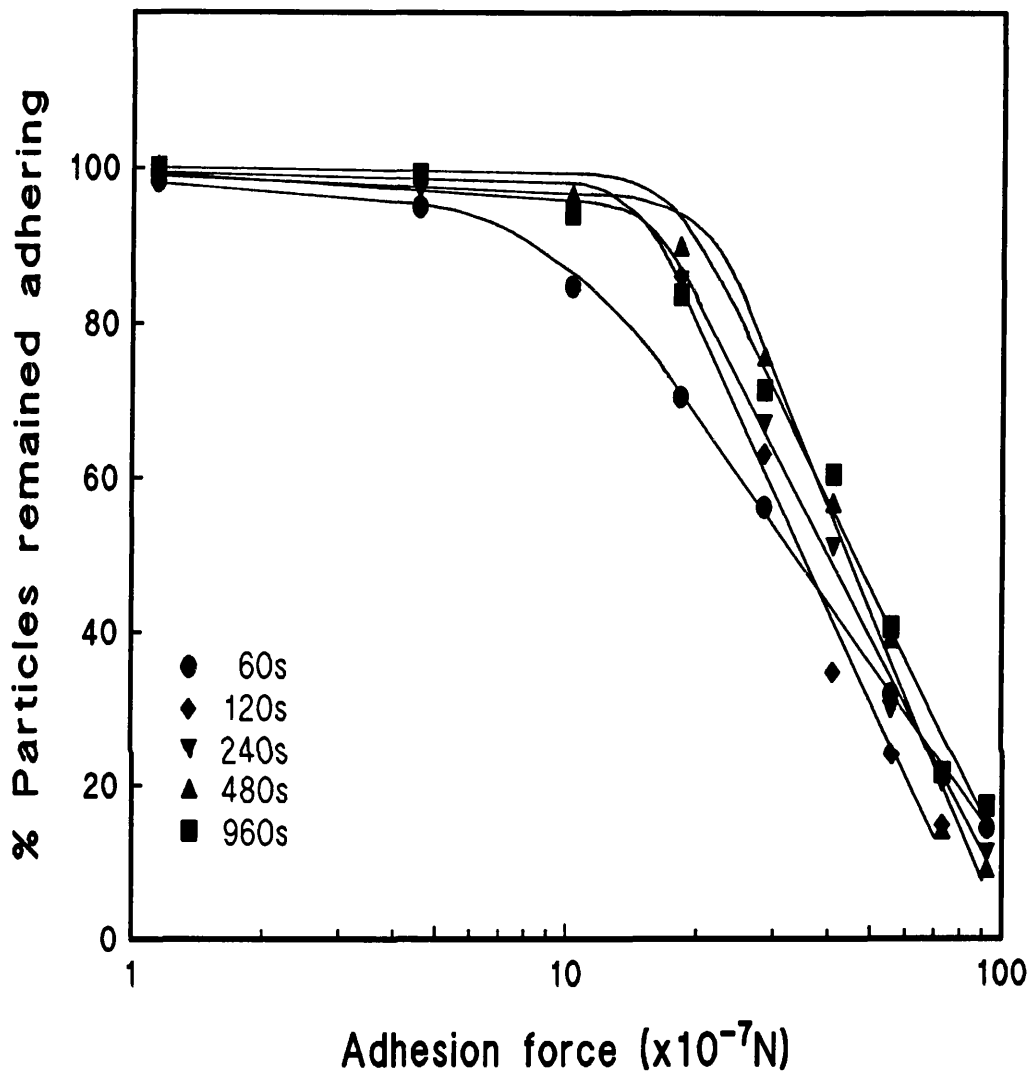


FIG. 5.2 Adhesion profiles of Starch 1500 to stainless steel, as a function of the duration (in seconds) of preliminary compression.

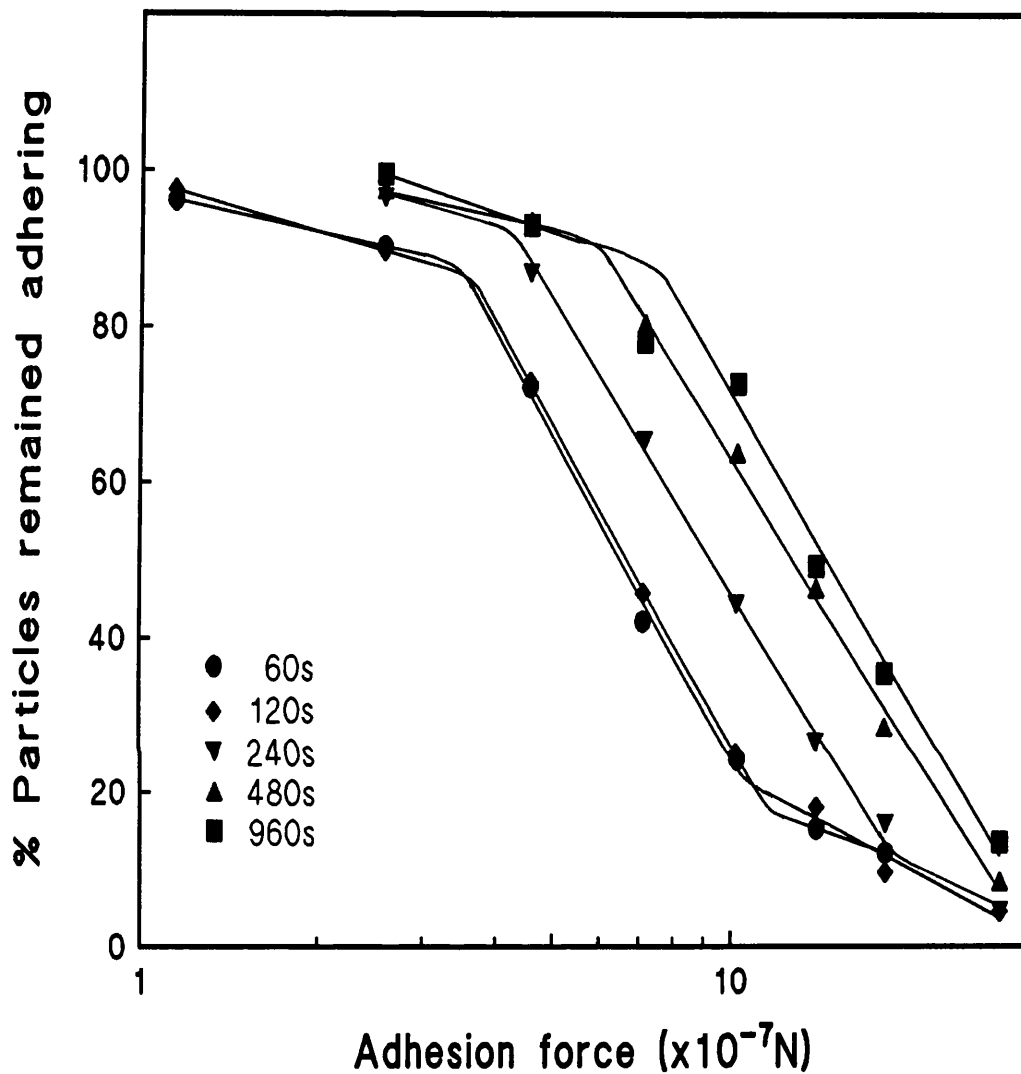


FIG. 5.3 Adhesion profiles of spray-dried lactose to stainless steel, as a function of the duration (in seconds) of preliminary compression.

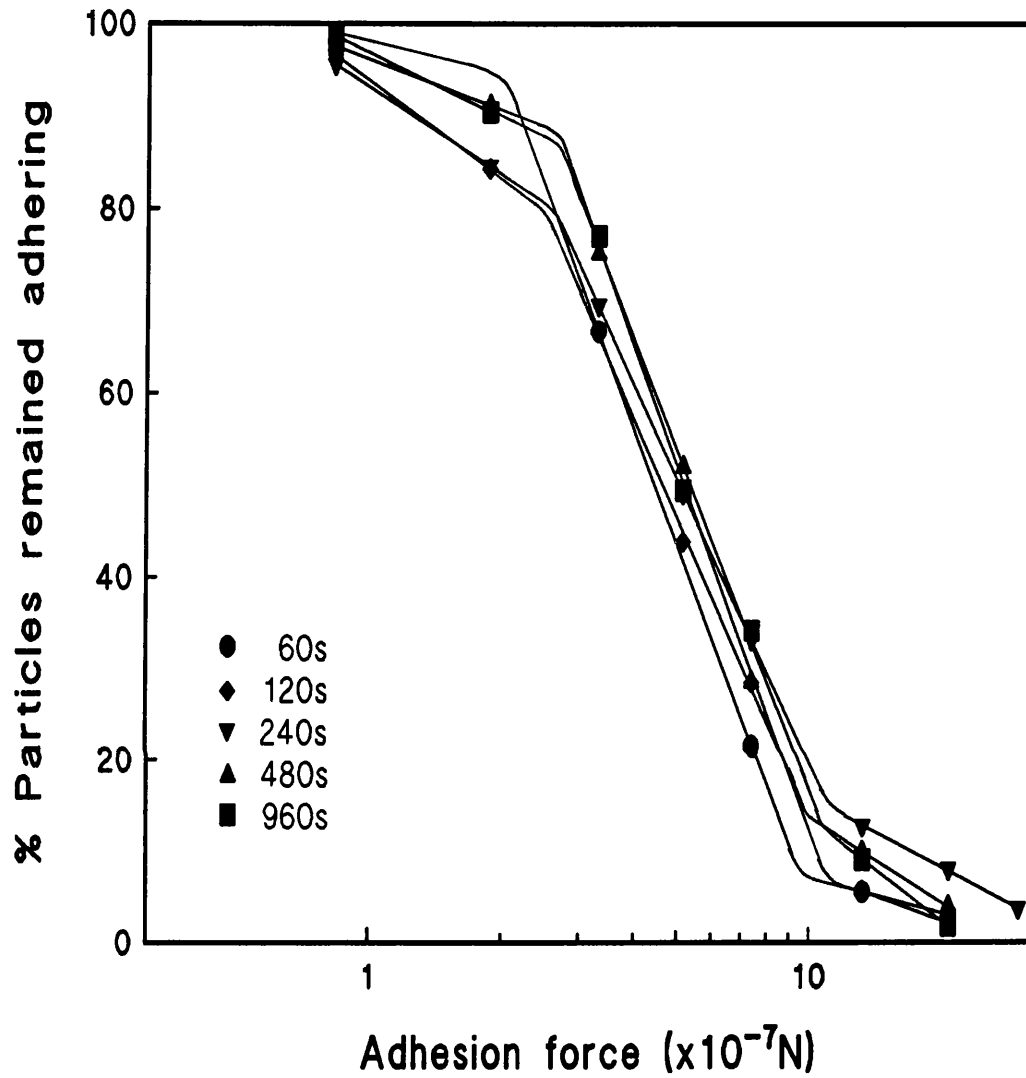


FIG. 5.4 Adhesion profiles of heavy precipitated calcium carbonate to stainless steel, as a function of the duration (in seconds) of preliminary compression.

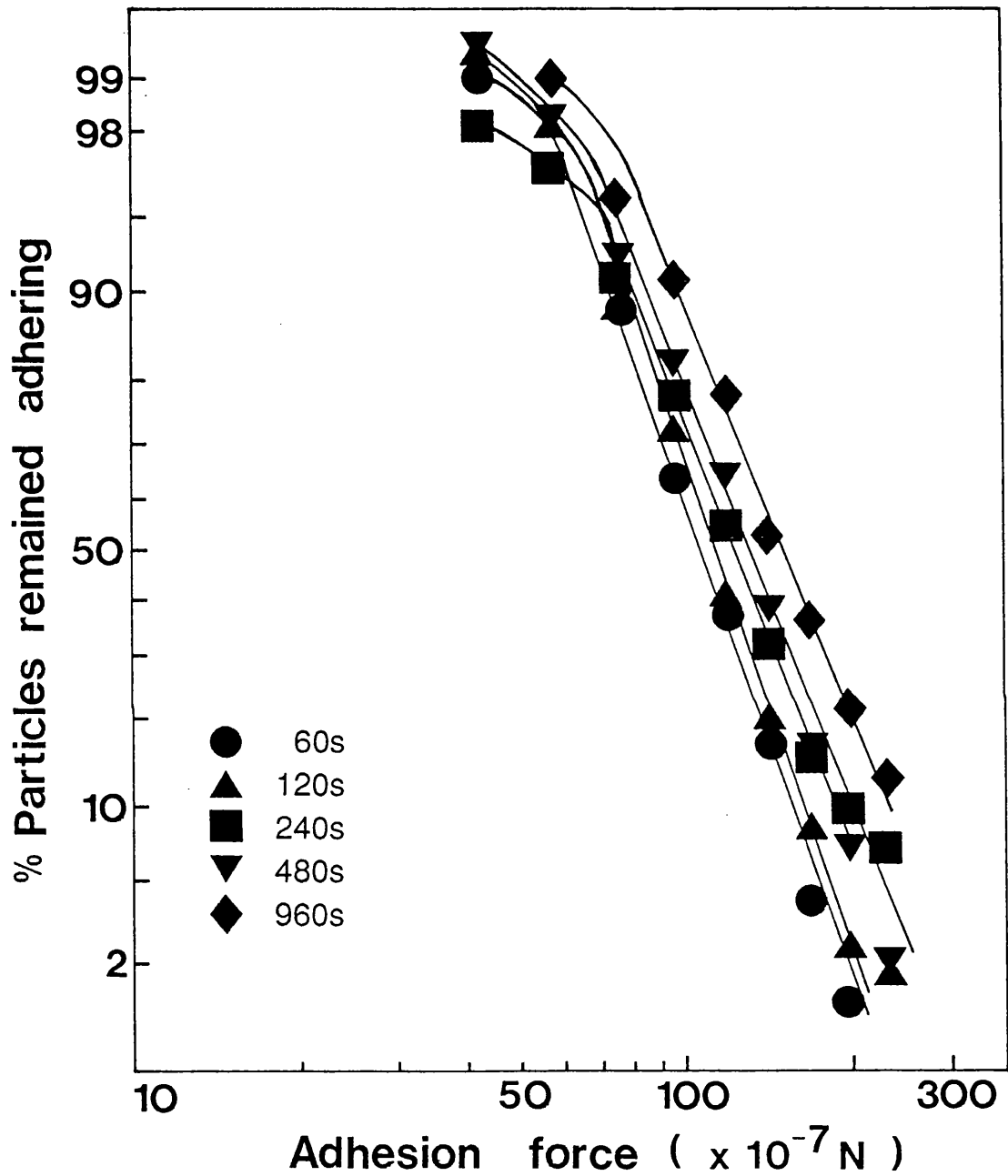


FIG. 5.5 Log-probability plots of the adhesion of PEG 4000 to stainless steel, as a function of the duration (in seconds) of preliminary compression.

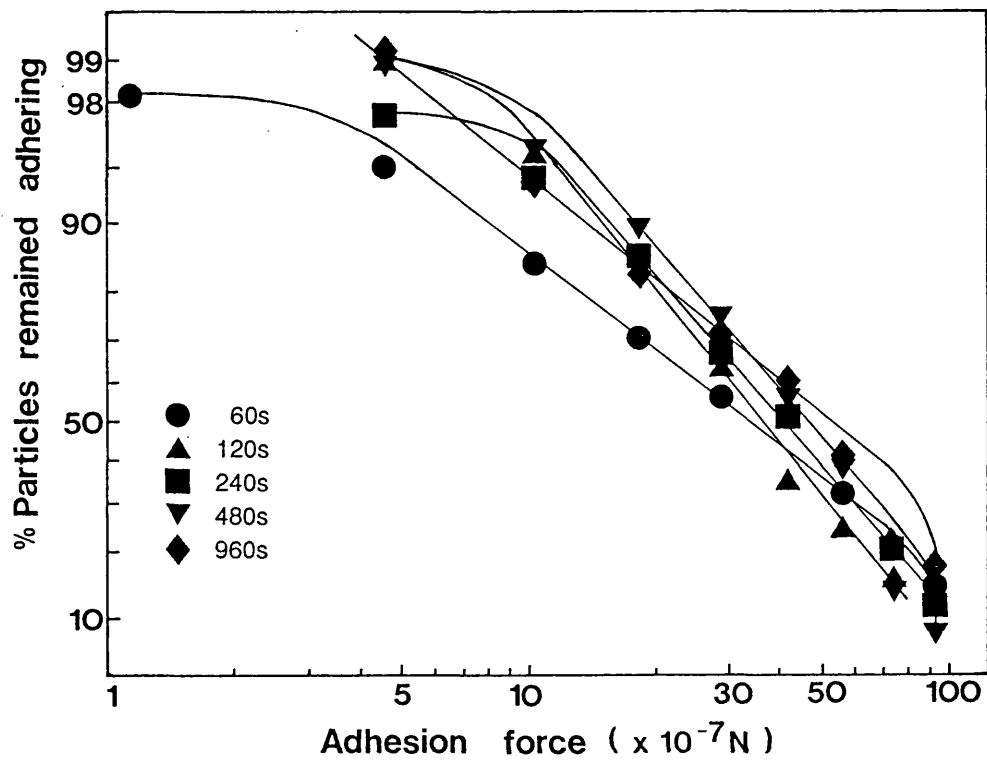


FIG. 5.6 Log-probability plots of the adhesion of Starch 1500 to stainless steel, as a function of the duration (in seconds) of preliminary compression.

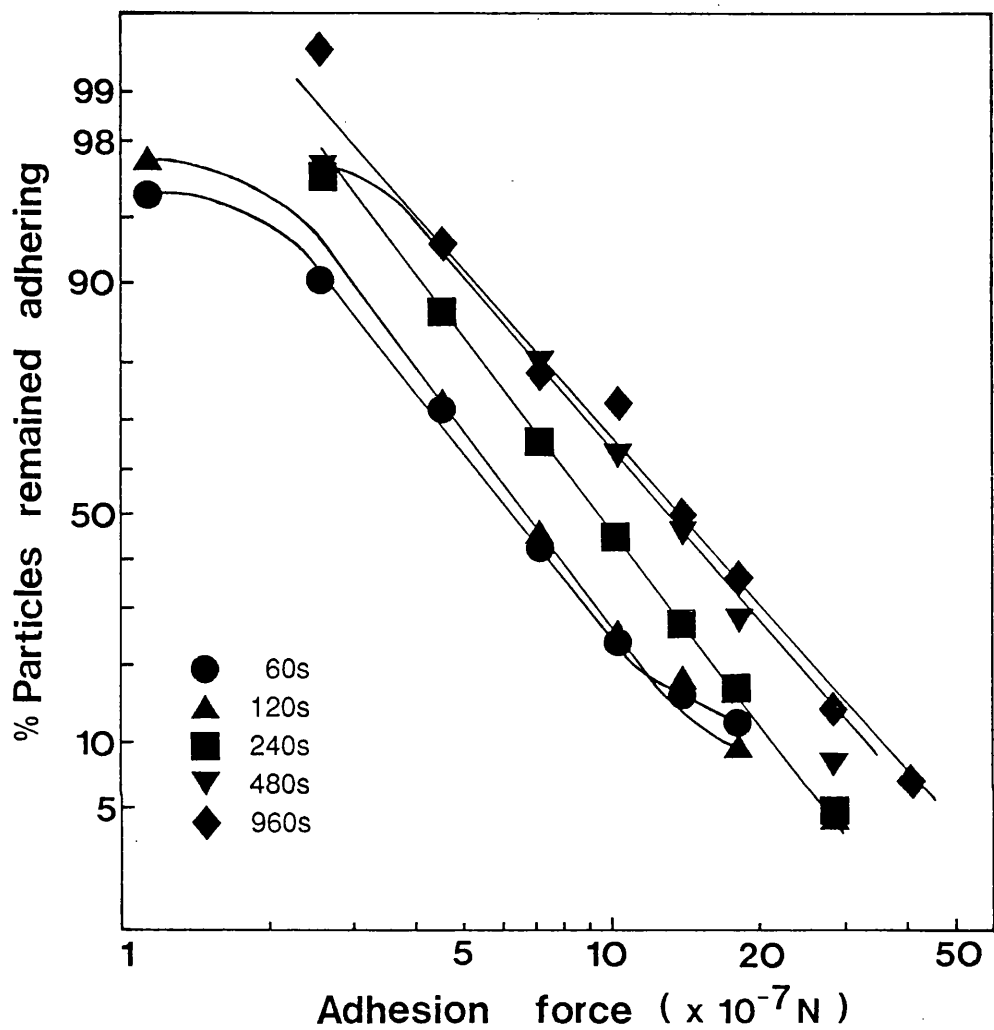


FIG. 5.7 Log-probability plots of the adhesion of spray-dried lactose to stainless steel, as a function of the duration (in seconds) of preliminary compression.

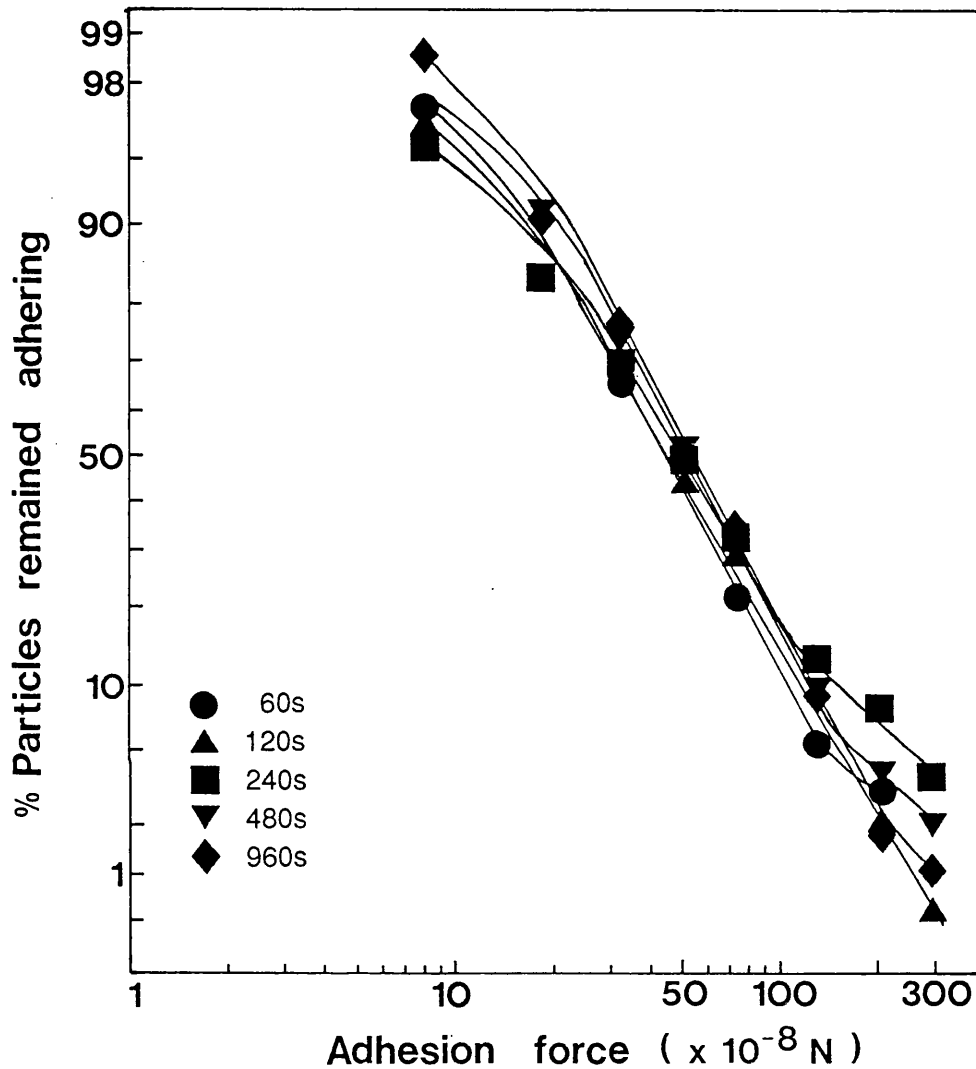


FIG. 5.8 Log-probability plots of the adhesion of heavy precipitated calcium carbonate to stainless steel, as a function of the duration (in seconds) of preliminary compression.

TABLE 5.1 Geometric median adhesion forces of powders and their corresponding geometric standard deviations, σ_g , over a press-on time period from 60 to 960 seconds, at 17,000rpm. Each experimental result is a mean of a minimum of 6 determinations.

Material	Duration of preliminary compression (s)	Median adhesion force ($\times 10^{-7}$ N)	σ_g (N)
PEG 4000	60	108.25	0.734
	120	112.58	0.732
	240	127.25	0.687
	480	129.67	0.744
	960	149.58	0.732
Starch 1500	60	32.42	0.344
	120	35.92	0.528
	240	40.60	0.538
	480	49.33	0.460
	960	53.50	0.347
Lactose, spray-dried	60	6.38	0.533
	120	6.77	0.532
	240	9.54	0.557
	480	12.48	0.568
	960	14.45	0.529
Calcium carbonate, heavy precipitated	60	4.44	0.511
	120	4.65	0.448
	240	4.99	0.405
	480	5.22	0.489
	960	5.36	0.459

difference among the different geometric standard deviation values at the various press-on duration, i.e., $\sigma_g \approx \text{constant}$. Under these circumstances, both powder-steel adhesive systems could be defined by just the median adhesion force parameter alone. In the case of Starch 1500 (${}^4F_{26}=97.96$, $p<10^{-6}$) and the calcium carbonate (${}^4F_{25}=4.772$, $p=5.34 \times 10^{-3}$), significant differences were obtained for their respective σ_g values.

The values of the median adhesion force for PEG 4000, Starch 1500 and calcium carbonate at the 60 seconds duration of compression, were the values determined in Chapter 4. The corresponding median adhesion force for spray-dried lactose, however, has poor agreement with its other median adhesion forces determined at longer compression time durations. Thus, this particular force value for the lactose was re-determined experimentally; the new mean value is shown in Table 5.1. This apparent disagreement reflected a possible kind of difficulties that could be encountered in particle adhesion experiments, albeit the experimental conditions were basically the same. As can be seen, the median adhesion force increased with the duration of preliminary compression, for all the powders. Over the experimental press-on time duration (i.e., from 60 to 960 seconds), the increase in the median adhesion force was about 38% for PEG 4000, 65% for Starch 1500, 126% for spray-dried lactose and 21% for heavy precipitated calcium carbonate. The relation between the time duration and the median adhesion force is shown in Fig. 5.9. On a log-log scale, linear relationships were depicted by all four powders. The correlation coefficients for the regression lines of PEG 4000, Starch 1500, spray-dried lactose and the calcium carbonate were 0.9738, 0.9924, 0.9821 and 0.9892, respectively. The slope of each regressed line represents the increase of the log of the median adhesion force per unit of the log of the time duration under the press-on load; the value calculated for PEG 4000 was 0.114, Starch 1500 0.190, spray-dried lactose 0.324 and heavy precipitated calcium carbonate 0.071, of which the highest rate of change was also shown by lactose.

The relative quantitative increase of the particle-steel adhesive strength per unit of the preliminary compression force, at the various time duration of compression, was expressed by the ratio of the median adhesion force to the preliminary press-on force.

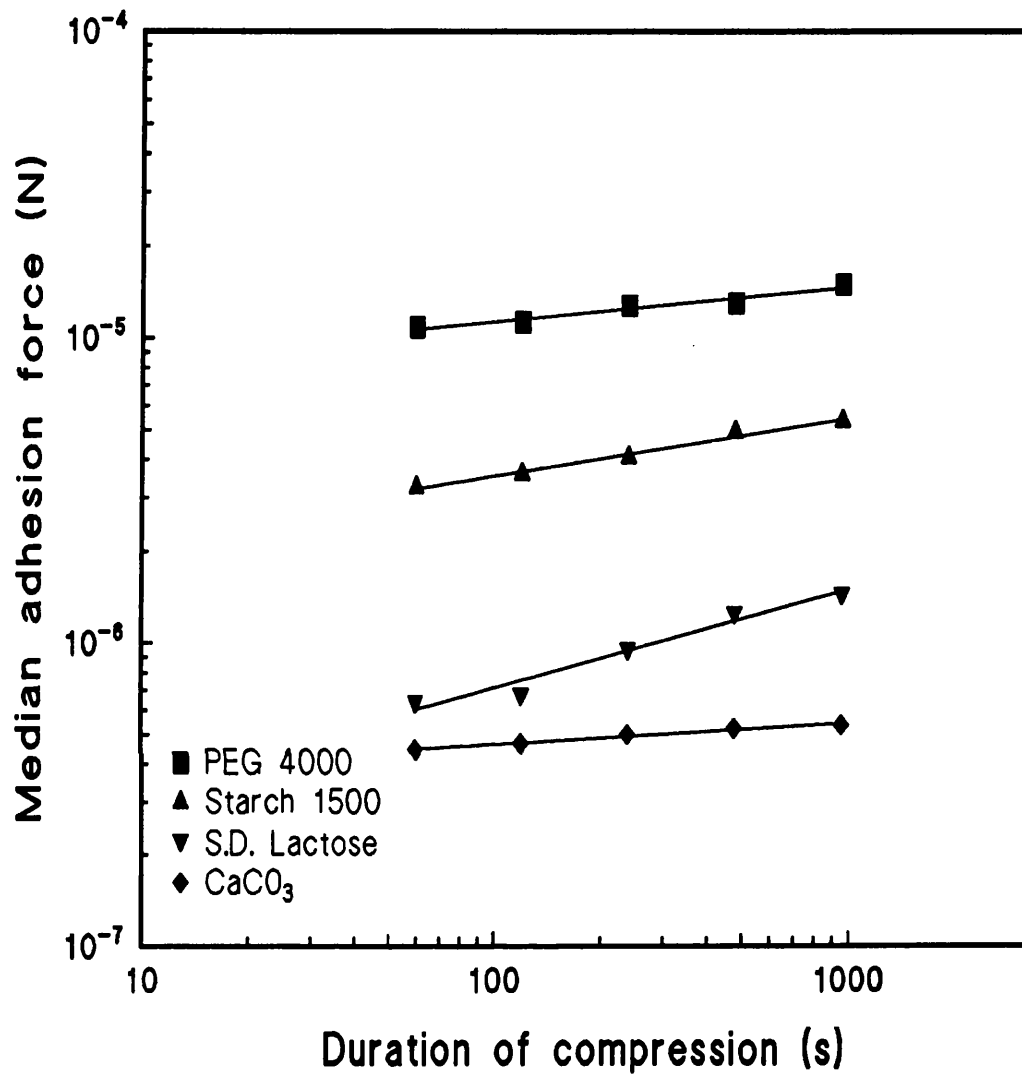


FIG. 5.9 Relationship between median adhesion force and duration of preliminary compression.

Table 5.2 shows the calculated values of this parameter for the powder materials. There was observed a general rise of this ratio with the time duration under load, and curves expressing this relationship are illustrated in Figs. 5.10 to 5.13. From the graphs, the increase of this ratio with time can be seen to depict signs of levelling off after a particular press-on time duration, with the exception for PEG 4000. This specific time duration varied with the powder; the value obtained graphically for Starch 1500 was about 744 seconds, spray-dried lactose 344 seconds and calcium carbonate 326 seconds. It indicated that a longer duration is associated with a softer or more adhesive material.

TABLE 5.2 Ratios of the geometric median adhesion force to the preliminary compression force, over a compression duration from 60 to 960 seconds, at 17,000rpm. The compression force exerted on the particles of PEG 4000 was $32.95 \times 10^{-6} \text{N}$, Starch 1500 $31.86 \times 10^{-6} \text{N}$, spray-dried lactose $31.86 \times 10^{-6} \text{N}$ and heavy precipitated calcium carbonate $23.07 \times 10^{-6} \text{N}$.

Material	Duration of preliminary compression (s)	Median adhesion force ($\times 10^{-7} \text{N}$)	Median adhesion force
			————— Compression force ($\times 10^{-2}$)
PEG 4000	60	108.25	32.9
	120	112.58	34.2
	240	127.25	38.6
	480	129.67	39.4
	960	149.58	45.4
Starch 1500	60	32.42	10.2
	120	35.92	11.3
	240	40.60	12.7
	480	49.33	15.5
	960	53.50	16.8
Lactose, spray-dried	60	6.38	2.00
	120	6.77	2.12
	240	9.54	2.99
	480	12.48	3.92
	960	14.45	4.54
Calcium carbonate, heavy precipitated	60	4.44	1.93
	120	4.65	2.01
	240	4.99	2.16
	480	5.22	2.26
	960	5.36	2.32

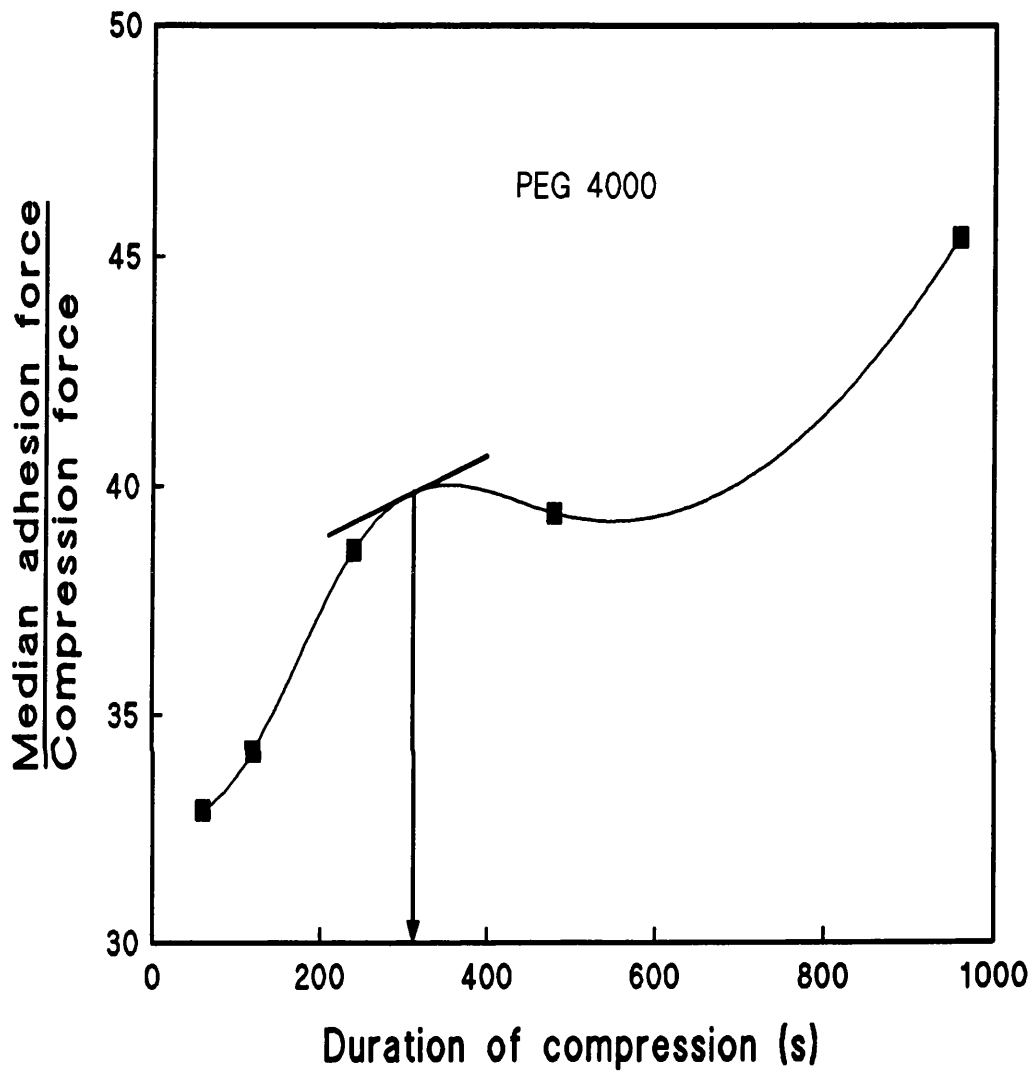


FIG. 5.10 Effect of the duration of preliminary compression on the amount of median adhesion force established per unit of the press-on force applied to PEG 4000.

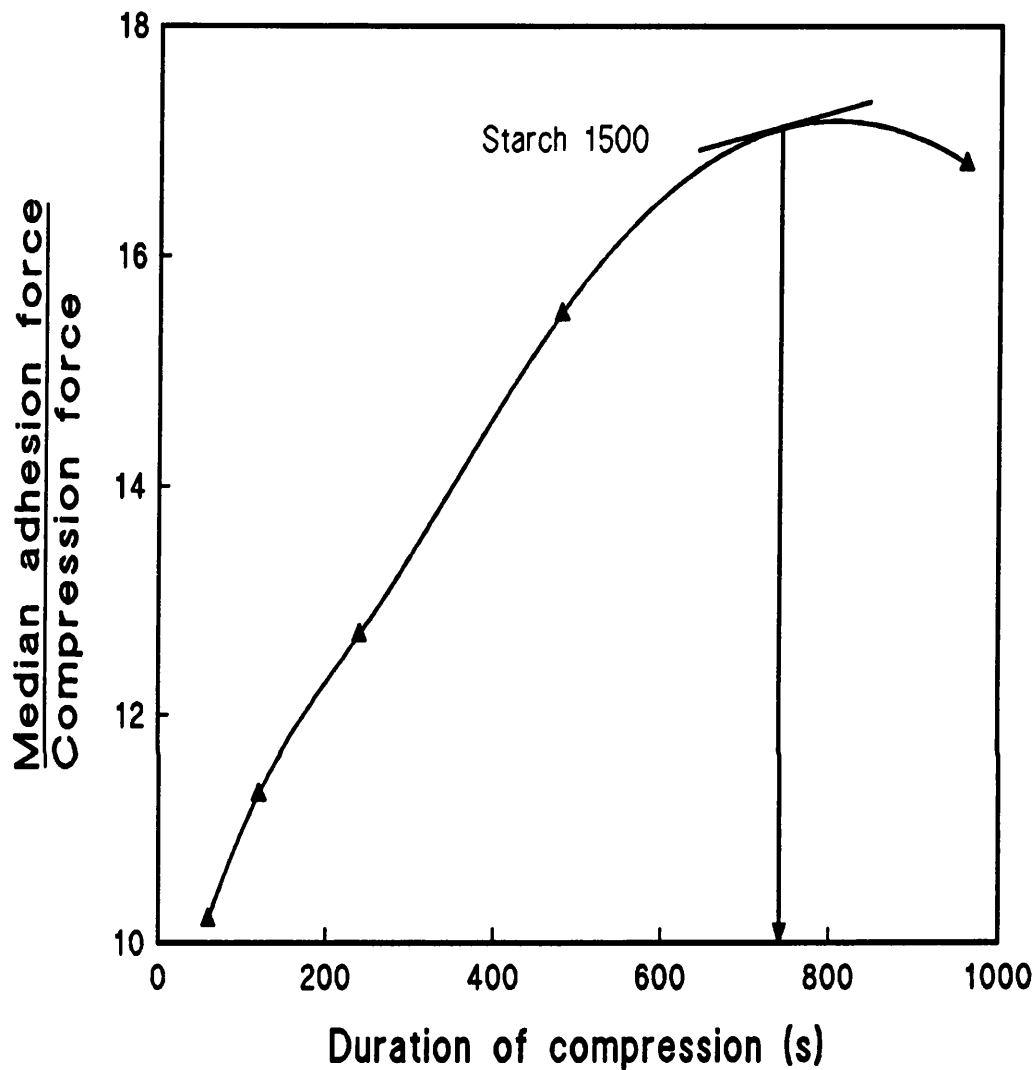


FIG. 5.11 Effect of the duration of preliminary compression on the amount of median adhesion force established per unit of the press-on force applied to Starch 1500.

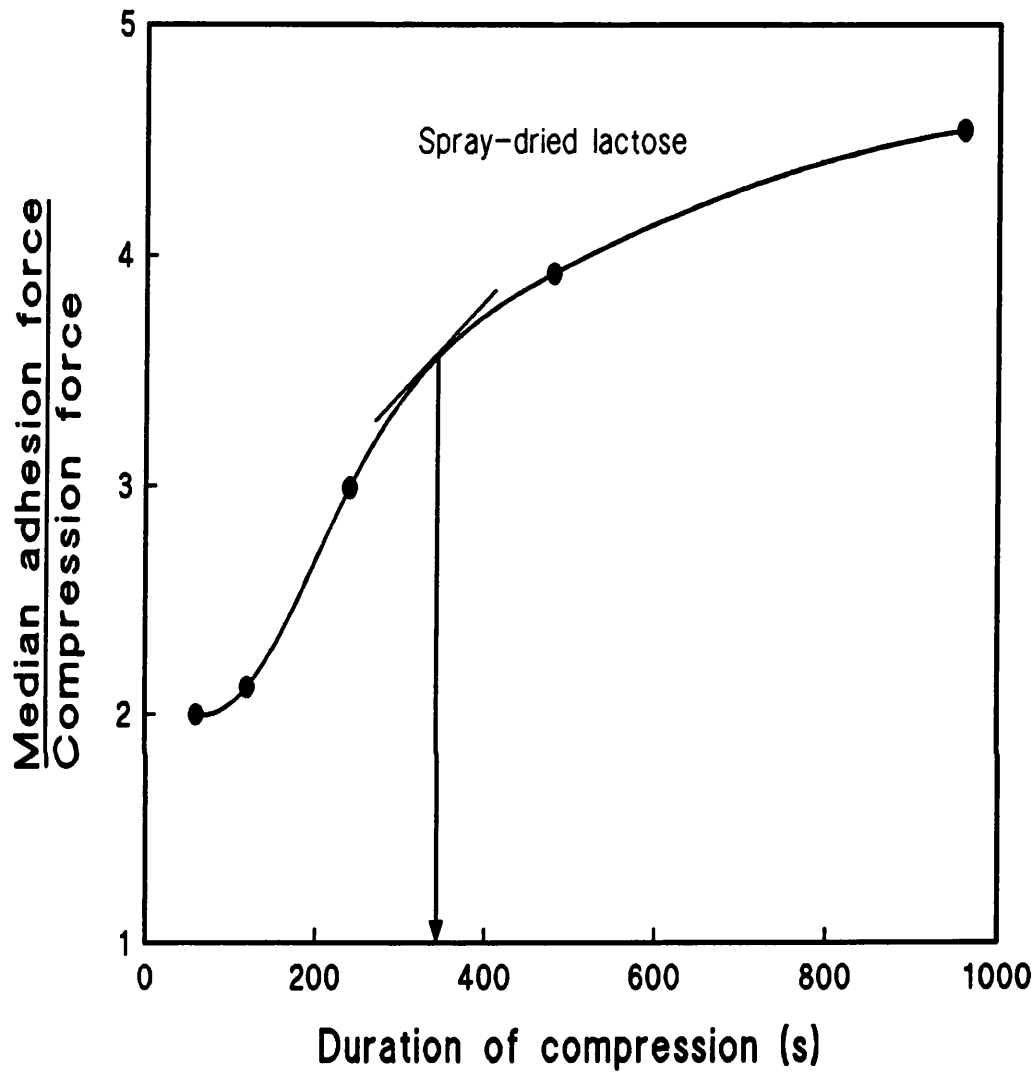


FIG. 5.12 Effect of the duration of preliminary compression on the amount of median adhesion force established per unit of the press-on force applied to spray-dried lactose.

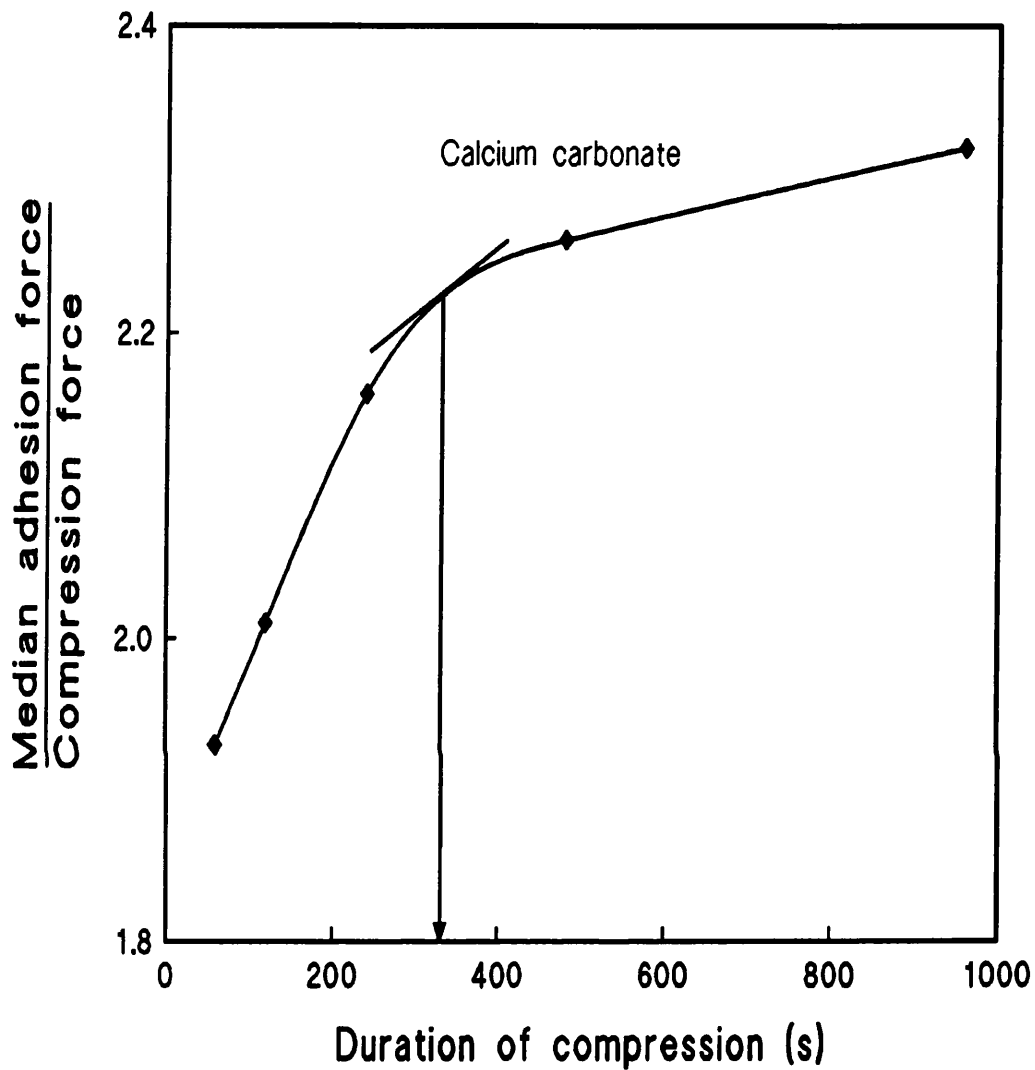


FIG. 5.13 Effect of the duration of preliminary compression on the amount of median adhesion force established per unit of the press-on force applied to heavy precipitated calcium carbonate.

5.4 DISCUSSION

The emergence of a plateau region in the initial part of the adhesion profile curves implied that almost all the particles were adhering to the steel disk with such strengths that the separation forces applied were insufficient to overcome the net adhesion forces to cause any significant detachment of particles from the substrate surface. The shifting of the adhesion profile to the right of a graph (see Figs. 5.1 to 5.4) indicated greater and greater adhesive interactions, in response to longer durations of the preliminary compression. The relatively wider spacing of the integral adhesion curves for spray-dried lactose showed apparently that, larger interaction changes occurred in the lactose-steel adhesive system. This could be substantiated by its 126% rise in the median adhesion force between the 960 and the 60 seconds compression duration. For PEG 4000, Starch 1500 and calcium carbonate, their respective increases (i.e., 38%, 65%, 21%) were much less.

The increase in the median adhesion force with the length of time the adhering particles were under a compressive load (see Table 5.1) could be accounted for as follows. When the powder solids were deposited on to the stainless steel surface, contacts would only be made at the most prominent surface microasperities of both bodies. During the stage of pressing-on at 17,000rpm (equivalent to an acceleration of about 28,000g (see Table 3.1)), the localized stresses in the minute contact structures would be taken up by the plastic deformation of the particle material; deformation of the comparatively much harder stainless steel surface could be neglected, as according to Tabor (1951). Since plastic deformations in organic materials are generally a time-dependent process, prolongation of the preliminary compression would therefore allow more adhesive bonds to be produced through extended plastic flow, leading to an increase in the magnitude of the adhesion force. This could particularly be occurring in the particle surface material in proximity to the micro-contact junctions, which was able to undergo stress relaxation significantly enough at longer (for instance, the 960 seconds) press-on period to yield further contacts with the stainless steel surface. Krupp (1967) suggested that, on prolonged application of loads and in the more amorphous areas of the plastic surface, the localized pressure would be sufficient to cause substantial non-elastic deformation. On

the other hand, if two surfaces were left in contact for a length of time, the roughnesses may interlock (*Bowden & Tabor, 1964*), as a consequence, the adhesion effect would be more marked the longer the time of loading.

A molecular mechanism was proposed by Deryaguin *et al.* (1978a) for polymers to account for the increase in adhesion forces with increasing time of contact. Their principle involves molecular diffusion across the contacting interface, leading to an increase in the engagement or coupling between the matching sections and resulting eventually in the disappearance of the physical interface. With regard to the experimental conditions used in this part of the study, molecular diffusion across the interface to strengthen the adhesion was, however, considered not to be of any real significance. The possible temperature rise due to the deformation process itself was assumed to be negligibly small, so that any form of chemical bonding was also improbable.

Some of the above effects causing increased adhesion are perhaps the basis of the phenomenon of creep. The process of creep may be defined as the slow progressive deformation of a material with time, especially at constant stress. The creep effect, to which most pharmaceutical particulate materials would be exposed to, will be dependent upon the mechanical properties of the solids (*Tsardaka et al., 1988; Tsardaka & Rees, 1990*). A higher creep compliance value was found by Tsardaka & Rees (1989) for Starch 1500 ($8.1 \times 10^{-7} \text{MPa}^{-1}$) than anhydrous lactose ($1.8 \times 10^{-7} \text{MPa}^{-1}$), indicating the former was more vulnerable to the creep effect. However, the theory in this field is incomplete and exact information is not available for many pharmaceutical powder materials. In practice, due to real particles usually possess^{-ing} rough surface profiles, increased adhesion with another surface can often be satisfactorily achieved just by prolonging the contact time under a high pressure to enable the contact area to be maximized. This process is called 'cold welding' or 'pressure welding' and is a common procedure employed in the metal industry.

The linear relationship shown in Fig. 5.9 may be expressed by the following empirical mathematical formula:

$$\log F_m = a_m \log t + b_i \quad (5.1)$$

where F_m is the median adhesion force, a_m is the slope, t is the length of time under a compression load and b_i is the intercept on the ordinate, which could correspond to a compression time of $t=1s$. The increase in the logarithm of the median adhesion force per unit change of the logarithm of the compression duration, expressed by the slope of the regressed line, was not found to bear any relationship to the known mechanical properties (such as the yield pressures and Young's moduli) of the powders or to their adhesion ratios determined in Chapter 4.

The percentage increase of the median adhesion force for PEG 4000 was smaller than those for Starch 1500 and spray-dried lactose, although the former was softer and more adhesive than the latter two materials. Moreover, spray-dried lactose depicted an exceptionally marked increase in its adhesive strength to the steel substrate. This apparent unexpected adhesional behaviour of spray-dried lactose could probably be explained by its brittle solid structure. Particulate materials prepared by the process of spray drying would have a porous solid structure, as was found by Fell & Newton (1971a) for lactose prepared by spray-drying. The spray-dried product exhibited a lower apparent particle density when compared with its crystalline form, which was explained as due to the former having hollow particles. On the other hand, because of the rapid rates of evaporation in a spray drying process, the solids produced could contain relatively higher proportions of crystal imperfections, causing them to be more vulnerable to a compression load. For instance, lactose solids obtained by spray drying was generally found to yield more readily under pressure than crystalline lactose (Fell & Newton, 1971b). Bowden & Tabor (1964) previously suggested that, brittle solids could become more ductile when under pressure, because the compression of the surface layers would heal the surface defects and cracks. Thus, for a porous particle under a plastic compression force for an extended period, there could possibly result in an incipient failure in the bulk solid or breakage of its surface structure. Such changes would allow additional solid materials to be in contact with the substrate surface, thereby enhancing the adhesion.

Starch 1500 was not prepared by spray drying, however, the use of the pre-gelatinization process in its manufacture could possibly introduce structural imperfections within the particles so that the above effects for spray-dried lactose might similarly be occurring in the starch. The extent of such effects should be smaller, but was perhaps significant enough to outweigh the percentage adhesional increase seen in PEG 4000. An additional contributory factor to this larger percentage force increase in Starch 1500 may be illustrated by the findings of Rees & Rue (1978), which indicated that plastic deformation of the starch can only take place slowly. Thus, at a longer duration under a compressive load, the effect of the plastic deformation in Starch 1500 was more fully manifested at the particle contact sites, resulting in its greater adhesional change than that observed in PEG 4000.

On the assumption of plastic deformation occurring in the adhesion, the initial rise of the curves in Figs. 5.10 to 5.13 could be attributed to an appreciable increase in the area of true contact. Owing to the probable effect of work hardening (particularly after prolonged compressions) in the particle materials at and in close proximity to the adhesive area, the increase in the contact area would be expected to be less upon further lengthening of the press-on process. This phenomenon was revealed in Starch 1500, spray-dried lactose and calcium carbonate, by probably the change in the slope of their curves after a certain compression duration. This particular time duration, beyond which the effect of deformation hardening began to predominate, was shorter for the harder calcium carbonate than the softer Starch 1500, which indicated that, the significance of the effect of work hardening appeared sooner in a harder solid than in a softer material.

5.5 CONCLUSIONS

The influence of the duration of preliminary compression on the adhesion of four pharmaceutical solids to stainless steel was investigated by a centrifuge technique. All the powders depicted an increase in the median adhesion force over the experimental length of press-on time from 60 to 960 seconds, which indicated that the duration of compression can significantly affect the subsequent adhesion properties of the particles to the substrate. A linear relationship was obtained between the logarithms of both the median adhesion force and the time of contact under load. In the case of spray-dried lactose, its time-dependent adhesion property to the steel substrate was overshadowed by the smaller magnitudes of its median adhesion force when compared with those of PEG 4000 and Starch 1500. This is because the largest adhesional change was seen in the lactose, though itself being a harder and less adhesive material than PEG 4000 and Starch 1500. The observed effect was attributed to the weaker inherent lactose particle structure, which allowed the solids considerable stress relaxation under prolonged application of a compressive load. It was also found that, the effect of deformation hardening occurred generally sooner in a harder solid than in a softer material. Thus, extended times of application of a compressive load can technically be important with regard to particle adhesion; due considerations should be given to the inherent particulate structure of a powder when processing the material in actual practice.

CHAPTER 6

Influence of Particle Size on Powder Adhesion to Stainless Steel

6. INFLUENCE OF PARTICLE SIZE ON POWDER ADHESION TO STAINLESS STEEL

6.1 INTRODUCTION

The behaviour and mechanical properties of particulate materials are, to a large extent, dependent on their particle size or size distributions. Indeed, particle size is almost always one of the primary variables in all experimental tests. Without exception, particle size can also be a key factor in the theory and practice of adhesive interaction.

Particle adhesion, as a function of particle size, has often been quantified in terms of the tensile strength of a powder mass (e.g. *Farley & Valentin, 1967/68; Kočova & Pilpel, 1971/72*). Another experimental method previously used to determine the relative magnitude of 'particle-particle' attraction force, in relation to particle size, was sedimentation. For this method, basically, particles of a known and narrow size distribution are dispersed in an inert liquid. The sedimentation volume, measured after centrifugation, will decrease if particle-particle attraction is more dominant than separation forces in the liquid medium. With regard to single particle adhesion, previous investigations into the effect of particle size usually employed ideal models of uniform spheres and smooth flat surfaces (e.g. *Bradley, 1932; Overbeek & Sparnaay, 1952, 1954; Vold, 1954*).

Different relationships between particle size and the force of adhesion to a solid plane exist in the literature. Both direct and inverse dependence of adhesive force on particle diameter were reported. Alternatively, complete independence of adhesive force on particle size, over a certain range characterizing the difference in sizes of these particles, was also observed. Bradley (1932), for example, found a direct proportionality between adhesion force and particle radius, in experiments with quartz and borate spheres. Later, Corn (1961) confirmed the linear relationship from experiments with freshly blown quartz and Perspex microspheres. On the other hand, by using metal styli in place of spherical particles, Kohno & Hyodo (1974) also

observed linear dependence of the adherence force on the tip radius. More recently, studies by Bowling (1988) indicated a direct variation between adhesion force and particle size. With very irregularly shaped quartz particles adhering to a hard metal surface, Krupp (1967) obtained an approximate proportionality between adhesive force and the square root of the particle size. An inverse relationship, however, was found in the adhesion of spherical glass particles to a steel surface by Deryaguin & Zimon (1961). Further examples of such inverse relationship are given in the monograph of Zimon (1982). In contrast to many studies, Böehme *et al.* (1962) reported an independence of adhesive force on particle size. All these adhesion studies involved mainly elastic particle contacts, and the prime adhesional attraction was assumed to be due to the van der Waals forces.

Research carried out by several workers (e.g. *Aleinikova et al., 1968, Deryaguin et al., 1968/69, 1976, 1984*) revealed the variation between adhesive force and the radius of certain particles to follow a power law with an exponent close to 2. In their work, experiments were carried out on the sticking of elastic polyvinyl chloride and polystyrene spheres to a steel surface, and investigated by means of a 'dynamic' method using a pneumatic adhesiometer (*Deryaguin et al., 1968/69*), in which an initial compression of the particles to the plane substrate was involved. The quadratic relationship was explained by the authors as being due to the effect of the electrical double layer formed within the zone of contact during the press-on stage. This explanation was corroborated quantitatively by direct measurement of the electrical charges removed by the particles after their tearing from the substrate surface. Therefore, under those circumstances, the electrostatic forces predominated in the adhesion, and the molecular effect was comparatively negligible. The possibility of any significant contribution from preliminary static electrifications to the electrostatic force from the electrical double layer was also considered small, agreeing with a similar conclusion reached by Krupp & Sperling (1966).

The above information illustrates that, both molecular and electrostatic forces are significant in particle adhesion, but the conflicting results tend to indicate that one force component can, in certain cases, predominate over the other. This effect is

probably dependent upon the adhesive system concerned. For a dry system, in which the capillary effect could usually be neglected, the total forces of adhesion are governed principally by the molecular van der Waals and electrostatic forces, both of which are related in different ways to particle size. In the interpretation of experiments on particle adhesion to a solid surface, one main difficulty has been the differentiation between the molecular and electrostatic forces as to which is the major contributor to the total adhesion forces. This problem could be tackled by determining both the force of adhesion and the electrical charge, after detachment, in the same experiment (Aleinikova *et al.*, 1968; Donald, 1969). For many systems, however, the materials or, perhaps, the experimental techniques available for the study do not possibly permit simultaneous measurements of both adhesion and the electrophysical parameters needed to characterize the electrical double layer. The identity of the dominant contributing force component may, alternatively, be found by considering, from a theoretical point of view, the nature of the forces responsible for adhesion. According to Zimon (1982), for particle-substrate adhesion, the various dependence on particle size of the different components of adhesive force are as follows:

Components of adhesive forces	Relationship with particle radius (R)
Van der Waals	R
Coulomb	R^{-1}
Electrical double layer	R^{-2}

From this, it can be seen that, only if the molecular van der Waals component plays a dominant role will the adhesion force then become proportional to the particle size. If Coulomb or electrical double layer forces predominate, the overall force of adhesion may very well not depict a direct variation with particle size.

A number of previous works associated with the adhesions of particles to a substrate, under small or zero loads, have been explained on the basis of elastic

contacts. In practice, solid-solid contacts invariably involve some plasticity, particularly when adhesion between two rough surfaces occurs at their surface rugosities, where the high localized pressures developed at these sites would bring about material flow. The purpose of this chapter is to examine the effect of particle size on the adhesions of some pharmaceutical particulate materials to stainless steel, after a compression force has initially been applied to force the particles on to the substrate surface. An attempt will also be made to identify the nature of the adhesive forces involved in the interactions.

6.2 EXPERIMENTAL METHOD

The influence of particle size on adhesion, after the particles have initially been forced on to the stainless steel substrate, was investigated for two previous pharmaceutical powders, Starch 1500 and spray-dried lactose. Experiments were performed with particles ranging between 32 and 75 μm in diameter. They were separated with test sieves using an air-jet sieve into five powder size fractions, namely, -40+32 μm , -45+40 μm , -56+45 μm , -63+56 μm and -75+63 μm (see Section 2.1.4) for this experiment. Representative powder fractions of each size fraction were 'dusted' on to the stainless steel substrate disk surface at ambient conditions and air relative humidities not over 50%.

The particles of each size fraction were preliminarily forced on to the substrate surface at an arbitrary chosen centrifuge speed of 10,000rpm (which is equal to an acceleration of about 9,700g (see Table 3.1)), following the procedure described in Section 4.2.3.1. Immediately after this compression stage, the adhesion profile which illustrates the distribution of the adherent particles in relation to the adhesion force, was determined for the particular powder size fraction, as in Section 4.2.2.1. The centrifugation temperature was maintained at about 20 \pm 2 $^{\circ}\text{C}$.

6.3 RESULTS

The distribution of the particle adhesion force for the five size fractions of Starch 1500 and spray-dried lactose are presented as the integral adhesion curves in Figs. 6.1 & 6.2. Each powder sieve fraction was observed to have some particles that adhered to the steel substrate with great as well as with little tenacity. It can also be seen that a broader distribution of the particle adhesion force occurred for the smaller than the larger particle size. Virtually, all the adhesive force distribution curves for both powder excipients display an initial plateau section, though this region became progressively shorter as the particle size investigated became larger.

Linearization of the adhesion results was performed by plotting the data on logarithmic probability coordinates. Representative plots are shown in Figs. 6.3 & 6.4. In general, experimental data points at the extremities of a probability line can usually be ignored in practice, because of their comparatively greater degree of scattering (discussed in Section 4.2.3.2). A straight line section of the probability curves was obtained between the probability regions of 85% and 10% for Starch 1500 and between the 80% and 10% regions for spray-dried lactose. Therefore, the distributions of particles of the various size fractions with regard to the adhesion force, for both powders, were considered to follow a log-normal function. From this, the adhesion of the powder particles to the steel substrate can be characterized by the geometric median adhesion force and the geometric standard deviation, σ_g ; the latter was calculated as the ratio of the 50% probability force value to the 16% probability force value. Mean values (of six results) of these two statistical parameters for the different particle size fractions of both materials are listed in Table 6.1. The average median adhesion force value given for the -56+45 μ m sieve fraction of spray-dried lactose was the value determined in Chapter 4, however, the corresponding force value for Starch 1500 showed disagreement with the median adhesion force values of its other particle size fractions. Thus, this particular force value for the latter solid was discarded and re-determined for the present experiment.

Preliminary experimentations with the same five particle sieve fractions of both powders indicated that, without the initial stage of forcing the particles to the

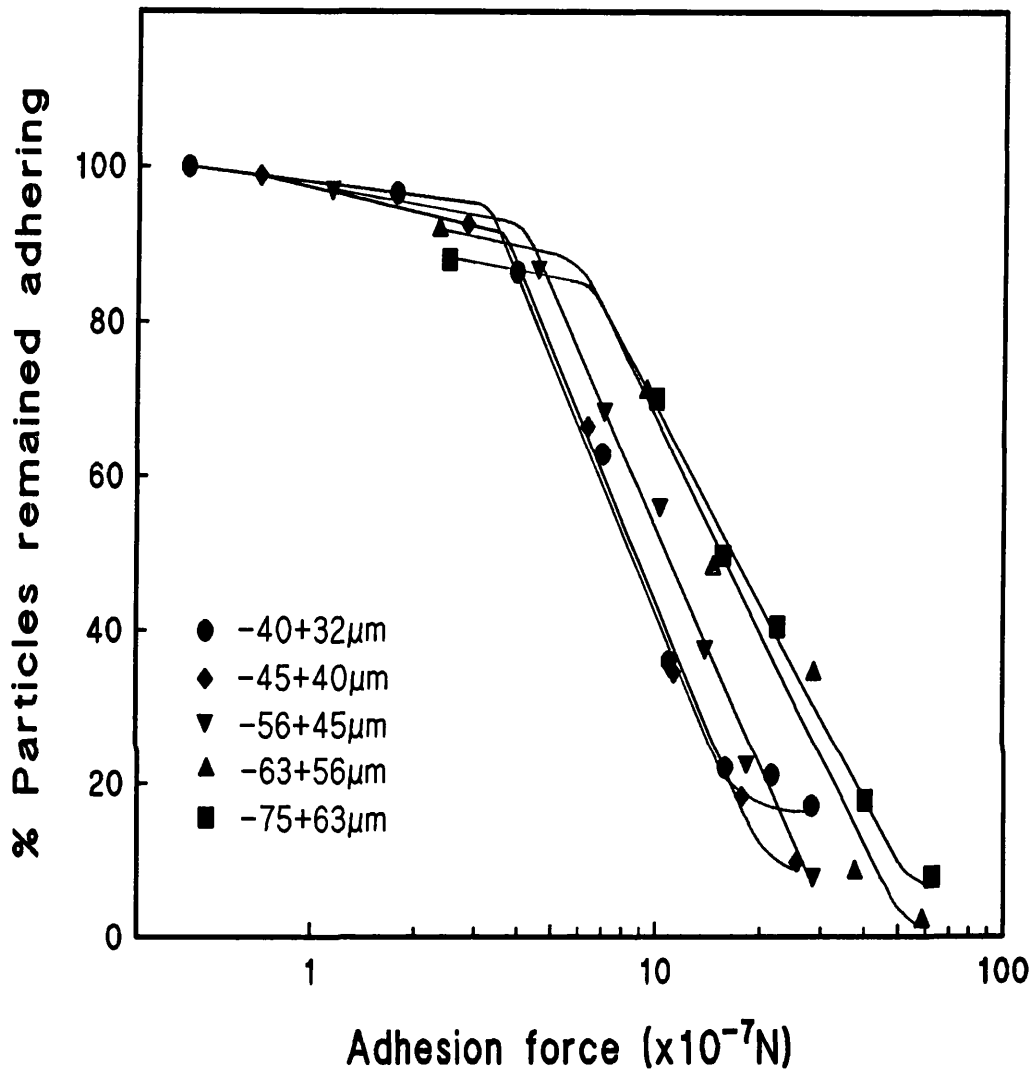


FIG. 6.1 Adhesion profiles of different particle size fractions of Starch 1500 to stainless steel, after preliminary compression.

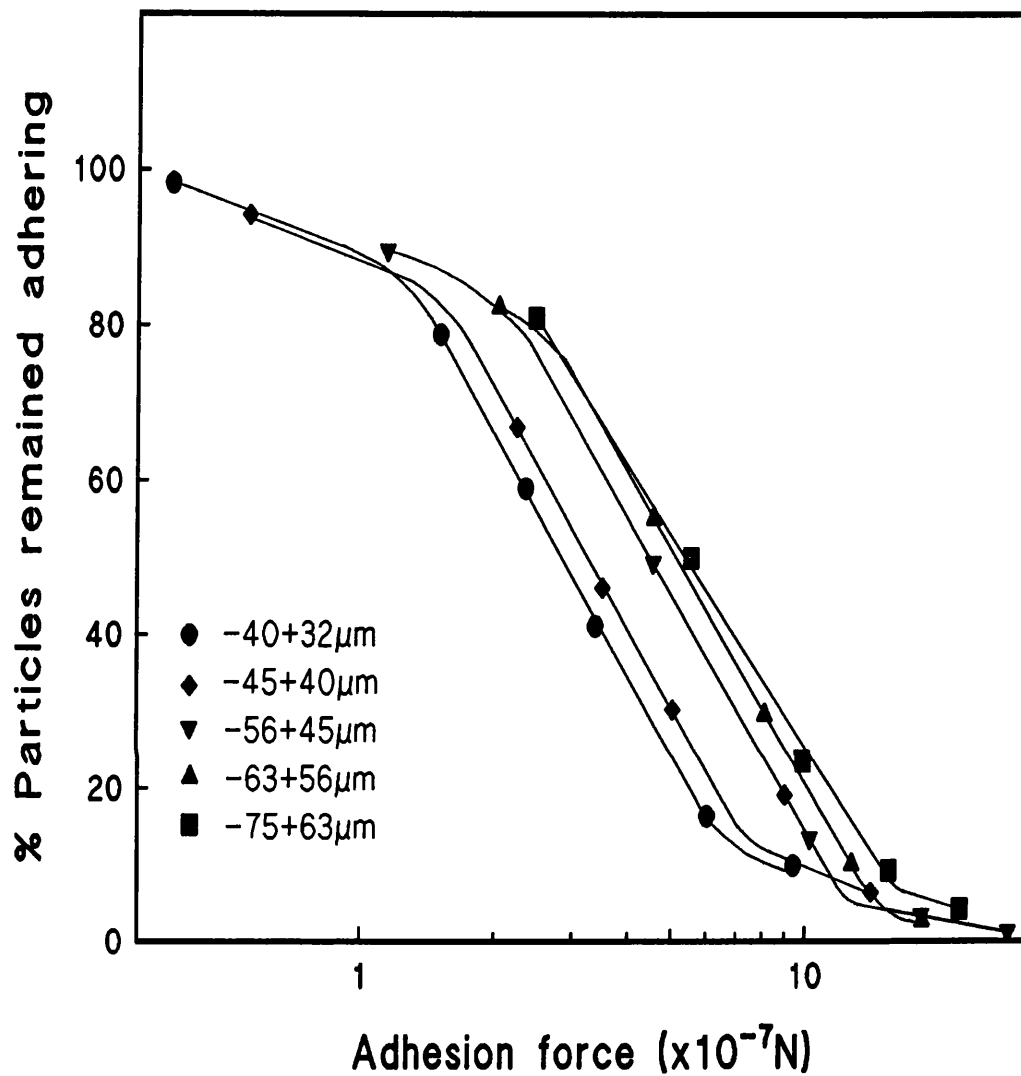


FIG. 6.2 Adhesion profiles of different particle size fractions of spray-dried lactose to stainless steel, after preliminary compression.

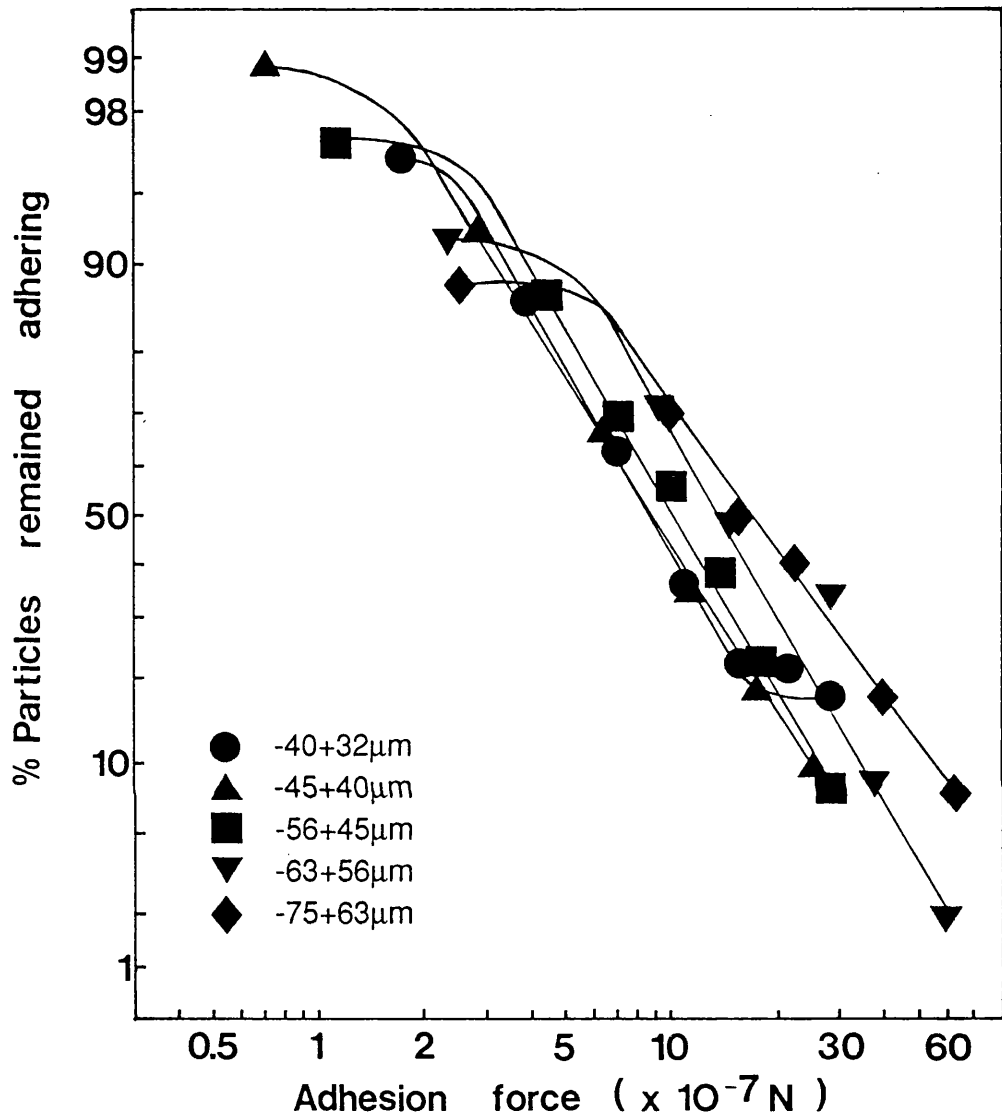


FIG. 6.3 Log-probability plots of the adhesion of different particle size fractions of Starch 1500 to stainless steel, after preliminary compression.

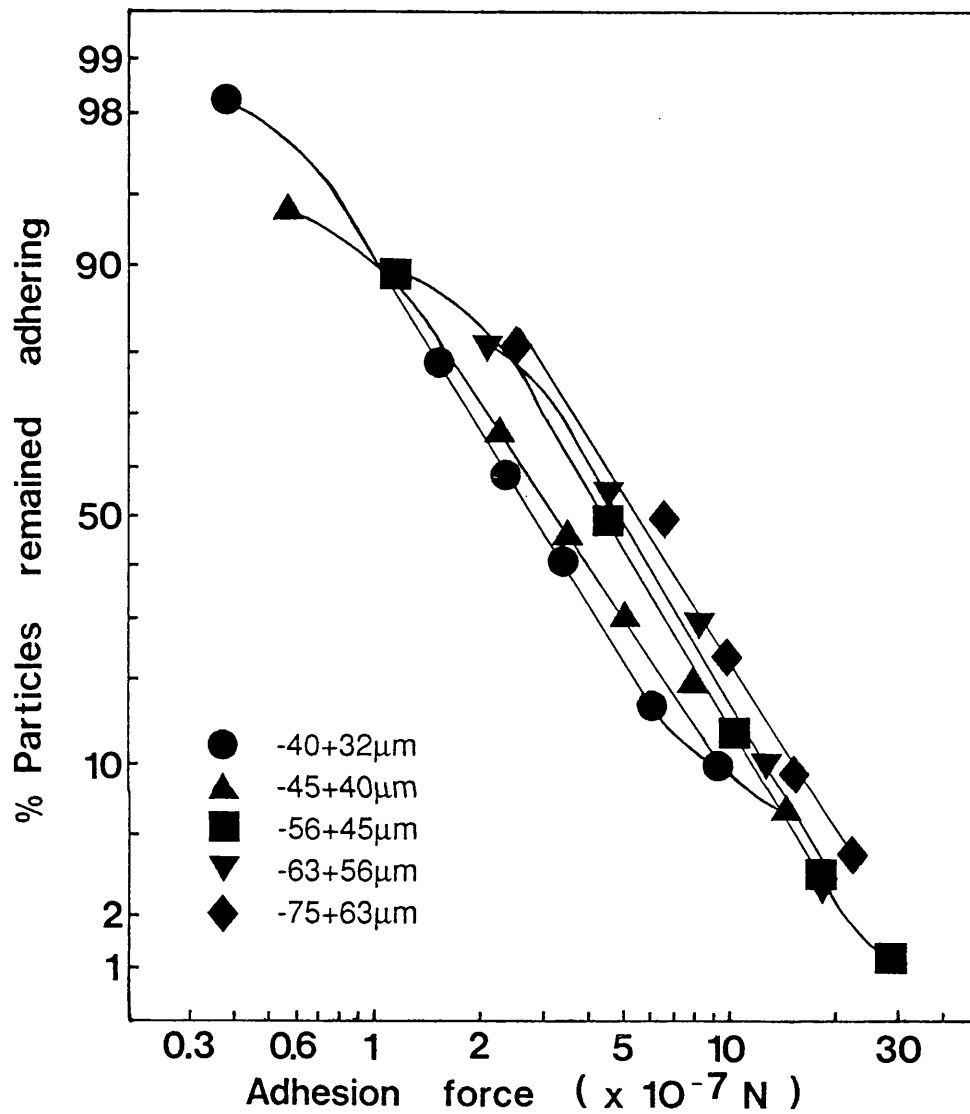


FIG. 6.4 Log-probability plots of the adhesion of different particle size fractions of spray-dried lactose to stainless steel, after preliminary compression.

TABLE 6.1 Values of the median adhesion force and geometric standard deviation, σ_g , of the various particle size fractions of Starch 1500 and spray-dried lactose.

Material	Particle sieve fraction (μm)	Calculated* particle radius, r (μm)	Median adhesion force ($\times 10^{-7}\text{N}$)	σ_g (N)
Starch 1500	-40+32	19.21	8.57	0.4907
	-45+40	22.53	8.84	0.4850
	-56+45	26.43	10.64	0.4877
	-63+56	33.57	14.23	0.4518
	-75+63	34.30	17.38	0.3862
Spray-dried lactose	-40+32	18.21	2.72	0.4857
	-45+40	20.82	3.21	0.4092
	-56+45	26.38	4.33	0.4670
	-63+56	31.96	4.98	0.4326
	-75+63	34.08	5.52	0.4698

* = see later text for calculation

substrate, the adhesion was very little. Determination of the median force of adhesion, under those circumstances, was not possible. After the preliminary pressing-on, particle adhesion greatly increased and the larger particle size fractions were observed to depict higher values of the median adhesion force. Although the adhesion force values obtained for Starch 1500 were all higher than the corresponding values for spray-dried lactose, both materials depicted an equivalent mean adhesional force increase from the lower to the higher size fraction, over the same range of particle size. In this particular case, the increase was found to be about 103%.

The average particle size of each sieve fraction was estimated from the apparent particle density (Section 2.1.5) and the mean particle mass (Section 2.1.6), by assuming the volume of the particles to approximate that of a sphere of equal mass. For a rough particle contacting a rough surface, the radii of curvature of the contacting asperities are of concern in adhesion. However, quantitative evaluation of the various dimensions of micro-contacts is still not feasible for many practical systems. This is, no doubt, why ideal models have often been chosen for many previous experimentations. Apart from the notion that the number of real contacts will usually be proportional to the size of a rough particle, nothing was known of any predictable relationship between the generally non-uniform geometries of the deformed surface asperities and the bulk particle radius, which would allow some theoretical estimations to be made on the magnitudes of the radii of the true contact areas. Under an external compression force, flattening of the particle surface elevations at the contact points was often assumed to approximate the theoretical case of a smooth surface. Moreover, because the particle rugosities were already minute, even after some degree of plastic flow, the dimensions of the contact areas, situated at the tips of the surface asperities, were assumed to be still a comparatively tiny fraction in relation to the bulk particle size. On the basis of these assumptions, adhesions may be interpreted in a way that, the substrate did not 'see' the various individual particle micro-contact sections clustering together, but it 'noticed' the full size of the adherent particle instead, so that adhesive interactions may be discussed, as a first approximation, in terms of the overall particle size, for the investigated size fractions of the two powders.

The experimental relationship between the median force of adhesion and the calculated average particle radius is given in Fig. 6.5. A reasonably good linear proportionality was observed for both Starch 1500 and spray-dried lactose; the correlation coefficients for the regression lines being 0.9790 and 0.9982, respectively.

The straight line sections of the probability curves (in Figs. 6.3 & 6.4) appear parallel to each other, the slopes of which were represented by their respective values of the geometric standard deviation, σ_g . By assuming that the adhesion data followed a Gaussian distribution, the values of σ_g for the different powder sieve fractions were analysed using the one-way analysis of variance. The results of the test indicated no significant difference among the σ_g values of the five particle size fractions for spray-dried lactose (${}^4F_{26}=2.243$, $p=9.19\times 10^{-2}$), but a significant difference among those for Starch 1500 (${}^4F_{25}=4.399$, $p=7.89\times 10^{-3}$). Further analysis of the σ_g data sets of Starch 1500 by means of a *posteriori* statistical test, the Tukey method (*Snedecor & Cochran, 1980*), revealed only the σ_g value of the -75+63 μ m size fraction was different, those for the other four powder fractions were statistically insignificant from each other. On the assumption that this apparent variation was due to some unrealized experimental discrepancy, the different values of σ_g were considered, by and large, constant, in the particle size range from 32 to 75 μ m, for either powder material. Under such circumstances, the median adhesion force could solely characterize the particle-substrate adhesion.

The relative extent of adhesion to the steel substrate between the different particle size fractions may be expressed numerically in terms of the ratio of the median adhesion force to the preliminary compression force. This ratio is dimensionless and its different calculated values are listed in Table 6.2. On the basis of using the bulk particle size, the variation of this ratio with particle radius is illustrated in Fig. 6.6. Inverse relationships were obtained, on log-log coordinates, for both Starch 1500 and spray-dried lactose; the correlation coefficients for the respective regressed lines being 0.9813 and 0.9985. This indicated that, larger particle size of the test powders showed relatively smaller extent of adhesion to the steel substrate.

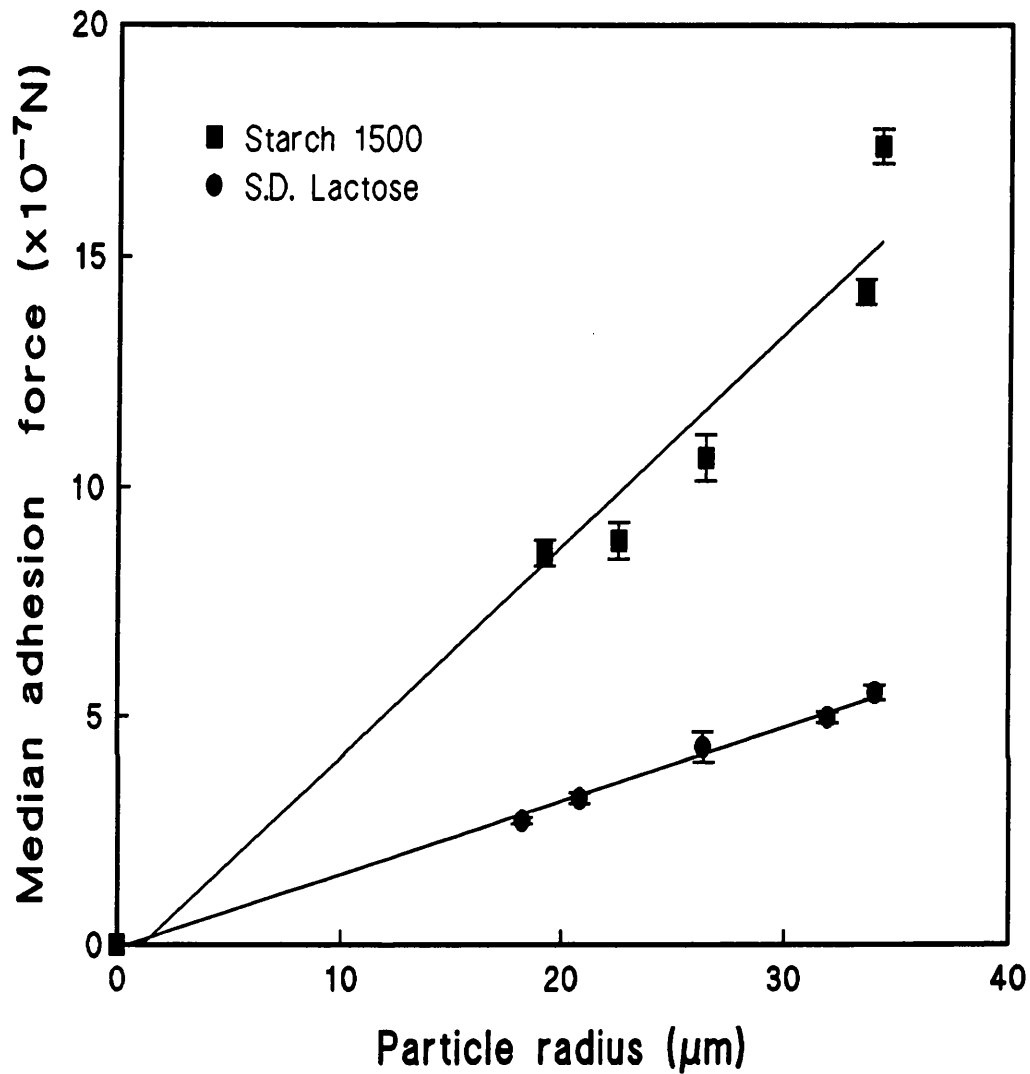


FIG. 6.5 Relationship between the median adhesion force and the calculated average particle size, when the powder solids have initially been forced on to the stainless steel surface. The error bar represents ± 1 s.e.m.

TABLE 6.2 Ratios of the median adhesion force to the preliminary compression force for the various calculated particle sizes of the test powders.

Material	Calculated particle radius, r	Preliminary compression force	Median adhesion force	Median adhesion force
	(μm)	($\times 10^{-5}\text{N}$)	($\times 10^{-7}\text{N}$)	$\frac{\text{Median adhesion force}}{\text{Compression force}}$ ($\times 10^{-2}$)
Starch 1500	19.21	0.426	8.57	20.1
	22.53	0.686	8.84	12.9
	26.43	1.10	10.64	9.67
	33.57	2.27	14.23	6.27
	34.30	2.42	17.38	7.18
Lactose, spray-dried	18.21	0.364	2.72	7.48
	20.82	0.544	3.21	5.90
	26.38	1.10	4.33	3.93
	31.96	1.97	4.98	2.53
	34.08	2.39	5.52	2.31

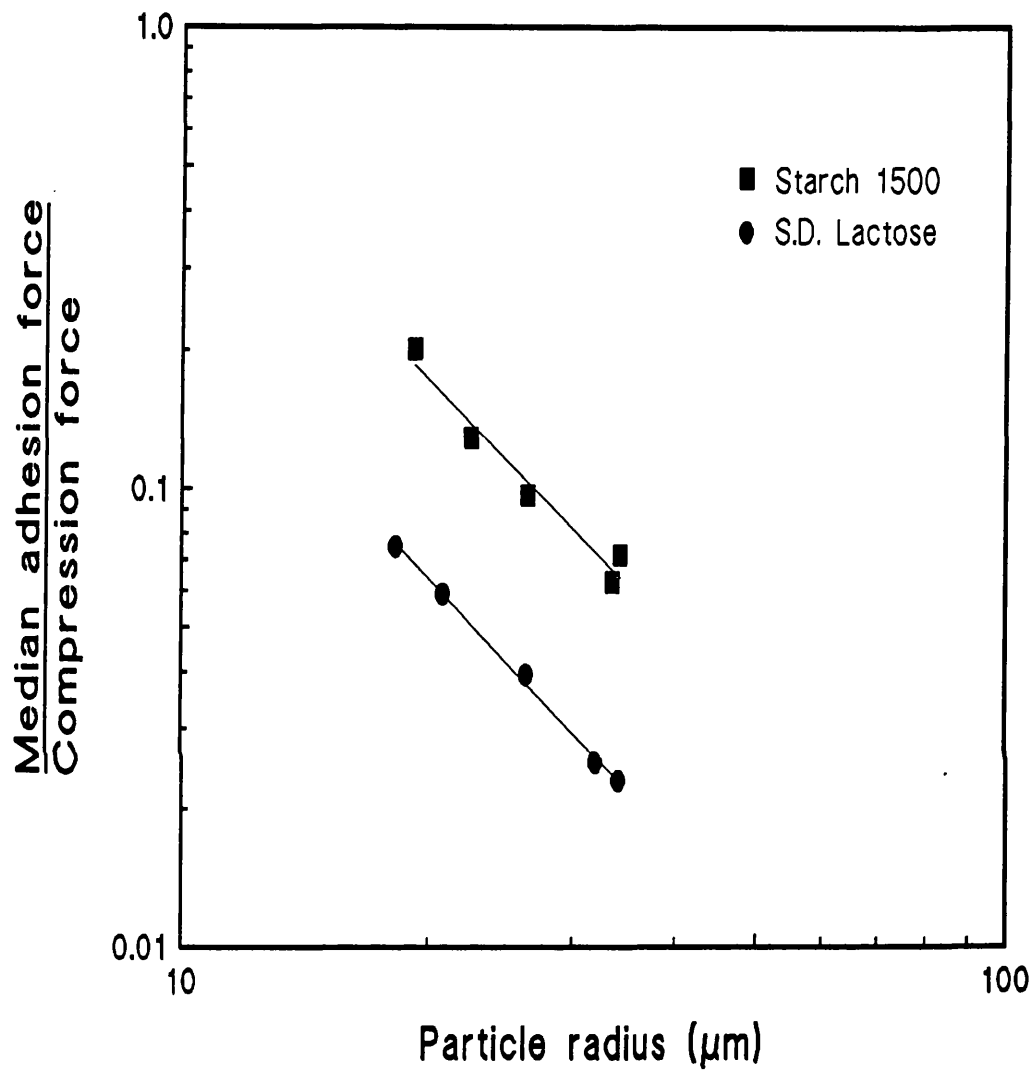


FIG. 6.6 Relative extent of adhesion of the different calculated average particle sizes of the powder solid fractions to stainless steel, after preliminary compression.

6.4 DISCUSSION

The observed increase in the particle adhesion force to the steel substrate with increase in particle size, could be explained by the nature of the contact between the contiguous bodies. On contact, a larger rough particle will generally lead to higher number of contact points being established with a rough plane surface (*Zimon, 1982*). Thus, due to a growth in the total area of true contact associated with an increase in the particle dimension, a greater force of adhesion would result. By assuming the predominance of the molecular effect in the adhesive interactions, since the 'retarded' Hamaker constant of molecular interaction (see Section 1.6.1.1), with allowance for deformation of the contact bodies, can increase with particle size (*Zimon, 1982*), a larger test particle would also bring about a proportionally larger attractive force.

The variation of the median adhesion force with particle size illustrated non-uniform particle size was a factor responsible partly for the adhesion force distribution of the particles when a powder sieve fraction was experimented. After the preliminary compression, the overall weaker adhesive strengths of spray-dried lactose implied that, the lactose solids could generally be considered as less adhesive than the starch particles to the steel substrate. This is consistent with the softer nature of the starch as well as agreeing with the findings in Chapter 4.

The direct proportionality relationship obtained in Fig. 6.5 infers that, within the specific range of particle sizes used for both powder materials, the median adhesion force varied with the first power of the bulk particle radius. This implies that the adhesive interactions involved in this study were governed mainly by the molecular van der Waals forces. This view could be substantiated by interpreting the adhesion force data in Table 6.2 as follows. When the calculated average particle radius was increased by a factor which was close to 2 (1.79 for Starch 1500 and 1.87 for spray-dried lactose), the median adhesion force was found to have increased also by a very similar factor; the value being about 2.03. This depicts a very close linear correlation, following the van der Waals relationship between adhesion force and particle size discussed earlier. A similar argument was used by Deryaguin *et al.* (1978a) as part of the interpretation of their results. In the experiments where the

electrostatic effects are claimed to be dominant in the adhesions, the adhesion force would be expected to vary over up to 4 orders of magnitude for a similar amount of particle size variation if based on the above argument, which was indeed observed experimentally (e.g. *Aleinikova, 1968; Deryaguin et al., 1968/69*). Thus, in this study, the molecular van der Waals forces could be considered as the predominating force component responsible for particle adhesions to the steel substrate. This finding may also support the assumption used in previous Chapters that van der Waals forces played a principal role in particle adhesions.

In certain cases of a rough particle contacting a plane surface where the surface rugosities of the particles are significant enough to remove the bulk of the particle from the contact points, the electrostatic forces are often considered to prevail over the van der Waals forces. This is due to the fact that, van der Waals forces decrease more rapidly with increasing distance between the adherents than the electrostatic forces, provided that there is no appreciable neutralization of the electrical double layer charges during the separation process. However, Bowling (1989) suggested that, because of the formation of multiple contact points from the multiple asperities present, the molecular effect can once again predominate. In addition, the closer contact between two bodies after deformation could bring about smaller attenuation of the van der Waals forces due to surface roughnesses. These effects altogether may make the molecular effect become significant in the adhesion.

Whilst emphasis in the particle-steel adhesion has been ascribed to the molecular van der Waals forces, the electrical force component and other possible forces cannot entirely be neglected in these adhesive interactions. From the relationship shown in Fig. 6.5, the dependence of the median adhesion force on particle size may be expressed by the following approximate equations for the two powder solids:

$$\text{Starch 1500, } F_{ad} = 0.0461R_c - 0.511 \times 10^{-7} \quad (6.1)$$

$$S.D. \text{ Lactose, } F_{ad} = 0.0161R_c - 0.069 \times 10^{-7} \quad (6.2)$$

where F_{ad} and R_c represent, respectively, the median adhesion force (in Newton) and the calculated average particle radius (in meter). The two regression lines do not pass through the coordinate origin; the intercept values on the ordinate may be considered as an estimation of the contribution from other interaction forces to the total adhesive forces (Zimon, 1982). These two empirical formulae can, however, only be considered specific for the particular adhesive systems used in this experiment.

When particle-substrate adhesion forces are determined by the centrifuge technique, the decisive factor will be the particle mass, which is in turn a function of the linear dimension of the particle. In this case, the centrifugal equation can be written as follows:

$$F_{det} = m\omega^2 r = 4\pi r\omega^2 \rho R^3/3 \quad (6.3)$$

where F_{det} is the detachment force, m is the mass of a particle, ω is the angular velocity, r is the centrifugal distance, ρ is the particle density and R is the particle radius. For particles from the same material, ρ is constant, the detachment force is then dependent upon the cube of the particle radius. At a particular speed of centrifugation, all the adherent particles will undergo the same acceleration; smaller adherent particles will thus experience smaller effective forces acting on them to pull them away from the substrate surface.

Values of the ratio of the median adhesion force to the preliminary compression force (in Table 6.2) indicate quantitatively the relative amount of interfacial adhesion force established per unit of the press-on force. For the various powder sieve fractions of both Starch 1500 and spray-dried lactose, this ratio was found to increase with decrease in the calculated particle radius. Whereas the magnitude of the detachment force, F_{det} , is dependent upon the particle mass, and

hence decreases as a function of the third power of the particle radius, the relevant median adhesion force, being considered molecular in nature, only decreases with the first power of the particle radius. Thus, as the particle size became smaller, due to a greater change in the particle mass than in the particle radius, this resulted in the above inverse relationship, as illustrated in Fig. 6.6.

The geometric standard deviation, σ_g , gives a numerical measure of the scatter of the particle adhesion force. By assuming the distribution of the particle surface asperities of the different powder sieve fractions was similar in nature, under the same compression force, the opportunities of forming adhesive bonds of various strengths would be equal in all size fractions. This may then be used to explain the insignificant statistical difference between the various σ_g values of the different powder size fractions in both Starch 1500 and spray-dried lactose. Furthermore, this may intuitively infer a similar statistical σ_g value be obtained if the corresponding unsieved powder material was experimented.

Adhesive Interaction Energy at Particle-Substrate Interface

Adhesion can be interpreted as a resistance to the breakdown of a contact between two unlike solids. To pull the contacting surfaces apart, a tensile force is required, i.e., the force of adhesion. The mechanical work expended by this force in overcoming the net adhesive forces can provide a measure of the strength of the mutual bonding between the adherents during their separation.

Various analyses have been made to evaluate the strengths of solid-substrate adhesions from a knowledge of the forces between the contacting surfaces, and the results expressed in terms of an energy function (e.g. *Deryaguin et al., 1975b; Kendall, 1988*). Since powders with different plastic deformational properties will absorb varying amounts of energy during compression, thereby, together with the adhesion force, the energy of interaction could also be a good measure of the physical toughness of a contact. Moreover, as particle adhesion is generally categorised as a

surface phenomenon, the interaction energy could be regarded as a result of the interaction between the surface free energies of two contacting solids.

The notion that the adhesive force between two unequal size spheres in elastic contact could be related to their energy of interaction, was considered in the early 30's by Bradley (1932). The following expression was obtained:

$$F_{ad} = 2\pi R_h \delta\gamma \quad (6.4)$$

where F_{ad} is the maximum pull-off force (equivalent to the adhesion force), R_h is the harmonic mean radius (given by $R_h = R_1 R_2 / (R_1 + R_2)$, where R_1 and R_2 are the radii of curvature of the contacting spheres. In the particular instance of a sphere adhering to a solid plane for which $R_2 = \infty$, R_h is equal to the sphere radius R_1), and $\delta\gamma$ is the specific energy of adhesion (given by $\delta\gamma = \gamma_1 + \gamma_2 - \gamma_{1,2}$, where γ_1 and γ_2 are the surface free energies of the adherents, and $\gamma_{1,2}$ is the interfacial free energy). The $\delta\gamma$ quantity in the above equation has the dimension of the surface free energy. Thus, for two identical bodies in contact, in which case $\gamma_1 = \gamma_2$ and $\gamma_{1,2} = 0$, $\delta\gamma = 2\gamma_1$, the surface free energy of the solid concerned can be determined by the above formula (e.g. *Bradley, 1932; Jordan, 1954; van den Tempel, 1972*).

Later, an alternative analysis was proposed by Johnson *et al.* (1971), the JKR theory, which indicated that, the surface molecular adhesion force was related to the geometry and the energy of adhesion by a relationship similar to Equation (6.4), but taking a coefficient 3/2 instead of 2 (see Section 1.9.2), i.e.,

$$F_{ad} = 3\pi R_h \delta\gamma / 2 \quad (6.5)$$

However, Deryaguin *et al.* (1975c), by adopting a different theoretical approach (the DMT theory) to that by Johnson *et al.* (1971), established a relationship in the form of Equation (6.4). This has, therefore, resulted in two different energy approaches to

the elastic contact of particles. In an attempt to clarify the situation, several researchers (e.g. *Tabor, 1977, 1978, 1980; Deryaguin et al., 1978b, 1980*) have made a number of observations relative to the region of applicability of the JKR and DMT models. The general conclusion arrived is that, in the absence of the electrostatic contribution and considering only the molecular component of the work of adhesion, the DMT theory is more precise in describing the force-energy relationship for relatively rigid particles (with modulus of elasticity, $E \geq 10^9 \text{Nm}^{-2}$), whereas considering the macroscopic geometry of the contact zone and the nature of particle detachment, corresponds better to the JKR theory (*Israelachvili et al., 1980; Muller & Yushchenko, 1980, 1982; Muller et al., 1980, 1983b*).

The specific adhesion energy, $\delta\gamma$, described above refers to the thermodynamic equilibrium energy of adhesion, which is valid for a process of reversible equilibrium elastic contact. Under an applied compression, plastic deformation or viscous flow of the materials at an interface would invariably arise. Also, with the centrifuge technique, the adhesive force can only be determined in a 'destructive' manner. Particles detachment, under these circumstances, do not therefore represent an equilibrium condition. By assuming, however, that the elastic energy from the applied compression force was entirely expended in the plastic deformation process, a pragmatic approach could be to interpret the equilibrium energy term, $\delta\gamma$, as the apparent work needed to break the plastic adhesive bonding (*Kendall, 1988*). By employing Equation (6.4), the value of this apparent adhesive interaction energy, ϕ_a , can be found from the slope of a plot of adhesion force versus particle radius. Since a linear relationship was obtained in Fig. 6.5, the values of ϕ_a thereby calculated for Starch 1500 was 7.34mJm^{-2} and for spray-dried lactose 2.56mJm^{-2} . The larger ϕ_a value obtained for the starch agreed with the previous conclusion (Chapter 4) that particle adhesive bondings with stainless steel was stronger for Starch 1500 than spray-dried lactose.

When compared with the order of magnitude of the solid surface dispersion energy values obtained in other types of experimental work, such as 34mJm^{-2} for rubber (*Fuller & Tabor, 1975*) and 40mJm^{-2} for spray-dried lactose (*Hiestand, 1985*), the

order of magnitude of the two estimated ϕ_a values was considered to be in sound agreement with the findings that the adhesive interactions, under the specific experimental conditions used in this part of the study, should arise principally from the London-van der Waals effect.

6.5 CONCLUSIONS

A centrifuge technique was employed to evaluate the relationship between adhesive force and particle size, for Starch 1500 and spray-dried lactose, over the size range from 32 to 75 μm . The results indicated that after the adherent particles were forced on to the steel substrate, their median adhesion force varied with the first power of the particle radius. Moreover, the experimental data provided grounds for the molecular van der Waals forces being the predominant force component in the adhesive interactions. Thus, this experiment was, to a first approximation, able to elucidate where the molecular force component was large for the test powder adhesive systems.

The ease with which a particle size fraction could be detached from the stainless steel surface was discussed quantitatively. Coarser particles were more easily removed than finer adherents, because as the particle size was decreased, the detachment force decreased at a greater rate than the adhesive force. The adhesive interactions between the steel substrate and particles were also expressed by an energy term, the apparent energy of adhesive interaction, ϕ_a . On the basis of the experimental data, the approximate values of ϕ_a obtained for the two powder adhesive systems indicated about 3 times more energy was required to dislodge a starch than a lactose particle from the substrate surface. Also, the order of magnitude of the ϕ_a values substantiates adhesive interactions were predominantly molecular in nature. Under the particular set of conditions and the particle size range used in this experiment, this energy parameter, ϕ_a , may further provide a comparative evaluation of the adhesion strength of the powder materials studied.

CHAPTER 7

Effect of Temperatures on Powder Adhesion to Stainless Steel

7. EFFECT OF TEMPERATURES ON POWDER ADHESION TO STAINLESS STEEL

7.1 INTRODUCTION

In general, less attention has been given to the mechanical properties of powders at the lower end of the temperature scale. The main reason for this, from the pharmaceutical point of view, is probably because most particulate materials are normally processed at ambient temperatures, and the moderate heat generated in the process can be allowed for, so that operations under such conditions can be carried out without serious restrictions. However, many organic powdered drugs have relatively low melting or softening points which might be sufficiently close to the ambient operating temperature range. Such materials include, for examples, polymers, fatty acids, thermosetting resins, gums and gelatin. Their incorporations into pharmaceutical solid dosage formulations could lead to significant changes in the properties of the subsequent products, if the process temperature is not properly controlled. For instance, additional cooling provision is sometimes employed in certain comminuting processes. Furthermore, the temperature range over which pharmaceutical powders are processed has been extended in recent years, to accommodate the increasingly wide nature of different types of drugs. At the low temperature end, there is the various pre-freezing processes as well as the freeze drying or sublimation drying technique used for manufacturing some biological products, such as certain antibiotic dry powders, blood products and vaccines. Also, there is an increasing concern and practice of storing powders at a low temperature for reasons of chemical and/or microbiological stability. Thus, there is a need to extend the knowledge of the behaviour of powders into the lower temperature region.

Adhesion of drug particles to a hard solid surface is strongly influenced by the viscoelastic property of the particle material. It is known that elasticity or plasticity of a solid material can be affected by temperature, for instance, cold can temporarily deprive plastic adhesives of their deformability, and extreme cold can convert highly elastic adhesives to rigid, often brittle substances. Most physico-chemical interactions

are temperature dependent, hence, varying the temperature will provide clear evidence of the nature of this dependency.

Temperature, therefore, is of basic importance to particle adhesion. This chapter will study the adhesion properties of some pharmaceutical particulate materials, in the region of low temperatures as these are more readily achievable with the current experimental system. The particles will be forced on to the substrate surface to enhance the adhesion.

7.2 EXPERIMENTAL METHOD

The test materials employed for the present experiment were samples of the same PEG 4000 (-56+45 μ m) and heavy precipitated calcium carbonate (-45+32 μ m) used in previous investigations (Chapter 4). Evaluations of the adhesion of the powder particles to the stainless steel substrate were performed at different temperatures over the range from 293 to 258K, which can be set by the thermostat on the control panel of the centrifuge (see Plate 3.2). In this study, it was not possible to deposit the particles on to the substrate surface at low temperatures and subsequently centrifuge at the same temperature. However, according to the experimental findings by Zimon (1982), such apparent discrepancy in this experimental procedure was thereby assumed not to cause any essential difference in results from those determined by performing the 'dusting' and detachment of particles at a constant temperature.

The relative humidities at which powder particles were deposited on to the steel disk surface were mostly below 45%. Although both powders have low moisture absorption potential at ambient conditions (*Handbook of Pharmaceutical Excipients, 1986*), and were stored all the time in a desiccator until required, there was an increasing opportunity of water vapour condensation from the environment and frost deposition at and around the contact interface, as the experimental temperature was lowered to the dew point and below. This could seriously affect the results of adhesion force measurements. To minimize these possible interfering effects, one way was to exclude moisture in the substrate compartment within the rotor tube. The procedure thus adopted for this purpose was to include a few dry silica gel crystals with the substrate disk, inside the rotor tube; the former being placed on the opposite side of the 'dusted' surface. After closing the protective cover, the rotor tube was left for a while at room conditions to allow the silica gel crystals to absorb moisture in the enclosed air space (<0.4cm³). During this period, the 'dusted' disk surface was faced downwards in order to minimize the effect of gravity on the adhesion. The rotor tube was subsequently positioned in the centrifuge rotor which has already been pre-conditioned to the required operating temperature. A digital thermometer was also employed to measure, independently, the temperature of the rotor while stationary, by placing its stainless steel probe into a rotor pocket.

At a chosen temperature within the specified range, the procedure to force the particles on to the disk surface (for 1 min.) and the subsequent determination of the adhesion profile, were performed as described in the respective Section 4.2.3.1 and Section 4.2.2.1. A press-on centrifugation speed of 10,000rpm was arbitrarily chosen for this experiment. Before beginning any centrifuging, the rotor tube was left resting in the pre-conditioned rotor for a fixed time, about 5 min., to allow temperature equilibration at the disk. It was assumed that over all the centrifugation periods, the average disk temperature would remain at about the set temperature. After the centrifuge has stopped and before opening up the adhesion tube to carry out particle counting, the tube was brought to room temperature by means of a hot air blower. The initial silica gel crystals were replaced by fresh ones when their colour indicated they had lost their dehydration ability.

Owing to the addition of silica gel crystals to the normal adhesion cell set-up, a control experiment was carried out to determine if the presence of silica gel crystals in the substrate disk compartment would possibly influence adhesion force determinations. The control was consisted of 3 parts, as follows:

- I. Comparison between the two mean median adhesion forces for calcium carbonate, determined with and without silica gel crystals, at the highest press-on speed of 17,000rpm for 1 min. and at 293K.
- II. Comparison between the two mean median adhesion forces for calcium carbonate, determined with and without silica gel crystals, at the highest press-on speed of 17,000rpm for 1 min. and at 273K.
- III. Comparison between the two mean median adhesion forces for calcium carbonate, determined for two time durations (1 & 8 mins.) at the highest press-on speed of 17,000rpm and at 273K, with silica gel crystals present.

7.3 RESULTS

The statistical test results for the control experiment are tabulated in Table 7.1. In Parts I & II of the table, it can be seen that, at both test temperatures (293K & 273K), even employing the highest press-on speed of 17,000rpm, there was no significant difference between the two mean median adhesion forces, determined with and without the presence of silica gel crystals. Thus, it was concluded that, the inclusion of silica gel crystals in the substrate compartment would impose no significant influence on the determination of the median adhesion force, but would serve the purpose of alleviating the problem of moisture condensation within the enclosed cell space. In Part III, a significant difference was obtained between the two mean median adhesion forces, determined for two press-on time durations at a low temperature. This illustrates that, variation of an experimental parameter at a low temperature could still be reflected by the expected changes in the magnitude of the median adhesion force, which would not be affected by the presence of silica gel.

Representative adhesion profiles of PEG 4000 and heavy precipitated calcium carbonate, as a function of the experimental press-on temperature, are illustrated in Figs. 7.1 & 7.2. For PEG 4000, the initial plateau region of the curve gradually disappeared as the temperature was decreased. For both powders, there appeared to be a change in the pattern of the profile curves at temperatures below 293K; the effect being more noticeable in PEG 4000. Figs. 7.3 & 7.4 show the adhesion data presented on logarithmic probability coordinates. In general, each set of experimental points can be joined by a good straight line. Thus, the adhesion force distribution for the two particulate solids, at low temperatures, can be considered to follow also a log-normal law, from adhesion force value of about $4.7 \times 10^{-7} \text{N}$ for PEG 4000 and $0.8 \times 10^{-7} \text{N}$ for the calcium carbonate. Values of the median adhesion force and the geometric standard deviation, σ_g , derived from the log-probability plots, are listed in Table 7.2; each of which was the mean from 6 results. The mean median force of adhesion at 293K for PEG 4000 was the value previously determined in Chapter 4. However, the corresponding median adhesion force value for the calcium carbonate showed some disagreement with its other force values obtained at the lower temperatures. As a result, this particular median adhesion force at 293K for heavy precipitated calcium

TABLE 7.1 Results of the statistical analysis of the control experiment.

Control experiment	Average median adhesion force ($\times 10^{-7}N$)		Student's <i>t</i> test
	Without silica gel (n=6)	With silica gel (n=6)	
Part I	4.44* (sem=0.23)	4.50 (sem=0.16)	NS (p=0.842)
Part II	3.28 (sem=0.09)	3.18 (sem=0.15)	NS (p=0.586)

	Compression duration=1min. (n=6)	Compression duration=8min. (n=6)	
Part III	3.18 (sem=0.15)	3.98 (sem=0.21)	significant (p=1.07 $\times 10^{-2}$)

* = result from Chapter 4
 NS = not significant
 sem = standard error of mean

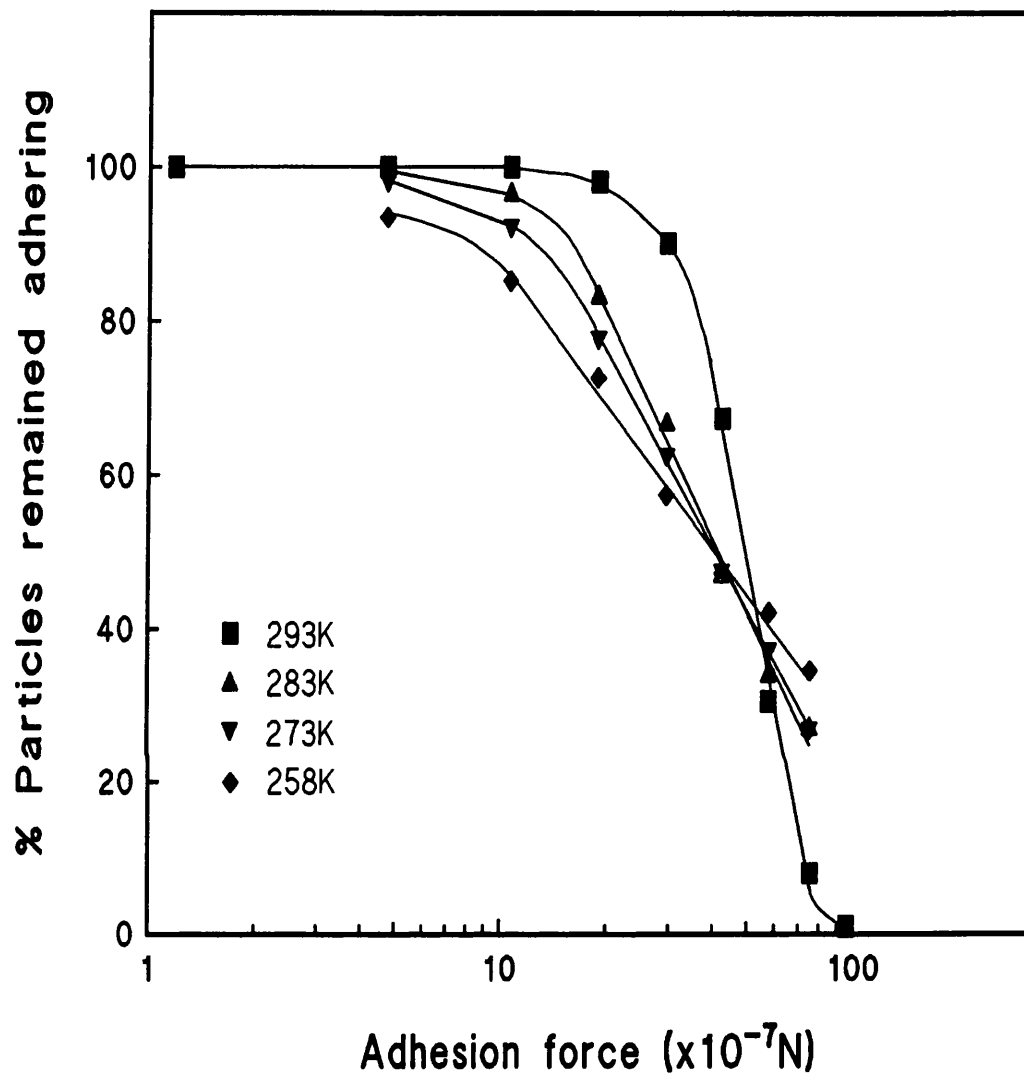


FIG. 7.1 Adhesion profiles of PEG 4000 to stainless steel at different preliminary press-on temperatures.

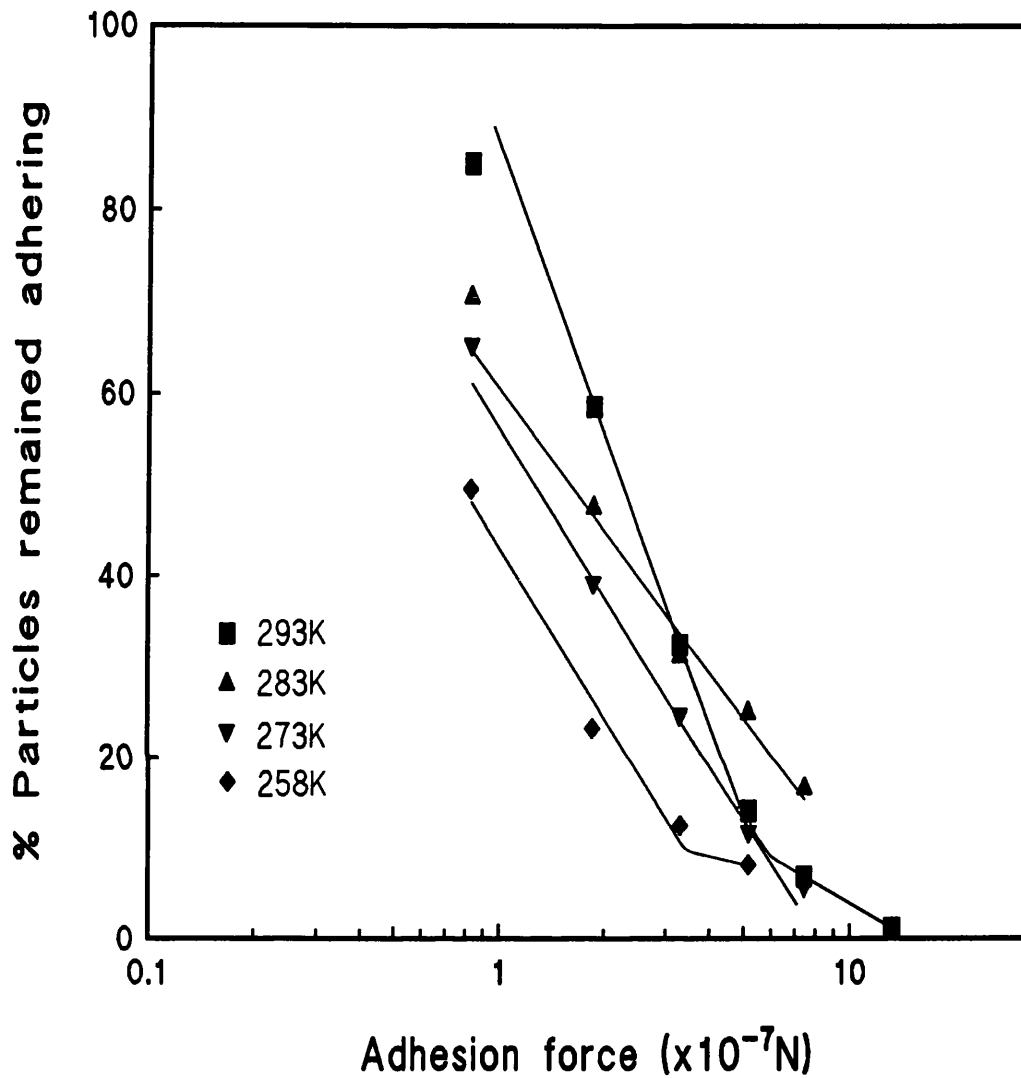


FIG. 7.2 Adhesion profiles of heavy precipitated calcium carbonate to stainless steel at different preliminary press-on temperatures.

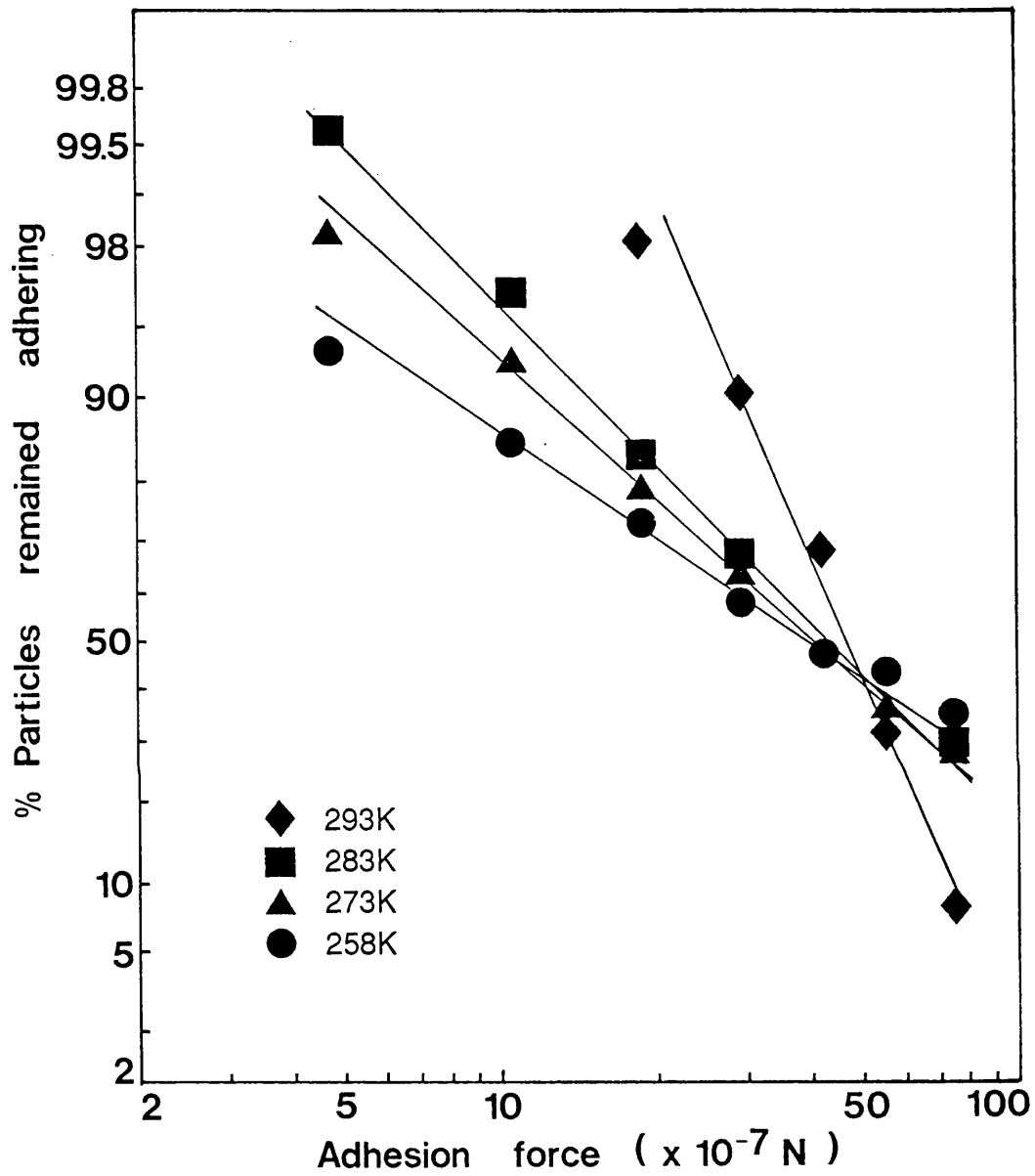


FIG. 7.3 Log-probability plots of the adhesion of PEG 4000 to stainless steel at different preliminary press-on temperatures.

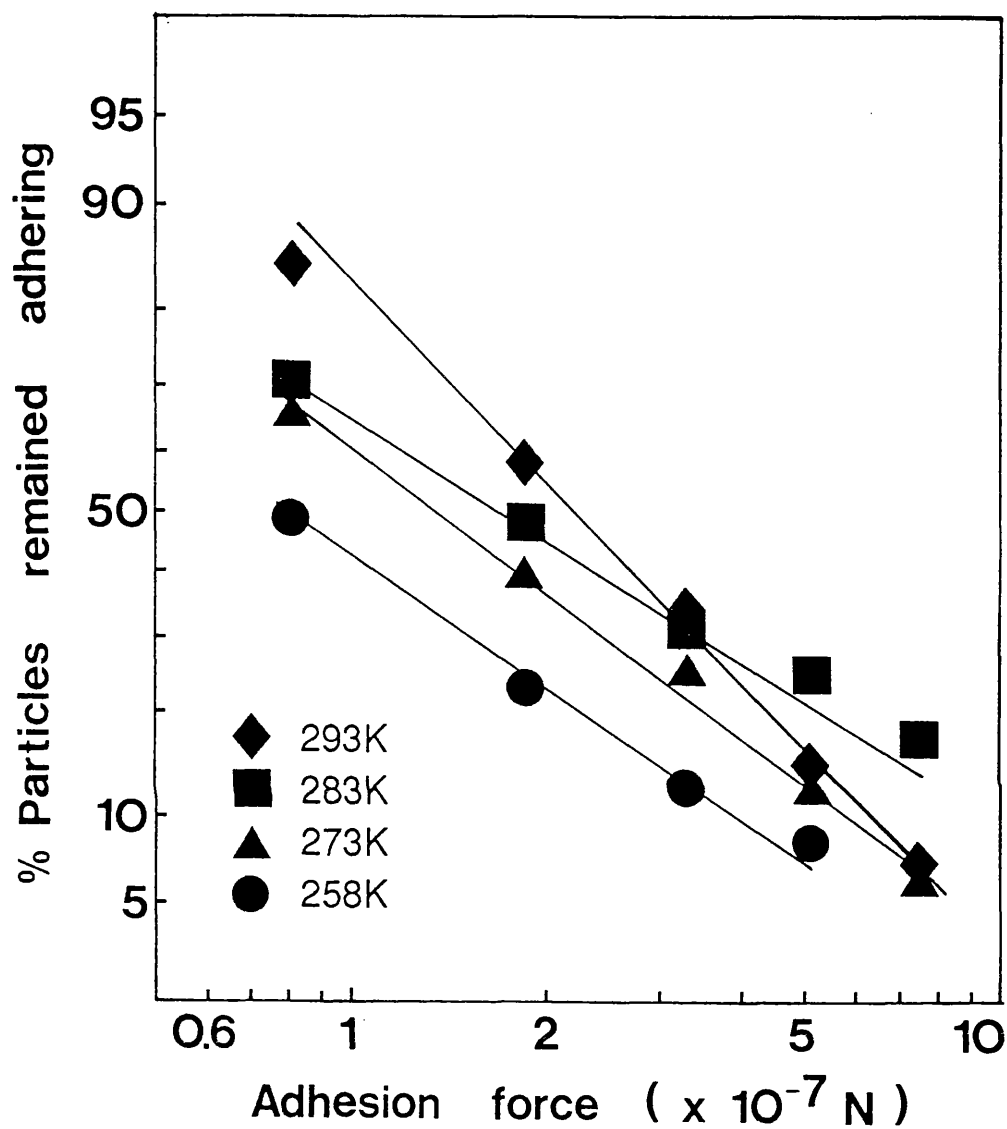


FIG. 7.4 Log-probability plots of the adhesion of heavy precipitated calcium carbonate to stainless steel at different preliminary press-on temperatures.

TABLE 7.2 Values of the two log-probability statistical parameters at the various experimental temperatures, for the two powder excipients.

Material	Preliminary compression temperature (K)	Median adhesion force ($\times 10^{-7}$ N)	Geometric standard deviation, σ_g (N)
PEG 4000	293	48.75	0.713
	283	41.62	0.460
	273	40.87	0.406
	258	37.48	0.284
Calcium carbonate, heavy precipitated	293	2.22	0.423
	283	1.79	0.235
	273	1.40	0.318
	258	0.82	0.308

carbonate was re-determined experimentally and the new mean value given. The geometric standard deviation was calculated as the ratio of the 84% probability force value to the 50% probability force value.

The numerical results in Table 7.2 indicate that, for the two pharmaceutical materials, the median adhesion force decreased with decreasing temperature at which the particles were forced on to and detached from the substrate surface. Over the temperature range (i.e., from 293 to 258K), PEG 4000 showed a reduction in the force of adhesion by about 23%, whereas for the calcium carbonate, the reduction was over 60%. Moreover, the log-probability line became less steep as the temperature was reduced from 293K, as illustrated by the smaller values of σ_g at lower temperatures.

Evaluation of the relative amount of adhesion established between the particles and the steel surface, at the different temperatures, could be quantitatively expressed by the ratio of the median adhesion force to the preliminary compression force applied to the particular powder solid. This ratio, τ , is dimensionless, and its values are listed in Table 7.3. The variation of τ with respect to temperature is represented in Fig. 7.5. From this graph, PEG 4000 was seen to exhibit an initial apparent change in form of the plot when the temperature was lowered from 293 to 283K. However, the change in heavy precipitated calcium carbonate appeared to be more gradual over the temperature range between 293 and 258K.

TABLE 7.3 Relative adhesions of the powder materials to the steel substrate, at the various press-on centrifugation temperatures. The press-on force for PEG 4000 was $11.40 \times 10^{-6} \text{N}$, and for heavy precipitated calcium carbonate $7.98 \times 10^{-6} \text{N}$.

Material	Preliminary compression temperature (K)	Median adhesion force ($\times 10^{-7} \text{N}$)	Median adhesion force
			Compression force ($\times 10^{-2}$)
PEG 4000	293	48.75	42.8
	283	41.62	36.5
	273	40.87	35.9
	258	37.48	32.9
Calcium carbonate, heavy precipitated	293	2.22	2.78
	283	1.79	2.25
	273	1.40	1.75
	258	0.82	1.02

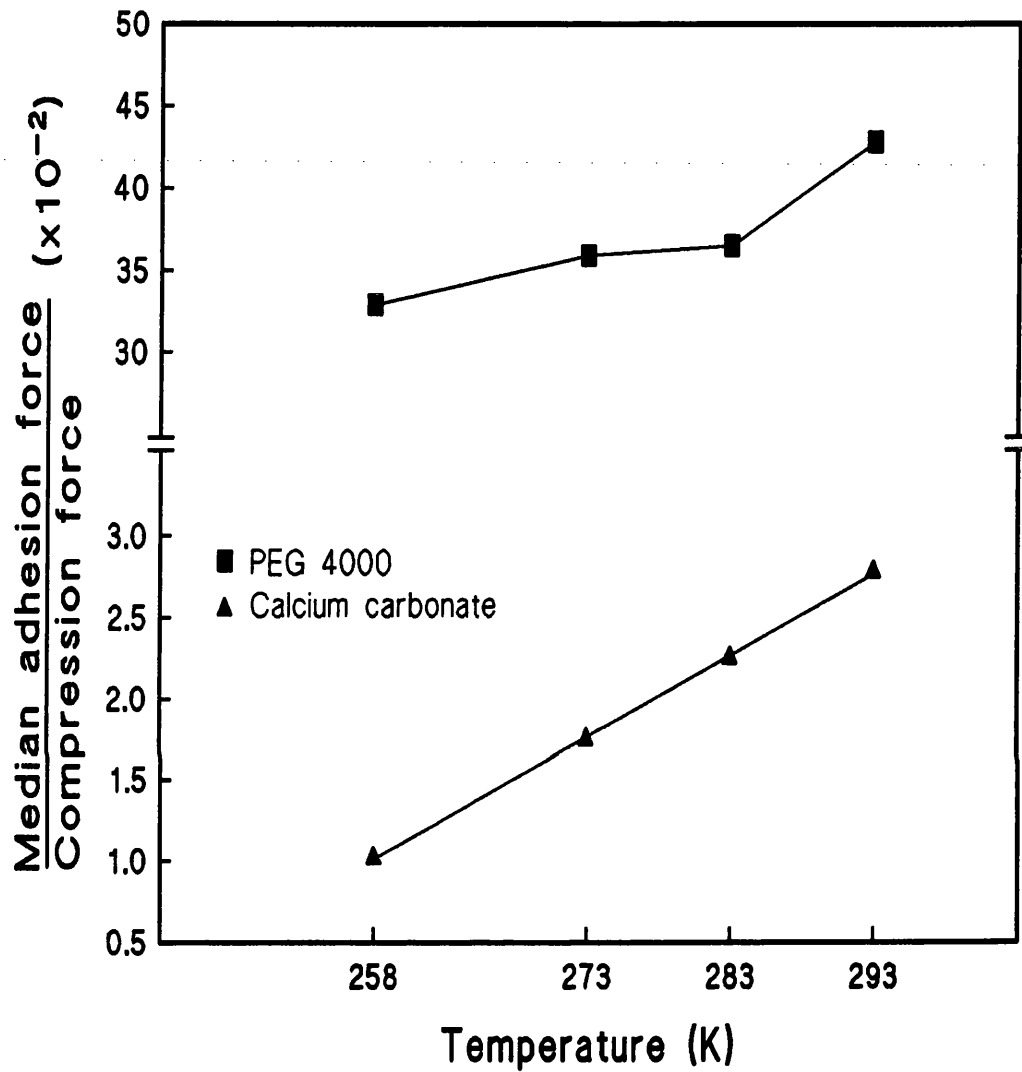


FIG. 7.5 Effect of lowering the preliminary press-on temperature on the relative extent of particle adhesion to stainless steel.

7.4 DISCUSSION

The gradual disappearance of the initial plateau section in the adhesion profile curve for PEG 4000 (see Fig. 7.1) showed that the general adhesive strength of the particles to the steel substrate surface was decreased as the temperature was reduced. On the assumption that the technique of using silica gel crystals has considerably reduced the moisture condensation, i.e., there was a minimal capillary effect, such decrease reflected a change taking place in the adhesion properties of the particles. Changes in the surface of the much harder stainless steel under those conditions were considered negligible.

The adhesion forces concerned in this study were considered mainly be the London forces, as discussed in Chapter 6. On this basis, the reduction in the median adhesion force with decrease in temperature could be accounted for in the following. In the Lifshitz equations for van der Waals forces (see Section 1.6.1.1), the Lifshitz constant, $\hbar\bar{\omega}$, for two interacting bodies can vary with temperature, due to the fact that it is derived from bulk material properties, such as optical data, and the light absorption properties of materials are influenced by ambient temperature changes. This is similarly inferred to in a review by Visser (1972). Thus, for this experiment, the smaller median adhesion forces obtained at the lower temperatures were partly due to weaker van der Waals attractions. On the other hand, temperature independencies for the Hamaker coefficient (which is related to the Lifshitz constant by Equation (1.11)) was observed by Osborne-Lee (1988). Though it seemed that the view about the relationship between the molecular interaction constant and temperature is uncertain due to limited available data, the temperature-dependent property of the material constant was considered to be an essential factor, as far as the present experiment was concerned, until more definite conclusions are arrived.

At elevated temperatures, especially at temperatures close to the melting points of materials, the increase in bond strength between particles was ascribed by some workers (*Pilpel & Britten, 1979; Malamataris & Pilpel, 1981; Esezobo & Pilpel, 1986*) to the powders being much softer and more plastic, thereby permitting the particles to undergo greater stress relaxation under a certain compression force. The

effect of heating in these cases is to increase the vibrational energy of the molecules, allowing them more mobility. Examination of the properties of wind-micronised snow by Bowden & Tabor (1964) found that the snow particles exhibited a more elastic behaviour at very low temperatures (e.g., 253K) than at just below 273K, with the consequence that, the snow displayed a lower adhesive strength. In practice, this presents the snow a higher tendency to slide and flow, producing avalanches. The above findings substantiate the notion that, whereas plasticity of a solid increases with increasing temperature, elasticity increases with decreasing temperature. With regard to the adhesion of the test particles to the steel surface, due to reduced thermal agitations of the molecules at low temperatures, the particle material will flow at a diminishing rate and become less plastic, giving rise to smaller area of contact and correspondingly less adhesion, under a particular load. In view of a relatively higher potential of elastic recovery of a material at low temperatures, which could possibly break the weaker adhesion junctions when the compression load was removed, there would be fewer intact adhesive bonds as the temperature was reduced. Thus, lowering the temperature in the press-on stage would inevitably decrease the resultant adhesion force, as supported by the experimental results in Table 7.2.

Adhesion of the test powder particles to the steel substrate was considered to occur at the asperities of the contacting surfaces. Owing to the minute area of contact, (of the order of 10^{-3} of their apparent contact area (*Bowden & Tabor, 1950*)), the pressure acting at the contact points would thus be tremendous during the stage of pressing-on at 10,000rpm (equivalent to an acceleration of about 9,700g (see Table 3.1)). In such instance, the melting point of the particle material at the localized points of asperity contact can be lowered, even at ambient temperature condition (*Jeffreys, 1935; Rankell & Higuchi, 1968*). On releasing the pressure during the slowing down of the centrifuge after the preliminary compression, welded bonds could be formed which would contribute to the overall adhesive strength. The amount of lowering of the melting point may be calculated according to an equation proposed by Skotnicky (1953), which was confirmed by other researchers (*Jayasinghe et al., 1969/70; York & Pilpel, 1972a, b*). The extent of this 'pressure-welding' phenomenon in strengthening an adhesive bond was, however, found to decrease with decreasing

temperature (*Britten & Pilpel, 1978; Adeyemi & Pilpel, 1984*). In the event of an adhesion process taking place at a low temperature, the significance of this effect would be less, thereby diminishing its contribution to the total adhesive strength.

Furthermore, as was found in metallurgical research, the homologous temperature which is sufficiently high to anneal and render ductile the junctions formed at the interface, was above about 0.5. The homologous temperature was defined as the ratio of the temperature of measurement to the melting point of the concerned material, both in absolute temperatures. Similar considerations were attempted on non-metal solids, and experiments with some pharmaceutical powders (*Pilpel & Esezobo, 1977; Pilpel & Britten, 1979; Otsuka et al., 1983; Danjo & Otsuka, 1990*) suggested that, the homologous temperature at which the above 'pressure-welding' mechanism took place was approximately in the range of 0.6 to 0.9. For the PEG 4000 used in this study, its homologous temperatures, with respect to the experimental temperatures in the range of 293 to 258K, were above 0.7; the upper limit of the melting point of PEG 4000, i.e., 331K (*Handbook of Pharmaceutical Excipients, 1986*) was used in the calculation. In the case of calcium carbonate, which decomposes at 1098K (*Chemical Engineers' Handbook, 1963*), its corresponding homologous temperatures were all below 0.3. Thus, it may be assumed that the 'pressure-melting' effect was operative, to a certain extent, in PEG 4000 during the press-on stage at 293K, but because of the temperature-dependent nature of this mechanism, the effect was less pronounced at low temperatures. This may perhaps also partly explain the smaller forces of adhesion for PEG 4000 at reduced temperatures. The greater percentage reduction of the median adhesion force in heavy precipitated calcium carbonate could probably be attributed, in part, to the relative absence of this 'pressure-welding' mechanism in the adhesion of the particles to the steel substrate during the preliminary compression.

With regard to the initial abrupt fall in τ for PEG 4000 as the press-on temperature was lowered from 293 to 283K (see Fig. 7.5), this might be due to some kind of deformational phase change occurring in the particles that led to such reduced solid adhesion to the steel substrate. By considering the plastic nature of the PEG

4000 solids at 293K, the observed phenomenon may be associated with a transition from essentially plastic to a more elastic deformational behaviour as the temperature was reduced to and below the dew point. This, however, requires further investigation.

Activation Energy of an Adhesion Bond

Interfacial reactions, such as sintering effects which consist of, for example, diffusion and condensation, diffusive mixing, mutual dissolution and alloying at the interface, are of importance to particle adhesion, mainly because they play a part in determining the size of the adhesive area when a particle comes into contact with a plane surface. This particular group of interfacial reactions are usually only greatly facilitated under certain conditions such as elevated temperatures. For instance, when powder compaction was performed at raised temperatures, the large increase in the tensile strength of a powder compact in the initial stage of the compaction process was attributed mainly to the sintering mechanism (*Pilpel & Britten, 1979; Esezobo & Pilpel, 1986; Danjo & Otsuka, 1990*). On the basis of the theory of sintering (*Kuczynski, 1950*), several workers (*Pilpel & Esezobo, 1977; Britten & Pilpel, 1978; Malamataris & Pilpel, 1981*) observed a relationship existing between the particle bond strength of a compressed powder bed and the temperature at which the cohesive bond was developed, which was found to follow the Arrhenius equation. On the other hand, *Jernot et al. (1981)* proposed an equation which could relate the particle specific surface area to the radius of a sinter neck formed between two spheres during sintering.

According to the above information, certain mechanical properties of solids bear a definite relationship with temperature. In the adhesion of particles to a hard substrate, the flow of the particle material at the contact sites is a temperature-dependent process; its initiation would require certain thermal activation energy. Also, due to the adhesive forces concerned being considered primarily molecular in nature, which would be influenced by temperature changes, it may intuitively be inferred that, the net adhesion forces between the steel substrate and the powder particles would vary with the temperature at which the adhesive bonds were established, possibly

following the Arrhenius relationship. Under such condition, it may be envisaged that, the relative amount of adhesion established, τ , would similarly conform to a form of the Arrhenius equation. These two particular relationships can be expressed by a common equation:

$$V_i = A_o e^{-\frac{E_a}{R_o T}} \quad (7.1)$$

where V_i can either be the median adhesion force, F_{ad} , or τ , A_o is a proportional constant for each particulate material under a specific press-on force, e is equal to 2.718, E_a is the apparent activation energy of bonding, R_o is the molar gas constant ($=8.31\text{JK}^{-1}\text{mol}^{-1}$) and T is the absolute temperature.

Arrhenius plots for PEG 4000 and heavy precipitated calcium carbonate, for both conditions of V_i , are shown in Fig. 7.6 & 7.7. Linear relationships were obtained for the two powder solids in both cases of V_i , although a rectilinear line of better correlation was indicated for the calcium carbonate than for PEG 4000. The apparent activation energy of adhesion, E_a , was evaluated from the slope ($=-E_a/2.303R_o$) of the regressed line, its values and those of A_o and the correlation coefficient, r , are shown in Table 7.4.

In either cases of V_i , a steeper slope of the straight line was observed for calcium carbonate than PEG 4000, which showed the former material was more sensitive to temperature changes, with regard to the adhesion to the steel substrate. The similarities of the E_a values in both conditions of V_i , for PEG 4000 and heavy precipitated calcium carbonate indicated that, either F_{ad} or τ can be an indicative parameter for defining the Arrhenius relationship between temperature and the adhesion of the above particulate solids to the substrate. A higher apparent activation energy value obtained for the calcium carbonate implied that its adhesive bond formation with stainless steel was relatively more difficult. Apparently, with the particular preliminary press-on centrifuge speed used, about 4.2 times as much thermal

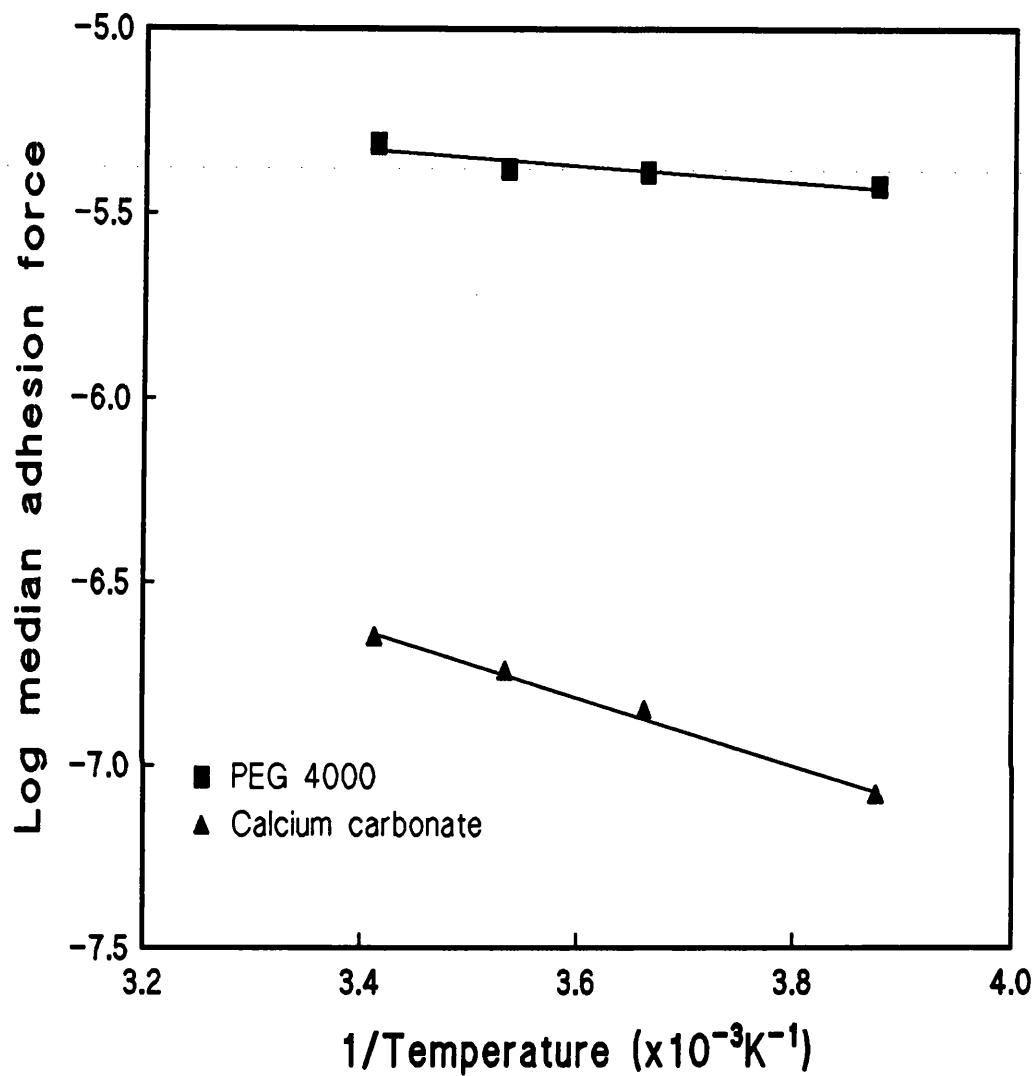


FIG. 7.6 Arrhenius plots of the median adhesion force of particles to stainless steel, as a function of the press-on temperature.

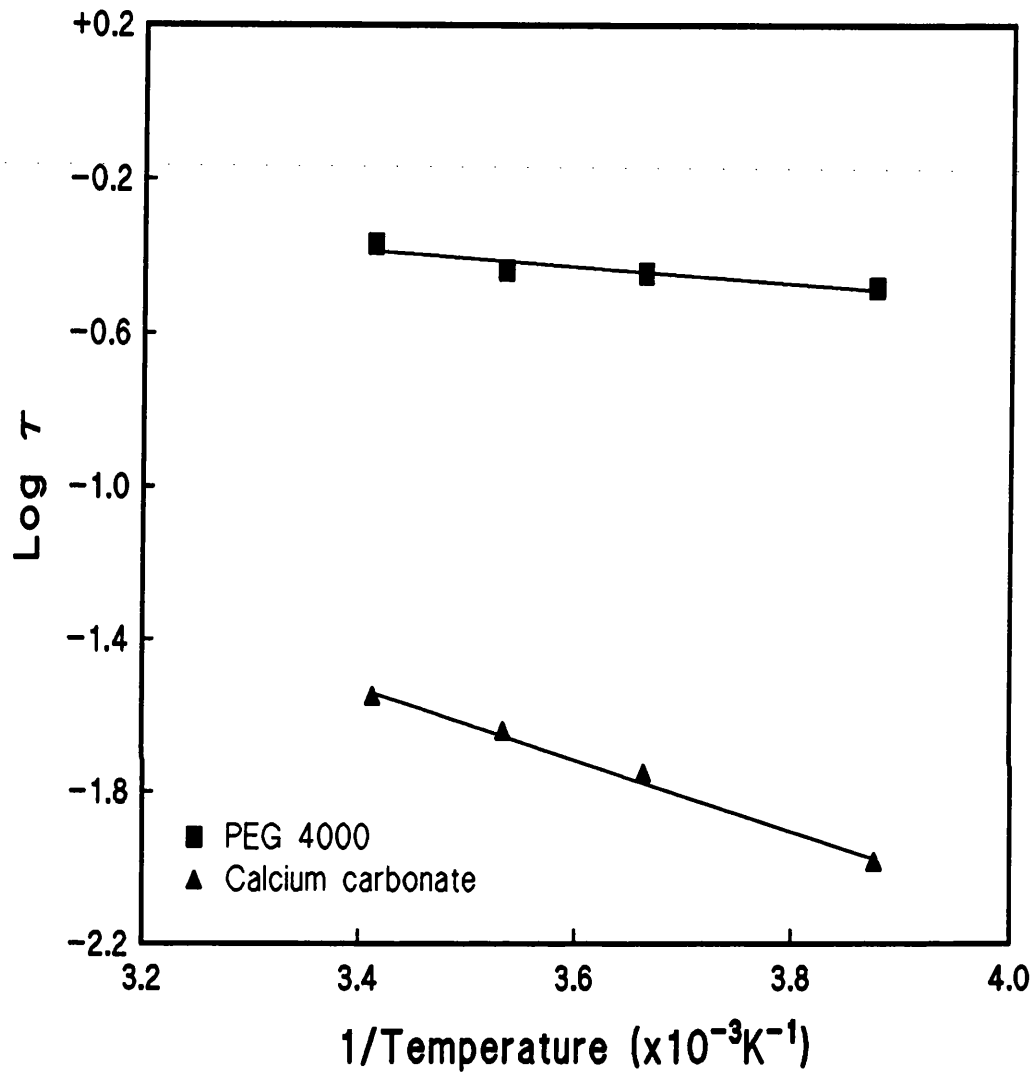


FIG. 7.7 Arrhenius plots of the relative extent of particle-steel adhesion (τ), as a function of the press-on temperature.

TABLE 7.4 Values of the apparent activation energy of bonding, E_a (kJmol^{-1}) and A_o , from Arrhenius plots for PEG 4000 and heavy precipitated calcium carbonate; r is the correlation coefficient.

V_i	PEG 4000			Calcium carbonate		
	E_a	A_o	r	E_a	A_o	r
F_{ad}	4.26	2.69×10^{-5}	0.9277	17.93	36.06×10^{-5}	0.9962
τ	4.26	2.36	0.9261	18.08	48.12	0.9960

energy of activation was required to initiate bond formation in the process of adhesion for the harder calcium carbonate as for the softer PEG 4000.

Nevertheless, by comparing with the magnitudes of the activation energy of bondings reported by other researchers (*Britten & Pilpel, 1978; Malamataris & Pilpel, 1981; Otsuka et al., 1983; Esezobo & Pilpel, 1986; Pilpel et al., 1991*), the E_a values obtained for the two experimental powder solids were of the order expected for interactions to be occurring by physical rather than chemical processes.

7.5 CONCLUSIONS

In this chapter, studies were made on the adhesion of PEG 4000 and heavy precipitated calcium carbonate to stainless steel, at temperatures between 293 and 258K, by means of a centrifuge method. In all cases at lower than the ambient temperature, i.e., 293K, the distribution of the particle adhesion forces also followed a log-normal law.

The median adhesion force decreased as the temperature employed for the preliminary compression stage was lowered. This can be explained in terms of a change in the deformational properties of the particles as well as reduced van der Waals dispersion forces generally. Reduction in the adhesive strength, over the temperature range, was more marked for the harder, less adhesive calcium carbonate than the softer, more adhesive PEG 4000.

Particle adhesion, as a function of temperature, could be defined by the Arrhenius relationship between the temperature at which adhesive bonds were established and either the median adhesion force, F_{ad} , or τ , the ratio expressing the relative extent of powder solid adhesion to the steel substrate. Values of the apparent activation energy of adhesion (in both cases of F_{ad} and τ) were basically no different for PEG 4000; the value being about 4.26kJmol^{-1} , and those for heavy precipitated calcium carbonate are also very close, being 17.93kJmol^{-1} and 18.08kJmol^{-1} . These E_a values reflect that, formation of adhesion bonds with stainless steel involved less thermal activation for the softer PEG 4000 than the harder calcium carbonate solid. This could be used to substantiate the previous findings (Chapter 4) that the former material was more adhesive than the latter to stainless steel.

CHAPTER 8

General Conclusions

8. GENERAL CONCLUSIONS

This work has been concerned with examining the adhesion characteristics of different types of pharmaceutical particulate excipients on a characterized stainless steel surface. The various statistical roughness parameters obtained for the substrate surface by a surface profilometry technique, together with the particle sizes chosen for this work, confirmed that all the particle adhesions to the steel surface should occur on the tops of the contacting asperities.

A centrifuge method was employed for evaluating particle-steel adhesion, and the data obtained was interpreted, basically, in terms of two statistical parameters, the geometric median adhesion force and the geometric standard deviation. In general, all the adhesion profiles followed a log-normal function, for the distributions of particle adhesion forces at the different experimental conditions. On a few occasions where consistency within a particular data set was not quite as sound, this was assumed to be due to a change in certain ambient conditions such as air humidity, which was perhaps significant enough to cause the discrepancy in the adhesion results. Nevertheless, in most cases, the results were reproducible.

Application of a preliminary compression to force the test powder particles to the stainless steel surface was found to bring about a significant increase in the subsequent adhesion of the solids to the substrate, on the basis that plastic deformation occurred during compression and the deformation remained after removal of the applied load. Investigations of the various compression forces on particle-steel adhesion showed that the softer PEG 4000 was more adhesive, indicated by the higher median adhesion forces, than the harder heavy precipitated calcium carbonate. This was substantiated by comparing the respective numerical values of a derived non-dimensional index, the adhesion ratio, obtained for the investigated pharmaceutical powders. The adhesion ratio values (in parentheses) indicated the following rank order of adherence to stainless steel: PEG 4000 (33.3×10^{-2}) > Starch 1500 (7.57×10^{-2}) > spray-dried lactose (1.72×10^{-2}) > heavy precipitated calcium carbonate (1.63×10^{-2}). An

inverse relationship was found between the adhesion ratios and the literature values of the yield pressure of the powder materials, this agreed with the softness (or hardness) nature of the powder solids, and suggested that the material mechanical properties could be grossly indicative of the relative adhesion behaviour of the particulate excipients.

The duration of preliminary compression has a considerable influence on the adhesion of the test powders to the steel substrate. Although the magnitude of the median adhesion force can allow some assessment to be made between different powders on their strength of adhesion at corresponding compression duration, for certain materials, it was found that the amount of change in the adhesion force was of greater concern. This could be illustrated by spray-dried lactose which, albeit being harder and established (with reference to the adhesion ratio) as less adhesive than PEG 4000, depicted the greatest change (126%) in the median adhesion force, over the experimental time period of the duration of preliminary compression. The observed phenomenon was attributed to the inherent porous and hence weak solid structure of the lactose particles, which was susceptible to the effect of a compression force over extended times. A similar observation was also found on Starch 1500, though the change (65%) was less pronounced. For PEG 4000 which was, amongst the test materials, considered to be the most adhesive to stainless steel (according to its adhesion ratio value), showed only minor increases (38%), and that (21%) for heavy precipitated calcium carbonate was even much less.

A linear relationship was obtained between the log of the median adhesion force and the log of the time duration of preliminary compression. The slope of the straight line, being a rate parameter, indicated the following decreasing order of the extent of adhesional force changes for the test powders, as: spray-dried lactose (0.340) > Starch 1500 (0.190) > PEG 4000 (0.114) > heavy precipitated calcium carbonate (0.071), where the numbers in parentheses are the calculated slope values. An implication of this particular finding to the industrial manipulation of powders having similar solid structure and nature to either that of spray-dried lactose or Starch 1500 could be that, during a lengthy process, an apparently not adhesive particulate material

could unexpectedly give rise to similar operation problems such blockages and jamming of certain parts, e.g. hoppers, nozzles, etc., commonly encountered generally for sticky materials.

Of the four experimental powder excipients, the softer Starch 1500 was observed to be able to sustain a relatively longer duration (about 744 seconds) under a particular compression force, followed by spray-dried lactose (about 344 seconds) and then the harder calcium carbonate (about 326 seconds), before the effect of deformation hardening began to exert a significant influence on affecting particle adhesion to the steel substrate.

With regard to particle size on adhesion, although larger particles of both Starch 1500 and spray-dried lactose similarly exhibited greater median forces of adhesion than their smaller particles to stainless steel, the larger ones were more easily dislodged by centrifugation. For these two powder-steel adhesive systems studied, after application of a preliminary press-on force, the median adhesion force was found to vary with the first power of the calculated average particle size of a powder sieve fraction. From this finding, and based on the Hamaker and Lifshitz force equations, the molecular van der Waals forces were considered to be the dominating force component involved in these interactions, although other types of forces (such as electrostatic forces, etc.) were not entirely neglected. The adhesions were evaluated in terms of surface energetics, from which an adhesive interaction energy parameter, the apparent energy of adhesion, was derived. The values of this energy parameter calculated for Starch 1500 and spray-dried lactose are 7.34mJm^{-2} and 2.56mJm^{-2} , respectively; their order of magnitude, when compared with other published results, substantiate that the particle-steel adhesive interactions for both Starch 1500 and spray-dried lactose were primarily molecular in nature. Furthermore, as the distribution of the particle adhesion forces to stainless steel (indicated by the geometric standard deviation parameter) was not statistically different between the various experimental solid size fractions of both Starch 1500 and spray-dried lactose, particle adhesion of the different powder size fractions as well as the unsieved powder of these two materials could thus be characterized by just the median adhesion force parameter alone.

The adhesions of PEG 4000 and the calcium carbonate particles to stainless steel were reduced when the temperature employed for the stage when the particles were forced on to the substrate surface was reduced. This was attributed to the particles being less plastically deformed at a low temperature, as well as to the reduced van der Waals attractions at temperatures towards and below the dew point. An Arrhenius relationship was obtained between the temperature at which adhesive bonds were formed and the median adhesion force or the amount of median adhesion force established per unit of the preliminary compression force (τ). The apparent energy of activation for adhesion bond formation, for either case, was about the same value of 4.26kJmol^{-1} for PEG 4000 and 17.93kJmol^{-1} & 18.08kJmol^{-1} , respectively, for heavy precipitated calcium carbonate. These values indicate that, either the median force parameter or τ can be indicative of the variation of particle adhesion to stainless steel. Moreover, the lower energy value obtained for PEG 4000 reflects that formation of adhesion bonds between the PEG 4000 particles and stainless steel would require less energy of activation than that for heavy precipitated calcium carbonate particles. This therefore implies that, under the same press-on force, PEG 4000 particles would deform more readily and as result, more adhesive than the calcium carbonate particles to stainless steel. Furthermore, the order of magnitude of these activation energies infers that adhesive interactions occurred by physical rather than chemical processes.

SUGGESTIONS FOR FURTHER WORK

1. The process by which adhesion occurs in pharmaceutical systems is complex, usually involving both compression and shear of one surface with the other. This could be studied by adapting the present rotor tube design so that when a compression force is exerted on to the adhering particles, it will be acting at an angle to the metal disk surface. Resolution of this force will yield two force components, namely, a normal compression force and a horizontal shearing (or frictional) force. After the press-on stage, the particles are detached by normal centrifugation. By varying the angle of application of the preliminary compression force (between 0 to 90°), the various relative extent of compression and shearing forces on particle adhesion to a substrate surface could be studied.
2. In adhesion experiments, particles are generally deposited on to a substrate surface in such a way that they are separated from each other at a reasonable distance, in order to minimize the effect of interparticle interactions on adhesion. However, in many practical situations, individual particles are in close contact with their neighbouring partners, and so studies should also be carried out to establish the significance of such effect on particle-substrate adhesion.
3. In this work, the preliminary compression force was applied relatively slowly on the adhering particles. Some powder materials, such as Starch 1500 has been observed to be capable of extensive plastic deformation, but can only occur slowly (Rees & Rue, 1978). Hence, the rate of application of the press-on force can be essential with respect to particle adhesion. With a centrifuge, an appreciable inertial effect (which simulates a high compression speed) can be generated by setting the centrifuge speed to the final desired speed, before the start of a press-on centrifugation process.

4. When the substrate material is a polymer (e.g. polypropylene, PTFE), the particle-substrate system may bear some similarity to that of two semi-conductive materials in contact. For this combination, electrical charges that arise due to, for instance, contact potential difference may not be as readily dissipated as when the substrate is a metal. Under such circumstances, the electrostatic effect could be significant in affecting the adhesion. Hence, studies may be considered on the adhesion between particles and a non-metal substrate, with particular reference to the relationship between particle size and adhesion force.

5. For the adhesion model used in this study, the metal disk can be replaced by a powder compact (e.g. a tablet) of the same material as the particles, so that the adhesion may be interpreted as particle-particle interactions. This model may then be utilised to study, perhaps, the effect of environmental factors, e.g. air humidity on particle-particle adhesions.

BIBLIOGRAPHY

- Adamson, A.W., *Physical Chemistry of Surfaces*, 4th Ed., J. Wiley and Sons, New York, 1982.
- Adeyemi, M.O. and Pilpel, N., The effects of interacting variables on the tensile strength, disintegration and dissolution of oxytetracycline-lactose tablets. *Int. J. Pharm.*, 20 (1984) 171-186.
- Al-Angari, A.A., Kennerley, J.W. and Newton, J.M., The compaction properties of polyethylene glycols. *J. Pharm. Pharmacol.*, 37 (1985) 151-153.
- Aleinikova, I.N., Deryaguin, B.V. and Toporov, Yu.P., The electrostatic component of adhesion of dielectric particles to a metal surface. *Kolloid. Zh.*, 30 (1968) 128-132.
- Archard, J.F., Contact and rubbing of flat surfaces. *J. Appl. Phys.*, 24 (1953a) 981-988.
- Archard, J.F., Elastic deformation and the contact of surfaces. *Nature*, 172 (1953b) 918-919.
- Asakawa, S. and Jimbo, G., Measurement of adhesion force of powder particles to solid surfaces by centrifugal method. *J. Soc. Mat. Sci., Japan*, 16 (1967) 358-363.
- Aulton, M.E., Travers, D.N. and White, P.J.P., Strain recovery of compacts on extended storage. *J. Pharm. Pharmacol.*, 25 (1973) Suppl., 79P-86P.
- Bailey, A.G., Electrostatic phenomena during powder handling. *Powder Technol.*, 37 (1984) 71-85.
- Bardina, J., Methods for surface particle removal: A comparative study. In Mittal, K.L. (Ed.), *Particles on Surfaces I*, Plenum Press, New York, 1988, pp. 329-338.
- Barouch, E., Wright, T.H. and Matijević, E., Kinetics of particle detachment. I. General considerations. *J. Colloid Interface Sci.*, 118 (1987) 473-481.
- Beams, J.W., Breazeale, J.B. and Bart, W.L., Mechanical strength of thin films of metals. *Phys. Rev.*, 100 (1955) 1657-1661.
- Benjamin, P. and Weaver, C., The adhesion of metals to crystal faces. *Proc. Roy. Soc. Lond.*, A274 (1963) 267-273.
- Bhattacharya, S. and Mittal, K.L., Mechanics of removing glass particulates from a solid surface. *Surface Technol.*, 7 (1978) 413-425.

- Bickel, W.S. and Wentzel, T.M., Crossed fibre models of the particle-substrate interaction. In Mittal, K.L. (Ed.), *Particles on Surfaces I*, Plenum Press, New York, 1988, pp. 225-236.
- Bikerman, J.J., Adhesion in friction. *Wear*, 39 (1976) 1-13.
- Böehme, Ing.G., Krupp, H., Rabenhorst, H. and Sandstede, G., Adhesion measurements involving small particles. *Trans. Instn. Chem. Engrs.*, 40 (1962) 252-259.
- Boland, D. and Geldart, D., Electrostatic charging in gas fluidised beds. *Powder Technol.*, 5 (1971/72) 289-297.
- Booth, S.W. and Newton, J.M., Experimental investigation of adhesion between powders and surfaces. *J. Pharm. Pharmacol.*, 39 (1987) 679-684.
- Bowden, F.P. and Rowe, G.W., The adhesion of clean metals. *Proc. Roy. Soc. Lond.*, A233 (1956) 429-442.
- Bowden, F.P. and Tabor, D., *The Friction and Lubrication of Solids*, Part I, Clarendon Press, Oxford, 1950.
- Bowden, F.P. and Tabor, D., *The Friction and Lubrication of Solids*, Part II, Clarendon Press, Oxford, 1964.
- Bowling, R.A., A theoretical review of particle adhesion. In Mittal, K.L. (Ed.), *Particles on Surfaces I*, Plenum Press, New York, 1988, pp. 129-142.
- Bradley, R.S., The cohesive force between solid surfaces and the surface energy of solids. *Phil. Mag.*, 13 (1932) 853-862.
- Brenner, S.S., Wriedt, H.A. and Oriani, R.I., Impact adhesion of iron at elevated temperatures. *Wear*, 68 (1981) 169-190.
- Briggs, G.A.D. and Briscoe, B.J., Effect of surface roughness on rolling friction and adhesion between elastic solids. *Nature*, 260 (1976) 313-315.
- British Standard (BS 410: 1969) Specification for test sieves.
- British Standard (BS 2955: 1958, amended 1965) Glossary of terms relating to powders.
- British Standard (BS 1449: Part II, 1983) Specification for stainless and heat-resisting steel plate, sheet & strip.
- Britten, J.R. and Pilpel, N., Effects of temperature on the tensile strength of pharmaceutical powders. *J. Pharm. Pharmacol.*, 30 (1978) 673-677.

- Buckley, D.H., Ferrante, J., Pashley, M.D. and Smith, J.R., Solids in contact. In Panel Report on Interfacial Bonding and Adhesion. *Mat. Sci. Eng.*, 83 (1986) 177-188.
- Butcher, A.E., Newton, J.M. and Fell, J.T., The tensile failure planes of powder compacts. *Powder Technol.*, 9 (1974) 57-59.
- Caddell, R.M., *Deformation and Fracture of Solids*, Prentice Hall, New Jersey, 1980.
- Cairns, R.J.R., Ottewill, R.H., Osmond, D.W.J. and Wagstaff, I., Studies on the preparation and properties of lattices in nonpolar media. *J. Colloid Interface Sci.*, 54 (1976) 45-51.
- Chemical Engineers' Handbook, by Perry, J.H., Chilton, C.H. and Kirkpatrick, S.D. (Eds.), 4th ed., McGraw-Hill, New York, 1963, Section 3, p. 8.
- Chestinov, A.L., An optical method for the determination of contact areas. *Stanki Instrum.*, 9 (1954).
- Chowhan, Z.T. and Chow, Y.P., Compression behaviour of pharmaceutical powders. *Int. J. Pharm.*, 5 (1980) 139-148.
- Coelho, M.C. and Harnby, N., The effect of humidity on the form of water retention in a powder. *Powder Technol.*, 20 (1978) 197-200.
- Cole, E.T., Rees, J.E. and Hersey, J.A., Relations between compaction data for some crystalline pharmaceutical materials. *Pharm. Acta Helv.*, 50 (1975) 28-32.
- Cook, G.D., Mechanical strength of compacts of binary mixtures. Ph.D. Thesis, University of London, 1987.
- Cooper, D.W., Wolfe, H.L. and Miller, R.J., Electrostatic removal of particles from surfaces. In Mittal, K.L. (Ed.), *Particles on Surfaces I*, Plenum Press, New York, 1988, pp. 339-349.
- Corn, M., The adhesion of solid particles to solid surfaces. II. *J. Air Pollution Control Assoc.*, 11 (1961) 566-575, 584.
- Corn, M., in Davies, C.N. (Ed.), *Aerosol Science*, Academic Press, New York, 1966, p. 359.
- Cottrell, G.A., The measurement of the contact charge density using soft rubber. *J. Phys. D: Appl. Phys.*, 11 (1978) 681-687.
- Czarnecki, J. and Dabroś, T., Attenuation of the van der Waals attraction energy in the particle/semi-infinite medium system due to the roughness of the particle surface. *J. Colloid Interface Sci.*, 78 (1980) 25-30.

- Dahneke, B., The capture of aerosol particles by surfaces. *J. Colloid Interface Sci.*, 37 (1971) 342-353.
- Dahneke, B., The influence of flattening on the adhesion of particles. *J. Colloid Interface Sci.*, 40 (1972) 1-13.
- Danjo, K. and Otsuka, A., Effect of temperature on the tensile strength of some organic powders. *Proc. Second World Congress Particle Technology*, Sept., 1990, pp. 221-226.
- David, S.T. and Augsburg, L.L., Plastic flow during compression of directly compressible fillers and its effect on tablet strength. *J. Pharm. Sci.*, 66 (1977) 155-159.
- Deryaguin, B.V., Aleinikova, I.N. and Toporov, Yu.P., On the role of electrostatic forces in the adhesion of polymer particles to solid surfaces. *Powder Technol.*, 2 (1968/69) 154-158.
- Deryaguin, B.V., Churaev, N.V. and Rabinovich, Ya.I., The modern state of the macroscopic theory of molecular forces and the results of its experimental verification for thin interlayers. *Adv. Colloid Interface Sci.*, 28 (1988) 197-244.
- Deryaguin, B.V., Krotova, N.A. and Smilga, V.P., *Adhesion of Solids*, Consultants Bureau, New York, 1978a.
- Deryaguin, B.V., Muller, V.M. and Toporov, Yu.P., Effect of contact deformation on particle adhesion. Determination of shape of surface of a spherical elastic particle close to the zone of particle contact with a flat rigid surface. *Kolloid. Zh.*, 37 (1975a) 412-416.
- Deryaguin, B.V., Muller, V.M. and Toporov, Yu.P., Influence of contact deformations on particle adhesion. 2. Macroscopic calculation of adhesive force with allowance for contact deformations in a spherical elastic particle. *Kolloid. Zh.*, 37 (1975b) 962-969.
- Deryaguin, B.V., Muller, V.M. and Toporov, Yu.P., Effect of contact deformations on the adhesion of particles. *J. Colloid Interface Sci.*, 53 (1975c) 314-326.
- Deryaguin, B.V., Muller, V.M. and Toporov, Yu.P., On the role of molecular forces in contact deformations (critical remarks concerning Dr. Tabor's Report). *J. Colloid Interface Sci.*, 67 (1978b) 378-379.
- Deryaguin, B.V., Muller, V.M. and Toporov, Yu.P., On different approaches to the contact mechanics. *J. Colloid Interface Sci.*, 73 (1980) 293.
- Deryaguin, B.V., Muller, V.M., Toporov, Yu.P. and Aleinikova, I.N., The role of the pressing-on in the adhesion of elastic particles. *Powder Technol.*, 37 (1984) 87-93.

- Deryaguin, B.V., Rabinovich, Ya.I. and Churaev, N.V., Measurement of forces of molecular attraction of crossed fibres as a function of width of air gap. *Nature*, 265 (1977a) 520-521.
- Deryaguin, B.V., Rabinovich, Ya.I. and Churaev, N.V., Direct measurement of molecular forces. *Nature*, 272 (1978c) 313-318.
- Deryaguin, B.V., Toporov, Yu.P. and Aleinikova, I.N., Electroadhesive properties of polymer particles in contact with the photoconductor surface. *J. Colloid Interface Sci.*, 54 (1976) 59-68.
- Deryaguin, B.V., Toporov, Yu.P., Muller, V.M. and Aleinikova, I.N., On the relationship between the electrostatic and the molecular component of the adhesion of elastic particles to a solid surface. *J. Colloid Interface Sci.*, 58 (1977b) 528-533.
- Deryaguin, B.V., Voropayeva, T.N., Kabanov, B.N. and Titiyevskaya, A.S., Surface forces and the stability of colloids and disperse systems. *J. Colloid Interface Sci.*, 19 (1964) 113-135.
- Deryaguin, B.V. and Zimon, A.D., Adhesion of powder particles to plane surfaces. *Kolloid. Zh.*, 23 (1961) 454-460.
- Donald, D.K., Electrostatic contribution to powder particle adhesion. *J. Appl. Phys.*, 40 (1969) 3013-3019.
- Drinker, P. and Hatch, T., *Industrial Dust*, 2nd Edn., McGraw Hill, New York, 1954.
- D'Yachenko, P.E.D., Tolkacheva, N.N., Andrew, G.A. and Karpova, T.M., *Actual Contact Area Between Touching Surfaces*, Consultants Bureau, New York, 1964.
- Dybwad, G.L., Sensitive new method for the determination of the adhesion force between a particle and a substrate. In Mittal, K.L. (Ed.), *Particles on Surfaces I*, Plenum Press, New York, 1988, pp. 237-243.
- Dyson, J. and Hirst, W., The true contact area between solids. *Proc. Roy. Soc. Lond.*, B67 (1954) 309-312.
- Edmonds, M.J., Jones, A.M., O'Callaghan, P.W. and Probert, S.D., A three-dimensional relocation profilometer stage. *Wear*, 43 (1977) 329-340.
- Esezobo, S. and Pilpel, N., The effect of temperature on the plasto-elasticity of some pharmaceutical powders and on the tensile strengths of their tablets. *J. Pharm. Pharmacol.*, 38 (1986) 409-413.
- Esmen, N.A., Ziegler, P. and Whitfield, R., The adhesion of particles upon inpaction. *J. Aerosol Sci.*, 9 (1978) 547-556.

- Farley, R. and Valentin, F.H.H., Effect of particle size upon the strength of powders. *Powder Technol.*, 1 (1967/68) 344-354.
- Fell, J.T. and Newton, J.M., The production and properties of spray-dried lactose. Part 2. The physical properties of samples of spray-dried lactose produced on an experimental drier. *Pharm. Acta Helv.*, 46 (1971a) 425-430.
- Fell, J.T. and Newton, J.M., Effect of particle size and speed of compaction on density changes in tablets of crystalline and spray-dried lactose. *J. Pharm. Sci.*, 60 (1971b) 1866-1869.
- Fujiwara, K., A method of observing the area of contact and the mechanical breakdown of a surface film. *Wear*, 50 (1978) 275-284.
- Fuller, K.N.G. and Tabor, D., The effect of surface roughness on the adhesion of elastic solids. *Proc. Roy. Soc. Lond.*, A345 (1975) 327-342.
- Gane, N., Pfaelzer, P.F. and Tabor, D., Adhesion between clean surfaces at light loads. *Proc. Roy. Soc. Lond.*, A340 (1974) 495-517.
- Gillespie, T., On the adhesion of drops and particles on impact at solid surfaces I. *J. Colloid Sci.*, 10 (1955) 266-280.
- Gillespie, T. and Rideal, E.K., On the adhesion of drops and particles on impact at solid surfaces. II. *J. Colloid Sci.*, 10 (1955) 281-298.
- Gillespie, T. and Settineri, W.J., The effect of capillary liquid on the force of adhesion between spherical solid particles. *J. Colloid Interface Sci.*, 24 (1967) 199-202.
- Goetzl, C.G., *Treatise on Powder Metallurgy*, Vol. 2, Interscience Publ. Inc., New York, 1950, pp. 797-861.
- Goldman, A.J., Cox, R.G. and Brenner, H., Slow viscous motion of a sphere parallel to a plane wall. II. Couette flow. *Chem. Eng. Sci.*, 22 (1967) 653-660.
- Good, R.J., in Lee, L.H. (Ed.), *Recent Advances in Adhesion*, Gordon Breach Sci. Publ., London, 1973.
- Good, R.J., Kvikstad, J.A. and Bailey, W.O., Anisotropic forces in the surface of a stretch-oriented polymer. *J. Colloid Interface Sci.*, 35 (1971) 314-327.
- Greenwood, J.A. and Rowe, G.W., Deformation of surface asperities during bulk plastic flow. *J. Appl. Phys.*, 36 (1965) 667-668.
- Greenwood, J.A. and Williamson, J.B.P., The contact of nominally-flat surfaces. *Proc. Roy. Soc. Lond.*, A295 (1966) 300-379.

- Gregory, J., The calculation of Hamaker constants. *Adv. Colloid Interface Sci.*, 2 (1969) 396-417.
- Gregory, J., Approximate expressions for retarded van der Waals interaction. *J. Colloid Interface Sci.*, 83 (1981) 138-145.
- Grunberg, L., Scott, D and Wright, K.H.R., The investigation of surface deformation. *Brit. J. Appl. Phys.*, 12 (1961) 134-140.
- Guerrero, J.L. and Black, J.T., Stylus tracer resolution and surface damage as determined by scanning electron microscopy. *Trans. A.S.M.E.*, 94B (1972) 1087-1093.
- Halling, J., The specification of surface quality - quo vadis? *The Production Engineer*, 51 (1972) 171-179.
- Hamaker, H.C., The London-van der Waals forces between spherical particles. *Physica*, 4 (1937) 1058-1072.
- Handbook of Pharmaceutical Excipients, American Pharmaceutical Association, Washington, DC, 1986, pp. 209-213.
- Hardman, J.S. and Lilley, B.A., Deformation of particles during briquetting. *Nature*, 228 (1970) 353-355.
- Harper, W.R., *Contact and Frictional Electrification*, Clarendon Press, Oxford, 1967.
- Hartley, P.A., Parfitt, G.D. and Pollock, L.B., The role of the van der Waals force in the agglomeration of powders containing submicron particles. *Powder Technol.*, 42 (1985) 35-46.
- Hayden, H.W., Moffatt, W.G. and Wulff, J., *The Structure and Properties of Materials. Volume III. Mechanical Behaviour*, J. Wiley & Sons, New York, 1965.
- Hays, D.A., Electric field detachment of charged particles. In Mittal, K.L. (Ed.), *Particles on Surfaces I*, Plenum Press, New York, 1988, pp. 351-360.
- Hertz, H., Study on the contact of elastic solid bodies. *J. Reine Angew. Math.*, 29 (1881) 156-171; SLA translations SLA-57-1164, 1882.
- Hiestand, E.N., Powders: particle-particle interactions. *J. Pharm. Sci.*, 55 (1966) 1325-1344.
- Hiestand, E.N., The determination of some important physical properties of powders. *Pharm. Ind.*, 34 (1972) 262-269.

- Hiestand, E.N., Dispersion forces and plastic deformation in tablet bond. *J. Pharm. Sci.*, 74 (1985) 768-770.
- Hinds, W.C., *Aerosol Technology*, Wiley, New York, 1982.
- Homola, A and Robertson, A.A., A compression method for measuring forces between colloidal particles. *J. Colloid Interface Sci.*, 54 (1976) 286-297.
- Hotta, K., Takeda, K. and Inoya, K., The capillary binding force of a liquid bridge. *Powder Technol.*, 10 (1974) 231-242.
- Hough, D.B. and White, L.R., The calculation of Hamaker constants from Lifshitz theory with applications to wetting phenomena. *Adv. Colloid Interface Sci.*, 14 (1980) 3-41.
- Israelachvili, J.N., Forces between surfaces in liquids. *Adv. Colloid Interface Sci.*, 16 (1982) 31-47.
- Israelachvili, J.N., Perez, E. and Tandon, R.K., On the adhesion force between deformable solids. *J. Colloid Interface Sci.*, 78 (1980) 260-261.
- Israelachvili, J.N. and Tabor, D., Measurement of van der Waals forces in the range 1.5 to 130nm. *Proc. Roy. Soc. Lond.*, A331 (1972) 19-38.
- James, M.B., Measurement of friction at a tablet metal interface. Ph.D. Thesis, University of London, 1986.
- James, M.B. and Newton, J.M., The influence of surface topography on the dynamic friction between acetylsalicylic acid compacts and steel. *J. Mat. Sci.*, 20 (1985) 1333-1340.
- Jayasinghe, S.S. and Pilpel, N., The cohesive properties of coal when heated. *J. Inst. Fuel*, 43 (1970) 51-55.
- Jayasinghe, S.S., Pilpel, N. and Harwood, C.F., The effect of temperature and compression on the cohesive properties of particulate solids. *Mat. Sci. Eng.*, 5 (1969/70) 287-294.
- Jeffreys, H., On the relation between fusion and strength. *Phil. Mag.*, 19 (1935) 840-846.
- Jenike, A.W., *Gravity Flow of Solids*, Bulletin 108, Utah Engineering Experiment Station, University of Utah, Salt Lake City, Utah, 1961.
- Jernot, J.P., Coster, M. and Charmant, J.L., Model of variation of the specific surface area during sintering. *Powder Technol.*, 30 (1981) 21-29.

- Johnson, K.L., A note on the adhesion of elastic solids. *Brit. J. Appl. Phys.*, 9 (1958) 199-200.
- Johnson, K.L., Kendall, K and Roberts, A.D., Surface energy and the contact of elastic solids. *Proc. Roy. Soc. Lond.*, A324 (1971) 301-313.
- Jones, T.M., *Formulation and Preparation of Dosage Forms*, Polderman, J. (Ed.), Elsevier, Amsterdam, 1977, pp. 29-44.
- Jones, W.D., *Fundamental Principles of Powder Metallurgy*, Edward Arnold, London, 1960, pp. 387-602.
- Jordan, D.W., The adhesion of dust particles. *Brit. J. Appl. Phys.*, 5 (1954) Suppl. 3, S194-S197.
- Kallay, N. and Matijević, E., Particle adhesion and removal in model systems. IV. Kinetics of detachment of hematite particles from steel. *J. Colloid Interface Sci.*, 83 (1981) 289-300.
- Kendall, K., The adhesion and surface energy of elastic solids. *J. Phys. D: Appl. Phys.*, 4 (1971) 1186-1195.
- Kendall, K., Thin-film peeling - the adhesion term. *J. Phys. D: Appl. Phys.*, 8 (1975) 1449-1452.
- Kendall, K., Theoretical aspects of solid-solid adhesion. *Sci. Prog., Oxf.*, 72 (1988) 155-171.
- Khilani, A., Cleaning semiconductor surfaces: facts and foibles. In Mittal, K.L. (Ed.), *Particles on Surfaces I*, Plenum Press, New York, 1988, pp. 17-35.
- Kitchener, J.A. and Prosser, A.P., Direct measurement of the long-range van der Waals forces. *Proc. Roy. Soc. Lond.*, A242 (1957) 403-409.
- Kočova, S. and Pilpel, N., The failure properties of lactose and calcium carbonate powders. *Powder Technol.*, 5 (1971/72) 329-343.
- Kohno, A. and Hyodo, S., Microadhesion between hard solids caused by very light loads. *Japan J. Appl. Phys.*, Suppl. 2, Pt. 1, (1974) 313-315.
- Kordecki, M.C. and Orr, C., Adhesion of solid particles to solid surfaces. *Am. Med. Assoc. Arch. Env. Hlth.*, 1 (1960) 13-21.
- Kragelskii, I.V, and Demkin, N.B., Contact area of rough surfaces. *Wear*, 3 (1960) 170-187.
- Krupp, H., Particle adhesion - theory and experiment. *Adv. Colloid Interface Sci.*, 1 (1967) 111-239.

- Krupp, H. and Sperling, G., Theory of adhesion of small particles. *J. Appl. Phys.*, 37 (1966) 4176-4180.
- Kuczynski, G.C., Measurement of self-diffusion of silver without radioactive tracers. *J. Appl. Phys.*, 21 (1950) 632-636.
- Kulvanich, P. and Stewart, P.J., Fundamental considerations in the measurement of adhesional forces between particles using the centrifuge method. *Int. J. Pharm.*, 35 (1987a) 111-120.
- Kulvanich, P. and Stewart, P.J., Correlation between total adhesion and charge decay of a model interactive system during storage. *Int. J. Pharm.*, 39 (1987b) 51-57.
- Kulvanich, P. and Stewart, P.J., Influence of relative humidity on the adhesion properties of a model interactive system. *J. Pharm. Pharmacol.*, 40 (1988) 453-458.
- Kuo, R.J. and Matijević, E., Particle adhesion and removal in model systems. III. Monodispersed ferric oxide on steel. *J. Colloid Interface Sci.*, 78 (1980) 407-421.
- Landau, L.D. and Lifshitz, E.M., *Theory of Elasticity*, Pergamon Press, Oxford, 1975.
- Larsen, R.I., The adhesion and removal of particles attached to air filter surfaces. *Am. Ind. Hyg. Assoc. J.*, 19 (1958) 265-270.
- Laycock, S. and Staniforth, J.N., Problems encountered in accurate determination of interparticle forces in ordered mixes. *Particulate Sci. Technol.*, 1 (1983) 259-268.
- Lee, M.H. and Jaffe, A.B., Toner adhesion in electrophotography. In Mittal, K.L. (Ed.), *Particles on Surfaces I*, Plenum Press, New York, 1988, pp. 169-177.
- Leenaars, A.F.M., A new approach to the removal of submicron particles from solid (silicon) substrates. In Mittal, K.L. (Ed.), *Particles on Surfaces I*, Plenum Press, 1988, pp. 361-372.
- Lifshitz, E.M., The theory of molecular attraction forces between solid bodies. *Sov. Phys.*, 2 (1956) 73-83.
- Lodge, K.B., Techniques for the measurement of forces between solids. *Adv. Colloid Interface Sci.*, 19 (1983) 27-73.
- Lodge, K.B. and Mason, R., Macroscopic attractive forces between solid surfaces separated by 10-100nm. 1. The theory of a novel dynamic-jump technique of measurement. *Proc. Roy. Soc. Lond.*, A383 (1982a) 279-294.

- Lodge, K.B. and Mason, R., Macroscopic attractive forces between solid surfaces separated by 10-100nm. 2. Experimental determination of attractive forces between mica cylinders by both dynamic-jump and static-jump methods. *Proc. Roy. Soc. Lond.*, A383 (1982b) 295-312.
- London, F., The general theory of molecular forces. *Trans. Faraday Soc.*, 33 (1937) 8-26.
- Lontz, J.F., in Borris, L.J. and Hausner, H.H. (Eds.), *Fundamental Phenomena in the Material Sciences*, Vol. 1, Plenum Press, New York, 1964, p. 37.
- Luckham, P.F., An invited review. The measurement of interparticle forces. *Powder Technol.*, 58 (1989) 75-91.
- Malamataris, S. and Pilpel, N., Effect of temperature on the tensile strength of lactose coated with fatty acids. Part 2. Tablets. *Powder Technol.*, 28 (1981) 35-42.
- Massimilla, L. and Donsi, G., Cohesive forces between particles of fluid-bed catalysts. *Powder Technol.*, 15 (1976) 253-260.
- Mattox, D.M. and Rigney, D.A., Adhesion processes in technological applications. In Panel Report on Interfacial Bonding and Adhesion. *Mat. Sci. Eng.*, 83 (1986) 189-195.
- Maugis, D., Overview of adherence phenomena. In Lee, L.H. (Ed.), *Adhesive Chemistry*, Plenum Press, New York, 1984.
- Maugis, D. and Barquins, M., Fracture mechanics and adherence of viscoelastic bodies. *J. Phys. D: Appl. Phys.*, 11 (1978) 1989-2023.
- Maugis, D. and Pollock, H.M., Surfaces forces, deformation and adherence at metal microcontacts. *Acta Metall.*, 32 (1984) 1323-1334.
- McFarlane, J.S. and Tabor, D., Adhesion of solids and the effect of surface films. *Proc. Roy. Soc. Lond.*, A202 (1950) 224-243.
- Mehrotra, V.P. and Sastry, K.V.S., Pendular bond strength between unequal-sized spherical particles. *Powder Technol.*, 25 (1980) 203-214.
- Mitrevej, A. and Augsburger, L.L., Adhesion of tablets in a rotary tablet press. I. Instrumentation and preliminary study of variables affecting adhesion. *Drug Dev. Ind. Pharm.*, 6 (1980) 331-377.
- Muller, V.M., Deryaguin, B.V. and Toporov, Yu.P., Effect of elastic contact deformation on the adhesion of particles. *Kolloid. Zh.*, 38 (1976) 41-47.

- Muller, V.M., Deryaguin, B.V. and Toporov, Yu.P., On two methods of calculation of the force of sticking of an elastic sphere to a rigid plane. *Colloids Surfaces*, 7 (1983a) 251-259.
- Muller, V.M. and Yushchenko, V.S., Influence of surface forces on deformation and adhesion of elastic particles to a rigid substrate or to each other. *Kolloid. Zh.*, 42 (1980) 411-419.
- Muller, V.M. and Yushchenko, V.S., Contact strains and mutual adhesion of spherical elastic particles with consideration of the surface forces. *Kolloid. Zh.*, 44 (1982) 811-818.
- Muller, V.M., Yushchenko, V.S. and Deryaguin, B.V., On the influence of molecular forces on the deformation of an elastic sphere and its sticking to a rigid plane. *J. Colloid Interface Sci.*, 77 (1980) 91-101.
- Muller, V.M., Yushchenko, V.S. and Deryaguin, B.V., General theoretical consideration of the influence of surface forces on contact deformations and the reciprocal adhesion of elastic spherical particles. *J. Colloid Interface Sci.*, 92 (1983b) 92-101.
- Nadkarni, P.D., Kildsig, D.O., Kramer, P.A. and Banker, G.S., Effect of surface roughness and coating solvent on film adhesion to tablets. *J. Pharm. Sci.*, 64 (1975) 1554-1557.
- Nakamura, T., *Bull. Jap. Soc. Precis. Engrs.*, 1 (1966) 241-248.
- Neumann, A.W., Visser, J., Smith, R.P., Omenyi, S.N., Francis, D.W., Spelt, J.K., Vargha-Butler, E.B., Zingg, W., van Oss, C.J. and Absolom, D.R., The concept of negative Hamaker coefficients. III. Determination of the surface tension of small particles. *Powder Technol.*, 37 (1984) 229-244.
- O'Callaghan, P.W. and Probert, S.D., Real area of contact between a rough surface and an optically-flat surface. *J. Mech. Eng. Sci.*, 12 (1970) 259-267.
- O'Callaghan, P.W. and Probert, S.D., Prediction and measurement of true areas of contact between solids. *Wear*, 120 (1987) 29-49.
- Okada, J., Matsuda, Y. and Fukumori, Y., Measurement of the adhesive force of pharmaceutical powders by the centrifugal method. I. *J. Pharm. Soc., Japan*, 89 (1969) 1539-1544.
- Onyekweli, A.O. and Pilpel, N., Effect of temperature changes on the densification and compression of griseofulvin and sucrose powders. *J. Pharm. Pharmacol.*, 33 (1981) 377-381.

- Osborne-Lee, I.W., Calculation of Hamaker coefficients for metallic aerosols from extensive optical data. In Mittal, K.L. (Ed.), *Particles on Surfaces 1*, Plenum Press, New York, 1988, pp. 77-90.
- Otsuka, A., Iida, K., Danjo, K. and Sunada, H., Measurements of the adhesive force between particles of powdered organic substances and a glass substrate by means of the impact separation method. I. Effect of temperature. *Chem. Pharm. Bull.*, 31 (1983) 4483-4488.
- Otsuka, A., Iida, K., Danjo, K. and Sunada, H., Measurement of the adhesive force between particles of powdered materials and a glass substrate by means of the impact separation method. III. Effect of particle shape and surface asperity. *Chem. Pharm. Bull.*, 36 (1988) 741-749.
- Overbeek, J.Th.G., Interparticle forces in colloid sciences. *Powder Technol.*, 37 (1984) 195-208.
- Overbeek, J.Th.G. and Sparnaay, M.J., Experiments on long-range attractive forces between macroscopic objects. *J. Colloid Sci.*, 7 (1952) 343-345.
- Overbeek, J.Th.G. and Sparnaay, M.J., Classical coagulation: London-van der Waals attraction between macroscopic objects. *Disc. Faraday Soc.*, 18 (1954) 12-24.
- Paronen, P., Heckel plots as indicators of elastic properties of pharmaceuticals. In Rubinstein, M.H. (Ed.), *Pharmaceutical Technology: Tableting Technology*, Volume 1, Ellis Horwood, Chichester, 1987, pp. 139-144.
- Paronen, P. and Juslin, M., Compression characteristics of four starches. *J. Pharm. Pharmacol.*, 35 (1983) 627-635.
- Parsegian, V.A. and Weiss, G.H., Spectroscopic parameters for computation of van der Waals forces. *J. Colloid Interface Sci.*, 81 (1981) 285-289.
- Pashley, M.D., Pethica, J.B. and Tabor, D., Adhesion and micromechanical properties of metal surfaces. *Wear*, 100 (1984) 7-31.
- Patrick, R.C., *Treatise on Adhesion and Adhesives, Vol. 2. Theory*, Marcel Dekkar Inc., New York, 1967.
- Pilpel, N. and Britten, J.R., Effects of temperature on the flow and tensile strengths of powders. *Powder Technol.*, 22 (1979) 33-44.
- Pilpel, N., Britten, J.R., Onyekweli, A.O. and Esezobo, S., Compression and tableting of pharmaceutical powders at elevated temperatures. *Int. J. Pharm.*, 70 (1991) 241-249.

- Pilpel, N. and Esezobo, S., The effect of temperature on the tensile strength and disintegration of paracetamol and oxytetracycline tablets. *J. Pharm. Pharmacol.*, 29 (1977) 389-392.
- Princen, H.M., Capillary phenomena in assemblies of parallel cylinders. I. Capillary rise between two cylinders. *J. Colloid Interface Sci.*, 30 (1969) 69-75.
- Rabinovich, Ya.I., Deryaguin, B.V. and Churaev, N.V., Direct measurements of long-range surface forces in gas and liquid media. *Adv. Colloid Interface Sci.*, 16 (1982) 63-78.
- Rabinowicz, E., in Wiley, J. (Ed.), *Friction and Wear of Materials*, J. Wiley & Sons, London, 1965.
- Ranade, M.B.A., Menon, V.B., Mullins, M.E. and Debler, V.L., Adhesion and removal of particles: effect of medium. In Mittal, K.L. (Ed.), *Particles on Surfaces I*, Plenum Press, New York, 1988, pp. 179-191.
- Rankell, A.S. and Higuchi, T., Thermodynamic and kinetic aspects of adhesion under pressure. *J. Pharm. Sci.*, 57 (1968) 574-577.
- Rees, J.E., Hersey, J.A. and Cole, E.T., The effect of rate of loading on the strength of tablets. *J. Pharm. Pharmacol.*, 22 (1970) Suppl., 64S.
- Rees, J.E. and Rue, P.J., Time-dependent deformation of some direct compression excipients. *J. Pharm. Pharmacol.*, 30 (1978) 601-607.
- Rice, R.W., In Krigel, W.W. and Palmour, H. (Eds.), *Materials Science Research*, Volume 5, Ceramics in Severe Environments, Plenum Press, New York, 1971, p. 197.
- Richmond, O., Morrison, H.L. and Devenpeck, M.L., Sphere indentation with application to Brinell hardness test. *Int. J. Mech. Sci.*, 16 (1974) 75-82.
- Richmond, P. and Ninham, B.W., Calculation of van der Waals forces across mica plates using Lifshitz theory. *J. Colloid Interface Sci.*, 40 (1972) 406-408.
- Ridgway, K., Aulton, M.E. and Rosser, P.H., The surface hardness of tablets. *J. Pharm. Pharmacol.*, 22 (1970) Suppl., 70S-78S.
- Ridgway, K., Glasby, J. and Rosser, P.H., The effect of crystal hardness on radial pressure at the wall of a tableting die. *J. Pharm. Pharmacol.*, 21 (1969) Suppl., 24S-29S.
- Roberts, R.J. and Rowe, R.C., The effect of the relationship between punch velocity and particle size on the compaction behaviour of materials with varying deformation mechanisms. *J. Pharm. Pharmacol.*, 38 (1986) 567-571.

- Roberts, A.D. and Thomas, A.G., The adhesion and friction of smooth rubber surfaces. *Wear*, 33 (1975) 45-64.
- Rogers, L.N. and Reed, J., The adhesion of particles undergoing an elastic-plastic impact with a surface. *J. Phys. D: Appl. Phys.*, 17 (1984) 677-689.
- Rowe, R.C., The adhesion of film coatings to tablet surfaces-the effect of some direct compression excipients and lubricants. *J. Pharm. Pharmacol.*, 29 (1977) 723-726.
- Rowe, R.C., The measurement of the adhesion of film coatings to tablet surfaces: the effect of tablet porosity, surface roughness and film thickness. *J. Pharm. Pharmacol.*, 30 (1978a) 343-346.
- Rowe, R.C., The effect of some formulation and process variables on the surface roughness of film-coated tablets. *J. Pharm. Pharmacol.*, 30 (1978b) 669-672.
- Rowe, R.C., Surface roughness measurements on both uncoated and film-coated tablets. *J. Pharm. Pharmacol.*, 31 (1979) 473-474.
- Rumpf, H., Particle adhesion. *Agglomeration*, 77 (1977) 97-129.
- Salpekar, A.M. and Augsburger, L.L., Magnesium lauryl sulphate in tableting: effect on ejection force and compressibility. *J. Pharm. Sci.*, 63 (1974) 289-292.
- Sano, S., Saito, F. and Yashima, S., Measurement of forces of adhesion of powders to glass plate by centrifugal method. *Kagaku Kogaku Ronbunshu*, 10 (1984) 17-24.
- Schubert, H., Capillary forces - modeling and application in particulate technology. *Powder Technol.*, 37 (1984) 105-116.
- Sendall, F.E. and Staniforth, J.N., A study of powder adhesion to metal surfaces during compression of effervescent pharmaceutical tablets. *J. Pharm. Pharmacol.*, 38 (1986) 489-493.
- Shapiro, I., Compaction of powders. In Vincenzini, P. (Ed.), *Ceramic Powders, Preparation, Consolidation and Sintering*, Elsevier, Amsterdam, 1983, p. 80.
- Shlanta, S. and Milosovich, G., Compression of pharmaceutical powders I. Theory and instrumentation. *J. Pharm. Sci.*, 53 (1964) 562-564.
- Siegel, S., Hanus, E.J. and Carr, J.W., Polytetrafluoroethylene tipped tablet punches. *J. Pharm. Sci.*, 52 (1963) 604-605.
- Skotnický, J., The dependence of the melting point on the pressure. *Czech. J. Phys.*, 3 (1953) 225-231.

- Snaith, B., Probert, S.D. and O'Callaghan, P.W., Thermal resistances of pressed contacts. *Appl. Energy*, 22 (1986) 31-84.
- Snedecor, G.W. and Cochran, W.G., *Statistical Methods*, 7th Ed., The Iowa State University Press, Iowa, USA, 1980.
- Sparnaay, M.J., Four notes on van der Waals forces. Induction effect, nonadditivity, attraction between a cone and a flat plate (asperities), history. *J. Colloid Interface Sci.*, 91 (1983) 307-319.
- Staniforth, J.N., Lai, F.K., Hersey, J.A. and Rees, J.E., Interparticle adhesion forces in ordered mixes. *J. Pharm. Pharmacol.*, 32 (1980) Suppl., 23P.
- Staniforth, J.N. and Patel, C.I., Creep compliance behaviour of direct compression excipients. *Powder Technol.*, 57 (1989) 83-87.
- Staniforth, J.N., Rees, J.E., Lai, F.K. and Hersey, J.A., Determination of interparticulate forces in ordered powder mixes. *J. Pharm. Pharmacol.*, 33 (1981) 485-490.
- Staniforth, J.N., Rees, J.E., Lai, F.K. and Hersey, J.A., Interparticle forces in binary and ternary ordered powder mixes. *J. Pharm. Pharmacol.*, 34 (1982) 141-145.
- Tabor, D., A simple theory of static and dynamic hardness. *Proc. Roy. Soc. Lond.*, A192 (1948) 247-274.
- Tabor, D., *The Hardness of Metals*, Clarendon Press, Oxford, 1951.
- Tabor, D., Recent studies of short range forces. *J. Colloid Interface Sci.*, 31 (1969) 364-371.
- Tabor, D., Surface forces and surface interactions. *J. Colloid Interface Sci.*, 58 (1977) 2-13.
- Tabor, D., On the role of molecular forces in contact deformations (critical remarks concerning Dr. Tabor's report). *J. Colloid Interface Sci.*, 67 (1978) 380.
- Tabor, D., Role of molecular forces in contact deformations. *J. Colloid Interface Sci.*, 73 (1980) 294.
- Tabor, D. and Winterton, R.H.S., Surface forces: direct measurement of normal and retarded van der Waals forces. *Nature*, 219 (1968) 1120-1121.
- Tabor, D. and Winterton, R.H.S., The direct measurement of normal and retarded van der Waals forces. *Proc. Roy. Soc. Lond.*, A312 (1969) 435-450.
- Taylor, G.I., The mechanism of plastic deformation of crystals. Part I. Theoretical. *Proc. Roy. Soc. Lond.*, A145 (1934) 362-387.

- Teer, D.G. and Arnell, R.D., in Halling, J. (Ed.), *Principles of Tribology*, Macmillan Press, London, 1975.
- The Merck Index, 10th Ed., Merck & Co. Inc., USA, 1983.
- Thomas, T.R., Recent advances in measurement and analysis of surface microgeometry. *Wear*, 33 (1975) 205-233.
- Timoshenko, S. and Goodier, J.N., *Theory of Elasticity*, McGraw Hill, New York, 1951.
- Toyoshima, K., Yasumura, M., Ohnishi, N. and Ueda, Y., Quantitative evaluation of tablet sticking by surface roughness measurement. *Int. J. Pharm.*, 46 (1988) 211-215.
- Train, D., Agglomeration of solids by compaction. *Trans. Instn. Chem. Engrs.*, 40 (1962) 235-240.
- Tsardaka, K.D. and Rees, J.E., Plastic deformation and retarded elastic deformation of particulate solids using creep experiments. *J. Pharm. Pharmacol.*, 41 (1989) Suppl., 28P.
- Tsardaka, K.D. and Rees, J.E., Relations between viscoelastic parameters and compaction properties of two modified starches. *J. Pharm. Pharmacol.*, 42 (1990) Suppl., 77P.
- Tsardaka, K.D., Rees, J.E. and Hart, J.P., Compression and recovery behaviour of compacts using extended Heckel plots. *J. Pharm. Pharmacol.*, 40 (1988) Suppl., 73P.
- Turner, G.A. and Balasubramanian, M., Investigations of the contributions to the tensile strength of weak particulate masses. *Powder Technol.*, 10 (1974) 121-127.
- Uppal, A. and Probert, S.D., Considerations governing the contact between a rough and a flat surface. *Wear*, 22 (1972) 215-234.
- Uppal, A., Probert, S.D. and Thomas, T.R., The real area of contact between a rough surface and a flat surface. *Wear*, 22 (1972) 163-183.
- Van Blokland, P.H.G.M. and Overbeek, J.Th.G., Dispersion forces between objects of fused silica. *J. Colloid Interface Sci.*, 68 (1979) 96-100.
- Van den Tempel, M., Mechanical properties of plastic-disperse systems at very small deformations. *J. Colloid Sci.*, 16 (1961) 284-296.
- Van den Tempel, M., Interaction forces between condensed bodies in contact. *Adv. Colloid Interface Sci.*, 3 (1972) 137-159.

- Van Oss, C.J., Good, R.J. and Chaudhury, M.K., The role of van der Waals forces and hydrogen bonds in hydrophobic interactions between biopolymers and low energy surfaces. *J. Colloid Interface Sci.*, 111 (1986) 378-390.
- Vincent, B., The van der Waals attraction between colloid particles having adsorbed layers. II. Calculation of interaction curves. *J. Colloid Interface Sci.*, 42 (1973) 270-285.
- Visser, J., Measurement of the force of adhesion between submicron carbon-black particles on a cellulose film in aqueous solution. *J. Colloid Interface Sci.*, 34 (1970) 26-31.
- Visser, J., On Hamaker constants. A comparison between Hamaker constants and Lifshitz-van der Waals constants. *Adv. Colloid Interface Sci.*, 3 (1972) 331-363.
- Visser, J., The concept of negative Hamaker coefficients. 1. History and present status. *Adv. Colloid Interface Sci.*, 15 (1981) 157-169.
- Visser, J., An invited review - van der Waals and other cohesive forces affecting powder fluidization. *Powder Technol.*, 58 (1989) 1-10.
- Vold, M.J., Van der Waals attraction between anisometric particles. *J. Colloid Sci.*, 9 (1954) 451-459.
- Vold, M.J., The effect of adsorption on the van der Waals interaction of spherical colloidal particles. *J. Colloid Sci.*, 16 (1961) 1-12.
- Voyutskii, S.S., *Autohesion and Adhesion of High Polymers*, Wiley, New York, 1963.
- Vromans, H., de Boer, A.H., Bolhuis, G.K., Lerk, C.F. and Kussendrager, K.D., Studies on the tableting properties of lactose: the effect of initial particle size on binding properties and dehydration characteristics of α -lactose monohydrate. In Rubinstein, M.H. (Ed.), *Pharmaceutical Technology: Tableting Technology*, Volume 1, Ellis Horwood, Chichester, 1987, pp. 31-42.
- Williamson, J.B.P. and Hunt, R.T., Relocation profilometry. *J. Phys. E: Appl. Phys.*, 2 (1968) 749-752.
- Woo, K.L. and Thomas, T.R., Contact of rough surfaces: a review of experimental work. *Wear*, 58 (1979) 331-340.
- York, P., Particle slippage and rearrangement during compression of pharmaceutical powders. *J. Pharm. Pharmacol.*, 30 (1978) 6-10.
- York, P. and Bailey, E.D., Dimensional changes of compacts after compression. *J. Pharm. Pharmacol.*, 29 (1977) 70-74.

- York, P. and Pilpel, N., The effect of temperature on the frictional cohesive and electrical conducting properties of powders. *Mat. Sci. Eng.*, 9 (1972a) 281-291.
- York, P. and Pilpel, N., The effect of temperature on the mechanical properties of some pharmaceutical powders in relation to tableting. *J. Pharm. Pharmacol.*, 24 (1972b) Suppl., 47P-56P.
- Zimon, A.D., Adhesion of solid particles to a plane surface 2. Influence of air humidity on adhesion. *Kolloid. Zh.*, 25 (1963) 265-268.
- Zimon, A.D., *Adhesion of Dust and Powder*, 2nd Ed., Consultants Bureau, New York, 1982.
- Zimon, A.D. and Volkova, T.S., Effect of surface roughness on dust adhesion. *Kolloid. Zh.*, 27 (1965) 306-307.